Université de Strasbourg

Institut de Biologie Chimique et Médecine Fondamentale Novossibirsk

2015

Ecole doctorale de la vie et de la santé

THÈSE

Présentée pour l'obtention du grade de

DOCTEUR DE L'UNIVERSITÉ DE STRASBOURG

Discipline : Science du Vivant

Domaine : Aspects Moléculaires et Cellulaires de la Biologie

par

Ilya DOVYDENKO

Mise au point d'aptamères aux capacités thérapeutiques basés sur les ARN importables dans les mitochondries humaines

Soutenue le 23 septembre 2015 devant la commission d'examen :

Pr Volkmar WEISSIG	**Rapporteur externe**
Pr Ruslan AFASIZHEV	**Rapporteur externe**
Dr Marie SISSLER	**Examinateur interne**
Pr Valentin VLASSOV	**Examinateur**
Dr Dmitrii PYSHNYI	**Examinateur**
Dr Ivan TARASSOV	**Examinateur**
Dr Nina ENTELIS	**Directeur de thèse**
Dr Alia VENYAMINOVA	**Co-directeur de thèse**

UMR7156 CNRS

«Génétique Moléculaire Génomique Microbiologie»

TABLE OF CONTENTS

ACKNOWLEDGEMENTS

ABBREVIATIONS

ACKNOWLEDGEMENTS

ABBREVIATIONS

AA	acrylamide
ADP	adenosine diphosphate
ATP	adenosine triphosphate
*bis*AA	*bis*-acrylamide
cal	calorie
CHEMS	cholesteryl hemisuccinate
CL	cationic lipid
CP	cationic polymer
CPP	cell-penetrating peptide
DC-Chol	3β-(N-(N′,N′-dimethylaminoethane)-carbamoyl) cholesterol
DNA	deoxyribonucleic acid
DOGS	dioctadecylamidoglycylspermine
DOPE	dioleoylphosphatidylethanolamine
DOSPA	N,N-dimethyl-N-[2-(sperminecarboxamido)ethyl]-2,3-bis(dioleyloxy)-1-propaniminium pentahydrochloride
DOTAP	1,2-dioleyl-3-trimethylammonium-propane
DOTMA	N-[1-(2,3-dioleyloxy) propyl]-N,N,N-trimethylammonium chloride
DTT	dithiothreitol
EDTA	ethylenediaminetetraacetic acid
$FADH_2$	flavin adenine dinucleotide hydroquinone form
GHS	glutathione
HEPES	4-(2-hydroxyethyl)-1-piperazineethanesulfonic acid
HF	fluoric acid
HDL	high-density lipoprotein
INs	inorganic nanoparticles
KSS	Kearns Sayre Syndrome
LDL	low-density lipoprotein
LNA	Locked Nucleic Acid
MELAS	Mitochondrial Encephalopathy, Lactic Acidosis and Stroke-like episodes
MEND	multifunctional envelope-type nanodevices
MERRF	Myoclonic Epilepsy and Red Ragged Fibres

MIF	membrane interaction factor
mRNA	messanger RNA
MTS	mitochondrial targeting sequence
MW	molecular weight
NA	nucleic acid
NADH	nicotinamide adenine dinucleotide reduced
NMP	N-methylpyrrolidone
OU	optical units
OXPHOS	oxidative phosphorylation
PA	phosphatidic acid
PAGE	polyacrylamide gel
PAMAM	polyamidoamine
PBS	phosphate buffered saline
PCR	polymerase chain reaction
PEI	polyethyleneimine
PEG	polyethylene glycol
PHPMA	poly[N-(2-hydoxypropyl)methacrylamide]
PLGA	poly lactic-co-glycolic acid
PLL	poly-L-lysine
PNA	Peptide Nucleic Acid
PNPase	Polynucleotide phosphorylase
RIC	RNA import complex
RNA	ribonucleic acid
rRNA	ribosomal RNA
SATE	S-acyl-2-thioethyl
SELEX	Systematic Evolution of Ligands by Exponential Enrichment
SDS	sodium dodecyl sulfate
siRNA	small interfering RNA
SM	sphingomyelin
SSC	Saline sodium citrate buffer
STR-R8	stearyl octaarginine
TALEN	Transcription Activator-like Effector Nucleases
TBDMS	*tert*-butyldimethylsilyl

TBE	Tris/Borate/EDTA buffer
TEA	triethylamine
TFAM	transcription factor A, mitochondrial
THF	tetrahydrofuran
Tris	tris(hydroxymethyl)aminomethane
tRNA	transfer RNA
UNA	unlocked nucleic acid
XNA	xylo nucleic acid

INTRODUCTION

INTRODUCTION

This chapter reviews different nucleic acids delivery strategies and discusses mitochondrial DNA-associated pathologies and the challenges of their treatment by gene or RNA therapy.

1. Nucleic acids delivery systems

Synthetic oligonucleotides and their conjugates are widely used in various fields of molecular biology, nanobiotechnology and medicine as tools for fundamental and applied research, as well as promising drugs for diagnosis and treatment of viral, cancer, genetic and others diseases of humans and animals (Ginn et al., 2013; Tan et al., 2011). Development of oligonucleotides as potential therapeutic agents is limited by their low efficiency of penetration into the target cells due to large size, negative charge and low stability. Many systems of gene targeting have been developed to overcome these barriers. Delivery vectors can be divided on two major groups: viral and non-viral systems (Kay, 2011). Each approach has advantages and disadvantages. Systems based on viral vectors have efficient mechanisms for entering the the cells, escaping endosomal entrapment and translocating gene cargo to the nucleus. Despite high efficiency of targeting, several limitations are associated with viral systems: insertional mutagenesis, immune response to viral proteins, tumorigenesis and cytopathic effects (Thomas et al., 2003; Walther and Stein, 2000).

The shortcomings in viral vectors stimulated development of non-viral vectors which can be readily synthesized and modified to facilitate biocompatibility. Improving of non-viral delivery systems depends on a detailed understanding of the barriers associated with the nucleic acids targeting into cells. The successful system for nucleic acids (NA) delivery shall meet a number of requirements: biocompatibility and low cytotoxicity, resistance to nuclease activity, possibility of endosomal escape and capability of entering the appropriate cellular compartment.

Mammalian cells internalise extracellular macromolecules by the endocytosis leading to formation of vesicle-like structures that fuse with early endosomes (De Haes et al., 2012), (Figure 1). Thus, the efficacy of transfection and the expected effect depend on both the ability of a vector to efficiently deliver the NA cargo with minimal toxicity, and its potential to overcome the endosomal compartmentalization.
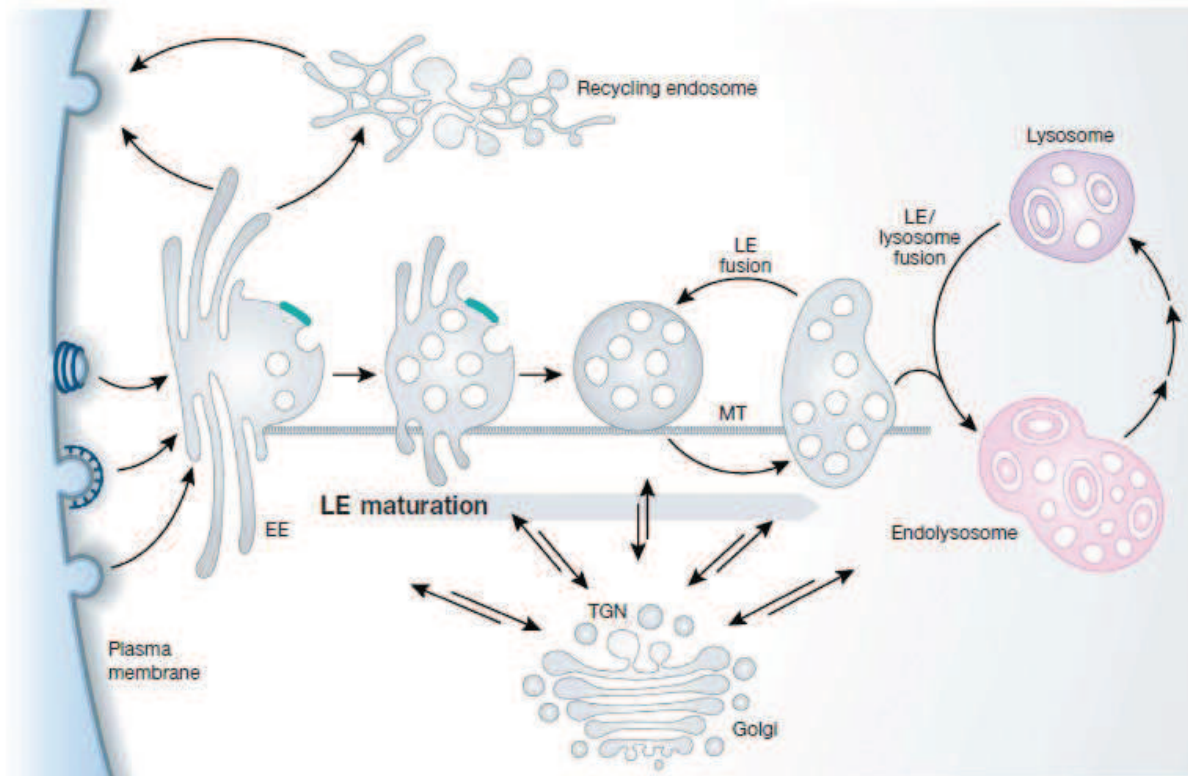
Figure 1. The endosome/lysosome system. Primary endocytic vesicles deliver their cargo to early endosomes (EEs) in the peripheral cytoplasm. During endosomal processing EEs move to the perinuclear space with the help of microtubules (MT) and mature into late endosomes (LEs). Processing of LEs results? in the increased size due to fusing and concentration of lysosomal hydrolases derived from the trans-Golgi network (TGN). Moreover, the LE pH drops from 6.8 to 4.9 during the maturation process. Finally, LEs fuse with a lysosome and form the endolysosome, in which active degradation takes place (Huotari and Helenius, 2011).

To faciliate NA escape into the cytosol, various compounds (endosomolytic agents, EA) have been used in combination with the delivery vectors. EAs vary in type (natural or synthetic compounds) as well as in their mechanisms of action, which include the endosomal membrane destabilization (TAT HIV, KALA or GALA peptides), pore formation (*e. g.* listeriolysin O toxin produced by *Listeria monocytogenes,* gp41HIV protein), and endosomal disruption *via* the "proton sponge" mechanism (*e. g.* PEI, ammonium chloride, chloroquine, methylamine) (Varkouhi et al., 2011).

The non viral delivery systems can be split in two groups: carrier-mediated and carrier-free systems.

1.1. Targeting of nucleic acids with nanocarriers

The carrier-mediated NA targeting systems can be further subdivided into three main groups:

- Polymeric system in which NA form complex with a polymer through charge interactions between the positive groups of the polymer and the negatively charged NA;

- Lipidic system in which cationic lipids interact with negatively charged NA and condensate it or encapsulate them;

- Inorganic carriers involving various materials such as gold nanoparticles, silica, carbon nanotubes, which can bind NA through different mechanisms.

1.1.1. Polymeric systems

Cationic polymers (CPs) are delivery vectors, which possess the ability to address nucleic acids into target cells (Bartlett and Davis, 2008; Davis, 2009; Heidel et al., 2007). Various types of polymers for NA delivery have been developed. They differ in both structure - linear, branched, or dendritic molecules -, and chemical nature - synthetic polymers, such as polyethyleneimine (PEI), poly-L-lysine (PLL), poly lactic-co-glycolic acid (PLGA), or natural compounds, such as chitosan and cyclodextrins (Figure 2) (Oliveira 2015).
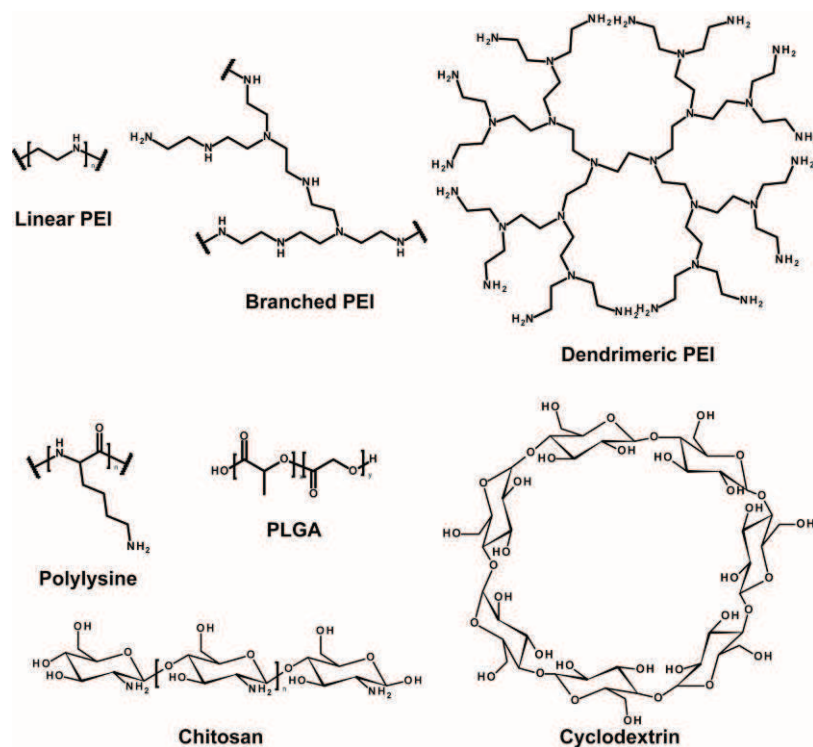

Figure 2. Polymers used in delivery of nucleic acids into cells.

Cationic polymers bind NA through spontaneous electrostatic interactions, neutralize their negative charge, and form nanoscale polymer-NA complexes (polyplexes), characterized by high stability and controllable size (Glodde et al., 2006). Internalisation of positively charged polyplexes occurs through nonspecific endocytosis *via* interactions with polyanionic glycosaminoglycans located on the cell surface (Mislick and Baldeschwieler, 1996; Ruponen et al., 2004). However, the polymers are of flexible design and can also be chemically crosslinked to a ligand in order to direct their delivery to specific target cells (Jager et al., 2012). The major challenges of NA delivery with the CP system are finding the optimal structure of the polymer that enables high efficacy of NA cargo internalisation and mitigates biocompatibility/cytotoxicity issues. For instance, some of the polymers, which had been found to be highly efficient *in vitro* (e.g. PEI and PLL), demonstrated high toxicity in a range of cell lines (Hunter, 2006).

Several structural parameters of CPs are important for successful NA delivery into cells: molecular weight, charge density, and type of charged centres. These properties may affect each step of the polyplex delivery: cellular uptake, endosomal escape, and release of NA cargo from the complex with CP. Cellular uptake directly depends on the polyplex stability. In turn, the stability of the complex positively correlates with the molecular weight (MW) and the charge density. Thus, CPs with high MW demonstrate more efficient targeting of genetic material into cells, but also display higher cytotoxicity than low MW polymers (Gebhart and Kabanov, 2001; Grayson et al., 2006). Certain polyamine-based polymers, such as PEI or polyamidoamine (PAMAM) dendrimers, are able to escape from the endosomes *via* the "proton sponge" mechanism (Behr, 1997; Boussif et al., 1995). The "proton sponge" mechanism is realized through active protonation of secondary and tertiary amino groups, resulting in proton and counter ions influx, which causes the rupture of the endosomal membrane and the release of the complexes into the cytosol. However, efficiency of recruiting nucleic acids in the polyplex increases with the number of substituted hydrogen atoms in the amino group. Thus, high efficacy of binding through secondary and tertiary amino groups can become an obstacle for NA release from the complex, which is one of the critical steps determining the efficiency of non-viral gene delivery systems (Cho et al., 2003). Therefore, a decrease of toxicity through reducing MW or charge of the polymer will usually lead to a loss of transfection efficiency.

One of the ways to save the high positive charge of the vector and increase its biocompatibility is the use of natural polymer molecules, such as chitosans (Jiang et al., 2008) and starch (Amar-Lewis et al., 2014), or introduction of biodegradable bridges in the

backbone of the molecule. Biodegradable carriers demonstrate improved transfection efficiencies by facilitating unpacking of the polyplexes after the cellular uptake. Many polymers containing cleavable bonds, such as poly-β-amino esters (Green et al., 2008), polyester amines (Yamanouchi et al., 2008), polyesters (Bikram et al., 2005), ketalized PEI (Shim and Kwon, 2009), polyphosphazenes (Luten 2003), and molecules containing reducible disulfide bonds (Oupicky and Li, 2014) have been developed as alternatives to non-biodegradable polymers. Another way to increase the biocompatibility and prevent interaction of CP-based system with blood components is to hide positive charges on the carrier surface by coating the complex with hydrophilic polyethylene glycol (PEG) or poly[N-(2-hydoxypropyl)methacrylamide] (PHPMA) (Miyata et al., 2012).

1.1.2. Lipidic systems

The pioneering work of Bangham et al. described formation of closed bilayered phospholipidic structures in aqueous systems, which led to the development of various lipid-based drug delivery methods (Bangham et al., 1965; Hope, 2014; Torchilin, 2005). Suspended in an aqueous environment, lipids can adopt a number of structured phases, such as spherical micelles, cylindrical micelles, flexible bilayers, vesicles, planar bilayers, and inverted hexagonal phase (Figure 3). Each type of phase can be predicted from the value of the packing parameter (P), which can be defined as $P=V/(a \times L)$, where V is the hydrophobic tail volume, a is the hydrophilic head area, and L is the hydrophobic tail length (Balazs and Godbey, 2011).
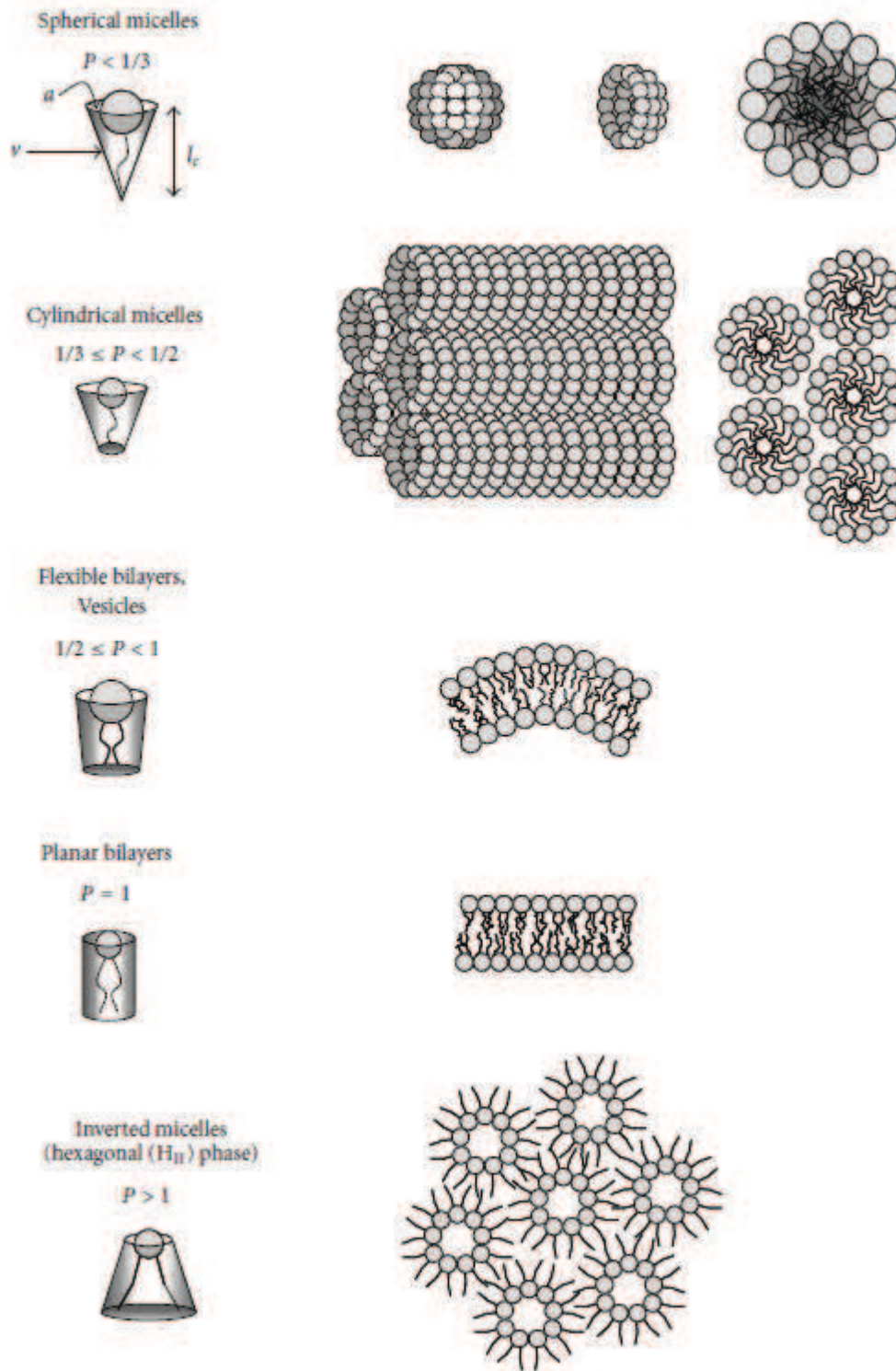
Figure 3. The structure of lipid phases (Balazs and Godbey, 2011).

In 1980, Fraley and co-workers demonstrated encapsulation of SV40 DNA in large phospholipid vesicles and their delivery in cultured monkey cells (Fraley et al., 1980). Later, in 1987, Felgner and co-workers showed a more efficient transfection with a synthetic cationic lipid, N-[1-(2,3-dioleyloxy) propyl]-N,N,N-trimethylammonium chloride (DOTMA)

(Figure 4), which spontaneously formed small, uniform liposomes capable of efficient DNA delivery into various mammalian cell lines (Felgner et al., 1987). Cationic lipids (CLs), similarly to cationic polymers, can form complexes (lipoplexes) with negatively charged nucleic acids. Their positive charge also plays a role in the delivery processes (binding to the negatively charged surface of the cell and induction of endocytosis) and the endosomal escape (through destabilization of the bilayer nonlamellar structure of the endosomal membrane) (Rehman et al., 2013). Release of NA cargo may be increased by addition of a helper lipid, dioleoylphosphatidylethanolamine (DOPE) (Figure 4).
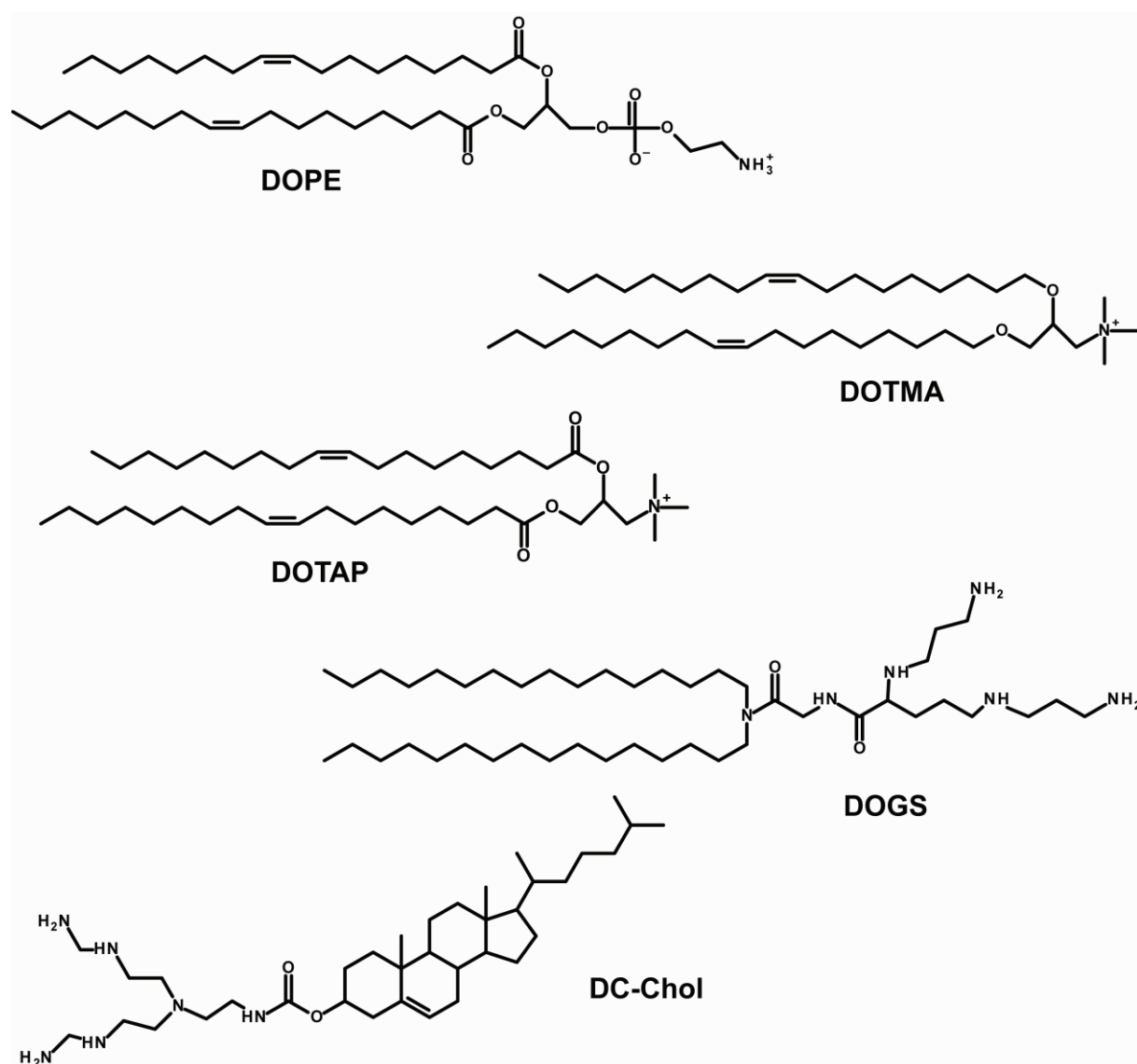
Figure 4. Lipids used for nucleic asids delivery.

Cationic lipids used for NA delivery can be classified according to the type of the hydrophobic moiety (aliphatic, such as DOTMA, and cholesterol-based derivatives, such as 3β-(N-(N′,N′-dimethylaminoethane)-carbamoyl) cholesterol, DC-Chol) and the nature of the

15

head group (monovalent lipids, such as 1,2-dioleyl-3-trimethylammonium-propane, DOTAP, and multivalent lipids, such as dioctadecylamidoglycylspermine, DOGS (Farhood et al., 1992; Freedland et al., 1996; Leventis and Silvius, 1990)) (Figure 4). The structure of CL affects the efficiency of NA internalisation and the cytotoxicity. For example, shortening of the aliphatic chain as well as the presence of unsaturated bonds leads to an increase of the delivery efficacy (Fletcher et al., 2006; Liu et al., 2008). The type of positively charged centres has an impact on the cytotoxicity. For instance, CLs, especially cholesterol derivatives, containing amino groups are characterised by high toxicity due to inhibition of the protein kinase C, which can be amended by changing the polar head to a heterocyclic cation, such as imidazolium or pyridinium (Lv et al., 2006). Another approach to decrease toxicity of CLs is to introduce cleavable bonds in the linker between the positively charged head and the hydrophobic part (Movahedi et al., 2015). Additionally, the delivery system with CLs can be shielded with PEG, it will decrease the toxicity and extend the *in vivo* circulation time (Li and Szoka, 2007). Alternative to CL lipoplexes is a system based on anionic lipids, in which all shortcomings inherent to CLs due to their positive charge are absent. Instead of using cationic lipids, some divalent cations, such as calcium, can be added to assemble the anionic lipid–NA complex (Balazs and Godbey, 2011); alternatively, NA should be pre-condensed with cationic polymers (Lee and Huang, 1996). To improve the cellular uptake and the endosomal escape the surface of negatively charged liposomes has been modified by addition of cell penetrating peptides (Akita et al., 2009).

1.1.3 Inorganic systems

Besides oraganic systems for targeting of NA, inorganic nanoparticles (INs) can be used as possible vectors. Gold, silica, carbon nanotubes, calcium phosphate, metal oxides represent some of the most popular materials for nucleic acids delivery (Dizaj et al., 2014). The surface of INs can be modified to increase the affinity of NAs for the carrier surface and the specificity of targeting (Ding et al., 2014). Interestingly, supraparamagnetic iron oxide-based nanoparticles can respond to a magnetic field, thus, the magnetic field can potentially direct the targeted delivery and improve the cellular uptake (Peng et al., 2008; Tang et al., 2014). Two pathways by which INs penetrate the cells, depending on the carrier size, are known: phagocytosis (for INs larger than 0.5 μm) and endocytosis (for smaller particles) (Rolland, 1999). Most INs are characterised as biocompatible and low cytotoxicity delivery vectors due to their inertness. On the other hand, toxic effects can be provoked by modifications used for immobilization of NA cargo (Xua et al., 2006). As an exception, carbon nanotubes

demonstrate high cytotoxicity *per se* which can, however, be reduced by modification of their surface with hydrophilic molecules (Bianco et al., 2005).

1.2. Carrier-free targeting systems

As mentioned above, another approach for delivery of oligonucleotides into the cells consists in conjugation of NA molecules with targeting ligands. The transporting molecule is capable of binding to the cell surface or to specific receptors on it, and inducing endocytosis (Juliano et al., 2008). The ligand molecule can be attached to NA directly or through a linker. Depending on the type of oligonucleotide and its purpose, the linker can be connected *via* the 2'-, 3'-, or 5'-terminus, the C5 atom of pyrimidine bases, the C8 atom of adenine, the exocyclic amino group of guanine, or an internucleoside phosphate (Winkler, 2013). In contrast to carrier-mediated systems of delivery, in conjugates NA is not protected and needs additional modifications shielding it from nucleases (see section 1.3.). For most carrier-free systems the endosomal escape is passive, which reduces the efficiency of transfection, thus, there is a necessity to use additional compounds to promote the release of oligonucleotides from endosomes before they are degraded and recycled. However, the simplicity of design and the small size, in comparison with nanoparticles, ensure a lower toxicity and a better biodistribution of NA conjugates. Vectors with sizes larger than 5 nm can only be used for NA delivery to certain types of tumours and to normal tissues with fenestrated endothelia, such as liver and spleen, whereas conjugates can reach many types of tissues (Juliano et al., 2009).

Various delivery systems through covalent attachment of addressing ligands to the NA cargo have been developed: carbohydrate–NA conjugates, peptide–NA conjugates, antibody–NA conjugates (Uckun et al., 2013), aptamer conjugates, and lipid–NA conjugates.

Carbohydrate–NA conjugates. The asialoglycoprotein receptor present on hepatocytes binds diverse chemotherapeutic agents, including galactose-glycoproteins, and helps their internalisation by endocytosis (Stockert, 1995). This permits the use of carbohydrate-based vectors for addressed NA delivery. For instance, 5'-glycoconjugates of oligonucleotides have demonstrated excellent cell-type specificity and cellular uptake in the nanomolar concentration range (Biessen et al., 1999). Triantennary N-acetyl galactosamine conjugates (Figure 5) facilitate the targeted delivery of siRNAs and antisence oligonucleotides to hepatocytes *in vivo* (Nair et al., 2014; Prakash et al., 2014).
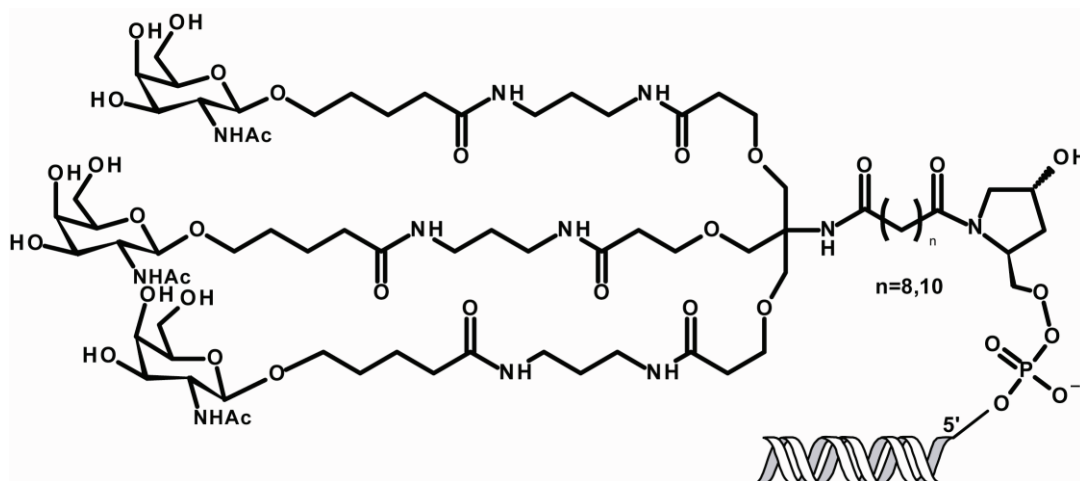
Figure 5. Triantennary N-acetyl galactosamine-NA conjugate.

Peptide–NA conjugates. The peptides used for delivery of NA can be divided in two classes. The first group includes cell-targeting peptides which are specific ligands for overexpressed surface receptors of diseased cells (Juliano et al., 2013; McGuire et al., 2014; Vives et al., 2008). For instance, the bombesin peptide (ligand for the gastrin-releasing peptide receptor) and a specific peptide for the IGF1R receptor (overexpressed in breast cancer) were conjugated with an oligonucleotide and siRNA, respectively, for targeted delivery (Cesarone et al., 2007; Ming et al., 2010). The second type is cell-penetrating peptides (CPPs), which are short, amphiphilic, basic amino acid-rich peptides. CPPs enter cells by two ways, *via* endocytosis through electrostatic interactions with negatively charged glycosaminoglycans, similarly to cationic polymers (see section 1.1.2.) (Juliano et al., 2008), or trough membrane translocation. The choice of entry pathway is influenced by such factors as the CPP sequence, temperature, and the CPP concentration (Boisguerin et al., 2015). CPPs also promote the endosomal escape as described above.

Aptamer–conjugates. Aptamers are small nucleic acids that fold into a well-defined three-dimensional structure, which determines their affinity and specificity for target molecules. They can be obtained by SELEX (Systematic Evolution of Ligands by Exponential Enrichment) (Tuerk and Gold, 1990). Aptamers can be *in vitro* evolved to bind small molecules, nucleic acids, proteins, carbohydrates, or cell surface receptors. Thus, these structured NA molecules can be used for delivery of other oligonucleotides (Tan et al., 2011).

1.2.1. Lipid-containing conjugates

One of the most popular methods of delivery of conjugated oligonucleotides is the use of lipids as vectors. Various lipophilic molecules have been conjugated to oligonucleotides, including phospholipids, fatty acids, bile acids (e.g. cholic acid), cholesterol, fat-soluble vitamins (e.g. α-tocopherol, folic acid) (Bhat et al., 1999; Li et al., 1998; Raouane et al., 2012). The structures of these compounds are shown in Figure 6. Among those, cholesterol, studied by various groups for the past 25 years, since the pioneering work of Letsinger and co-workers (Letsinger et al., 1989), is by far the most extensively characterized addressing agent.
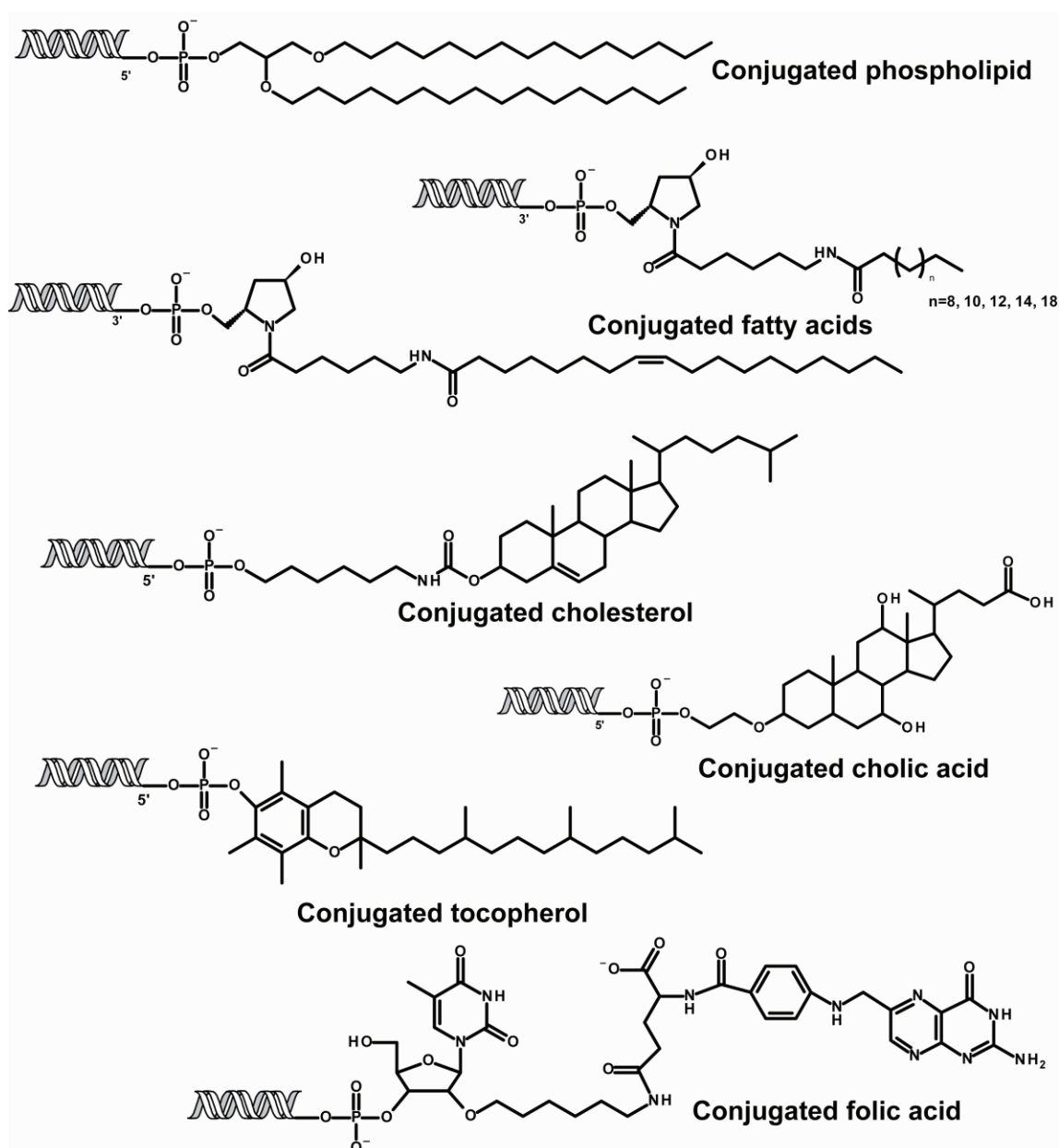
Figure 6. Lipophilic molecules used for conjugation with oligonucleotides.

Cholesterol is an essential lipid of cell membranes of many eukaryotes, which made it an attractive agent for addressing various therapeutic molecules into cells. For instance, intravenous administration of cholesterol-containing siRNA conjugates resulted in significant levels of those in liver, heart, kidney, adipose, and lung tissue (Soutschek et al., 2004). In yet another study, accumulation of a cholesterol-conjugated siRNA in brain cells upon intrastriatal injection was shown (DiFiglia et al., 2007). Cholesterol-containing conjugates were found to accumulate in various tumor cells (Moschos et al., 2007; Petrova et al., 2011). Altogether, these studies demonstrate that cholesterol conjugation significantly improves delivery of NAs. Cellular uptake of cholesterol-conjugated oligonucleotides *in vivo* depends on complex formation between the conjugates and circulating high-density (HDL) and low-density lipoprotein (LDL) (Wolfrum et al., 2007). Binding of conjugates to the LDL receptor leads to the uptake in the liver, whereas in other tissues the internalization proceeds through HDL receptors.

Conjugates of oligonucleotides with cholesterol have been developed by many research groups, wherein attachment to an oligonucleotide was performed through either the 5'- or the 3'-terminus. Introduction of a cholesterol residue into an oligonucleotide is carried out through the unique hydroxyl group of the steroid. Cholesterol can be attached either directly (MacKellar et al., 1992; Seo et al., 2006b) or *via* various linear or branched linkers. Examples of linear linkers are molecules based on diamines, proposed by Letsinger and co-workers (Letsinger et al., 1989) (Figure 7). Amino alcohols with various lengths of aliphatic chain (Lorenz et al., 2004; Petrova et al., 2011) and polyethylene glycol (Kubo et al., 2007) have also been used as linear linker (Figure 7).
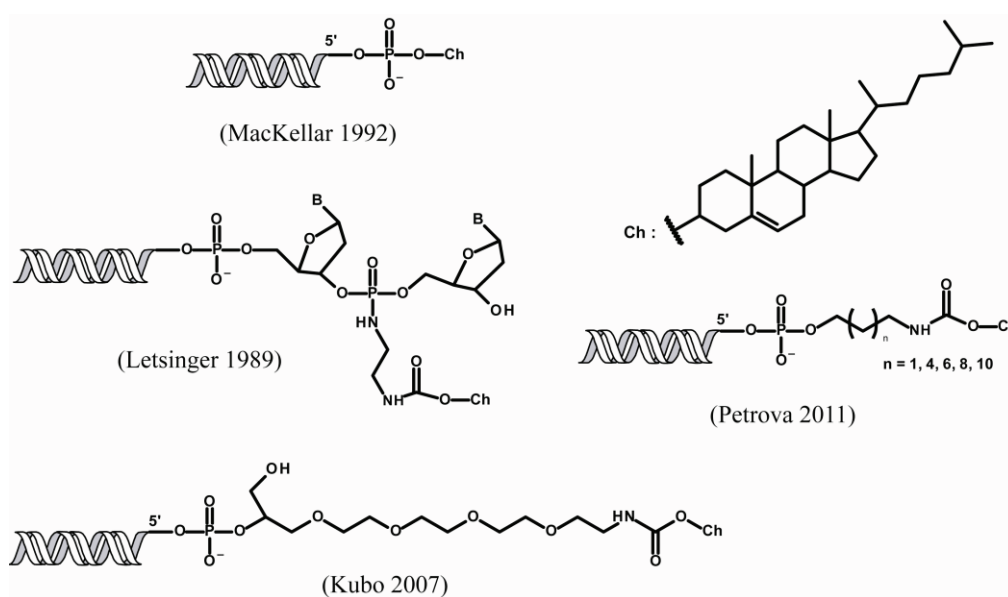
Figure 7. Cholesterol conjugated with oligonucleotides trough linear linkers.

Another approach to the synthesis of cholesterol-conjugated oligonucleotides is introducing the steroid residue at the 5'- or the 3'-terminus of the oligonucleotide chain through branched linkers containing several reactive groups. The compounds used as the branched linkers include glycerol (Ueno et al., 2008; Vu et al., 1993), 2-aminobutyl-1,3-propanediol (Rump et al., 1998), serinol (Manoharan et al., 2005), trans-4-hydroxy-L-proline (Manoharan et al., 2005; Reed et al., 1991), lysine (Stetsenko and Gait, 2001) or serine (Chaltin et al., 2005) (Figure 8).
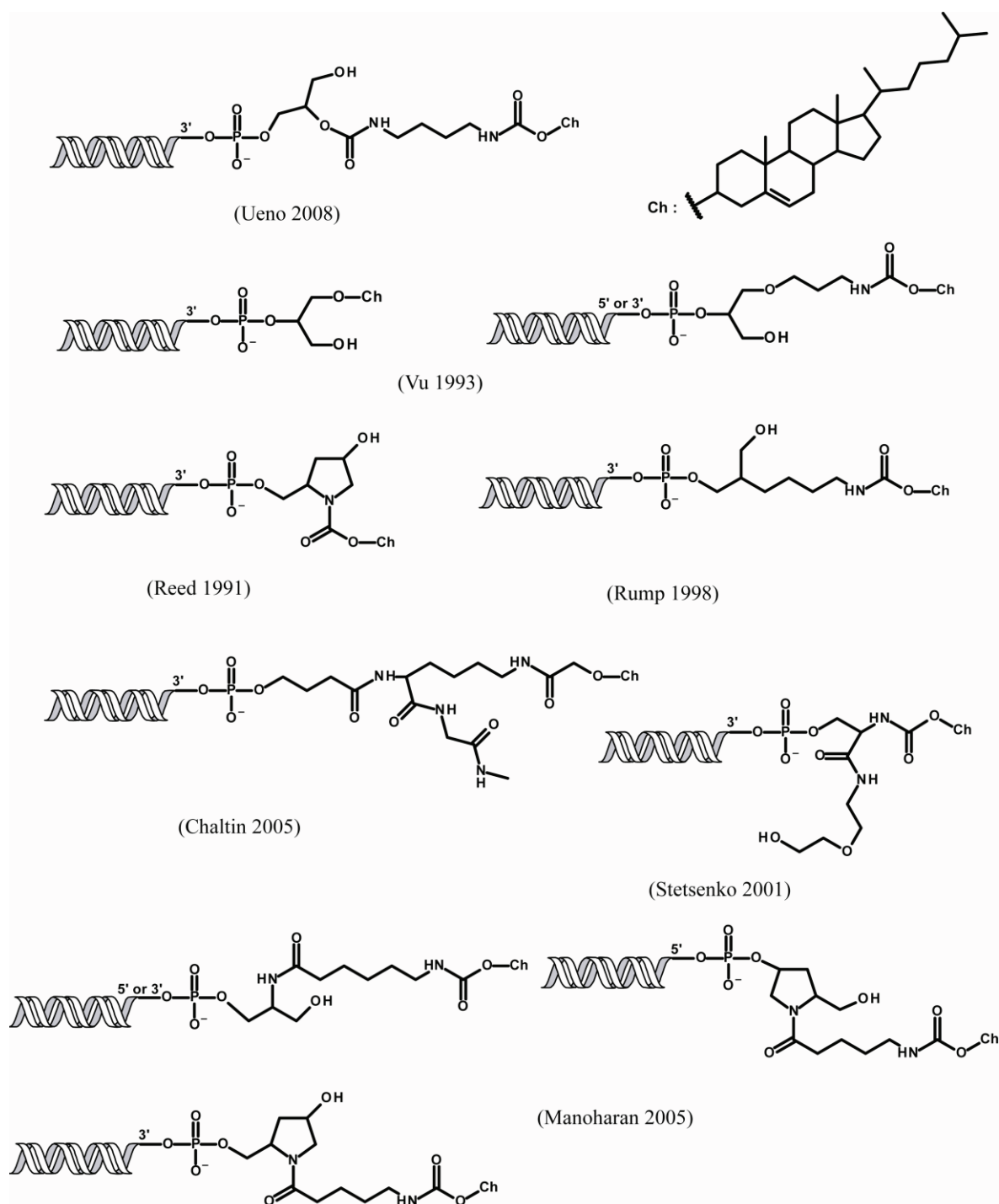
Figure 8. Cholesterol conjugated with oligonucleotides trough branched linkers.

A cholesterol residue may negatively affect the therapeutic effect by anchoring the cargo NA to the lipid bilayer membrane or by reducing the efficiency of annealing with the target molecule. To alleviate these effects, a cholesterol residue, conjugated with siRNA, is introduced at the sense chain, or it can be added through a cleavable arm, usually containing a disulfide bond (Boutorine and Kostina, 1993; Chen et al., 2010; Manoharan et al., 2005; Moschos et al., 2007; Oberhauser and Wagner, 1992) (Figure 9).
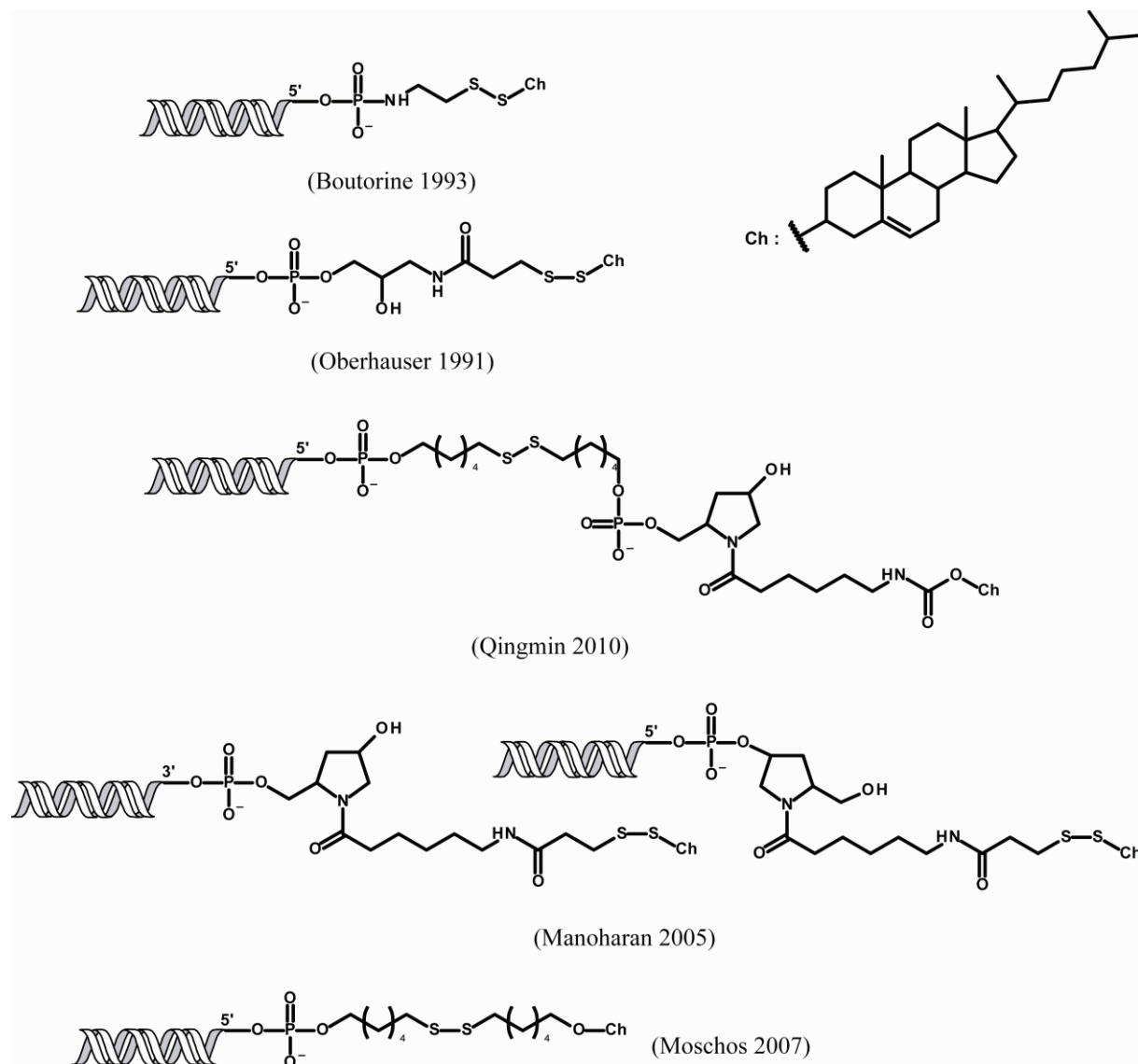
Figure 9. Cholesterol conjugated with oligonucleotides trough cleavable linkers.

The length of the linker can influence the cellular uptake, the optimal efficiency achieved for the RNA chain and the cholesterol spaced by 6-10 methylene units (Petrova et al., 2011).
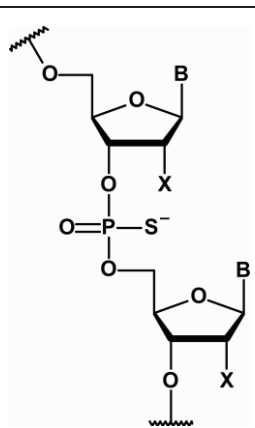
It is interesting that after penetration of the conjugates into cells, they do affect the target gene expression, suggesting that they successfully escape from endosomes. So far, the mechanism
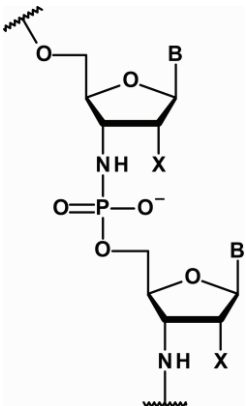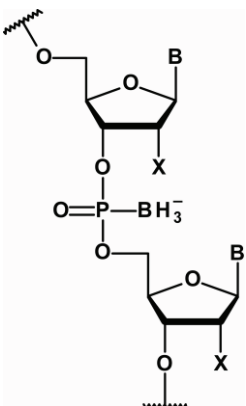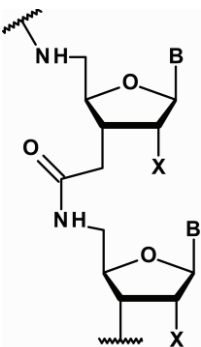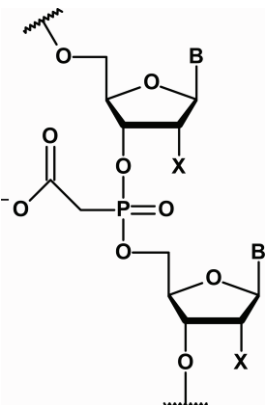
of such a release from endosomes is currently not understood, but it may be related to the intracellular traffic of cholesterol (Maxfield and Wustner, 2013).
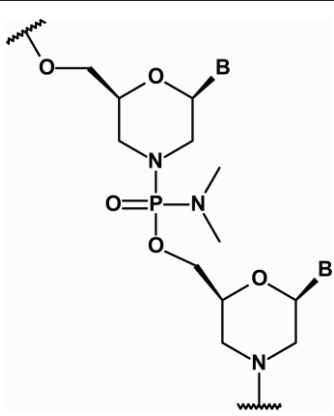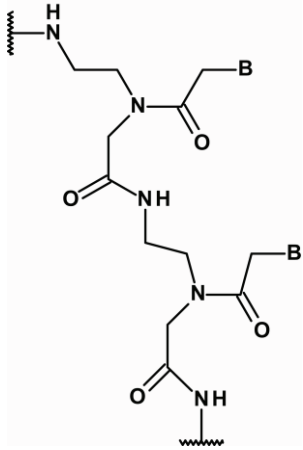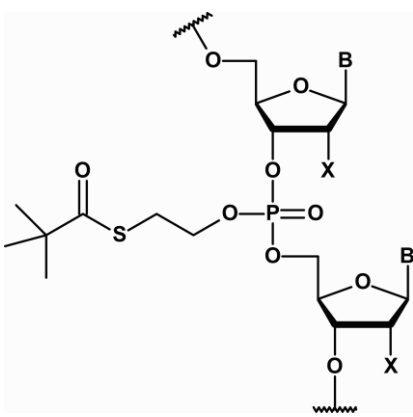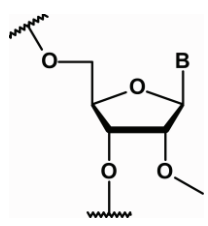
1.3. Modification of nucleic acids
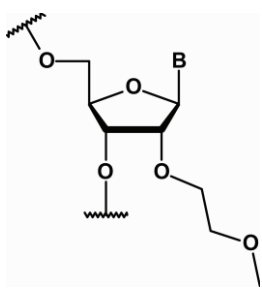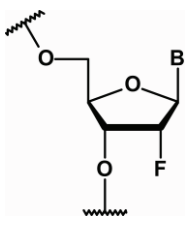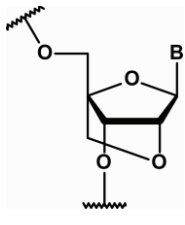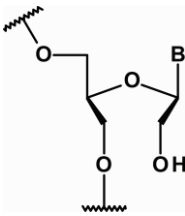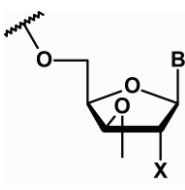
In the previous sections we have reviewed the main approaches of non-viral nucleic acids delivery. As we can see, one of the differences between the carrier-free and the carrier-mediated delivery is the absence/presence of protection of NA from nucleases during transfection. However, in both cases, after the cell penetration the carrier-NA complex should break up and release NA into the cytoplasm, where it will again become vulnerable to nuclease attack. This complication can be circumvented if the oligonucleotide cargo is chemically modified to improve its stability. Chemical modifications of nucleic acids can be classified into three distinct categories: internucleoside linkage modifications, sugar modifications, and nucleobase modifications (the latter, not considered here, affects the thermal stability of the duplex (Herdewijn, 2000) (Table 1). The different classes of modifications may be used within the same molecule, depending on the desired effect. However, any modifications should be introduced with caution as they may change NA properties, such as binding affinity for RNA/DNA targets and toxicity.

Table 1. Chemical modifications of nucleic acids.

Modification	Structure	Properties	References
Modification of internucleoside link			
Phosphorothioate		Highly resistant to nuclease cleavage; decreases the duplex stability; binds to serum albumin; toxic.	(Bennett and Swayze, 2010; Milligan et al., 1993)

N3' Phosphoramidate		Confers resistance to nucleases; increases T_m of duplex by 2°C per residue for an RNA target.	(Gryaznov et al., 1995; Heidenreich et al., 1997)
Boranophosphate		Confers high nuclease resistance.	(Hall et al., 2004)
Amide-linkage		Confers nuclease resistance; leads to the duplex T_m change from -4 to +0,9°C per residue for an RNA target.	(De Mesmaeker et al., 1994; Mutisya et al., 2014)
Phosphonoacetate		Confers nuclease resistance; uncharged; decreases T_m of duplex by 1.2°C per residue for an RNA target.	(Sheehan et al., 2003)

Morpholino		Highly resistant to nuclease cleavage; uncharged.	(Summerton and Weller, 1997)
Peptide Nucleic Acid (PNA)		Highly resistant to nuclease cleavage; uncharged; decreases T_m of duplex by 1° C per residue for a DNA target.	(Shabi et al., 2006)
SATE		Highly resistant to nuclease cleavage; uncharged; reversible protection group (cleaved off by thioesterase in the cytoplasm).	(Meade et al., 2014)
Sugar modifications			
2'-O-Me		Confers nuclease resistance; increases the duplex stability; decreases the innate immune response induction.	(Bennett and Swayze, 2010)

2'-O-MOE		Confers nuclease resistance; increases T_m of duplex by 2°C per residue for an RNA target.	
2'F-RNA		Confers nuclease resistance; increases T_m of duplex by 2.2^{o}C per residue for an RNA target.	(Kawasaki et al., 1993)
LNA		Confers nuclease resistance; increases T_m of duplex by 5.1^o C per residue for an RNA target and by 4°C per residue for a DNA target.	(Koshkin et al., 1998)
UNA		Decreases T_m of duplex by 5-10°C per residue for an RNA target and by 7-10°C per residue for a DNA target.	(Campbell and Wengel, 2011)
XNA		Confers nuclease resistance; decreases duplex stability.	(Poopeiko et al., 2003)
X – H (DNA) or OH (RNA); B – nucleobases: A, C, G, T, U.			

2. Mitochondria and mitochondrial diseases

Mitochondria are essential eukaryotic cell organelles discovered in the 19th century (Ernster and Schatz, 1981). The first structural characterisation of mitochondria was performed over 60 years ago by transmission electron microscopy (Palade, 1952; Sjostrand, 1953) (Figure 10). These studies showed that the mitochondrion is encapsulated by outer and inner membranes which divide the organelle into the intermembrane space and the matrix compartments. The inner membrane invaginates into the matrix space, forming cristae, which increases the surface of the inner membrane. Mitochondria are dynamic organelles and can

change their morphology depending on the cell type and physiological conditions. For instance, they can form interconnected networks or numerous separate small organelles (Westermann, 2012). The interconnectivity and dynamics of the mitochondria are determined by processes of mitochondrial fusion and fission.
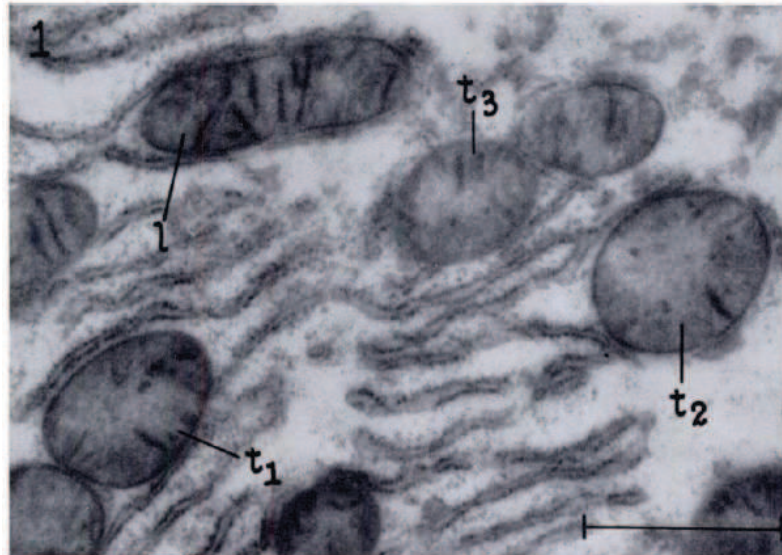
Figure 10. Transmission electron microscopy of the cytoplasm of rat liver cell, t1-3 are mitochondria (Palade, 1953).

Mitochondria are responsible for a multitude of metabolic and signalling pathways such as metabolism of fatty acids, carbohydrates and amino acids, steroid and heme biosynthesis, calcium and iron homeostasis, production and scavenging of reactive oxygen species, programmed cell death, *etc*. However, their most known function is participation in the process of oxidative phosphorylation (OXPHOS) resulting in production of ATP from ADP. OXPHOS is much more efficient (36 ATP molecules are generated per one molecule of glucose) than glycolysis (2 ATP molecules produced per one molecule of glucose). Most proteins involved in OXPHOS (with the exception of cytochrome c) are embedded in the inner mitochondrial membrane and constitute five multi-protein enzyme complexes: NADH dehydrogenase (complex I), succinate dehydrogenase (complex II), cytochrome c oxidoreductase (complex III), cytochrome c oxidase (complex IV), and ATP synthase (complex V), which altogether form the respiratory chain (Figure 11). Electrons from NADH and $FADH_2$, which have been obtained in the Krebs cycle and from fatty acid oxidation, enter the respiratory chain *via* complexes I and II, respectively, and become transferred onto ubiquinone (coenzyme Q). Thereafter, complex III transfers electrons from ubiquinone to cytochrome c. Complex IV catalyses the last step of electron transfer from cytochrome c onto an oxygen molecule, reducing it to water. The energy obtained from the electron flux is used

for proton pumping across the inner membrane into the intermembrane space, resulting in an electrochemical gradient, which is exploited by complex V to phosphorylate ADP to ATP (Boyer et al., 1973).

Figure 11. Mitochondrial respiratory chain and oxidative phosphorylation (Nijtmans et al., 2004).

Mitochondria are semi-autonomous organelles that contain their own genome (mtDNA) and protein synthesis machinery. In humans, supercoiled circular mtDNA localizes to the mitochondrial matrix and is anchored to the inner membrane. It is 16 568 bp-long and encodes 37 genes: 13 for protein subunits of respiratory complexes, 22 for mitochondrial tRNAs, and 2 for rRNAs (Figure 11).

Figure 11. The human mitochondrial genome (Wanrooij and Falkenberg, 2010). Heavy "(H-strand") and light ("L-strand") mtDNA strands are shown. Complex I NADH dehydrogenase (ND) genes are shown in green; complex III cytochrome b (cyt b) gene is shown in red; complex IV cytochrome c oxidase (COX) genes are shown in light blue; complex V ATP synthase (ATPase) genes are shown in gray. Transfer RNA genes are set in black and ribosomal RNA genes (rRNA) in yellow.

Most mitochondrial proteins (>1000) are encoded by nuclear genes and imported into the organelle. Mutations in both mitochondrial genome and in the nuclear genes encoding

mitochondrial proteins or involved in regulation of mitochondrial functions, can lead to a number of human pathologies, mostly neuromuscular syndromes (Angelini et al., 2009; Koopman et al., 2012; Pinto and Moraes, 2014; Schon et al., 2012).

2.1. Approaches for treatment of mitochondrial disorders associated with mtDNA.

Diseases caused by mtDNA mutations have a cumulative prevalence of at least 1:5000 (Chinnery et al., 2000). Various strategies of treatment can be envisaged for such disorders, including symptomatic approaches, directed on alleviating the symptoms caused by a disease, and disease-modifying strategies. The latter may include restoring the respiratory chain functions, eliminating toxic metabolites, altering the mitochondrial dynamics, changing the whole mitochondrial population, or intervening in the mitochondrial gene expression system. Genetic approaches include gene therapy (allotopic or xenotopic expression of artificially introduced gene products from the nucleus) and methods to directly impact mtDNA.

Allotopic expression, when normally mtDNA-encoded protein genes are transferred into the nucleus, is based on the natural pathway of import of nuclear-encoded proteins into mitochondria (Becker et al., 2012). This approach was first applied on a yeast model: the gene for the ATPase subunit 8 combined with a mitochondrial targeting peptide was expressed from the nucleus (Nagley et al., 1988). It was shown that the expressed protein incorporated into the mitochondrial complex V and supported the respiratory function. This idea was also implemented on cultured human cells, where the genes for ATPase subunit 6 (complex V) (Manfredi et al., 2002) and ND4 subunit (complex I) (Guy et al., 2002) were nuclearly expressed. Corral-Debrinski with colleagues optimized the allotopic expression of highly hydrophobic mitochondrial proteins, which can form aggregates in the cytosol preventing the mitochondrial targeting, by introducing the 3'-UTR of the SOD2 mRNA, which localizes to the mitochondrial surface, to facilitate the translocation of the synthesized proteins ATP6, ND1 and ND4 through the mitochondrial membranes (Bonnet et al., 2008; Kaltimbacher et al., 2006). This strategy was then tested on animal models with AAV-based vector (Lechauve et al., 2014).

Xenotopic expression consists in the allotopic expression of genes coming from other species. For example, Yagi and coworkers showed that the single-subunit rotenone-insensitive NADH-quinone oxidoreductase (Ndi1) of *Saccharomyces cerevisiae* can restore the NADH oxidation in complex I-deficient mammalian cells (Seo et al., 2006a).

Alternative allotopic methods involve production of mitochondrial tRNAs from nuclear genes and their import into mitochondria. The mitochondrial targeting of nuclear DNA-encoded tRNAs has been described for diverse organisms (Rubio et al., 2008; Tarassov et al., 2013). Many mitochondrial disorders are associated with mutations in mitochondrial tRNA genes and importing non-mutated tRNAs into mitochondria may be a potential treatment strategy for such defects. It has been shown that yeast tRNA^{Lys} (tRK1) and some tRK1-derived molecules can be internalized by isolated human mitochondria (Kolesnikova et al., 2002; Kolesnikova et al., 2000). The yeast tRNA^{Lys} derivatives expressed in immortalized human cells and in primary human fibroblasts were found to be partially imported into mitochondria (Kolesnikova et al., 2004). In *trans*mitochondrial cybrid cells carrying a mutation in the mitochondrial tRNA^{Lys} gene which causes the MERRF (Myoclonic Epilepsy and Red Ragged Fibres) syndrome, import of the yeast tRNA^{Lys} was accompanied by a partial rescue of the mitochondrial translation (Kolesnikova et al., 2004). The efficacy of this approach was also demonstrated on *trans*mitochondrial cybrid cells carrying the mutation in the mitochondrial tRNA^{Leu} gene causing MELAS (Mitochondrial Encephalopathy, Lactic Acidosis and Stroke-like episodes) (Karicheva et al., 2011). In this study, recombinant tRNA^{Lys} with the identity elements for the human mitochondrial leucyl-tRNA synthetase have been designed and used to complement the mutation. It was demonstrated that nuclear expression and mitochondrial targeting of such transgenic tRNAs result in an improvement of mitochondrial translation, increased levels of mitochondrial DNA-encoded respiratory complex subunits, and a significant rescue of respiration. Mitochondrial import of nuclearly expressed tRNA^{Lys}, tRNA^{Leu} and the *COX2* mRNA, which were fused with another determinant of RNA import (so-called "RP sequence"), was also reported by another research team (Wang et al., 2012).

Instead of targeting complementing gene products into mitochondria, the mutated mtDNA may be repaired to "solve the problem from inside". In the vast majority of clinical cases, both wild-type and mutant mtDNA molecules are simultaneously present in the same cell, a phenomenon known as ''heteroplasmy''. The ratio between the "healthy" and pathology-associated mitochondrial genomes determines whether the mitochondrial function will be affected. Therefore, shifting this ratio in favor of wild-type mtDNA may prevent the disease development. There are two kinds of approaches aiming to do so: selective destruction of mutant mitochondrial genomes or inhibition of their replication. The first approach was applied to a hybrid cell line containing both mouse (carrying two sites for endonuclease *PstI*) and rat (without *PstI* sites) mtDNA. The use of a construct encoding a mitochondrially targeted *PstI* restriction endonuclease resulted in an increase of the proportion of the rat

mtDNA (Srivastava and Moraes, 2001). Similar use of mitochondrially addressed restriction enzymes was reported in later studies (Alexeyev et al., 2008; Tanaka et al., 2002). One important limitation of this strategy is the rarity of specific and unique restriction sites in the mutant mtDNA. However, this hurdle can be overcome by using designer zinc-finger nucleases (Minczuk et al., 2008) or TALENs (Transcription Activator-like Effector Nucleases) (Bacman et al., 2012; Reddy et al., 2015) directed against specific mutations.

Another strategy for shifting the level of heteroplasmy, proposed by Taylor and coworkers, consists in selective inhibition of mutant mtDNA replication (Taylor et al., 1997). It relies on constructs which can penetrate into mitochondria, selectively bind to the mutated mtDNA and at least transiently block its replication while allowing the wild-type mtDNA to multiply. For example, mitochondrially targeted peptide nucleic acids (PNAs) were shown to have a remarkable binding selectivity, associating with mutated mtDNA but not with the wild-type one at physiological salt concentrations and temperatures *in vitro* (Taylor et al., 1997). Unfortunately, they proved to be inefficient in living cells (Muratovska et al., 2001). Recently, this approach was successfully applied to RNA molecules which contained determinants of import (Kolesnikova et al., 2011) and a region of complementarity to a mutated locus of mtDNA (Comte et al., 2013). A high binding specificity and an efficient mitochondrial import of these designed RNAs were paralleled by a shift of the level of heteroplasmy in cybrid cells.

So far, the low efficacy of cellular and mitochondrial addressing nucleic acids remains the main challenge in treating diseases associated with mutations in the mitochondrial genome by using these approaches.

2.2. Targeting of nucleic acids into mitochondria

Currently, a few strategies were developed for delivery of exogenous nucleic acids into the mitochondria, the first group is based on the pathways of the natural import of proteins and RNA, the second – on the targeting carried out by synthetic molecules and particles.

2.2.1. Carrier-mediated import

Carrier-mediated import of nucleic acids into the mitochondria comprises systems based on modified cationic polymers, micelle-like particles and liposomal structure, as well as inorganic carriers. As described previously, cationic polymers are capable to deliver nucleic acid into the cells, some of them are able to escape from endosomes, and can be easily modified for imparting of additional properties. Lee and co-workers conjugated PEI with MTS (Lee et al., 2007). In this study, a modified cationic polymer was used for plasmid DNA condensation resulting in cell penetrance, and DNA internalization into mitochondria. In addition, it was shown that modified PEI exerted lower cytotoxicity than PEI. An alternative system is based on amphiphilic cation - dequalinium, which can form liposome-like particles (DQAsomes) (Figure 12). DQAsomes can condense DNA, which can be used for cell transfection (Weissig et al., 1998). It had been demonstrated that these cationic vesicles can dissociate and release DNA cargo upon contact with the surface of isolated mitochondria (Weissig et al., 2001). Further studies showed effective targeting of DQAsome/DNA complex to live cells, endosomal escape and partial adressing of DNA cargo to mitochondrial sites (D'Souza et al., 2003). The use of DQAsome system for adressing of NA to mitochondria sites in combination with DNA conjugated with MTS provides the DNA cargo accumulation in mitochondria of living cells (D'Souza et al., 2005).
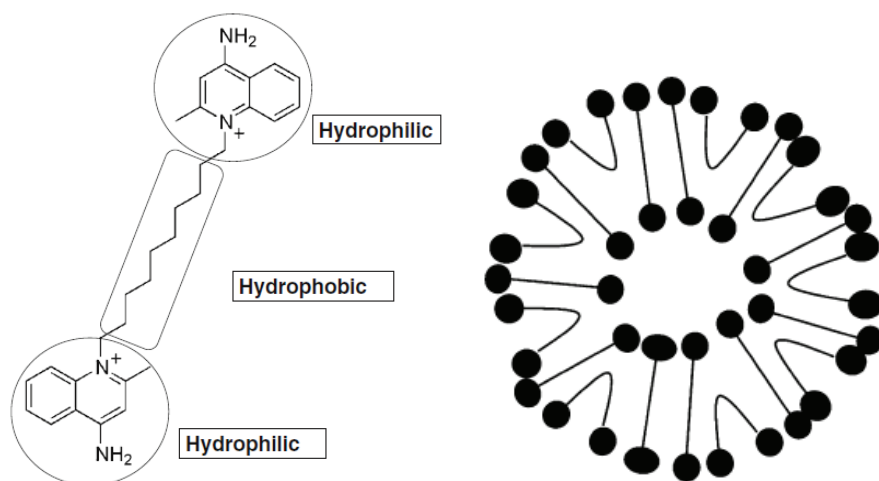
Figure 12. Chemical structure of dequalinium and hypothetical scheme illustrating the self-assembly of dequalinium cations into liposome-like vesicles (Weissig, 2011).

One more example of oligonucleotides delivery into mitochondria using cationic amphiphiles was demonstrated by Muratovska and co-workers by conjugation of PNA oligonucleotide with a triphenylphosphonium moiety (Muratovska et al., 2001). The conjugate successfully penetreted human cell and was targeted to mitochondria. Another approach to the delivery of

macromolecules into mitochondria was proposed in Harashima laboratory (Yamada et al., 2008). The basis of this method is the use of multifunctional envelope-type nanodevices (MEND), core shell construction modified with CPP and functional ligands (Yamada et al., 2012a) (Figure 13). MENDs targeted to mitochondria were termed "Mito-porter". The method consists in sequential and specific membrane fusion of liposomal carrier with organelle membranes (Figure 13).
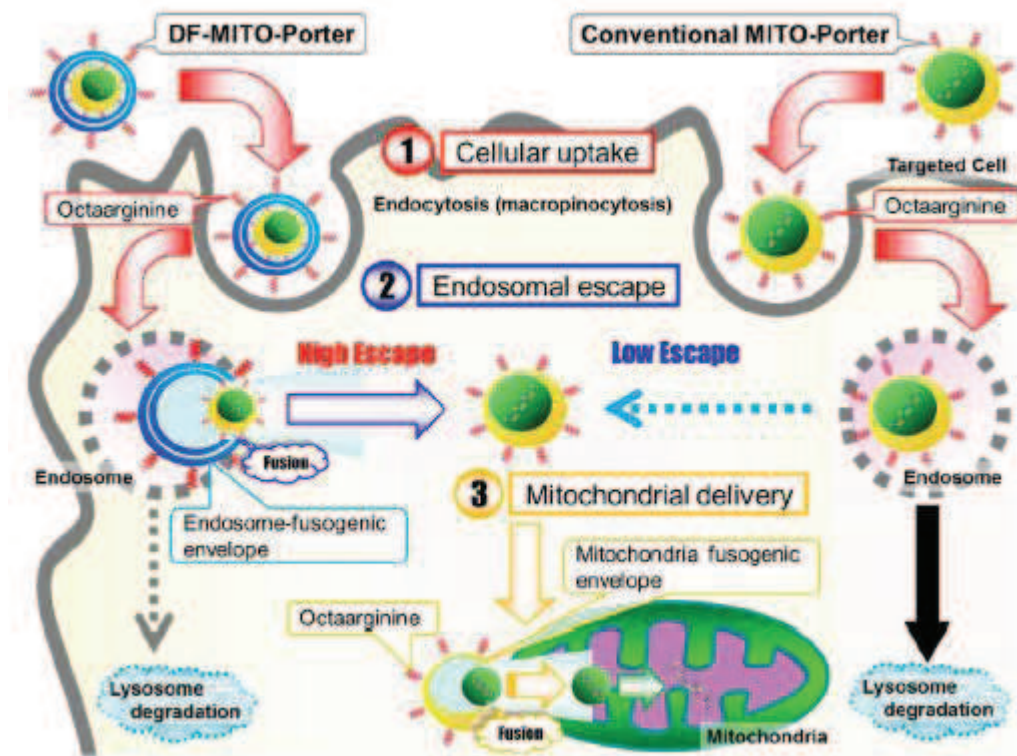
Figure 13. Schematic image of mitochondrial delivery of DNA cargo *via* a series of membrane fusions using dual function (DF)-MITO-Porter (Yamada et al., 2012b).

For fusing of the liposome with mitochondrial membranes, its lipid composition was optimised (Yamada et al., 2008). The core part of MEND contains DNA condensed with R8-peptide which is enveloped by the first shell [DOPE/SM/CHEMS/STR-R8 (9:2:1:1, molar ratio)] and the second shell [DOPE/PA/STR-R8 (7:2:1, molar ratio)], optimised for endosomal escape (Akita et al., 2009; El-Sayed et al., 2008) and further delivery of DNA cargo into mitochondria (Yamada et al., 2012b). Recently, the same group demonstrated mitochondrial delivery of an antisense oligonucleotide bearing 23-nucleotide D-arm of *Leishmania tropica* tRNA^{Tyr} encapsulated in Mito-porter system (Furukawa et al., 2015).

2.2.2. Mechanisms of the natural import of proteins and RNA

Mitochondrial targeting sequence (MTS), the N-terminal peptide involved in the protein import pathway, can be used for addressing various macromolecules through TOM and TIM translocation complexes. Thus, transfection of isolated yeast mitochondria by DNA conjugated with MTS had been demonstrated (Vestweber and Schatz, 1989). This approach has also been implemented to isolated rat mitochondria (Seibel et al., 1995). *In vivo* experiments demonstrated accumulation of PNA oligonucleotide conjugated with MTS in mitochondria after cell delivery of conjugate with PEI polyplex (Flierl et al., 2003). Another approach to the transfection of mammalian mitochondria, termed "protofection", is also based on the protein import. This method invokes targeting of mtDNA-binding protein TFAM (mitochondrial transcription factor A) fused with a protein transduction domain and MTS (Iyer et al., 2011; Keeney et al., 2009; Khan and Bennett, 2004). This fusion protein binds mtDNA and transports it through three membranes into mitochondria.

Natural pathway which can be also used for addressing of exogenous nucleic acids to mitochondria is import of small non-coding RNA. RNA trafficking into mitochondria is poorly understood due to the complexity of its mechanism and its variability between species. This pathway has been described in phylogenetic groups as diverse as protozoan, plants, fungi and animals (Entelis et al., 2001; Rubio et al., 2008; Salinas et al., 2008). Several teams studied RNA structural determinants necessary for mitochondrial import and their implications for therapeutic purposes. Studies of tRNA import into mitochondria of *Leishmania tropica* resulted in a model of RNA targeting into mammalian mitochondria by use of the tag sequence comprising the 23-nucleotide D-arm of tRNA^{Tyr} and a protein complex RIC, detected only in this particular protozoan organism (Mahato et al., 2011). Another team proposed to use the 20-nucleotide stem-loop sequence of the RNase P RNA component (H1 RNA) as a signal, that enables longer fusion RNAs to be imported into human mitochondria (Wang et al., 2012). It was demonstrated that 5S rRNA import occurs through interaction with two cytosolic precursors of mitochondrial proteins: preMRP-L18 and rhodanese (Smirnov et al., 2010; Smirnov et al., 2011), which bind α-and γ-domains of 5S RNA whereas β-domain can be deleted or replaced (Smirnov et al., 2008), thus transforming the 5S rRNA in a vector (Comte et al., 2013). Analysis of artificial import of yeast lysine tRNA (tRK1) and its derivatives into mitochondria demonstrated that protein factors binding and subsequent RNA import require formation of an alternative structure, different from a classic L-form tRNA model, characterized by bringing together the 3′-end and TΨC loop and

forming the structure referred to as F-hairpin. RNAs comprising two domains of tRK1 alternative structure, D-arm and F-hairpin, were characterized by a high efficiency of mitochondrial targeting in living human cells (Kolesnikova et al., 2011) (Figure 14). These tRNA derivatives also can therefore also serve as vectors (Comte et al., 2013).
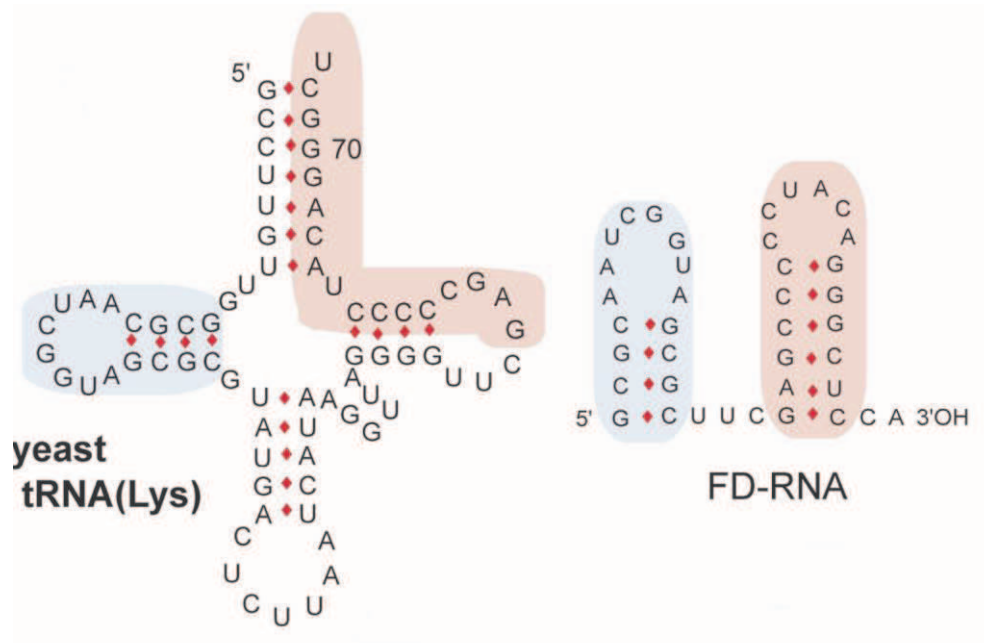
Figure 14. The structures of yeast tRNALys and short synthetic FD-RNA obtained by fusing both determinants of import: D-arm and F-hairpin (Comte et al., 2013).

The main advantage of the use of pathways of protein or RNA mitochondrial targeting is that they are natural mechanisms, rather efficient in living cells and which are not likely to significantly alter the mitochondrial functioning. The approaches developed during my thesis exploit this advantage.

OBJECTIVES

Thesis project and objectives

Defects in mitochondrial genome often cause neuromuscular pathologies, for which no efficient therapy exists. Because most of deleterious mitochondrial mutations are heteroplasmic (functional and mutated mitochondrial DNA (mtDNA) coexist in the same cell), the shift in proportion between two types of molecules could restore mitochondrial functions. The anti-replicative strategy aims to decrease the heteroplasmy level by targeting specifically designed molecules into mitochondria and thereby decreasing the rate of mutant mtDNA replication. Recently, my host research team in Strasbourg University developed mitochondrial RNA vectors that can address anti-replicative oligoribonucleotides into human mitochondria and thus reduce the level of mtDNA bearing a large deletion associated with Kearns Sayre Syndrome.

The efficiency of the anti-replicative molecules depends on their capacity to achieve the following objectives:

(i) translocation of oligonucleotide through the cellular membrane;

(ii) resistance to intracellular nucleases;

(iii) import into mitochondria;

(iv) specific binding to mutant mtDNA.

My PhD project aimed to improve steps (i) and (ii), RNA cell delivery and protection. For this, I developed and optimized the protocols of chemical synthesis which have been introduced by my home laboratory in IBCFM, Novosibirsk.

First, we designed and tested a set of new antireplicative molecules containing various chemically modified nucleotides, aiming to improve their protection from endogenous nucleases. At this step, we used Lipofectamine to transfect small antireplicative RNA into cells, but this reagent is not compatible with potential medicinal applications. Various cell transfection strategies have been developed (see Introduction section), but not all of them possess low toxicity and high efficacy of transfection. The efficiency of antireplicative RNA delivery into cells is a limiting factor which determines their potential therapeutic effect. The conjugation of RNA to the ligand which can be internalized by the cell via natural transport mechanisms is a promising approach to improve cell transfection and to decrease toxicity. Thus, we used the strategy of RNA conjugation with a lipophilic agent, cholesterol, aiming to improve the carrier-free cell delivery of the therapeutic molecules.

Main objectives of my PhD project are:

1. Design and synthesize new antireplicative molecules containing various chemically modified nucleotides, for improved protection against endogenous nucleases. Investigate the modified oligonucleotide's capacity to shift the heteroplasmy level for pathogenic mutations in human mitochondrial DNA, including a point mutation in ND5 gene.

2. Optimize fluorescent labeling of antireplicative molecules and analyze their mitochondrial targeting by laser confocal microscopy.

3. Developt and optimize methods for the chemical synthesis of cholesterol-containing antireplicative RNA attached *via* various cleavable bridges to improve the carrier-free cell delivery of the therapeutic molecules.

The long term objective of these studies is development of a therapeutic strategy leading to a stable and reproducible decrease of the level of heteroplasmy for pathogenic mutations in mtDNA.

RESULTS AND DISCUSSION

3. RESULTS AND DISCUSSION

3.1. Characterization of chemically modified oligonucleotides targeting a pathogenic mutation in human mitochondrial DNA.

Previously, my host laboratory in Strasbourg University developed RNA aptamers based on the structural elements of yeast tRNA(Lys) (D-arm and F-stem loop), characterized by high efficiency of import into yeast and human mitochondria (Kolesnikova et al., 2011). These molecules were successfully applied for targeting of antireplicative oligonucleotides into human mitochondria (Comte et al., 2013). Mitochondrially imported antireplicative RNAs demonstrated ability to specifically reduce the proportion of mtDNA bearing a large deletion associated with the Kearns Sayre Syndrome in cultured *trans*mitochondrial cybrid cells. However, the obtained heteroplasmy shift was transient, disappearing in 7-8 days after transfection of cells with RNA molecules. Rapid restoration of the mutant mitochondrial DNA proportion can be explained by different time periods needed for replication of wild type and mutant DNA molecules, due to their size difference (16.7 and 8.3 kb correspondingly). Therefore, upon a rapid intracellular degradation of antireplicative RNA molecules, the initial heteroplasmy level can be restored. The problem can be solved by use of chemical modifications to increase RNA stability in cells and mitochondria. For this purpose, we introduced various chemically modified oligonucleotides into antireplicative RNA molecules and tested their impact on the efficiency of the hybridisation with mtDNA *in vitro*, RNA stability, mitochondrial targeting and the effect on heteroplasmy in cultured human cybrid cells (**Publication 1**).

My contribution to this study consisted in the chemical synthesis of modified versions of antireplicative RNAs, experimental tests and statistical analysis of their stability in transfected cells. Chemical synthesis of long RNA molecules containing various modified nucleotides has been optimized in ICBFM, Novosibirsk with my participation (**Publication 6**).

We used a small artificial RNA, which was previously shown to be imported into human mitochondria, referred to as D22L (Gowher et al., 2013). This molecule represents the fusion of the D-arm of imported tRNA^{Lys} (tRK1) (Kolesnikova et al., 2011) with a 22-nucleotide sequence corresponding to a fragment of human mtDNA (L-strand) at the boundaries of a large deletion found in patients with Kearns Sayre Syndrome (KSS) (Comte et al., 2013). Since this anti-genomic part of the molecule (referred to as KSS-part) should be the most sensitive to nucleases, we synthesized a set of D22L derivatives containing substitutions at the

2′-hydroxyl group with or without addition of inverted 3′-3′ thymidine nucleotide at the 3′ terminus (see **Fig. 1 in Publ. 1**). All the pyrimidine nucleotides of the KSS-part contained 2′-OMe and 2′-F groups in the versions D22L-Me and D22L-F correspondingly. In the D22L-4Me molecule, only four nucleotides localized in the nuclease-sensitive sites (Volkov et al., 2009) contained the 2′-OMe groups. In D22L-DNA molecules, all the nucleotides of KSS-part were in 2′-deoxy form, thus forming a set of chimerical RNA–DNA molecules. We also synthesized and tested chimerical RNA–DNA molecules containing RNA F-hairpin structure as the mitochondrial import determinant (Kolesnikova et al., 2011) and DNA KSS-part of 13 nucleotides complementary to either H- or L-strand of mtDNA (F13H and F13L correspondingly). Almost all obtained molecules were characterized by extended intracellular half-life time comparing with non-modified molecule (see **Fig. 2 in Publ. 1**).

Contrary to our expectation, only one version (RNA/DNA chimera) could induce a slight shift of heteroplasmy level in transfected cells. All the other modified oligonucleotides did not cause a significant effect on the heteroplasmy level in transfected *trans*mitochondrial cybrid cells bearing a pathogenic mtDNA deletion, proving to be less efficient than non-modified antireplicative RNA molecules (see **Fig. 5 in Publ. 1**).

Nevertheless, we should take into account that the most part of the modified antireplicative RNA molecules tested above contained only one import determinant and the KSS-part corresponding to the L-strand of mtDNA. To broaden the variations of modified molecules, we synthesized two RNA molecules containing both determinants of mitochondrial import (D-arm and F-hairpin) and antireplicative part of 16 nucleotides corresponding to H-strand of mtDNA. We introduced 2′-OMe nucleotides in the major cleavage sites for endonucleases (Volkov et al., 2009) in five positions of the antireplicative part (FD16H-5Me) and in the loop regions (FD16H-10Me) (Figure 15 A**,** data not published). After cell transfection, these molecules showed the same intracellular stability as completely methylated version D22L-Me (Figure 15 B). Moreover, for FD16H-10Me molecule, in contrast to all the other methylated versions, we demonstrated a decrease of heteroplasmy level of KSS deletion (Figure 15 C). These data indicate that: 1) there is no direct correlation between RNA stability and its effect on heteroplasmy level; 2) protection of the import determinants loop regions can improve the antireplicative activity. We hypothesise that only non-modified oligoribonucleotide stretches complementary to the mutated region of mtDNA can significantly influence its replication by stalling the replisome progression. At the same time, nucleotide modifications introduced into loop regions of hairpin domains could have a positive impact on the RNA protection against nucleases and stabilisation of its secondary structure, thus improving anti-replicative activity.

41

In perspective, RNA molecules containing 2′-OMe nucleotides in loop regions, should be synthetised and tested for mitochondrial targeting and capacity to decrease the heteroplasmy level.
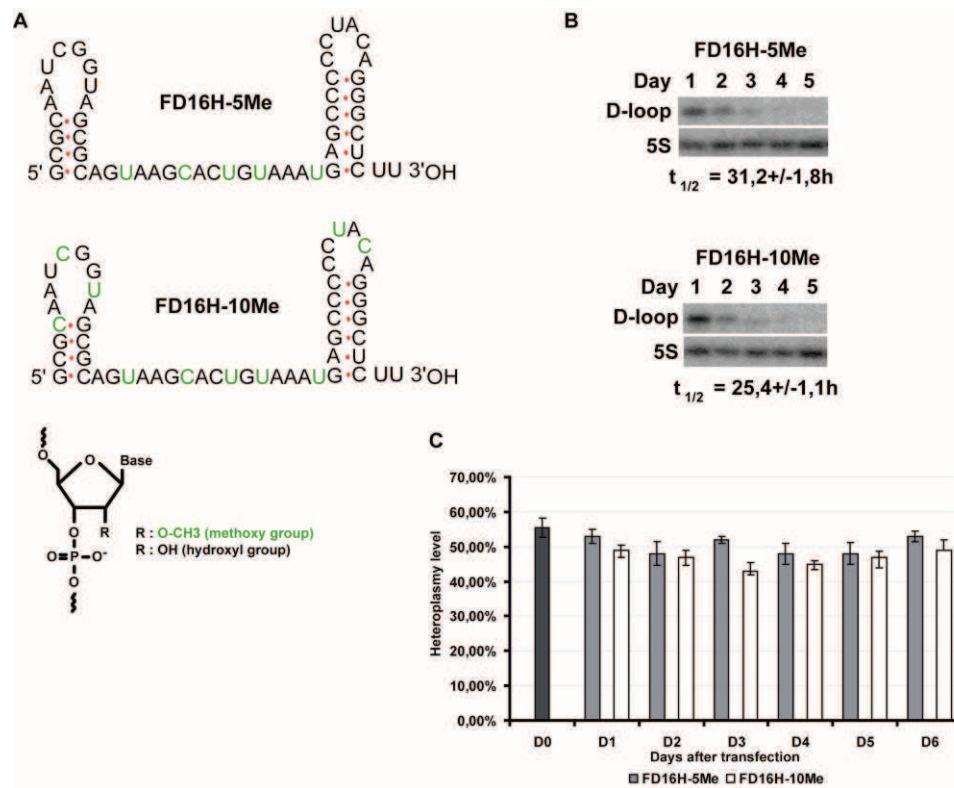
Figure 15. (A) Modified oligonucleotides FD16H-5Me and FD16H-10Me. 2′-OMe nucleotides are shown in green. (B) Stability of synthetic oligonucleotides in transiently transfected cybrid cells. Northern hybridization of total RNA isolated in 1-5 days after cell transfection (as indicated above the lanes) with ^{32}P-labeled probes (indicated at the left): D-loop, specific for oligonucleotide used for transfection; 5S, against 5S rRNA to quantify the level of oligonucleotide in the cells. Below each panel, a half-life time is indicated; ±SD was calculated from n=3 independent experiments. (C) The effect of FD16H-5Me and FD16H-10Me oligonucleotides on heteroplasmy level in transfected cybrid cells. Time dependence of KSS deletion heteroplasmy level followed during 6 days after transfection of cybrid cells with FD16H-5Me and FD16H-10Me.

3.2. Publication 1.

Yann Tonin, Anne-Marie Heckel, Ilya Dovydenko, Mariya Meschaninova, Caroline Comte, Alya Venyaminova, Dmitrii Pyshnyi, Ivan Tarassov, Nina Entelis. Characterization of chemically modified oligonucleotides targeting a pathogenic mutation in human mitochondrial DNA. Biochimie, 2014, 100, 192-199.

Research paper

Characterization of chemically modified oligonucleotides targeting a pathogenic mutation in human mitochondrial DNA

Yann Tonin [a,1], Anne-Marie Heckel [a,1], Ilya Dovydenko [a,b], Mariya Meschaninova [b], Caroline Comte [a], Alya Venyaminova [b], Dmitrii Pyshnyi [b], Ivan Tarassov [a], Nina Entelis [a,*]

[a] Department of Molecular and Cellular Genetics, UMR 7156 Génétique Moléculaire, Génomique, Microbiologie (GMGM), Strasbourg University – CNRS, Strasbourg 67084, France
[b] Laboratory of RNA Chemistry, Institute of Chemical Biology and Fundamental Medicine SB RAS, Novosibirsk, Russia

ARTICLE INFO

ABSTRACT

Defects in mitochondrial genome can cause a wide range of clinical disorders, mainly neuromuscular diseases. Most of the deleterious mitochondrial mutations are heteroplasmic, meaning that wild type and mutated forms of mtDNA coexist in the same cell. Therefore, a shift in the proportion between mutant and wild type molecules could restore mitochondrial functions. The anti-replicative strategy aims to induce such a shift in heteroplasmy by mitochondrial targeting specifically designed molecules in order to inhibit replication of mutant mtDNA. Recently, we developed mitochondrial RNA vectors that can be used to address anti-replicative oligoribonucleotides into human mitochondria and impact heteroplasmy level, however, the effect was mainly transient, probably due to a rapid degradation of RNA molecules. In the present study, we introduced various chemically modified oligonucleotides in anti-replicative RNAs. We show that the most important increase of anti-replicative molecules' lifetime can be achieved by using synthetic RNA–DNA chimerical molecules or by ribose 2′-O-methylation in nuclease-sensitive sites. The presence of inverted thymidine at 3′ terminus and modifications of 2′-OH ribose group did not prevent the mitochondrial uptake of the recombinant molecules. All the modified oligonucleotides were able to anneal specifically with the mutant mtDNA fragment, but not with the wild-type one. Nevertheless, the modified oligonucleotides did not cause a significant effect on the heteroplasmy level in transfected *trans*mitochondrial cybrid cells bearing a pathogenic mtDNA deletion, proving to be less efficient than non-modified RNA molecules.

© 2013 Elsevier Masson SAS. All rights reserved.

1. Introduction

RNA is increasingly used in clinical application [1]. RNA-based therapeutics includes inhibitors of mRNA translation, agents of RNA interference, ribozymes and aptamers binding various molecular targets. However, RNA is relatively unstable *in vivo* due to the plethora of ribonucleases in serum and in cells. Challenges with the delivery, specificity and stability of RNA therapeutics have spawned the development of chemically modified oligonucleotides [2]. Recently, we developed RNA vectors that can be used to address therapeutic oligoribonucleotides into human mitochondria [3].

Mitochondrial disorders represent a heterogeneous group of genetic diseases characterized by an oxidative phosphorylation deficiency, resulting from either nuclear or mitochondrial gene mutations [4,5]. Human mitochondrial genome (mtDNA) is a closed circular double-stranded molecule of 16,5 kb able to replicate autonomously and encoding only 13 polypeptides, 2 ribosomal RNA (12S and 16S) and 22 tRNA, the vast majority of mitochondrial proteins and several RNAs being encoded in the nucleus and imported *via* the cytosol. Various defects in the mitochondrial genome (deletions, duplications, point mutations) can cause a wide range of clinical disorders, mainly neuromuscular diseases. Up to now, no efficient therapeutic treatment has been developed against these pathologies. Since most of the deleterious mitochondrial mutations are heteroplasmic, meaning that wild type and mutated forms of mtDNA coexist in the same cell, the shift in proportion between mutant and wild type molecules is expected to restore mitochondrial functions [6].

We demonstrated that replication of mitochondrial DNA containing a pathogenic mutation can be specifically affected by RNA

molecules bearing oligonucleotide stretches complementary to the mutated region. These molecules can be targeted into human mitochondria using artificially engineered RNA based on the 5S rRNA or tRNA as vectors [3]. We have previously developed several successful models based on the mitochondrial import determinants of the yeast tRNA$^{Lys}_{CUU}$ (further referred to as tRK1). Analysis of conformational rearrangements in this RNA demonstrated that protein factors binding and subsequent RNA import require formation of an alternative structure, different from a classic L-form tRNA model, characterized by bringing together the 3′-end and TΨC loop and forming the structure referred to as F-hairpin. Exploiting these data, we designed a set of short synthetic RNAs comprising two domains of tRK1 alternative structure, D-arm and F-hairpin, characterized by a high efficiency of mitochondrial targeting [7]. These molecules, fused to oligonucleotide stretches complementary to the mtDNA mutated region, were able to shift a heteroplasmy level in cells containing a large deletion in mtDNA. However, the effect was not permanent, disappearing in 7—8 days after transient transfection, probably due to a rapid degradation of RNA molecules [3].

In the present study, we attempted to increase the stability of the "anti-replicative" RNA molecules in human cells. For this purpose, we introduced into these molecules various chemically modified oligonucleotides and tested their impact on the efficiency of their hybridization with mtDNA *in vitro*, RNA stability, mitochondrial targeting and the effect on heteroplasmy in human cybrid cells in culture.

2. Materials and methods

2.1. Transmitochondrial cybrid cell line, transient transfection with RNA

Cultured skin fibroblasts derived from a patient diagnosed with a Kearns Sayre Shy syndrome were fused to a human rho0 osteosarcoma cell line (143B) as described [3]. Cybrid cells used in this study contained 65 ± 2% mutant mtDNA bearing a large deletion spanned from nucleotide 8363 to 15,438 thus removing 7075 base pairs including 9 structural genes and 6 tRNA genes.

Transient transfection with synthetic RNAs was performed as described in Refs. [8,9], with minor modification: for 2 cm^2 wells of 80%-confluent cells we used 0.25 μg of RNA. Transfections were performed with Lipofectamin-2000 in OptiMEM medium (Invitrogen), as described in the supplier's protocol. OptiMEM was changed to a standard DMEM medium the following day after the transfection. Transfection procedure did not lead to any detectable decrease of viability of the cells or to significant change of the overall mtDNA amount (measured by qPCR as described in Ref. [3]), suggesting the absence of synthetic RNAs toxicity.

2.2. Mitochondria isolation, assays for RNA stability and mitochondrial import

Mitochondria from cultured cybrid human cells were isolated as described in Ref. [10] by several rounds of high (20,000 g) and low (4000 g) centrifugations. After the second round of high-speed centrifugation of mitochondria, they were re-suspended in the breakage buffer (0.44 M mannitol, 20 mM Tris—HCl (pH 7.0), 20 mM NaCl, 1 mM EDTA) and centrifuged through two layers of sucrose (0.5 M and 1.5 M). Mitochondria were collected on the top of the 1.5 M layer and harvested by high-speed centrifugation. Mitochondria were treated with RNase A and digitonin to get rid of non-specifically attached RNA. Total and mitochondrial RNA were isolated with TRIzol reagent (Invitrogen).

Stability and mitochondrial import of synthetic RNA molecules were analysed by Northern hybridization of total and mitochondrial RNA with ^{32}P-labelled oligonucleotide probes against synthetic RNAs or against control cytosolic and mitochondrial RNA. The following probes were used: D-loop (5′-GAGTCA-TACGCGCTACCGATTGCGCCAACAAGGC-3′); 5.8S (5′-GGCCGCAAGT GCGTTCGAAG-3′); 5S (5′-CATCCAAGTACTACCAGGCCC-3′); tRNA^{Thr} (5′-TCTCCGGTTTACAAGAC-3′); KSS part (5′-GCTAAGTAAGCACTGT A-3′). To compare the stability of different recombinant RNA, relative concentration (R_0, …, R_t) of each RNA in various time period (t) after transfection was calculated as a ratio between the specific probe signal and the signal for 5S rRNA probe. The half-life period of RNA was calculated as $t_{1/2} = \ln 2/k$, where the degradation constant k can be estimated according to the formula: $\ln R_t/R_0 = kt$.

Relative amounts of each imported RNA inside mitochondria were estimated after quantification in the Typhoon-Trio scanner as a ratio between the signal obtained after hybridization with a specific probe and the signal obtained after hybridization with a probe against the mitochondrial tRNA^{Thr} in the same RNA preparation, as described previously [8].

2.3. Mutant mtDNA heteroplasmy level analysis

Heteroplasmy level was measured by real-time PCR using SYBR Green (iCycler, MyiQ™ Real-Time Detection System, BioRad) as described previously [3]. Two pairs of primers were used: (1) amplifying the 210 bp fragment of 12S rRNA gene region (nucleotides 1095—1305 in mtDNA) not touched by the KSS deletion as a value showing all mtDNA molecules, and (2) amplifying the 164 bp fragment of the deleted region (nucleotides 11,614—11,778) as a value showing wild type mtDNA molecules. All reactions were performed in a 20 μl volume in triplicates. PCR using water instead of template was used as a negative control. PCR was performed by initial denaturation at 95 °C for 10 min, followed by 40 cycles of 30 s at 95 °C, 30 s at 60 °C, and 30 s at 72 °C. Specificity was verified by melting curve analysis and gel electrophoresis.

2.4. Chemical synthesis of modified oligonucleotides

All the oligonucleotides (Fig. 1) were synthesized on an automatic ASM-800 RNA/DNA synthesizer (Biosset, Novosibirsk, Russia) at 0.4 μmol scale using solid phase phosphoramidite synthesis protocols [11] optimized for this instrument. The DNA phosphoramidites, 2′-O-TBDMS-protected RNA phosphoramidites, 2′-OMe-pyrimidine RNA phosphoramidites, 2′-F-pyrimidine RNA phosphoramidites and appropriate supports were purchased from Glen Research (USA). Attachment of 3′-O-DMTr-thymidine [12] to the CPG-500 solid carrier (Sigma—Aldrich) containing carboxylic groups was carried out as in Ref. [13]. A 5-ethylthio-*H*-tetrazole has been used as activator with 5, 10, 6 and 10 min coupling steps respectively for the phosphoramidites mentioned above. After standard deprotection, oligonucleotides were isolated *via* preparative electrophoresis in 12% polyacrylamide/8 M urea gel, followed by elution with 0.3 M NaOAc (pH 5.2)/0.1% SDS solution and precipitated with ethanol. Purified oligonucleotides were characterized by electrophoretic mobility in 12% denaturing polyacrylamide gel and by MALDI-TOF mass spectrometry (Autoflex III, Bruker Daltonics, Germany).

2.5. Synthetic RNA hybridization and thermal denaturation assays

To predict melting temperatures for DNA—DNA and RNA—DNA duplexes, we used IDT Sci-Tools OligoAnalyser 3.1 software [14]. Thermal denaturation experiments were performed on a Cary 300 BioMelt Spectrophotometer equipped with Temperature Probes

D22L

D22L-F

D22L-F-T

5' G ∘ C CUCUUUACAGUGCUUAGUUCUC 3'$_{OH}$

5' G ∘ C CUCUUUACAGUGCUUAGUUCUC 3'$_{OH}$

5' G ∘ C CUCUUUACAGUGCUUAGUUCUC T$_{inv}$ 3'

D22L-Me

D22L-Me-T

D22L-4Me

5' G ∘ C CUCUUUACAGUGCUUAGUUCUC 3'$_{OH}$

5' G ∘ C CUCUUUACAGUGCUUAGUUCUC T$_{inv}$ 3'

5' G ∘ C CUCUUUACAGUGCUUAGUUCUC 3'$_{OH}$

D22L-DNA

D22L-DNA-T

D22L -T

5' G ∘ C CTCTTTACAGTGCTTAGTTCTC 3'$_{OH}$

5' G ∘ C CTCTTTACAGTGCTTAGTTCTC T$_{inv}$ 3'

5' G ∘ C CUCUUUACAGUGCUUAGUUCUC T$_{inv}$ 3'

D13L-DNA

D13H-DNA

F13L-DNA

F13H-DNA

5' G ∘ C TTACAGTGCTTAC 3'$_{OH}$

5' G ∘ C AGTAAGCACTGTA 3'$_{OH}$

TTACAGTGCTTAC G ∘ C UU 3'$_{OH}$

GTAAGCACTGTAA G ∘ C UU 3'$_{OH}$

Legend:
- RNA import déterminant
- A T C G Nucleotides with methyl group
- A T C G Nucleotides with fluor group
- A T C G DNA
- T$_{inv}$ Inverted thymidine

R : - H
R : - O - CH$_3$
R : - F
R : - H

Base

Thymidine

Fig. 1. Structures and nucleotide modifications of synthetic oligonucleotides used in the study.

Accessory Series II (Varian Inc., Australia) in a buffer containing 10 mM sodium cacodylate, pH 7.4, 150 mM NaCl and 2 mM MgCl$_2$. The oligonucleotides (2.0 μM each strand) were mixed, denatured by heating and subsequently cooled to the starting temperature of the experiment. The rate of temperature change was 0.5 °C/min. Duplex melting temperatures (T_m) were calculated using the thermodynamic parameters ΔH and ΔS that have been obtained by fitting procedure of UV−melting curves registered at two different wavelengths (260 and 270 nm) [15] according to the two-state model [16]. The parameter determination error did not exceed 5−10%. Specific hybridization with target mtDNA was tested using Southern-blot hybridization of wild type (nucleotides 15,251−

15,680 of mtDNA) and KSS (nucleotides 8099−8365/15,438−15,680 of mutant mtDNA) fragments with ^{32}P-labelled synthetic RNAs in 1xPBS at 37 °C as described previously [3].

3. Results

3.1. Stability of modified oligonucleotides in human cells

Chemical substitutions at the 2′-hydroxyl group with 2′-OMe, 2′-F and 2′-deoxy in combination with terminus capping chemistry often improve the stability of therapeutic oligonucleotides [17]. To test this methodology, we used a small artificial RNA D22L (Fig. 1),

which was previously shown to be imported into human mitochondria [18]. This molecule represents the fusion of the D-arm of imported tRNA^Lys (tRK1) [7] with a 22-nucleotide sequence corresponding to a fragment of human mtDNA at the boundaries of a large deletion found in patients with Kearns Sayre Syndrome (KSS) [3]. Since this anti-genomic part of the molecule (referred to as KSS-part) should be the most sensitive to nucleases, we synthesized a set of D22L derivatives containing substitutions at the 2'-hydroxyl group with or without addition of inverted 3'-3' thymidine nucleotide at the 3' terminus (Fig. 1). All the pyrimidine nucleotides of the KSS-part contained 2'-OMe and 2'-F groups in the versions D22L-Me and D22L-F correspondingly. In the D22L-4Me molecule, only four nucleotides localized in the nuclease-sensitive sites [17] contained the 2'-OMe groups. In D22L-DNA molecules, all the nucleotides of KSS-part were in 2'-deoxy form, thus forming a set of chimerical RNA–DNA molecules. We also synthesized and tested chimerical RNA–DNA molecules containing RNA F-hairpin structure as the mitochondrial import determinant [7] and DNA KSS-part of 13 nucleotides complementary to either H- or L-strand of mtDNA (F13H and F13L correspondingly).

All versions were tested for their stability in human cells. For this, cultured cybrid cells were transfected with synthetic oligonucleotides (referred to as SO). The transfection procedure did not lead to detectable decrease of viability of the cells, suggesting the absence of SO toxicity. The amounts of SO internalized by cells and their degradation rate was evaluated by Northern hybridization of total cellular RNA with specific probes at different time points spanning a 6-day period after transfection (Fig. 2). The non-modified RNA molecule D22L demonstrated a rather low stability in cells, characterized by a half-life period of 17.7 +/− 0.8 h. On the other hand, protection of its 3'-terminus by inverted 3'-3' thymidine resulted in an increase of stability to 36.0 +/− 1.5 h. Surprisingly, 2'-modifications of all the pyrimidine nucleotides in D22L-Me and D22L-F molecules did not lead to further increase of their stability comparing to D22L, while 2'-O-methylation in only four positions, representing the U-A, C-A and U-G sites, previously identified as major cleavage sites for serum endoribonucleases [19], resulted in a strongly increased lifetime of the D22L-4Me molecule. A strong effect on SO stability was also detected for molecules

containing a DNA KSS-part. For these chimerical SO, increased stability was detected if 3' terminus had been protected by RNA hairpin structure in F13L-DNA or by inverted 3'-3' thymidine in D22L-DNA-T (Figs. 1 and 2).

The above data indicate that an increase of anti-replicative molecules lifetime in transfected cells can be achieved either by the use of RNA–DNA chimerical versions and RNA molecules bearing 2'-OMe groups in nuclease-sensitive sites.

3.2. Mitochondrial import of SO and mtDNA heteroplasmy analysis

To determine the impact of modified nucleotides on the mitochondrial import of SOs, we compared the amounts of D22, D22-Me, D22-Me-T, D22-DNA and D22-DNA-T in purified RNase-treated mitochondria 2 days after transfection (Fig. 3). Hybridization data using SO-specific probes were quantified and normalized to the amounts of loaded mtRNA, estimated by hybridization with a probe to a mitochondrial transcript (mt tRNA^Thr). The results demonstrate that chemical modifications do not inhibit the mitochondrial import of the molecules. Moreover, for the versions contained 2'-OMe groups, we detected an increased efficiency of import in comparison with the non-modified RNA D22L. Amounts of chimerical molecules inside mitochondria were comparable to those of non-modified RNA D22L. Therefore, the presence of inverted thymidine at 3' terminus and modifications of ribose in KSS-part of SO had no negative effect on the mitochondrial uptake of these molecules, probably indicating on a correct interaction of the modified SO with protein import factors and mitochondrial membrane receptors and channels.

To induce a shift of the mutant mtDNA proportion, the therapeutic anti-replicative molecules should anneal in a very specific manner to mutant mitochondrial genomes, but not to wild-type ones. Predicted and experimentally measured melting temperature values for the hybrids between the SO and mutant KSS mtDNA show the increased stability of the duplex for chimerical and 2'-O-modified oligonucleotides comparing to D22 (Table 1). To assay the specificity of modified SO annealing to mtDNA, we performed Southern blot-hybridization of labelled SO with fragments of mutant and wild-type mtDNA at 37 °C in buffer containing
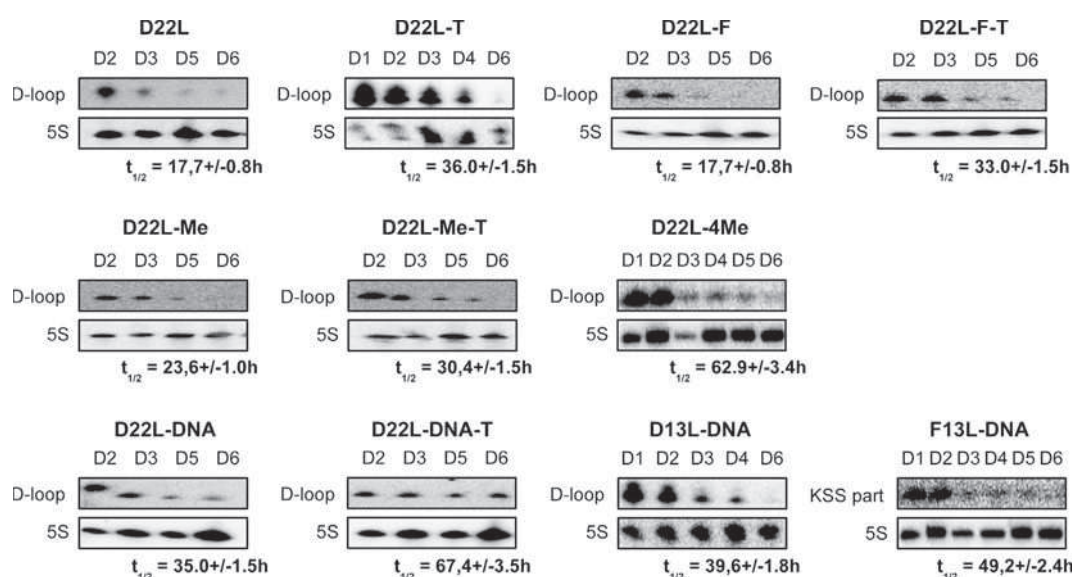
Fig. 2. Stability of synthetic oligonucleotides in transiently transfected cybrid cells. Northern hybridization of total RNA isolated in 2–6 days after cell transfection ("D2-6", as indicated above the lanes) with various SO-specific ^32P-labelled probes (the SO is indicated above each panel, the probe − at the left). Probes used for hybridization: D-loop or KSS-part, specific for SO used for transfection; 5S, against 5S rRNA to quantify the level of SO in the cells. Below each panel, a half-life time for corresponding SO is indicated; ±SD was calculated from $n = 3$ independent experiments.
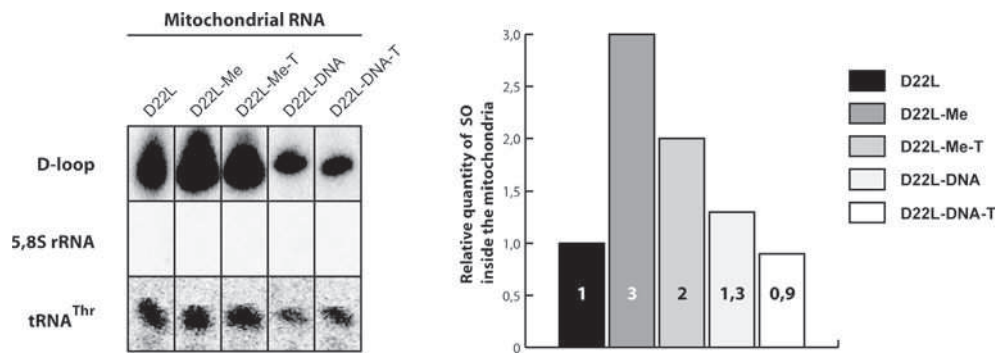
Fig. 3. Mitochondrial import of synthetic oligonucleotides in transiently transfected cybrid cells. On the left panel, an example of Northern hybridization of RNA extracted from purified mitochondria 48 h after transfection. Above the autoradiographs, SO used for transfection are indicated. On the left, hybridization probes: D-loop, specific for SO used for the transfection; 5.8S, against 5.8S rRNA to check the absence of cytosolic contamination in mitochondrial samples; tRNA[Thr], against mitochondrial tRNA to normalize the level of recombinant RNA to amount of loaded material. On the right panel, the diagram shows relative efficiencies of mitochondrial import. Import efficiency of D22L RNA was taken as 1. In all series ±SD = 0.1, resulting from $n = 3$ independent experiments.

physiological concentrations of NaCl (150 mM) (Fig. 4). The results clearly demonstrate that all the SO analysed could hybridize only with mtDNA fragment containing the deletion boundaries, but not with the wild-type mtDNA fragment.

Modified SOs are thus capable to be targeted into human mitochondria in living cells and to anneal with the mutant form of mtDNA, so we anticipated to detect their effect on the KSS deletion heteroplasmy level. We therefore measured the percentage of mutant KSS mtDNA to all mtDNA molecules by real-time qPCR in cybrid cells transfected with various SO at different time points spanning a 6–8 day period after transfection (Fig. 5). Contrary to our expectations, only non-modified RNA D22H induced a reproducible decrease of hetroplasmy level by 20 +/− 2% with a 5–6 day delay in respect to the cell transfection. The effect had a temporal character, since the proportion of mutant mtDNA re-increased within 7–8 days after transfection, as it was previously shown for molecules containing two import determinants [3]. Among all the modified SO tested, only chimerical molecule D22-DNA induced a 15% shift of the heteroplasmy in 4 days after cell transfection. The other versions did not cause any significant effect on the heteroplasmy level. Therefore, the modifications of 2′-OH ribose group, as well as inverted thymidine residue added to 3′ terminus, had a negative effect on the anti-replicative abilities of the SO, most probably due to the inability of the modified molecules to form correct and stable complex with mutant mtDNA *in vivo*.

4. Discussion

4.1. Stability of the modified oligonucleotides in human cells

Serum and cell homogenates are known to contain ribonucleases that belong to the RNase A-, 3′-exonuclease-, and phosphatase families, which cleave RNA more readily at sites within single strand regions and loops [19]. Modifications at the 2′ position of the sugar ring, including 2′-OMe and 2′-F, confer to the oligonucleotide the capacity to adopt an RNA-like C3′-endo (N-type) sugar pucker, which is the most energetically advantageous conformation of RNA. Thus, such modifications increase Watson–Crick binding affinity and, due to the proximity of the 2′-substituent and the 3′-phosphate, improve nuclease resistance [20]. In full agreement with the expectation, the degradation rate of chimeric RNA–DNA molecules in human cells was much lower than that of non-modified RNA D22L. Protection of the 3′ terminus by 3′-3′ inverted thymidine was also very efficient for all the versions, indicating that 3′-exonucleolitic degradation has a very important impact on the SO decay in cells.

Surprisingly, we detected only a very slight increase in stability for the molecule D22-Me, in which all the pyrimidine residues bore 2′-OMe groups, and no effect of 2′-F groups in D22-F version. At the same time, methylation of four predicted nuclease-sensitive sites resulted in a very important increase of a half-life time of the D22-4Me molecule. To explain these data, one can hypothesize that

Table 1
Predicted and measured melting temperatures for hybrids between synthetic oligonucleotides (SO) and mutant (KSS) or wild-type (WT) mtDNA regions (SD = 2.7°).

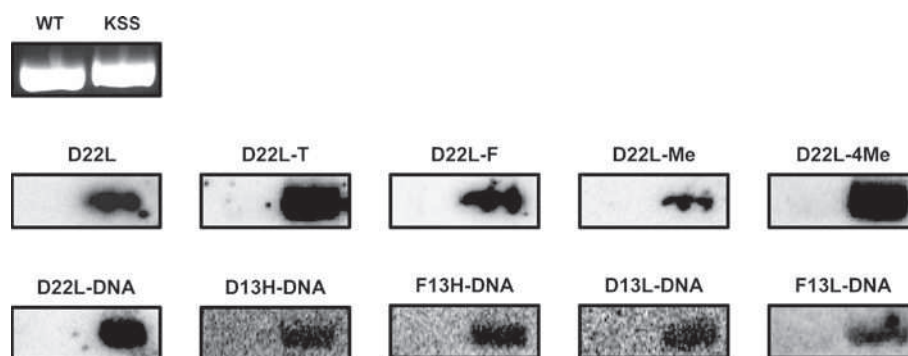| SO	Homology with KSS mtDNA (b)	Measured T_m for KSS mtDNA (°C)	Predicted T_m for KSS mtDNA (°C)	Homology with WT mtDNA (5′ deletion boundary) (b)	T_m for 5′ boundary deletion (°C)	Homology with WT mtDNA (3′ deletion boundary) (b)	T_m for 3′ boundary deletion (°C)
D22L	22	50	52.1	12	34,4	11	33.5
D22L-Me	22	56	52.1	12	34,4	11	33.5
D22L-4Me	22	ND	52.1	12	34,4	11	33.5
D22L-Me-T	22	56.5	ND	12	ND	11	ND
D22L-F	22	62	ND	12	ND	11	ND
D22L-F-T	22	62.5	ND	12	ND	11	ND
D22L-DNA	22	61.5	62.8	12	45.3	11	43.5
D22L-DNA-T	22	61.5	ND	12	ND	11	ND
D13H-DNA	13	ND	50.8	7	21.2	7	20.2
D13L-DNA	13	ND	49.6	8	26.9	6	12.4
F13H-DNA	13	ND	49.6	6	12.4	8	26.9
F13L-DNA	13	ND	49.6	8	26.9	6	12.4

Fig. 4. Ability of synthetic oligonucleotides to discriminate wild type and mutant mtDNA. Southern hybridization of wild-type (WT) or mutant (KSS) mtDNA fragments with labelled SO (indicated above each panel) under physiological conditions. The Ethidium Bromide stained gel is presented in the upper panel.

modification of 16 pyrimidine nucleotides of 22-nucleotide anti-mtDNA part of the molecule might induce substantial changes in the geometry of RNA molecule, the instability of the D-helix and, therefore, the vulnerability of the 5′- part of the molecule. Noteworthy, modification of only 4 nucleotides did not disturb the structure of the D-arm, thus improving the stability of the whole molecule.

4.2. Mitochondrial import of modified oligonucleotides

To target SO molecules into mitochondria, we used the native RNA mitochondrial import, a pathway that appears to be the unique natural mechanism of nucleic acids targeting into these organelles. While protein mitochondrial import mechanisms are well studied, RNA trafficking into mitochondria is not totally understood due to the complexity of its mechanism and the variability between species. This pathway has been detected in phylogenetic groups as diverse as protozoan, plants, fungi and animals [21–23]. Several teams studied RNA structural determinants necessary for mitochondrial import and their implications for therapeutic purposes. Studies of tRNA import into mitochondria of *Leishmania tropica* resulted in a model of RNA targeting into mammalian mitochondria by use of the tag sequence comprising the 23-nucleotide D-arm of tRNA^{Tyr} and a protein complex RIC, detected only in this particular protozoan organism [24]. Another team proposed to use the 20-nucleotide stem-loop sequence of the RNase P RNA component (H1 RNA) as a signal, that enables longer fusion RNAs to be imported into human mitochondria [25].

We have developed several successful therapeutic cellular models based on import determinants of a yeast tRNA, tRK1 [26,27]. Recently, we demonstrated that anti-replicative ribonucleotides flanked by only one stem-loop structures, D or F, can be efficiently imported into human mitochondria *in vitro* and *in vivo* [18]. In the present study, we show that not only RNA, but also DNA oligonucleotides as well as sequences contained modified nucleotides can be efficiently imported into mitochondria of living human cells if flanked by an RNA stem-loop structure. We can hypothesize that such small hairpin RNA domains might be recognized by mitochondrial membrane proteins allowing subsequent translocation of RNA molecules into the organelles. Mammalian polynucleotide phosphorylase (PNPase), enzyme at least partially localized in the mitochondrial intermembrane space [28,29], may function as such an RNA receptor to recognize these import signals and to allow the translocation of correctly tagged "importable" RNA molecules.

4.3. The low anti-replicative capacity of modified oligonucleotides

Our data show that all of the ribose modifications used in the study, as well as inverted thymidine residue added to 3′ terminus,

led to a loss of the anti-replicative activity of the oligonucleotides. This may be explained in several ways. First, the increased stability of RNA–mtDNA duplex might have a negative effect. To check this possibility, we synthesized a set of RNA–DNA chimerical molecules with a shorter, 13-nucleotide KSS-part (D13 and F13 versions, Fig. 1). The choice of the length was driven by melting temperature prediction (Table 1), aiming to adjust the T_m of the chimerical molecules to those of non-modified RNA D22L. Contrary to D22L and D22L-DNA, the chimerical molecules of D13 and F13 series had no effect on the heteroplasmy level, indicating that there is no direct correlation between the melting temperature of the duplex of SO with mutant mtDNA and the anti-replicative effect of SO.

The second possible explanation consists in non-specific annealing of SO not only to mutant mitochondrial genomes, but also to wild-type ones. Even if *in vitro* hybridization of all the modified SO with mutant mtDNA fragment was very specific, the situation *in vivo* might be different due to specific ionic conditions in the mitochondrial matrix and the implication of proteins. So far, the version D22-DNA, characterized by a high T_m of duplex with mutant mtDNA and also by rather high ($>37°$) T_m values for 5′ and 3′ boundaries of KSS deletion (Table 1), was the only one among the modified SO that demonstrated the expected effect on the heteroplasmy level. This indicates that the predicted annealing with wild-type mtDNA does not correlate with the absence of the specific stalling of mutant mtDNA replication.

All these considerations led us to a conclusion that the most important feature could be the nature of the anti-replicative nucleic acid. Apparently, only oligoribonucleotide stretches complementary to the mutated region of mtDNA can significantly influence its replication by stalling the replisome progression. Deoxyoligonucleotides are much less efficient, probably due to the ability of the mitochondrial replisome helicase to denature DNA–DNA hybrids, but not the regions of short RNA–DNA duplexes [30]. All the SO versions bearing ribose 2′-OH modifications and inverted thymidine residues revealed the total loss of anti-replicative efficiency. One can hypothesize that the C3′-endo sugar conformation and 3′-3′ inverted nucleotides might be recognized by the replisome or by other mitochondrial nucleoid proteins as non-natural and quickly eliminated. The RITOLS model of mtDNA replication suggests the presence of displaced H-strand not in the single-stranded form, but essentially in the form of RNA–DNA hybrid [31]. Therefore, short RNA–DNA duplexes will not be eliminated by mitochondrial proteins and could cause a stall of the mutant mtDNA replication, leading to a shift in proportion between mutant and wild-type mitochondrial genomes.

The data presented here show that various nucleotide modifications protect RNA molecules introduced into human cells against nucleolitic degradation. Modified oligonucleotides fused to import determinants can be imported into mitochondria in living cells and
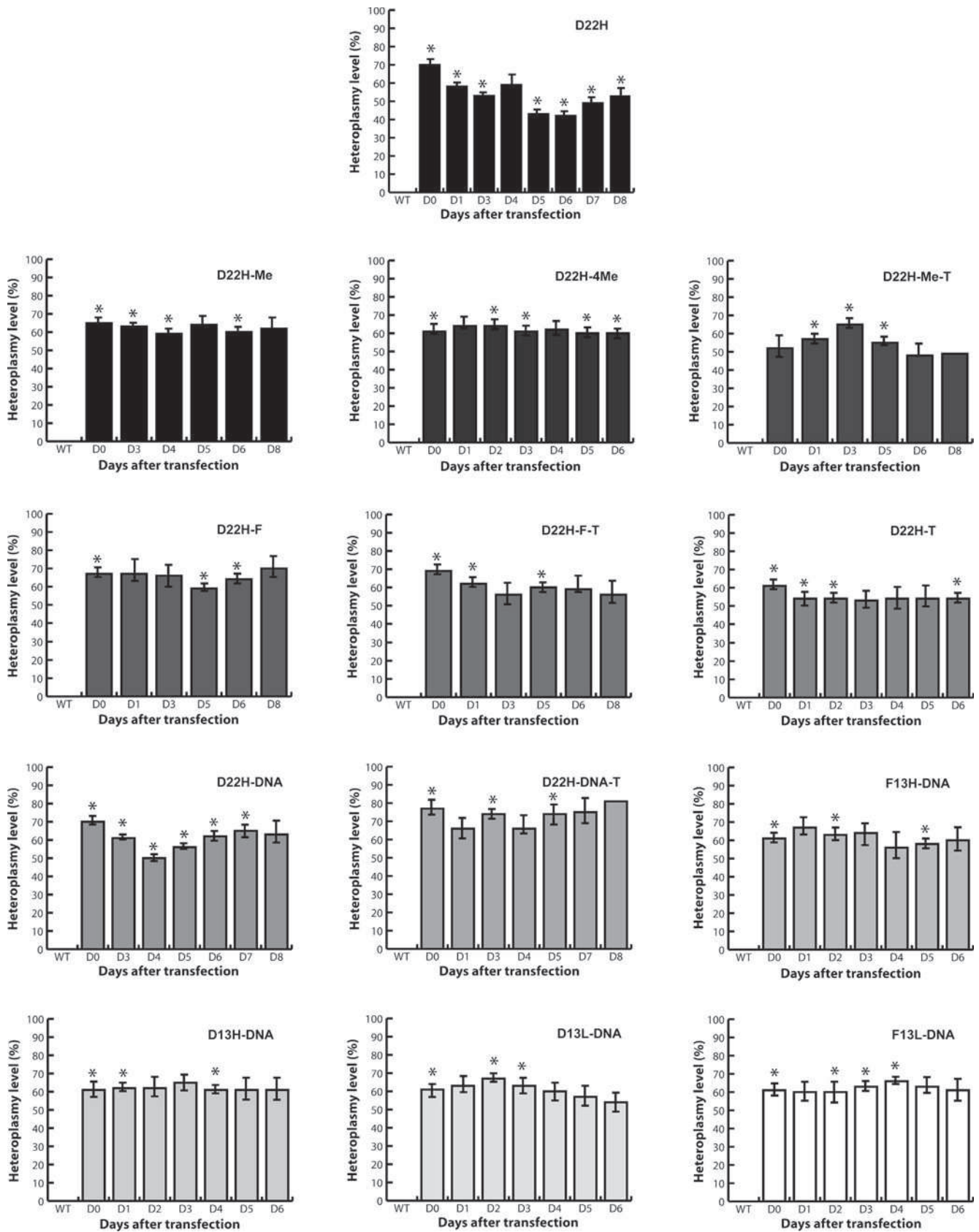
Fig. 5. Effect of synthetic oligonucleotides on heteroplasmy level in transfected cybrid cells. Time dependence of KSS deletion heteroplasmy level followed during 6–8 days after transfection of cybrid cells with various SO, indicated above each graph. ±SD was calculated from at least three independent experiments; *, statistically significant data.

can specifically anneal with mutant mtDNA. However, despite their increased stability, such modified oligonucleotides are not likely to be used as anti-replicative therapeutic agents. Thus, the problem of the transient effect of short RNA molecules on the heteroplasmy level [3] should be resolved by other means. For instance, a stable expression of specific RNA molecules in the nucleus, or the use of a non-toxic transfection procedure, allowing several consecutive transfections of human cells with therapeutic RNA, may prove promising for the future progress of RNA-based approaches of the therapy of mitochondrial diseases.

Acknowledgements

References

[1] J.C. Burnett, J.J. Rossi, RNA-based therapeutics: current progress and future prospects, Chem. Biol. 19 (2012) 60–71.
[2] D. Peer, J. Lieberman, Special delivery: targeted therapy with small RNAs, Gene Ther. 18 (2011) 1127–1133.
[3] C. Comte, Y. Tonin, A.M. Heckel-Mager, A. Boucheham, A. Smirnov, K. Aure, A. Lombes, R.P. Martin, N. Entelis, I. Tarassov, Mitochondrial targeting of recombinant RNAs modulates the level of a heteroplasmic mutation in human mitochondrial DNA associated with Kearns Sayre syndrome, Nucleic Acids Res. 41 (2013) 418–433.
[4] R.N. Lightowlers, P.F. Chinnery, D.M. Turnbull, N. Howell, Mammalian mitochondrial genetics: heredity, heteroplasmy and disease, Trends Genet. 13 (1997) 450–455.
[5] A. Rotig, Genetic bases of mitochondrial respiratory chain disorders, Diabetes Metab. 36 (2010) 97–107.
[6] D.C. Wallace, Mitochondrial DNA mutations in disease and aging, Environ. Mol. Mutagen. 51 (2010) 440–450.
[7] O. Kolesnikova, H. Kazakova, C. Comte, S. Steinberg, P. Kamenski, R.P. Martin, I. Tarassov, N. Entelis, Selection of RNA aptamers imported into yeast and human mitochondria, RNA 16 (2010) 926–941.
[8] A. Smirnov, I. Tarassov, A.M. Mager-Heckel, M. Letzelter, R.P. Martin, I.A. Krasheninnikov, N. Entelis, Two distinct structural elements of 5S rRNA are needed for its import into human mitochondria, RNA 14 (2008) 749–759.
[9] C. Kohrer, L. Xie, S. Kellerer, U. Varshney, U.L. RajBhandary, Import of amber and ochre suppressor tRNAs into mammalian cells: a general approach to site-specific insertion of amino acid analogues into proteins, Proc. Natl. Acad. Sci. U. S. A. 98 (2001) 14310–14315.
[10] A.M. Mager-Heckel, N. Entelis, I. Brandina, P. Kamenski, I.A. Krasheninnikov, R.P. Martin, I. Tarassov, The analysis of tRNA import into mammalian mitochondria, Methods Mol. Biol. 372 (2007) 235–253.
[11] L. Bellon, Oligoribonucleotides with 2'-O-(tert-butyldimethylsilyl) groups, Curr. Protoc. Nucleic Acid Chem. (2001) (Chapter 3), Unit 3 6.
[12] J.F. Ortigao, H. Rosch, H. Selter, A. Frohlich, A. Lorenz, M. Montenarh, H. Seliger, Antisense effect of oligodeoxynucleotides with inverted terminal internucleotidic linkages: a minimal modification protecting against nucleolytic degradation, Antisense Res. Dev. 2 (1992) 129–146.
[13] V.A. Efimov, S.V. Reverdatto, O.G. Chahmahcheva, Use of N-methylimidazolide phosphotriester method for the synthesis of oligonucleotides useful in recombinant DNA studies, Bioorg. Khim. 9 (1983) 1367–1381.
[14] N. Sugimoto, S. Nakano, M. Katoh, A. Matsumura, H. Nakamuta, T. Ohmichi, M. Yoneyama, M. Sasaki, Thermodynamic parameters to predict stability of RNA/DNA hybrid duplexes, Biochemistry 34 (1995) 11211–11216.
[15] D.V. Pyshnyi, A.A. Lomzov, I.A. Pyshnaya, E.M. Ivanova, Hybridization of the bridged oligonucleotides with DNA: thermodynamic and kinetic studies, J. Biomol. Struct. Dyn. 23 (2006) 567–580.
[16] M. Petersheim, D.H. Turner, Base-stacking and base-pairing contributions to helix stability: thermodynamics of double-helix formation with CCGG, CCGGp, CCGGAp, ACCGGp, CCGGUp, and ACCGGUp, Biochemistry 22 (1983) 256–263.
[17] A.A. Volkov, N.S. Kruglova, M.I. Meschaninova, A.G. Venyaminova, M.A. Zenkova, V.V. Vlassov, E.L. Chernolovskaya, Selective protection of nuclease-sensitive sites in siRNA prolongs silencing effect, Oligonucleotides 19 (2009) 191–202.
[18] A. Gowher, A. Smirnov, I. Tarassov, N. Entelis, Induced tRNA import into human mitochondria: implication of a host aminoacyl-tRNA-synthetase, PLoS One 8 (2013) e66228.
[19] D. Findlay, D.G. Herries, A.P. Mathias, B.R. Rabin, C.A. Ross, The active site and mechanism of action of bovine pancreatic ribonuclease, Nature 190 (1961) 781–784.
[20] C.F. Bennett, E.E. Swayze, RNA targeting therapeutics: molecular mechanisms of antisense oligonucleotides as a therapeutic platform, Annu. Rev. Pharmacol. Toxicol. 50 (2010) 259–293.
[21] N.S. Entelis, O.A. Kolesnikova, R.P. Martin, I.A. Tarassov, RNA delivery into mitochondria, Adv. Drug Deliv. Rev. 49 (2001) 199–215.
[22] M.A. Rubio, J.J. Rinehart, B. Krett, S. Duvezin-Caubet, A.S. Reichert, D. Soll, J.D. Alfonzo, Mammalian mitochondria have the innate ability to import tRNAs by a mechanism distinct from protein import, Proc. Natl. Acad. Sci. U. S. A. 105 (2008) 9186–9191.
[23] T. Salinas, A.M. Duchene, L. Marechal-Drouard, Recent advances in tRNA mitochondrial import, Trends Biochem. Sci. 33 (2008) 320–329.
[24] B. Mahato, S. Jash, S. Adhya, RNA-mediated restoration of mitochondrial function in cells harboring a Kearns Sayre syndrome mutation, Mitochondrion 11 (2011) 564–574.
[25] G. Wang, E. Shimada, J. Zhang, J.S. Hong, G.M. Smith, M.A. Teitell, C.M. Koehler, Correcting human mitochondrial mutations with targeted RNA import, Proc. Natl. Acad. Sci. U. S. A. 109 (2012) 4840–4845.
[26] N.S. Entelis, S. Kieffer, O.A. Kolesnikova, R.P. Martin, I.A. Tarassov, Structural requirements of tRNALys for its import into yeast mitochondria, Proc. Natl. Acad. Sci. U. S. A. 95 (1998) 2838–2843.
[27] O.Z. Karicheva, O.A. Kolesnikova, T. Schirtz, M.Y. Vysokikh, A.M. Mager-Heckel, A. Lombes, A. Boucheham, I.A. Krasheninnikov, R.P. Martin, N. Entelis, I. Tarassov, Correction of the consequences of mitochondrial 3243A>G mutation in the MT-TL1 gene causing the MELAS syndrome by tRNA import into mitochondria, Nucleic Acids Res. 39 (2011) 8173–8186.
[28] G. Wang, H.W. Chen, Y. Oktay, J. Zhang, E.L. Allen, G.M. Smith, K.C. Fan, J.S. Hong, S.W. French, J.M. McCaffery, R.N. Lightowlers, H.C. Morse 3rd, C.M. Koehler, M.A. Teitell, PNPASE regulates RNA import into mitochondria, Cell 142 (2010) 456–467.
[29] V. Vedrenne, A. Gowher, P. De Lonlay, P. Nitschke, V. Serre, N. Boddaert, C. Altuzarra, A.M. Mager-Heckel, F. Chretien, N. Entelis, A. Munnich, I. Tarassov, A. Rotig, Mutation in PNPT1, which encodes a polyribonucleotide nucleotidyltransferase, impairs RNA import into mitochondria and causes respiratory-chain deficiency, Am. J. Hum. Genet. 91 (2012) 912–918.
[30] M. Bowmaker, M.Y. Yang, T. Yasukawa, A. Reyes, H.T. Jacobs, J.A. Huberman, I.J. Holt, Mammalian mitochondrial DNA replicates bidirectionally from an initiation zone, J. Biol. Chem. 278 (2003) 50961–50969.
[31] T. Yasukawa, A. Reyes, T.J. Cluett, M.Y. Yang, M. Bowmaker, H.T. Jacobs, I.J. Holt, Replication of vertebrate mitochondrial DNA entails transient ribonucleotide incorporation throughout the lagging strand, EMBO J. 25 (2006) 5358–5371.

3.3. Modeling of antigenomic therapy of mitochondrial diseases by mitochondrially addressed RNA targeting a pathogenic point mutation in mitochondrial DNA.

Next part of my work aimed to show that antireplicative strategy is not limited to large rearrangements in mtDNA but can be applied to point mutations. To address this question, we designed oligonucleotides able to anneal to the mtDNA bearing a point mutation but not to the wild type mtDNA and tested their hybridization specificity *in vitro*. A series of chimeric molecules, including RNA-DNA chimera, have been synthesised and tested for mitochondrial import in human cultured cells by Northern blot hybridization and laser scanning confocal microscopy. We also tested ability of antireplicative molecules to induce a shift of the heteroplasmy level in *trans*mitochondrial cybrid cells and patient fibroblasts bearing A13514G mutation inducing amino acid replacement D393G in ND5 gene of human mtDNA, which encodes one of membrane domain subunits of the respiratory complex I. We demonstrated that RNA molecules containing mitochondrial targeting determinants and a 20-nucleotide sequence corresponding to the mutated region of mtDNA are able to selectively target mutated mitochondrial genomes. After being imported into mitochondria of cultured *trans*mitochondrial human cells bearing a pathogenic point mutation in ND5 gene, these RNA significantly decreased the proportion of mutated mtDNA molecules (**Publication 2**).

My contribution in this work consisted in synthesis and analysis of RNA-DNA chimeric molecules, fluorescent labeling of the antireplicative molecules and analysis of their mitochondrial import by laser scanning confocal microscopy.

To obtain a reliable picture of RNA import into human mitochondria in living cells by confocal microscopy, we analysed the characteristics of various fluorescent dyes and tested some of them (Table 2). The data led us to conclude that there are two characteristics that should be taken into account in the mitochondria – related studies: the charge of the fluorescent dye and its possible interaction with lipid bilayers.

Positively charged fluorophores conjugated with RNA can lead to non specific accumulation of oligonucleotide on the mitochondrial surface (Rhee and Bao, 2010), providing false positive results of mitochondrial targeting. The possibility of fluorescent dye interaction with lipid bilayer (Hughes et al., 2014) can lead to a decline or an absence of fluorescently labelled RNA import into mitochondria. Moreover, such fluorophores can prevent the release of RNA from lipoplex formed with Lipofectamine, which was used in the present study as a transfection agent to assure the RNA targeting into human cells. Finally, for the RNA

localization experiments, we have chosen UTP-Alexa-488, which was introduced into RNA by T7 transcription. We demonstrated significant colocalization of fluorescently labeled RNA with mitochondrial network stained by TMRM. Confocal microscopy data were confirmed by Northern blot hybridization of RNA from isolated mitochondria.

Dye	MIF	Charge
Carboxyfluorescein	n<0.1	-2
Alexa 488 SE	n<0.1	-2
ATTO 488 SE	n<0.1	-1
Alexa 532 M	0.1<n<1	-1
Alexa 532 SE	n<0.1	-1
ATTO 532 SE	n<0.1	-1
TMRM	0.1<n<1	+1
Sulfo-Cy3 M	0.1<n<1	-1
Alexa 546 SE	0.1<n<1	-2
ATTO 550 M	n>1	+1
Cy3 SE	n>1	+1
ATTO 565 biotin	0.1<n<1	0
Alexa 568 hydrazide	n<0.1	-2
Alexa 594 M	0.1<n<1	-2
ATTO 647N M	n>1	+1
ATTO 647 SE	0.1<n<1	0
Sulfo-Cy5 M	0.1<n<1	-1
Alexa 647 SE	n<0.1	-3
Alexa 647 M	n<0.1	-3
ATTO 655 SE	0.1<n<1	0

Table 2. Dye charge and membrane interaction factor (MIF) . Dyes with MIF values less than 0.1 indicate low or no membrane association, dyes with MIF>1 can strongly interact with membranes, intermediate MIF values indicate moderate levels of membrane interaction (Hughes et al., 2014).

3.4. Publication 2.

Yann Tonin, Anne-Marie Heckel, Mikhail Vysokikh, Ilya Dovydenko, Mariya Meschaninova, Agnès Rötig, Arnold Munnich, Alya Venyaminova, Ivan Tarassov, Nina Entelis. Modeling of antigenomic therapy of mitochondrial diseases by mitochondrially addressed RNA targeting a pathogenic point mutation in mitochondrial DNA. Journal of Biological Chemistry, 2014, 289, 13323-13334.

Modeling of Antigenomic Therapy of Mitochondrial Diseases by Mitochondrially Addressed RNA Targeting a Pathogenic Point Mutation in Mitochondrial DNA*[S]

Yann Tonin[‡1], Anne-Marie Heckel[‡], Mikhail Vysokikh[‡2], Ilya Dovydenko[‡§], Mariya Meschaninova[§], Agnès Rötig[¶], Arnold Munnich[¶], Alya Venyaminova[§], Ivan Tarassov[‡], and Nina Entelis[‡3]

From the ‡UMR 7156 Génétique Moléculaire, Génomique, Microbiologie (GMGM), Strasbourg University-CNRS, Strasbourg 67084, France, the §Laboratory of RNA Chemistry, Institute of Chemical Biology and Fundamental Medicine SB RAS, Novosibirsk 630090, Russia, and the ¶Université Paris Descartes-Sorbonne Paris Cité, INSERM U781, Hôpital Necker-Enfants Malades, Paris 75015, France

Background: Point mutations in mitochondrial genome cause severe clinical disorders.
Results: We designed recombinant RNA molecules imported into mitochondria of human cells, which are able to decrease the proportion of mitochondrial DNA molecules bearing a pathogenic point mutation.
Conclusion: Imported recombinant RNAs can function as anti-replicative agents in human mitochondria.
Significance: This is a new approach for therapy of mitochondrial diseases.

Defects in mitochondrial genome can cause a wide range of clinical disorders, mainly neuromuscular diseases. Presently, no efficient therapeutic treatment has been developed against this class of pathologies. Because most of deleterious mitochondrial mutations are heteroplasmic, meaning that wild type and mutated forms of mitochondrial DNA (mtDNA) coexist in the same cell, the shift in proportion between mutant and wild type molecules could restore mitochondrial functions. Recently, we developed mitochondrial RNA vectors that can be used to address anti-replicative oligoribonucleotides into human mitochondria and thus impact heteroplasmy level in cells bearing a large deletion in mtDNA. Here, we show that this strategy can be also applied to point mutations in mtDNA. We demonstrate that specifically designed RNA molecules containing structural determinants for mitochondrial import and 20-nucleotide sequence corresponding to the mutated region of mtDNA, are able to anneal selectively to the mutated mitochondrial genomes. After being imported into mitochondria of living human cells in culture, these RNA induced a decrease of the proportion of mtDNA molecules bearing a pathogenic point mutation in the mtDNA ND5 gene.

RNA is increasingly used in therapeutic applications, including the agents of RNA interference, catalytically active RNA molecules, and RNA aptamers that bind proteins and other ligands (reviewed in Ref. 1). Here, we use RNA molecules imported into human mitochondria to suppress negative effects of mutations in mtDNA.[4] Involved in many metabolic pathways varying from cellular respiration to apoptosis, mitochondria are subcellular organelles essential for eukaryotic cells containing their proper genome, mtDNA. Human mtDNA is a closed circular double-stranded molecule of 16.5 kb able to replicate autonomously and encoding only 13 polypeptides, two ribosomal RNA (12 S and 16 S), and 22 tRNA, with the vast majority of mitochondrial proteins and several RNAs being encoded in the nucleus and imported from the cytoplasm. Multiple alterations may occur in the mitochondrial genome (deletions, duplications, and point mutations), resulting in severe impact on cellular respiration and therefore leading to many diseases, essentially muscular and neurodegenerative disorders. To date, >250 pathologic diseases were shown to be caused by defects in mtDNA (2). The majority of these mutations are heteroplasmic, meaning that mtDNA coexists in two forms, wild type and mutated, in the same cell. The occurrence and severity of pathologic effects depend on the heteroplasmy level, clinical symptoms appearing at the threshold of the order of 60 to 80%, depending on the mutation and the type of cells (3).

Various strategies have been proposed to address these pathologies, unfortunately, for the vast majority of cases, no efficient treatment is currently available. In some cases, defects may be rescued by targeting into mitochondria nuclear DNA-expressed counterparts of the affected molecules, an approach called allotopic strategy (4, 5). Allotopic expression of mtDNA-encoded polypeptides has been demonstrated in yeast, but in mammalian mitochondria, results are contradictory (reviewed

in Ref. 6). We have exploited the RNA mitochondrial import pathway, which is the only known natural mechanism of nucleic acid delivery into mitochondria (reviewed in Ref. 7), to develop two successful models of allotopic rescue of an mtDNA mutation by targeting recombinant tRNA into mitochondria (8, 9).

Another strategy that might be termed as "anti-genomic," which consists of addressing into mitochondria endonucleases specifically eliminating mutated mtDNA, was also described (10, 11). Another approach, referred to as anti-replicative, aims to induce a shift in heteroplasmy level by targeting specifically the replication of mutant mtDNA, thus giving a propagative advantage to wild type genomes. This strategy has first been tested *in vitro* using peptide nucleic acids with high affinity to mutant mtDNA (12). It was demonstrated that peptide nucleic acid oligomers complementary to mutant mtDNA can specifically inhibit its replication *in vitro*; however, it remained non-applicable to living cells because of the impossibility of introducing peptide nucleic acid molecules into mitochondria *in vivo* (13). To overcome this obstacle, we proposed to use RNA mitochondrial import.

Analysis of the yeast tRNA$^{Lys}_{CUU}$ mitochondrial import mechanism demonstrated that binding to mitochondrial targeting protein factors and subsequent RNA translocation across mitochondrial membranes require formation of an alternative structure, different from a classic L-form tRNA model, characterized by bringing together the 3′-end and TΨC loop and forming the structure referred to as F-hairpin. Exploiting these data, we designed a short synthetic RNA comprising two domains of the yeast tRNA$^{Lys}_{CUU}$ alternative structure, D-arm and F-hairpin (referred to as FD RNA) (see Fig. 1), characterized by a high efficiency of mitochondrial targeting (14). These molecules, fused to oligonucleotide stretches complementary to the mtDNA-mutated region, were able to shift a heteroplasmy level in cells containing a large deletion in mtDNA, providing the first validation of the anti-replicative approach *in vivo* (15).

Here, we show that this approach is not limited to large rearrangements in mtDNA but can be applied to point mutations. We provide a protocol to design an oligonucleotide able to anneal to mtDNA bearing a point mutation but not to wild type mtDNA and an original assay to test the specificity of hybridization *in vitro*. A series of recombinant molecules, including RNA-DNA chimera, have been tested for mitochondrial import in human cultured cells and their ability to induce a shift of the heteroplasmy level. We demonstrate that RNA molecules containing mitochondrial targeting determinants and a 20-nucleotide sequence corresponding to the mutated region of mtDNA are able to selectively target mutated mitochondrial genomes. After being imported into mitochondria of cultured *trans*-mitochondrial human cells bearing a pathogenic point mutation in *ND5* gene, these RNA significantly decreased the proportion of mutated mtDNA molecules.

EXPERIMENTAL PROCEDURES

Recombinant RNA Modeling and Synthesis—To predict secondary structures of recombinant RNA and estimate their free energy (dG), the Mfold (16), IDT Sci-Tools OligoAnalyser (version 3.1), and ViennaRNA platforms were used. To estimate melting temperatures for DNA-DNA and RNA-DNA duplexes, we used IDT Sci-Tools OligoAnalyser software (version 3.1) (17).

The recombinant RNAs were obtained by T7 transcription using the T7 RiboMAX Express Large Scale RNA Production System (Promega) on the corresponding PCR products and were gel-purified. For PCR, the following oligonucleotides containing a T7 promoter (*underlined*) were used: *FD16L* (5′-<u>TAA TAC GAC TCA CTA TAG</u> CGC AAT CGG TAG CGC ACT CCA AAG GCC ACA TGA GCC CCC TAC AGG GCT C-3′); *FD16H* (5′-<u>TAA TAC GAC TCA CTA TAG</u> CGC AAT CGG TAG CGC ATG TGG CCT TTG GAG TGA GCC CCC TAC AGG GCT C-3′); *FD20L* (5′-<u>TAA TAC GAC TCA CTA TAG</u> CGC AAT CGG TAG CGC ACT CCA AAG GCC ACA TCA TCG AGC CCC CTA CAG GGC TC-3′); *FD20H* (5′-<u>TAA TAC GAC TCA CTA TAG</u> CGC AAT CGG TAG CGC GAT GAT GTG GCC TTT GGA GTG AGC CCC CTA CAG GGC TC-3′); *FD25L* (5′-<u>TAA TAC GAC TCA CTA TAG</u> CGC AAT CGG TAG CGC GTT TCT ACT CCA AAG GCC ACA TCA TGA GCC CCC TAC AGG GCT C-3′); *FD25H* (5′-<u>TAA TAC GAC TCA CTA TAG</u> CGC AAT CGG TAG CGC ATG ATG TGG CCT TTG GAG TAG AAA CGA GCC CCC TAC AGG GCT C-3′) with primers T7 (5′-GGG ATC CAT AAT ACG ACT CAC TAT A-3′) and FD-rev (5′-AAG AGC CCT GTA GGG-3′).

To test recombinant RNA annealing to target mtDNA, fragments of wild type and mutant mtDNA were amplified using primers hmtGluRT (5′-GTT CTT GTA GTT GAA ATA C-3′) and CRC-F (5′-CAT ACC TCT CAC TTC AAC CTC C-3′), separated on 1% agarose gel, blotted to Hybond-N membrane, and hybridized with ^{32}P-labeled recombinant RNAs in 1× PBS at 37 °C. After PhosphorImager quantification (Typhoon Trio, GE Healthcare), the hybridization signals were normalized to amounts of corresponding mtDNA fragments calculated after ethidium bromide staining of the agarose gel (before transfer to Hybond membrane) by densitometry using G-Box and GeneTools analysis software. Thereafter, hybridization specificity was calculated for each RNA as one minus ratio between normalized signals for wild type and mutated DNA fragments. Thus, for recombinant RNA annealed only to mutant DNA fragment, the hybridization specificity value reached 1, and for RNA annealed equally to mutant and wild type fragments, this value was close to 0. At least three independent experiments were performed for each RNA.

Chimeric Oligonucleotide Synthesis—Chimeric oligonucleotides D20L DNA and D20H DNA were synthesized on an automatic ASM-800 RNA/DNA synthesizer (Biosset) at 0.4-μmol scale using solid phase phosphoramidite synthesis protocols (18) optimized for this instrument. The DNA and 2′-*O*-TBDMS (*tert*-butyldimethylsilyl)-protected RNA phosphoramidites and appropriate supports were purchased from Glen Research. A 5-ethylthio-*H*-tetrazole has been used as activator with 5- and 10-min coupling steps, respectively. After standard deprotection, oligonucleotides were purified by 12% polyacrylamide/8 M urea gel and characterized by MALDI-TOF mass spectrometry (Autoflex III, Bruker Daltonics).

Synthesis of Fluorescently Labeled RNA Transcript—Alexa Fluor 488-5 UTP (Molecular Probes) was incorporated into RNA during 2-h T7 transcription by T7 RNA polymerase (Promega). A reaction mixture of 20 μl total volume contained 0.5 μg of DNA template, 80 units of T7-RNA polymerase (two additions of 40 units each), 0.5 mM ATP, 0.5 mM CTP, 0.5 mM GTP, 0.37 mM UTP, 0.125 mM Alexa Fluor 488-5-UTP, 10 mM DTT, and 40 units of RNaseOUT (Invitrogen). T7 transcript was purified by PAGE. To check the incorporation of the label in purified transcript, we compared the dye absorbance at 492 nm with the absorbance at 260 nm using NanoDrop ND1000 Microarray software (version 3.5.2). The efficiency of labeling obtained was approximately two labeled uridines per one RNA molecule.

RNA FD20H, used for the microscopy, contains 13 uridine residues (see Fig. 2): one at the end of F-stem region, three in the loops, and nine in the anti-replicative part of the molecule, which is not responsible for the mitochondrial import efficiency. Therefore, the labeling should not significantly alter the secondary structure and mitochondrial import of the RNA molecule.

Transient Transfection of Cybrid Cells—Trans-mitochondrial cybrid cell lines obtained by fusion of fibroblast-derived cytoplast from patient and a 143B rho⁰ cell line (19) were kindly provided by M. Zeviani (National Neurological Institute "Carlo Besta," Milan, Italy).

Primary skin fibroblasts were from patient 1: a boy born to non-consanguineous healthy parents. He was completely normal until 13 years of age when he developed dystonia of the left hand that worsened progressively. A brain MRI at 14 years of age revealed hypersignal of basal ganglia and abnormalities of brain system consistent with the diagnosis of Leigh syndrome. Two years later, he had tonicoclonic seizures with nystagmus and dysarthria. Stroke-like pattern was detected by brain MRI. Measurement of respiratory chain activities detected an isolated complex I deficiency related to a mitochondrial DNA mutation in the *ND5* gene (A13514G). Fibroblasts were characterized by a 30% heteroplasmy level. Cells were cultivated at 37 °C and 5% CO_2 in DMEM (Sigma) containing 4.5 g/liter of glucose supplemented with fetal calf serum (Invitrogen), penicillin/streptomycin, uridine (50 mg/liter), and fungizone (2.50 mg/liter) (Invitrogen).

Transient transfection of cells with RNA and chimeric molecules was performed as described in Refs. 20 and 21 with some modifications: for 2 cm² well of 80% confluent cells, we used 0.25 μg of RNA and 1 μl of Lipofectamine 2000 in OptiMEM medium (Invitrogen). OptiMEM was changed to a standard DMEM medium 8 h after transfection. In these conditions, ~80% of fibroblasts and 95% of cybrid cells were transfected with RNA (evaluated by fluorescent microscopy and by flow cytometry using CyFlow FACS 24 h post transfection). We also compared Northern hybridization signals obtained on total cellular RNA and on the known amounts of T7 transcripts loaded on the same gel. We could estimate that ~15% of RNA added to cybrid cells and 20% RNA for fibroblasts were internalized and can be detected in full-size form 24 h post transfection (data not shown). Transfection procedure did not lead to detectable decrease of viability of the cells or to a significant change of the

overall mtDNA amount verified by real-time quantitative PCR as described (15).

RNA Stability and Mitochondrial Import in Vivo—Mitochondria were isolated from the cybrid cells as described previously (22, 23) and treated with digitonin to generate mitoplasts (mitochondria devoid of the outer membrane) and RNase A to get rid of non-specifically attached RNA. This treatment allows us to obtain mitochondria free of cytosolic RNA contamination, which was tested using a probe for cytosolic 5.8 S rRNA usually strongly attached to the outer mitochondrial membrane. Total and mitochondrial RNA was isolated with TRIzol reagent (Invitrogen). Stability and mitochondrial import of recombinant molecules were analyzed by Northern hybridization of total and mitochondrial RNA with ³²P-labeled oligonucleotide probes followed by PhosphorImager quantification (Typhoon-Trio, GE Healthcare).

The probes used were as follows: "D-loop" probe-specific for recombinant molecules (see Fig. 1), 5′-GAG TCA TAC GCG CTA CCG ATT GCG CCA ACA AGG C-3′, hybridization temperature of 50 °C; cytosolic 5.8S rRNA probe, 5′-GGC CGC AAG TGC GTT CGA AG-3′, hybridization temperature of 50 °C; probe against the mitochondrial tRNA^Val, 5′-GAA CCT CTG ACT GTA AAG-3′, hybridization temperature of 45 °C; probe against the nuclear snRNA U3, 5′-CGC TAC CTC TCT TCC TCG TGG-3′, hybridization temperature of 50 °C. To compare the stability of different recombinant RNA, the relative concentration of each RNA in various time periods after transfection was calculated as a ratio between the D-loop probe signal and the signal for cytosolic 5.8 S rRNA.

The relative amount of each imported RNA inside the mitochondria was estimated as a ratio between the signal obtained after hybridization with the D-loop probe and the signal with a probe against the mitochondrial tRNA^Val in the same RNA preparation. To compare import efficiencies of different RNA molecules, the total level of each RNA molecule in transfected cells was taken into account and normalized as described previously (22). At least three independent experiments were performed for each RNA.

Confocal Microscopy—Cybrids cells cultivated in 2-cm² chamber slides (Lab-Tek) were transfected with Alexa Fluor 488-5-UTP-labeled RNA. At different time periods after transfections, living cells were stained with 5 μM tetramethylrhodamine methyl ester (TMRM) for 15 min at 37 °C, washed, and imaged in DMEM without red phenol. The LSM 700 confocal microscope (Zeiss) was used in conjunction with Zen imaging software, and images were acquired with a Zeiss 63×/1.40 oil immersion objective with a resolution of 1024 × 1024. The excitation/emission laser wavelengths were 488 nm (green channel) and 555 nm (red channel). Images were analyzed using ImageJ software (24) and JACoP plugin (25). Co-localization analyses were performed on multiple cells and optical sections. Pearson's and Manders' coefficients were estimated (26, 27). Pearson's correlation coefficient provides a measure of correlation between the intensities of each channel in each pixel. The overlap coefficients according to Manders indicate an actual overlap of the signals and represent the true degree of co-localization. In control experiments, cells were transfected with

Alexa Fluor 488-5-UTP-labeled RNA, which is not imported into mitochondria (28).

mtDNA Heteroplasmy Level Analysis—To isolate total DNA from transfected cells, 1 cm^2 of cells were solubilized in 0.5 ml of buffer containing 10 mM Tris-HCl, pH 7.5, 10 mM NaCl, 25 mM Na-EDTA, and 1% SDS, then 10 μl of proteinase K solution (20 mg/ml) was added, and the mixture was incubated for 2 h at 50 °C; 50 μl of 5 M NaCl was added, the DNA was precipitated with isopropyl alcohol and used for PCR amplification. Heteroplasmy level was analyzed by restriction fragment length polymorphism on a 125-bp PCR fragment encompassing nucleotides 13430 to 13555 of mtDNA obtained with primers CRC-F 5′-CAT ACC TCT CAC TTC AAC CTC C-3′ and CRC-R 5′-AGG CGT TTG TGT ATG ATA TGT TTG C-3′ (19). The A13514G mutation creates a HaeIII-specific cleavage site, giving two fragments of 80 and 45 bp. The HaeIII-digested fragments were separated on a 10% PAGE and stained with ethidium bromide. The proportion of mutant *versus* total mtDNA was calculated by densitometry using G-Box and GeneTools analysis software (Syngene). At least four independent transfections were performed with each recombinant RNA. Each DNA sample was analyzed twice by PCR amplification followed by at least three gel separation and quantification experiments.

The digestion control was performed for each reaction. For this, a 600-bp PCR fragment encompassing nucleotides 1216 to 1813 of mtDNA obtained with the primers CRS-F (5′-CGA TAA ACC CCG ATC AAC CTC-3′) and CRS-R (5′- GGT TAT AAT TTT TCA TCT TTC CC-3′) was cleaved by HaeIII to 350- and 250-bp fragments in the same tube as 125-bp PCR fragment containing the A13514G mutation site.

Mitochondria Quantification—2-cm^2 wells of 80% confluent cybrid cells and control wild type 143B cells, transfected with FD20H RNA, were stained with 5 μM TMRM and 200 nM MitoTracker® Green during 15 min in culture medium. The intensity of fluorescence was directly measured in a culture plate in DMEM without red phenol by VICTOR^{TM} X3 multilabel plate reader (PerkinElmer Life Science) at 485 nm (green channel) and 555 nm (red channel) in triplicate for each sample. After fluorescence measurement, cells were detached and quantified by flow cytometry using CyFlow FACS and FloMax software (Partec). Activity of complex I was measured using a MitoSciences® kit (Abcam).

Statistical Analyses—Pairwise comparisons were performed using two-tailed Student's *t* test and Excel software (Microsoft). Data are expressed as means ± S.D.

RESULTS

Design of Anti-replicative RNA Molecules—As it was reported previously, the helix-loop domains of FD RNA can serve as signals for RNA mitochondrial import, and this molecule can be used as a vector to deliver various sequences into the organelles (15). Recently, we also demonstrated that only one D-arm structure can be sufficient for targeting of recombinant molecule to mitochondria in living cells (28, 29).

To apply the anti-genomic strategy to point mutations, we used as a model the A13514G mutation inducing amino acid replacement D393G in the *ND5* gene of human mtDNA, which encodes one of the membrane domain subunits of the respiratory complex I (30). This mutation was initially found in two unrelated patients with MELAS (mitochondrial encephalopathy, lactic acidosis, and stroke-like episodes)-like syndrome (19). To target the mutant mitochondrial genome, a series of RNA molecules were constructed, bearing sequences complementary to a mutated region of *ND5* gene inserted between two helix-loop domains of a short artificial FD RNA (Fig. 1).

First, we analyzed the secondary structure predictions for FD RNA molecules bearing insertions of 16, 20, and 25 nucleotides corresponding to a fragment of the *ND5* gene, referred to as FD16L, FD16H, FD20L, FD20H, FD25L, and FD25H; R for sequence of H-strand and S for L-strand of mtDNA. For each sequence, a series of insertions bearing nucleotide G or C corresponding to the mutation A13514G (for either H- or L-strand) in various positions (Fig. 1) were analyzed by several types of software (see "Experimental Procedures") with similar results. Only molecules with a low probability of alternative folding were retained for further studies (Fig. 1). To check the ability of the selected versions for a specific annealing with mutated, but not wild type mtDNA, labeled recombinant RNAs were hybridized under physiological conditions with PCR-amplified mtDNA fragments either containing the mutation or not (Fig. 2). Versions FD25L and FD25H were not able to discriminate between mutant and wild type mtDNA; the shorter RNA molecule FD20H (but not FD20L) demonstrated specific annealing with the A13514G bearing mtDNA but not wild type. Annealing of molecules FD16H and FD16L was rather specific for mutant mtDNA; however, the efficiency of their hybridization at 37 °C was reproducibly lower when compared with FD20H. We also tested chimeric molecules, containing a stem-loop RNA import determinant and DNA inserts corresponding to FD20H and FD20L sequences, referred to as D20H-DNA and D20L-DNA (Fig. 2). Chimeric RNA-DNA molecule D20L-DNA demonstrated a higher ability to discriminate between mutant and wild type mtDNA when compared with FD20L. Thus, the recombinant molecules with 20 nucleotide insertions (FD20L, FD20H, D20L-DNA, and D20H-DNA) have been selected for the further analysis.

Mitochondrial Import of Recombinant RNA—To study the localization of recombinant RNA molecules in cultured human cells, an approach was developed consisting in cell transfection with Alexa Fluor 488-labeled RNA FD20H and its subsequent co-localization with the mitochondrial network by means of fluorescent confocal microscopy (Fig. 3). RNA molecules (green fluorescence) were detectable in cells in 24 h after transfection (day 1) as *green dots*, most probably representing the RNA-Lipofectamine complexes, with only slight co-localization with the mitochondria (red fluorescence). In 2–4 days after transfection, the distribution of the green label changed drastically, the amount of dots was reduced, and RNA molecules were now mostly dispersed within the cell, displaying clear partial co-localization with the mitochondrial network (Fig. 3*B* and supplemental movies). To perform quantitative co-localization analysis of confocal microscopy images, we estimated the values of Pearson's correlation coefficient and Manders' overlap coefficients M1 and M2 (26). For control RNA that is not imported into mitochondria (28), all of the coefficient values were very low (Fig. 3*A*), thus excluding the coincidental overlap
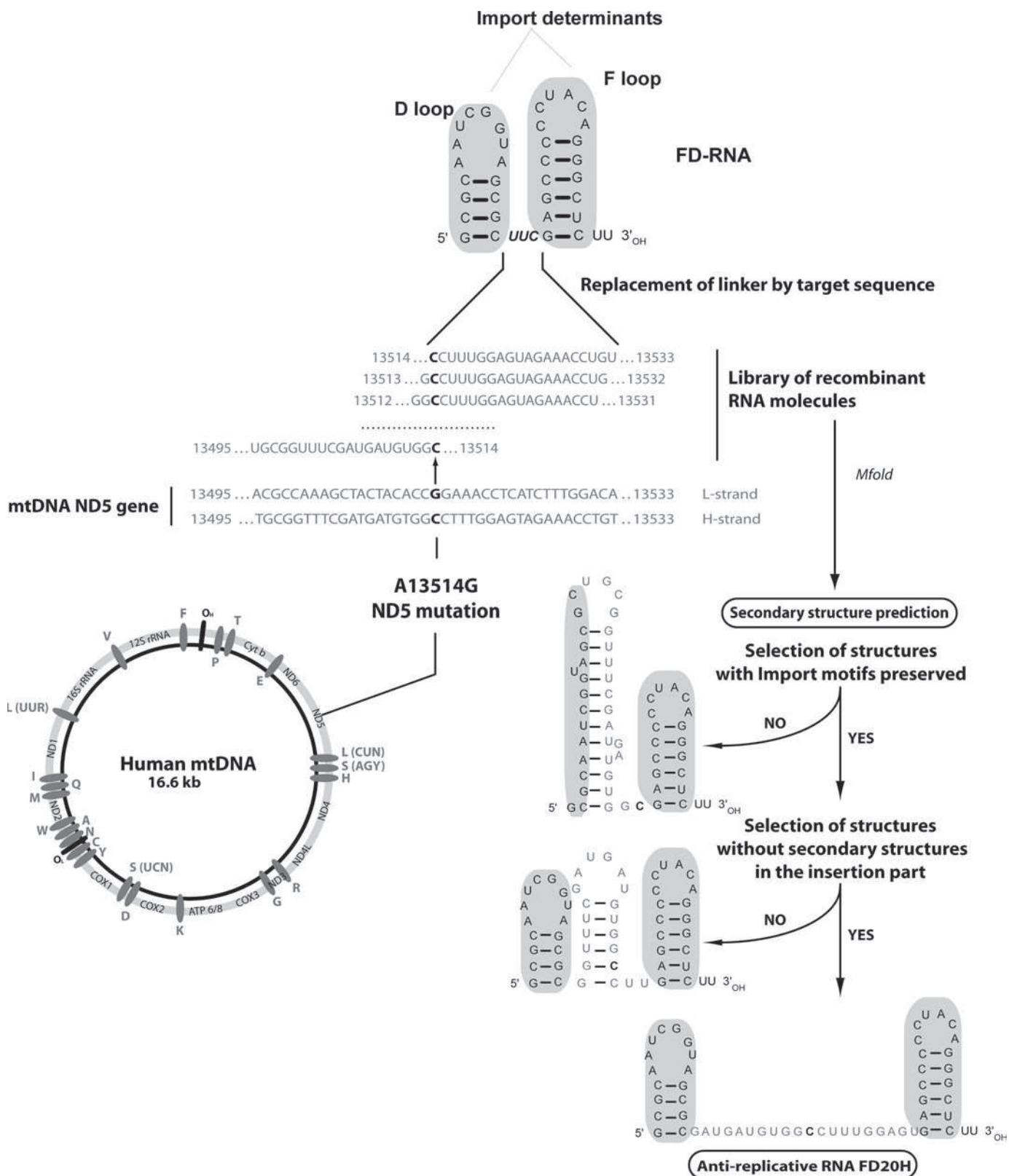
FIGURE 1. **Design of anti-replicative RNAs targeting A13514G mutation in human mtDNA.** Human mtDNA genetic map and sequence of the mutated region of *ND5* gene are presented, A13514G mutation is shown in *boldface type*; the FD-RNA stem-loop import determinants are colored *gray*. Design of recombinant RNA FD20H containing 20-mer corresponding to the H-strand of mtDNA is shown (see text for details).

of green and red signals. For FD20H RNA, the M1 values indicated that in 2 days post transfection, ~50% of green fluorescence (RNA) has been co-localized with red fluorescence (mitochondria), and this level did not significantly change between 2 and 4 days post transfection. M2 values representing the percentage of the red fluorescence (mitochondria) overlap-

	Control	Day 1	Day 2	Day 3	Day 4
PC	0.03±0.007	0.15±0.04	0.22±0.06	0.33±0.06	0.54±0.1
M1	0.05±0.01	0.38±0.07	0.49±0.06	0.50±0.08	0.55±0.1
M2	0.005±0.001	0.08±0.025	0.10±0.06	0.40±0.07	0.70±0.1
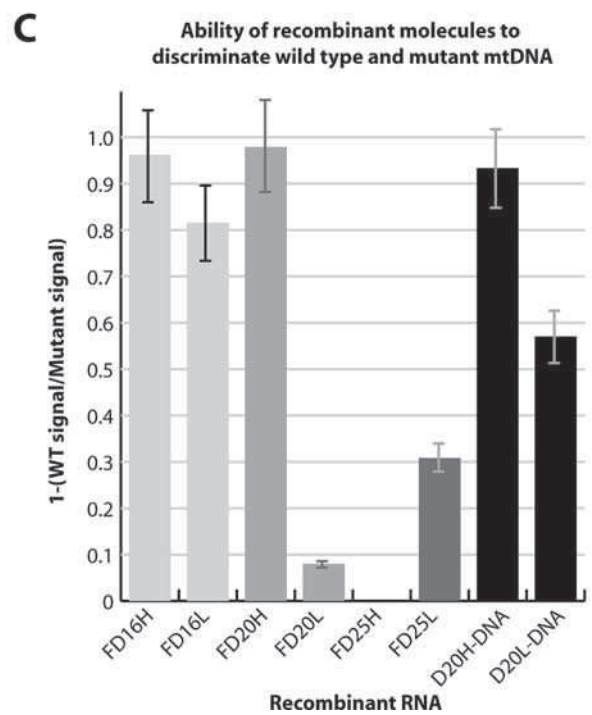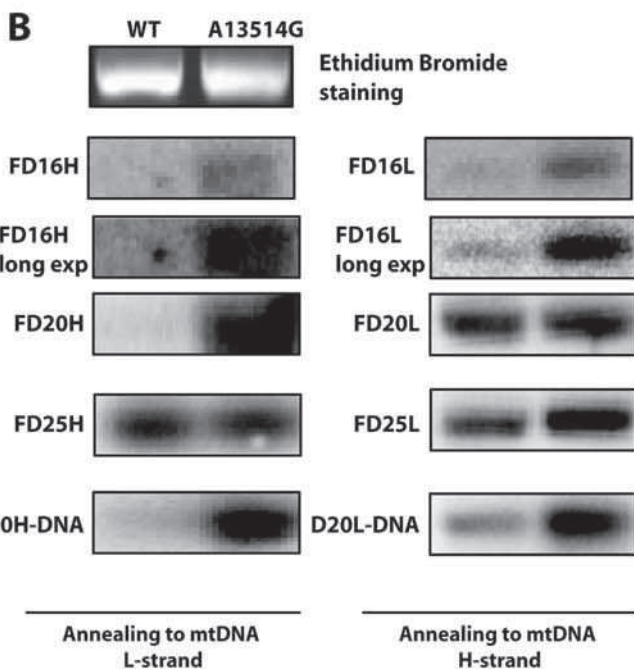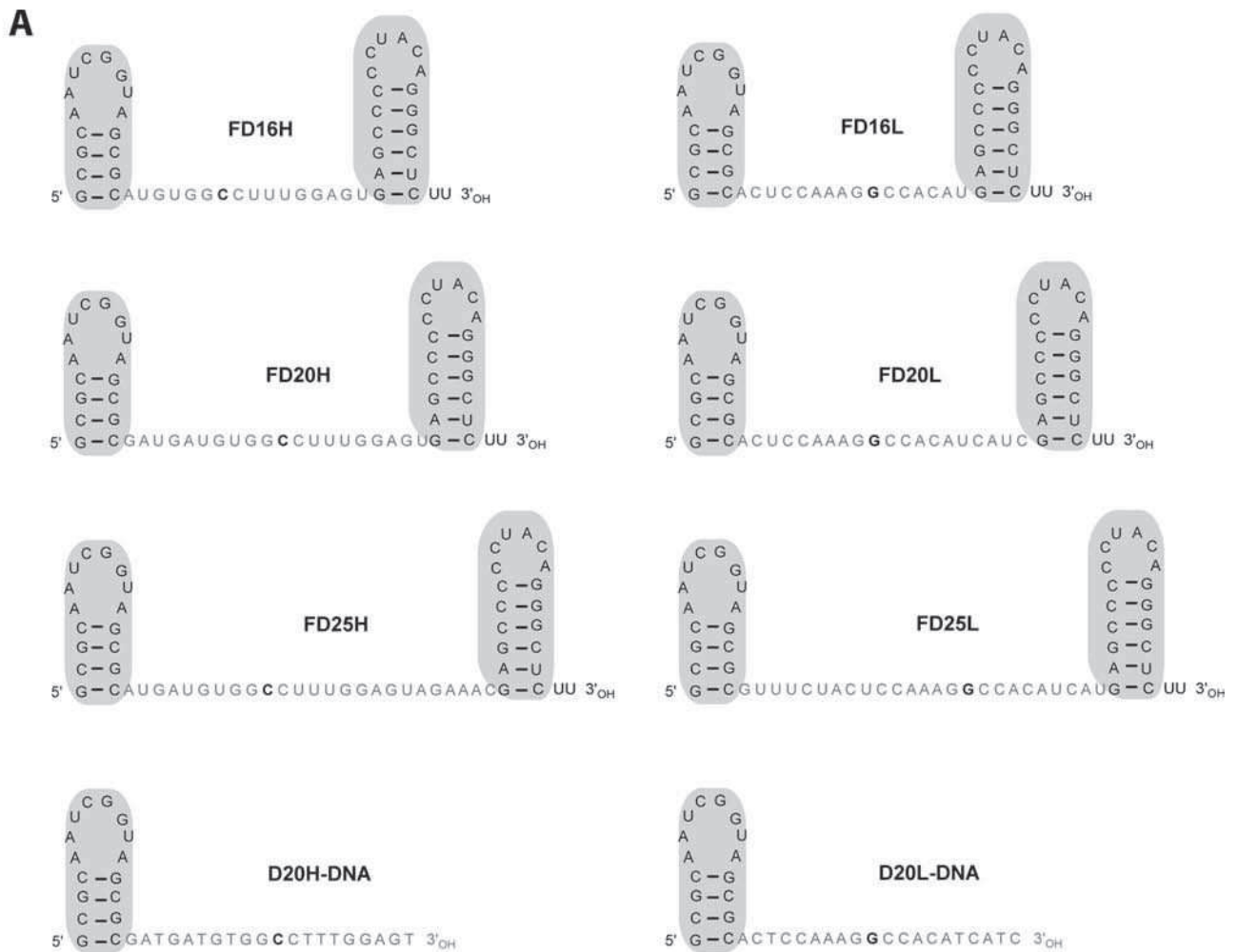
FIGURE 3. **Confocal microscopy of human cells transfected with fluorescently labeled RNA.** *A*, confocal microscopy of 143B cells transfected with Alexa Fluor 488-labeled FD20H RNA (*green*) at various time periods after transfection (as indicated *above* the panels). Control, cells transfected with Alexa Fluor 488-5-UTP-labeled RNA, which is not imported into mitochondria, 3 days post transfection. *TMRM*, visualization of mitochondrial network by red staining. *Below* the panels, shown is quantification of RNA co-localization with mitochondria, estimated for multiple cells and 6–10 optical sections in two independent experiments. *PC*, Pearson's correlation coefficient; *M1* and *M2*, Manders' overlap coefficients, representing the percentage of green fluorescence co-localized with red fluorescence (for M1) and the percentage of red fluorescence co-localization with green fluorescence (for M2). *B*, magnification of the image corresponding to day 4 post transfection. A three-dimensional reconstruction of the confocal microscopy image by ImageJ software is presented in the supplemental movies.

ping with the green fluorescence (RNA) indicate that only 10% of mitochondria contained RNA in 2 days post transfection. This proportion has been increased in 3 and 4 days up to 70%, probably due to the mitochondrial dynamic events, fusion and fission, resulting in more homogenous RNA distribution. These data clearly indicate on mitochondrial targeting of FD20H RNA in living human cells.

To measure recombinant RNA stability in cultured cells and the efficiency of their import into the mitochondrial matrix, cybrid cells were transfected with *in vitro*-synthesized recombinant RNAs and chimeric molecules. Their degradation rate in transfected cells was evaluated by Northern hybridization of

total cellular RNA at different time points spanning a 6-day period after transfection (Fig. 4*A*). Recombinant molecules were detectable in cybrid cells at least 6 days after transfection. The chimeric version D20L DNA revealed to be more stable than FD20L and FD20H. Such result suggests that the "insertion" part, lacking strong secondary structures, gives a prominent impact on the degradation of recombinant molecules. Thus, recombinant molecules in which RNA insertions were replaced by DNA sequences demonstrated improved stability in the living cells.
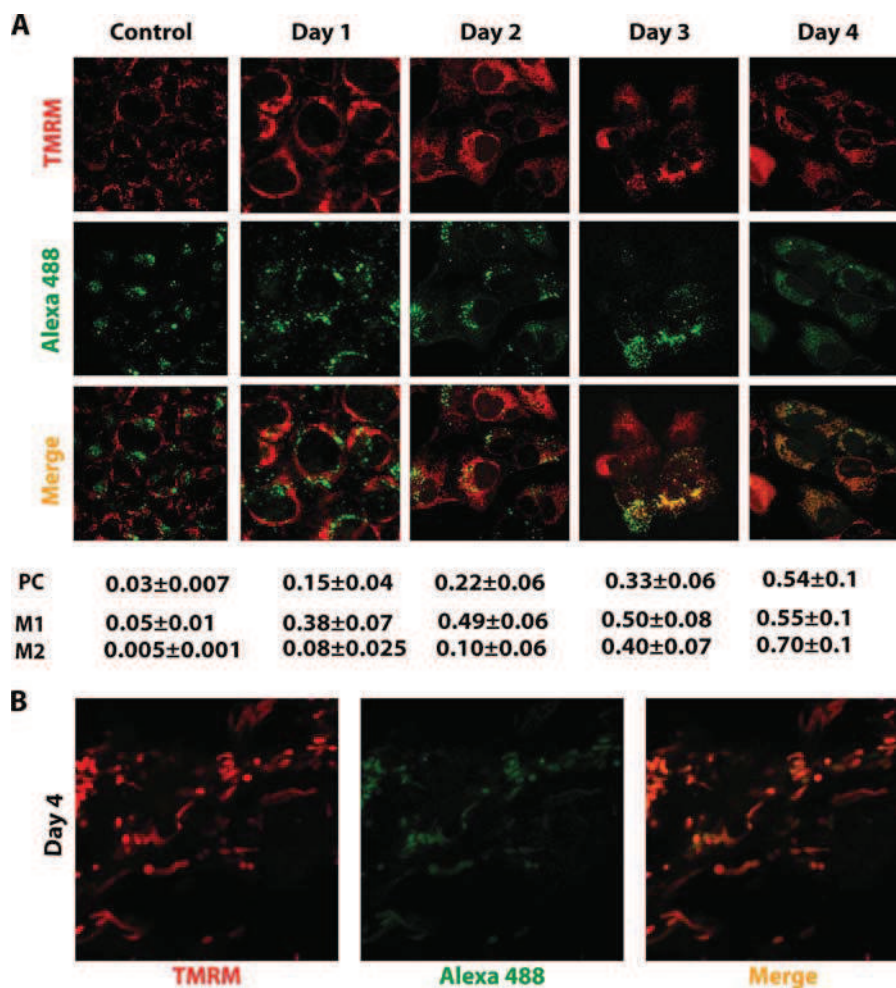
Because the microscopy data can give only a rough indication on the mitochondrial import of RNA molecules, we performed

FIGURE 2. **Ability of recombinant molecules to discriminate wild type and mutant mtDNA.** *A*, predicted secondary structures of anti-replicative molecules. Stem-loop import determinants are shown in *gray*. D20H DNA and D20L DNA, chemically synthesized chimeric molecules, RNA insertion has been replaced by DNA. *B*, Southern hybridization of WT or mutant (A13514G) mtDNA fragments with labeled recombinant RNAs (indicated at the *left*) under physiological conditions. *Long exp.*, radiogram after longer exposure for FD16H and FD16L. The specific radioactivity of all of the RNA probes was comparable. *C*, graphical representation of hybridization specificity of different recombinant molecules (indicated *below* the graphs). The hybridization specificity was calculated for each RNA as 1 − (ratio between hybridization signals for wild type and mutated DNA fragments). Thus, for recombinant RNA annealed only to the mutant DNA fragment, the hybridization specificity value reached 1, and for RNA annealed equally to mutant and wild type fragments, this value was close to 0. Data are ± S.D. calculated from three independent experiments.
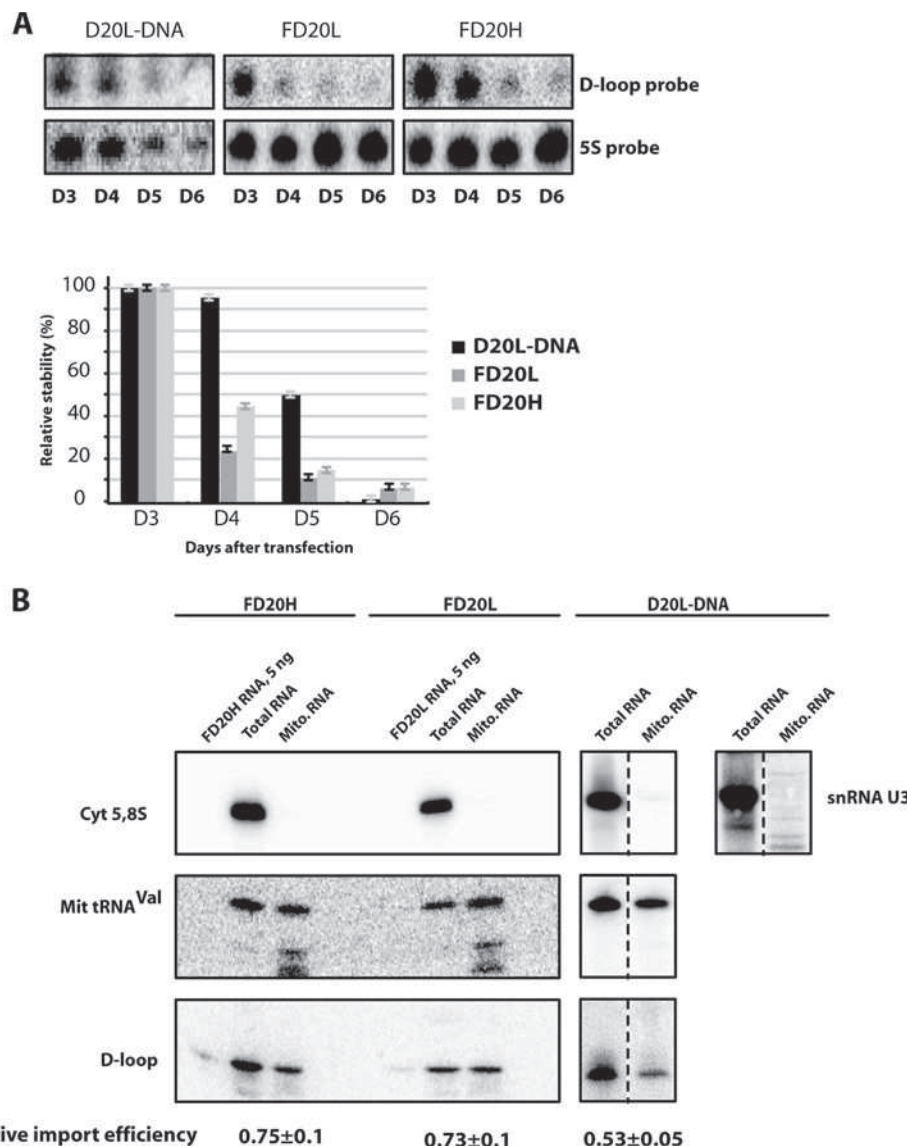
FIGURE 4. **Anti-replicative RNA stability and mitochondrial import in transiently transfected cybrid cells.** *A*, an example of Northern hybridization of total RNA isolated in 3–6 days after cell transfection (as indicated *below*) with various recombinant molecules (indicated *above* the panels). Probes used for hybridization: D-loop, specific for all recombinant molecules used for transfection; *5S*, against 5 S rRNA to quantify the level of recombinant RNA in the cells. Time dependence of RNA decay is shown below (means ± S.D. calculated from at least four independent experiments). *B*, mitochondrial import of recombinant molecules in transiently transfected cybrid cells. Northern hybridizations of RNA extracted from cells (*Total RNA*) or purified mitoplasts (*Mito RNA*) 48 h after transfection. *Above*, RNAs used for transfection are indicated. On the *left*, hybridization probes: D-loop, specific for recombinant molecules used for the transfection; *Cyt 5.8S*, against 5.8 S rRNA to check the absence of cytosolic RNA in mitochondrial samples; *snRNA U3*, demonstrating that the mitoplast fraction was not contaminated by the small nuclear RNAs; *Mit tRNA*^{Val}, to normalize the level of recombinant RNA to amount of loaded material. Import efficiency was estimated as a ratio of mitochondrial to total signal for the D-loop probe after normalization of the both signals to those for mitochondrial tRNA^{Val} probe.

Northern blot hybridization experiments. For this, cells were transfected with purified recombinant molecules. The mitochondrial import was analyzed by hybridization of the whole cell RNA and RNA isolated from purified and RNase-treated mitoplasts (mitochondria where the outer membrane was removed by digitonin) as described previously (15, 22, 29). The absence of signal in the mitochondrial RNA preparation after hybridization with the probe against the cytoplasmic 5.8 S rRNA indicates that the treatment of mitochondria with ribonuclease and digitonin removed all contamination by cytoplasmic RNA (Fig. 4*B*). Hybridization signals obtained with the D-loop probe specific for all of the recombinant molecules were normalized to the amounts of loaded RNA, estimated by hybrid-

ization with a probe to a mitochondrial transcript (*mito tRNA*^{Val}). The data show that the import efficiencies of RNA molecules FD20H and FD20L were close to each other; import of the chimeric molecule D20L-DNA was only slightly decreased (Fig. 4*B*).

Imported RNA Can Shift Point Mutation Heteroplasmy Level in Cybrid Cells—Trans-mitochondrial cybrid cell line containing a patient's mitochondria with 35% of mtDNA molecules bearing an A13514G mutation (referred thereafter as *ND5* mutation) were transfected with *in vitro* synthesized recombinant RNA and chimeric RNA-DNA molecules. Heteroplasmy levels (percentage of mutant *ND5* mtDNA to all mtDNA molecules) were measured at different time points after transfection by restriction fragment length polymorphism analysis of

FIGURE 5. **The effect of recombinant RNA on heteroplasmy level in transfected cybrid cells.** *A*, time dependence of A13514G mutation heteroplasmy level (axis Y) followed during 7–8 days. *D0–D8*, days after transfection of cells with different recombinant molecules. *Mut*, mock-transfected cybrid A13514G cells; *WT*, mo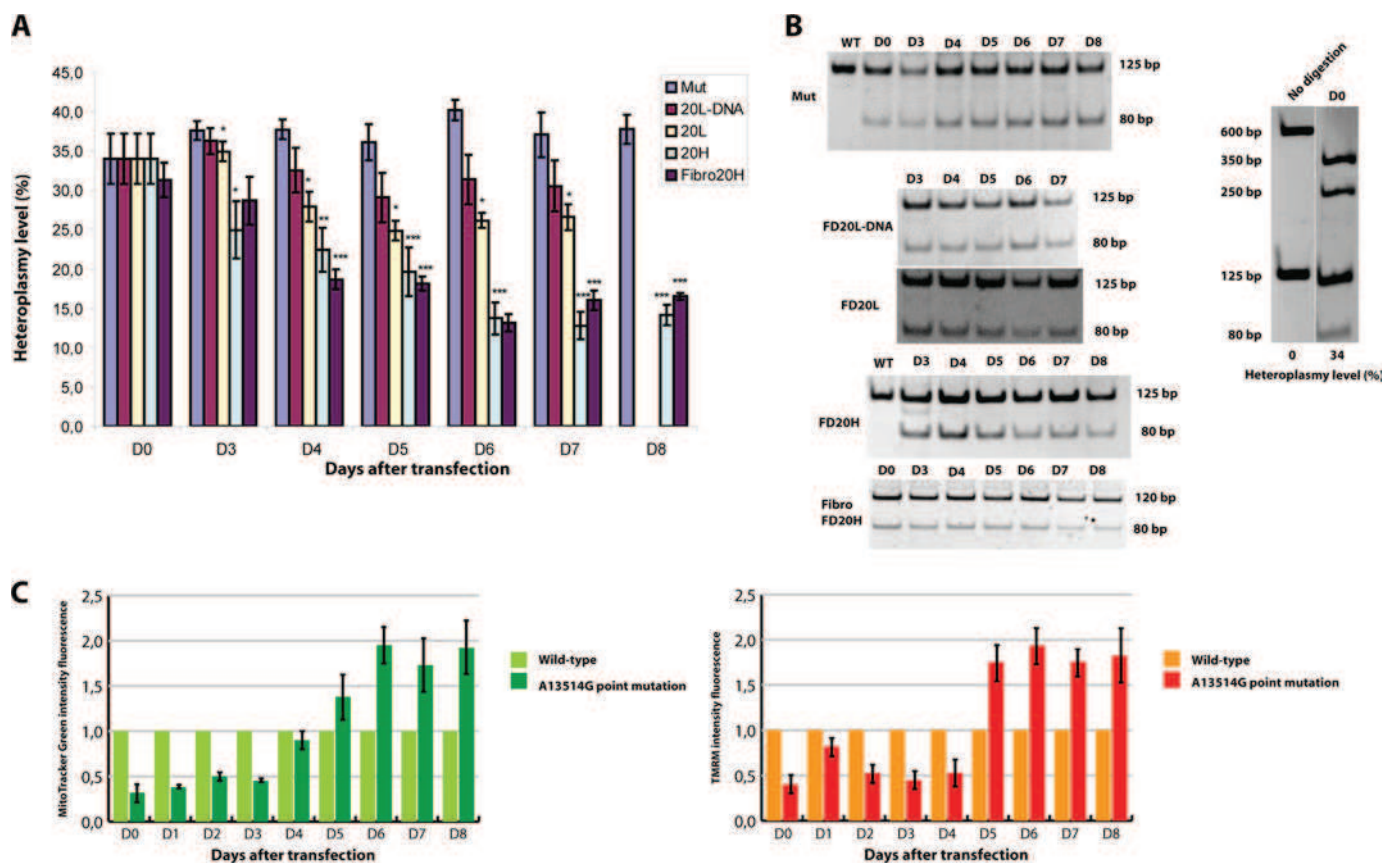ck-transfected 143B cells; FD20L, FD20H, or FD20L-DNA, cybrid cells transfected with corresponding recombinant molecule; *Fibro 20H*, primary fibroblasts transfected with FD20H RNA. Data are expressed as mean ± S.D. for 3–5 independent experiments. Shown is an unpaired *t* test between values for mutant and transfected cells; *, $p < 0.02$; **, $p < 0.003$; ***, $p < 0.0009$. *B*, an example of restriction fragment length polymorphism (*RFLP*) analysis for DNA samples isolated in 3–8 days (as indicated above) after cybrid cell transfection with recombinant molecules indicated at the left. Digestion control was performed for each reaction, as shown at the *right panel*. For this, 600-bp PCR fragment of mtDNA was cleaved by HaeIII to 350- and 250-bp fragments in the same tube as 125-bp PCR fragment spanning A13514G mutation site. The A13514G mutation creates an HaeIII-specific cleavage site, giving the fragment of 80 bp. Fragment size is indicated for each panel. *C*, evaluation of total and energised mitochondria content in 143B (wild type) and cybrid cells (A13514G) transfected with RNA FD20H during 8 days after cell transfection. MitoTracker Green (*left panel*) and TMRM (*right panel*) fluorescence normalized to the number of cells; values of wild type cells were taken as 1.

PCR-amplified mtDNA fragment (Fig. 5, *A* and *B*). We observed a reproducible decrease of the proportion of mutant mtDNA in cells transfected by recombinant RNA containing FD20H inserts. The heteroplasmy shift became visible 3 days after transfection, and then the heteroplasmy continued to decrease and reached the stable level of 13 ± 2% in 6 days post transfection. To affirm these data, we performed transfection of patient's fibroblasts, harboring the A13514G mutation, with FD20H RNA (Fig. 5, *A* and *B*). This completely independent experiment on primary human cells gave the same result of heteroplasmy shift, as obtained on the cybrid cells model.

Remarkably, in cells transfected with FD20H RNA, the decrease of mutant mtDNA correlated to increased amount of mitochondria per cell measured as MitoTracker Green fluorescence (Fig. 5*C*). Moreover, the same increase of the fluorescence was detected by TMRM dye that is readily sequestered by active mitochondria, indicating on a fully energized state of mitochondrial membranes (31).

In parallel experiments, mock-transfected cybrid cells demonstrated no heteroplasmy shift (Fig. 5, *A* and *B*). Cell transfection with FD20L RNA led to a very small heteroplasmy

decrease, reaching the level of 27 ± 5% in 7 days (Fig. 5*A*). Different effects of FD20H and FD20L RNA molecules are in perfect correlation with the more specific hybridization of FD20H RNA with mutant mtDNA (Fig. 2). Surprisingly, chimeric molecule D20L DNA, characterized by a rather specific hybridization with mutant mtDNA *in vitro*, high stability in cells, and efficient import into mitochondria, was not able to influence the heteroplasmy level. Our data show that mitochondrially imported RNA (but not DNA) molecules can function as anti-genomic agents in human cells, affecting the amount of mitochondrial genomes bearing a point mutation.

DISCUSSION

Specific Annealing of RNA to mtDNA Bearing a Point Mutation—The anti-replicative approach aiming to shift heteroplasmy levels in mtDNA below the pathogenic threshold has been recently applied to cells containing a large 7-kb deletion in mtDNA (15). In this case, a new sequence generated at the fusion of the deletion boundaries has been inserted into RNA vector molecules, and specific annealing only with the mutant but not with wild type mtDNA was demonstrated for recombi-

TABLE 1

Melting temperature predictions for hybrids between recombinant RNAs and mutated or WT mtDNA regions

RNA	Insert (bp)	T_m for mutated DNA	T_m for WT DNA[a]	ΔT_m
FD16L	16	48.4 °C	40.2 °C	8.2 °C
FD16H	16	48.4 °C	35.0 °C	13.4 °C
FD20L	20	54.9 °C	49.3 °C	5.6 °C
FD20H	20	52.8 °C	42.9 °C	9.9 °C
FD25L	25	59.0 °C	54.9 °C	4.1 °C
FD25H	25	59.0 °C	52.2 °C	6.8 °C

[a] Shown are values predicted by IDT Sci-Tools OligoAnalyser software (version 3.1) for mismatch containing DNA-DNA hybrids. ΔT_m, predicted decrease of T_m for wild type mtDNA compared with mutated mtDNA.

nant RNA molecules. In the present study, we investigated whether this strategy can be extended to point mutations in the mitochondrial genome. The first question we addressed was as follows: could a recombinant RNA importable into human mitochondria anneal in a specific way with only the mutant mtDNA containing a point mutation but not with wild type?

Using Southern hybridization under conditions designed to approximate the intracellular ionic environment, we demonstrated that the sequence of 20 nucleotides corresponding to H-strand of the mutated (A13514G) region of mtDNA (FD20H) can discriminate between fragments of mutant and wild type mtDNA. This was rather surprising, because the melting temperature predictions for hybrids between recombinant RNAs and mutated or wild type mtDNA (Table 1) show T_m values >37 °C. Thus, all RNA molecules tested are likely to anneal to mutant and wild type mtDNA fragments in the permissive conditions applied. According to the T_m predictions, we have started our experiments with shorter insertions of 8–10 nucleotides, which should anneal to mutant but not to wild type mtDNA. Surprisingly, we were not able to detect any signal with these RNA molecules used as probes for Southern blot hybridization and no effect on heteroplasmy level in transfected cells (data not shown). Then, we gradually increased the length of the complementary part from 11 to 25 nt and obtained specific hybridization (Fig. 2) for molecules containing 16- and 20-nt insertions. We suppose that the discrepancy between predictions and experimental data is due to the absence of software adapted to calculate the T_m of RNA-DNA duplexes containing a mismatch. Another possible explanation consists in formation of alternative secondary structures in RNA molecules that cannot be predicted by available software.

Another interesting issue is that the hybridization of RNA containing an insertion of the same length corresponding to the complementary L-strand of mtDNA (FD20L) was much less selective. This discrepancy can be explained by base mismatches: for FD20H, C-A pairing decreases the T_m of hybridization with wild type mtDNA by 10 °C (Table 1) compared with mutant mtDNA (predicted by IDT Sci-Tools OligoAnalyser software (version 3.1) for mismatch containing hybrids). In contrast, for FD20L, G-T pairing decreases T_m by only 5.5 °C and allows annealing of FD20L RNA with both mtDNA fragments at 37 °C. The above data show that a point mutation can be selectively addressed by RNA containing a 20-nucleotide stretch; however, for transitions A to G (in L-strand of mtDNA), sequences corresponding to H-strand would have a

more selective effect and vice versa, for G to A transitions, only L-strand sequences should be used.

Pathogenic Mutation in ND5 Gene—mtDNA mutation A13514G, which we used as a model in the present study, is localized in NADH dehydrogenase ND5 subunit of the respiratory complex I. This is the first and largest enzyme of the respiratory chain (45 subunits, total size ~ 1 MDa), coupling electron transfer between NADH and ubiquinone to the translocation of four protons across the inner mitochondrial membrane (32). The L-shaped complex consists of hydrophilic and membrane domains. Three largest transmembrane subunits ND2, -4, and -5 at the far end of the membrane arm are homologous to each other and likely participate in the conformation-coupled proton translocation (33). Mutation A13514G induces amino acid replacement D393G localized in a very conserved region of ND5 transmembrane helix 12 (34, 35), forming the second half of the proton channel, and is involved in a cascade of conformational changes leading to proton translocation. Therefore, any mutation exchanging the negatively charged Asp-393 to uncharged amino acid residue could disturb the transport of the proton through the ND5 subunit channel of respiratory complex I.

The *ND5* gene turned out to be mutated frequently (30). Point mutation A13514G-inducing amino acid replacement D393G has been detected in four unrelated patients with MELAS-like and Leigh syndromes (19, 36, 37). Another transition, the frequently reported and well documented G13513A, affects the same Asp-393 residue in the *ND5* gene, but the amino acid replacement is different, D393N (reviewed in Ref. 30). A prominent clinical feature detected in patients with these mutations was a visual loss due to optic atrophy, indicating an exquisite sensitivity of the optic nerve to damage caused by alteration of the ND5 Asp-393 residue (38). Thus, search for Asp-393 mutations has been proposed to be a part of the routine screening for mitochondrial disorders (19).

More recently, among the patients with Leigh-like syndrome and D393N mutation in *ND5*, several cases were reported characterized by normal complex I activity in muscle (36, 39). The authors suggested that the relatively low mutant heteroplasmy and normal respiratory chain activities in muscle do not necessarily represent the situation in affected tissue such as brain and/or optic nerve. Thus, even low mutation load in Asp-393 in the presence of normal respiratory chain analysis may be considered as pathogenic (36), illustrating the complexities of correlating A13514G heteroplasmy levels with biochemical phenotype in patient's muscle and fibroblasts. This can be a characteristic feature of NADH dehydrogenase complex because it was recently demonstrated that even a low dose of wild type *ND6* gene is sufficient to drive assembly of near normal levels of complex I (6). All of these data taken together indicate that a low load of mutation A13514G might cause a functional defect of ND5 protein, but this defect would be very low and hardly noticeable. This is exactly the case of cells used in the present study.

Effect of Imported RNAs on mtDNA Heteroplasmy—As we have shown previously, mitochondrially imported anti-replicative RNAs can cause a replication stalling at the site of RNA annealing to the mutant mtDNA because of slowdown of the

replication fork progression (15). Nevertheless, we obtained only a transient shift of heteroplasmy in cells bearing a large deletion in mtDNA, the initial heteroplasmy level being restored in 6–8 days after cell transfection with anti-replicative RNA. This can be explained by recombinant RNA degradation, followed by preferential replication of shorter mitochondrial genomes bearing deletion, due to the previously reported effect of "replicative advantage of deleted mtDNA" (40). In the present study, we successfully obtained a stable decrease of the proportion of mtDNA molecules containing *ND5* point mutation after transfection of cybrid cells and primary fibroblasts with anti-replicative RNA FD20H (Fig. 5). Because no difference was expected in the rate of replication for wild type and mutant mtDNA, we can suggest that even after degradation of recombinant RNA, the induced shift in *ND5* point mutation heteroplasmy level may become stable. The maintenance of wild type mtDNA enrichment was previously reported for several mutations (41, 42).

Among several anti-replicative recombinant molecules, characterized by comparable stability in cells and mitochondrial import efficiency (Fig. 4), only FD20H was able to induce a prominent heteroplasmy shift. This RNA molecule demonstrated the highest ability to discriminate between mutant and wild type mtDNA (Fig. 2). The chimeric molecule, containing the same sequence of the insertion part as FD20H, but in the form of DNA, was not capable to shift the heteroplasmy level (Fig. 5). These data provide an additional proof of recombinant RNA action at the level of mtDNA replication because it was suggested that mitochondrial replisome helicase can separate DNA-DNA hybrids but not regions of short RNA-DNA hybrids in the mtDNA D-loop (43). Thus, only mitochondrially imported RNA (but not DNA) molecules are likely to function as anti-replicative agents in human mitochondria.

Cybrid cells used in the present study, containing 35% of mtDNA molecules bearing the A13514G mutation, were almost asymptomatic, characterized by a very slight decrease of all of the measurable parameters as oxygen consumption, levels of ATP, reactive oxygen species, and complex I enzymatic activity compared with wild type 143B cell line (data not shown). Nevertheless, we observed a prominent decrease of amount of mitochondria in cybrid cells, measured by use of MitoTracker Green, a mitochondria-selective fluorescent label, accumulating in the matrix (Fig. 5*C*) (44). Notably, transfection with anti-replicative RNA FD20H, leading to an important decrease of the level of *ND5* point mutation, caused, at the same time, a recovery of mitochondrial content. Unexpectedly, if the MitoTracker Green fluorescence increased gradually from day 4 to day 6 post transfection and then reached a plateau, the shift of the TMRM fluorescence between days 4 and 5 was rather sharp. Thus, we observe some temporary hyperpolarization of mitochondria only at day 5 post transfection. We can hypothesize that following the heteroplasmy decrease observed for *ND5* cybrid cells in 3–4 days post transfection, the synthesis of increased amounts of normal, fully active ND5 protein might create a temporary unbalance in the assembly of respiratory complexes, resulting in a rise of the basal production of reactive oxygen species (at the 5th day) and increasing mitochondrial biogenesis (days 6–8).

Mitochondrial Import of RNA as a Therapeutic Tool

All of our data indicate on the possibility to obtain a curative effect of mitochondrial dysfunctions in human cells by a heteroplasmy shift induced by short RNA molecules targeted into mitochondria. Although the inhibitory effect was partial, it may have a long term therapeutic interest because only high levels of mutations in human mtDNA become pathogenic. The validation of the anti-replicative RNA strategy for a point mutation in mtDNA in cultured human cells can be considered as an important step to further develop an efficient therapy of mitochondrial diseases.

REFERENCES

1. Burnett, J. C., and Rossi, J. J. (2012) RNA-based therapeutics: current progress and future prospects. *Chem. Biol.* **19,** 60–71
2. Ruiz-Pesini, E., Lott, M. T., Procaccio, V., Poole, J. C., Brandon, M. C., Mishmar, D., Yi, C., Kreuziger, J., Baldi, P., and Wallace, D. C. (2007) An enhanced MITOMAP with a global mtDNA mutational phylogeny. *Nucleic Acids Res.* **35,** D823–828
3. Wallace, D. C. (2010) Mitochondrial DNA mutations in disease and aging. *Environ. Mol. Mutagen.* **51,** 440–450
4. Rustin, P., H, T. J., Dietrich, A., R, N. L., Tarassov, I., and Corral-Debrinski, M. (2007) Targeting allotopic material to the mitochondrial compartment: new tools for better understanding mitochondrial physiology and prospect for therapy. *Med. Sci.* **23,** 519–525
5. Manfredi, G., Fu, J., Ojaimi, J., Sadlock, J. E., Kwong, J. Q., Guy, J., and Schon, E. A. (2002) Rescue of a deficiency in ATP synthesis by transfer of MTATP6, a mitochondrial DNA-encoded gene, to the nucleus. *Nat. Genet.* **30,** 394–399
6. Perales-Clemente, E., Fernández-Silva, P., Acín-Pérez, R., Pérez-Martos, A., and Enríquez, J. A. (2011) Allotopic expression of mitochondrial-encoded genes in mammals: achieved goal, undemonstrated mechanism or impossible task? *Nucleic Acids Res.* **39,** 225–234
7. Schneider, A. (2011) Mitochondrial tRNA import and its consequences for mitochondrial translation. *Annu. Rev. Biochem.* **80,** 1033–1053
8. Karicheva, O. Z., Kolesnikova, O. A., Schirtz, T., Vysokikh, M. Y., Mager-Heckel, A. M., Lombès, A., Boucheham, A., Krasheninnikov, I. A., Martin, R. P., Entelis, N., and Tarassov, I. (2011) Correction of the consequences of mitochondrial 3243A→G mutation in the MT-TL1 gene causing the MELAS syndrome by tRNA import into mitochondria. *Nucleic Acids Res.* **39,** 8173–8186
9. Kolesnikova, O. A., Entelis, N. S., Jacquin-Becker, C., Goltzene, F., Chrzanowska-Lightowlers, Z. M., Lightowlers, R. N., Martin, R. P., and Tarassov, I. (2004) Nuclear DNA-encoded tRNAs targeted into mitochondria can rescue a mitochondrial DNA mutation associated with the MERRF syndrome in cultured human cells. *Hum. Mol. Genet.* **13,** 2519–2534
10. Bacman, S. R., Williams, S. L., Garcia, S., and Moraes, C. T. (2010) Organ-specific shifts in mtDNA heteroplasmy following systemic delivery of a mitochondria-targeted restriction endonuclease. *Gene. Ther.* **17,** 713–720
11. Bacman, S. R., Williams, S. L., Hernandez, D., and Moraes, C. T. (2007) Modulating mtDNA heteroplasmy by mitochondria-targeted restriction endonucleases in a 'differential multiple cleavage-site' model. *Gene Ther.* **14,** 1309–1318
12. Taylor, R. W., Chinnery, P. F., Turnbull, D. M., and Lightowlers, R. N. (1997) Selective inhibition of mutant human mitochondrial DNA replication *in vitro* by peptide nucleic acids. *Nat. Genet.* **15,** 212–215

13. Muratovska, A., Lightowlers, R. N., Taylor, R. W., Turnbull, D. M., Smith, R. A., Wilce, J. A., Martin, S. W., and Murphy, M. P. (2001) Targeting peptide nucleic acid (PNA) oligomers to mitochondria within cells by conjugation to lipophilic cations: implications for mitochondrial DNA replication, expression and disease. *Nucleic Acids Res.* **29,** 1852–1863

14. Kolesnikova, O., Kazakova, H., Comte, C., Steinberg, S., Kamenski, P., Martin, R. P., Tarassov, I., and Entelis, N. (2010) Selection of RNA aptamers imported into yeast and human mitochondria. *RNA* **16,** 926–941

15. Comte, C., Tonin, Y., Heckel-Mager, A. M., Boucheham, A., Smirnov, A., Auré, K., Lombès, A., Martin, R. P., Entelis, N., and Tarassov, I. (2013) Mitochondrial targeting of recombinant RNAs modulates the level of a heteroplasmic mutation in human mitochondrial DNA associated with Kearns Sayre Syndrome. *Nucleic Acids Res.* **41,** 418–433

16. Zuker, M. (2003) Mfold web server for nucleic acid folding and hybridization prediction. *Nucleic Acids Res.* **31,** 3406–3415

17. Sugimoto, N., Nakano, S., Katoh, M., Matsumura, A., Nakamuta, H., Ohmichi, T., Yoneyama, M., and Sasaki, M. (1995) Thermodynamic parameters to predict stability of RNA/DNA hybrid duplexes. *Biochemistry* **34,** 11211–11216

18. Bellon, L. (2001) Oligoribonucleotides with 2′-O-(*tert*-butyldimethylsilyl) groups. in *Current Protocols in Nucleic Acid Chemistry*, pp. 1:3.6.1–3.6.13, John Wiley & Sons, Inc., New York

19. Corona, P., Antozzi, C., Carrara, F., D'Incerti, L., Lamantea, E., Tiranti, V., and Zeviani, M. (2001) A novel mtDNA mutation in the ND5 subunit of complex I in two MELAS patients. *Ann. Neurol.* **49,** 106–110

20. Smirnov, A. V., Entelis, N. S., Krasheninnikov, I. A., Martin, R., and Tarassov, I. A. (2008) Specific features of 5S rRNA structure: its interactions with macromolecules and possible functions. *Biochemistry* **73,** 1418–1437

21. Köhrer, C., Xie, L., Kellerer, S., Varshney, U., and RajBhandary, U. L. (2001) Import of amber and ochre suppressor tRNAs into mammalian cells: a general approach to site-specific insertion of amino acid analogues into proteins. *Proc. Natl. Acad. Sci. U.S.A.* **98,** 14310–14315

22. Smirnov, A., Tarassov, I., Mager-Heckel, A. M., Letzelter, M., Martin, R. P., Krasheninnikov, I. A., and Entelis, N. (2008) Two distinct structural elements of 5S rRNA are needed for its import into human mitochondria. *RNA* **14,** 749–759

23. Mager-Heckel, A. M., Entelis, N., Brandina, I., Kamenski, P., Krasheninnikov, I. A., Martin, R. P., and Tarassov, I. (2007) The analysis of tRNA import into mammalian mitochondria. *Methods Mol. Biol.* **372,** 235–253

24. Schneider, C. A., Rasband, W. S., and Eliceiri, K. W. (2012) NIH Image to ImageJ: 25 years of image analysis. *Nat. Methods* **9,** 671–675

25. Bolte, S., and Cordelières, F. P. (2006) A guided tour into subcellular co-localization analysis in light microscopy. *J. Microsc.* **224,** 213–232

26. Zinchuk, V., Zinchuk, O., and Okada, T. (2007) Quantitative colocalization analysis of multicolor confocal immunofluorescence microscopy images: pushing pixels to explore biological phenomena. *Acta Histochem. Cytochem.* **40,** 101–111

27. Zinchuk, V., and Grossenbacher-Zinchuk, O. (2009) Recent advances in quantitative colocalization analysis: focus on neuroscience. *Prog. Histochem. Cytochem.* **44,** 125–172

28. Gowher, A., Smirnov, A., Tarassov, I., and Entelis, N. (2013) Induced tRNA import into human mitochondria: implication of a host aminoacyl-tRNA-synthetase. *PLoS One* **8,** e66228

29. Tonin, Y., Heckel, A. M., Dovydenko, I., Meschaninova, M., Comte, C., Venyaminova, A., Pyshnyi, D., Tarassov, I., and Entelis, N. (2014) Characterization of chemically modified oligonucleotides targeting a pathogenic mutation in human mitochondrial DNA. *Biochimie* **100,** 192–199

30. Blok, M. J., Spruijt, L., de Coo, I. F., Schoonderwoerd, K., Hendrickx, A., and Smeets, H. J. (2007) Mutations in the ND5 subunit of complex I of the mitochondrial DNA are a frequent cause of oxidative phosphorylation disease. *J. Med. Genet.* **44,** e74

31. Davidson, S. M., Yellon, D., and Duchen, M. R. (2007) Assessing mitochondrial potential, calcium, and redox state in isolated mammalian cells using confocal microscopy. *Methods Mol. Biol.* **372,** 421–430

32. Efremov, R. G., and Sazanov, L. A. (2012) The coupling mechanism of respiratory complex I: a structural and evolutionary perspective. *Biochim. Biophys. Acta* **1817,** 1785–1795

33. Ohnishi, T., Ohnishi, S. T., Shinzawa-Itoh, K., Yoshikawa, S., and Weber, R. T. (2012) EPR detection of two protein-associated ubiquinone components (SQ(Nf) and SQ(Ns)) in the membrane *in situ* and in proteoliposomes of isolated bovine heart complex I. *Biochim. Biophys. Acta* **1817,** 1803–1809

34. Baradaran, R., Berrisford, J. M., Minhas, G. S., and Sazanov, L. A. (2013) Crystal structure of the entire respiratory complex I. *Nature* **494,** 443–448

35. Efremov, R. G., and Sazanov, L. A. (2011) Structure of the membrane domain of respiratory complex I. *Nature* **476,** 414–420

36. Brautbar, A., Wang, J., Abdenur, J. E., Chang, R. C., Thomas, J. A., Grebe, T. A., Lim, C., Weng, S. W., Graham, B. H., and Wong, L. J. (2008) The mitochondrial 13513G→A mutation is associated with Leigh disease phenotypes independent of complex I deficiency in muscle. *Mol. Genet. Metab.* **94,** 485–490

37. Bugiani, M., Invernizzi, F., Alberio, S., Briem, E., Lamantea, E., Carrara, F., Moroni, I., Farina, L., Spada, M., Donati, M. A., Uziel, G., and Zeviani, M. (2004) Clinical and molecular findings in children with complex I deficiency. *Biochim. Biophys. Acta* **1659,** 136–147

38. Chol, M., Lebon, S., Bénit, P., Chretien, D., de Lonlay, P., Goldenberg, A., Odent, S., Hertz-Pannier, L., Vincent-Delorme, C., Cormier-Daire, V., Rustin, P., Rötig, A., and Munnich, A. (2003) The mitochondrial DNA G13513A MELAS mutation in the NADH dehydrogenase 5 gene is a frequent cause of Leigh-like syndrome with isolated complex I deficiency. *J. Med. Genet.* **40,** 188–191

39. Sudo, A., Honzawa, S., Nonaka, I., and Goto, Y. (2004) Leigh syndrome caused by mitochondrial DNA G13513A mutation: frequency and clinical features in Japan. *J. Hum. Genet.* **49,** 92–96

40. Diaz, F., Bayona-Bafaluy, M. P., Rana, M., Mora, M., Hao, H., and Moraes, C. T. (2002) Human mitochondrial DNA with large deletions repopulates organelles faster than full-length genomes under relaxed copy number control. *Nucleic Acids Res.* **30,** 4626–4633

41. Bayona-Bafaluy, M. P., Blits, B., Battersby, B. J., Shoubridge, E. A., and Moraes, C. T. (2005) Rapid directional shift of mitochondrial DNA heteroplasmy in animal tissues by a mitochondrially targeted restriction endonuclease. *Proc. Natl. Acad. Sci. U.S.A.* **102,** 14392–14397

42. Suen, D. F., Narendra, D. P., Tanaka, A., Manfredi, G., and Youle, R. J. (2010) Parkin overexpression selects against a deleterious mtDNA mutation in heteroplasmic cybrid cells. *Proc. Natl. Acad. Sci. U.S.A.* **107,** 11835–11840

43. Bowmaker, M., Yang, M. Y., Yasukawa, T., Reyes, A., Jacobs, H. T., Huberman, J. A., and Holt, I. J. (2003) Mammalian mitochondrial DNA replicates bidirectionally from an initiation zone. *J. Biol. Chem.* **278,** 50961–50969

44. Presley, A. D., Fuller, K. M., and Arriaga, E. A. (2003) MitoTracker Green labeling of mitochondrial proteins and their subsequent analysis by capillary electrophoresis with laser-induced fluorescence detection. *J. Chromatogr. B. Analyt. Technol. Biomed. Life Sci.* **793,** 141–150

CELL BIOLOGY

RNA

Cell Biology:

Modeling of Antigenomic Therapy of Mitochondrial Diseases by Mitochondrially Addressed RNA Targeting a Pathogenic Point Mutation in Mitochondrial DNA

Yann Tonin, Anne-Marie Heckel, Mikhail Vysokikh, Ilya Dovydenko, Mariya Meschaninova, Agnès Rötig, Arnold Munnich, Alya Venyaminova, Ivan Tarassov and Nina Entelis

Access the most updated version of this article at doi: 10.1074/jbc.M113.528968

Find articles, minireviews, Reflections and Classics on similar topics on the JBC Affinity Sites.

Alerts:
- When this article is cited
- When a correction for this article is posted

Click here to choose from all of JBC's e-mail alerts

Supplemental material:
http://www.jbc.org/content/suppl/2014/04/01/M113.528968.DC1.html

This article cites 44 references, 16 of which can be accessed free at
http://www.jbc.org/content/289/19/13323.full.html#ref-list-1

3.5. Lipophilic conjugates of anti-replicative molecules.

3.5.1. Cell transfection with RNA/DNA duplexes

Successful application of antireplicative strategy on *trans*mitochondrial cybrid cells and patients fibroblasts bearing a large deletion or a point mutation in mtDNA, opens a possibility to develop an approach for therapy of mitochondrial deseases. The major limitation for antireplicative RNAs rests in low efficiency of nucleic acids penetration into cells targets.The previous studies were performed with Lipofectamine transfection, which is not aplicable to animal/human models due to high toxicity of Lipofectamine (Lv et al., 2006). Moreover, we demonstrated an extremely high intracellular stability of non-modified "naked" RNA due to lipoplex formation ($t_{1/2}$=17.7h, **Publication 1**). In fact, strong interaction of cationic lipid DOSPA (N,N-dimethyl-N-[2-(sperminecarboxamido)ethyl]-2,3-bis(dioleyloxy)-1-propaniminium pentahydrochloride, a part of Lipofectamine reagent) (Weecharangsan et al., 2007) with RNA molecules may create a barrier for the RNA release from the complex with lipids, resulting in a decreased amount of antireplicative RNA available for the import into mitochondria and, therefore, a transient heteroplasmy shift (Comte et al., 2013).

To decrease the toxicity of cell transfection procedure and create a universal approach of targeting various anti-replicative RNAs into living human cells, we designed molecules containing a cholesterol residue. Cholesterol is a natural lipid and an essential structural component of animal cell membranes, and its transporting efficiency and low toxicity were demonstrated previously by targeting siRNA in human cells (Petrova et al., 2011). Nevertheless, cholesterol can stall the mitochondrial import of therapeutic anti-replicative RNA due to attachment to the mitochondrial membranes. To address this problem, we designed RNA/DNA duplexes of synthetic antireplicative RNA FD20H (**Publication 2)**, and DNA oligonucleotide conjugated with cholesterol (referred to as DNA-probe) (Figure 16 A). RNA FD20H consists of the antireplicative part, flanked by two import determinants (D-arm and F hairpin). Thus, we can anneal the DNA oligonucleotide conjugated with cholesterol to one of the flanking regions. The problem of the duplex formation consisted in the competition between various annealing processes: DNA/RNA hybridization; formation of RNA hairpin, RNA dimer (due to self-compliment parts) and DNA hairpin (Figure 15).
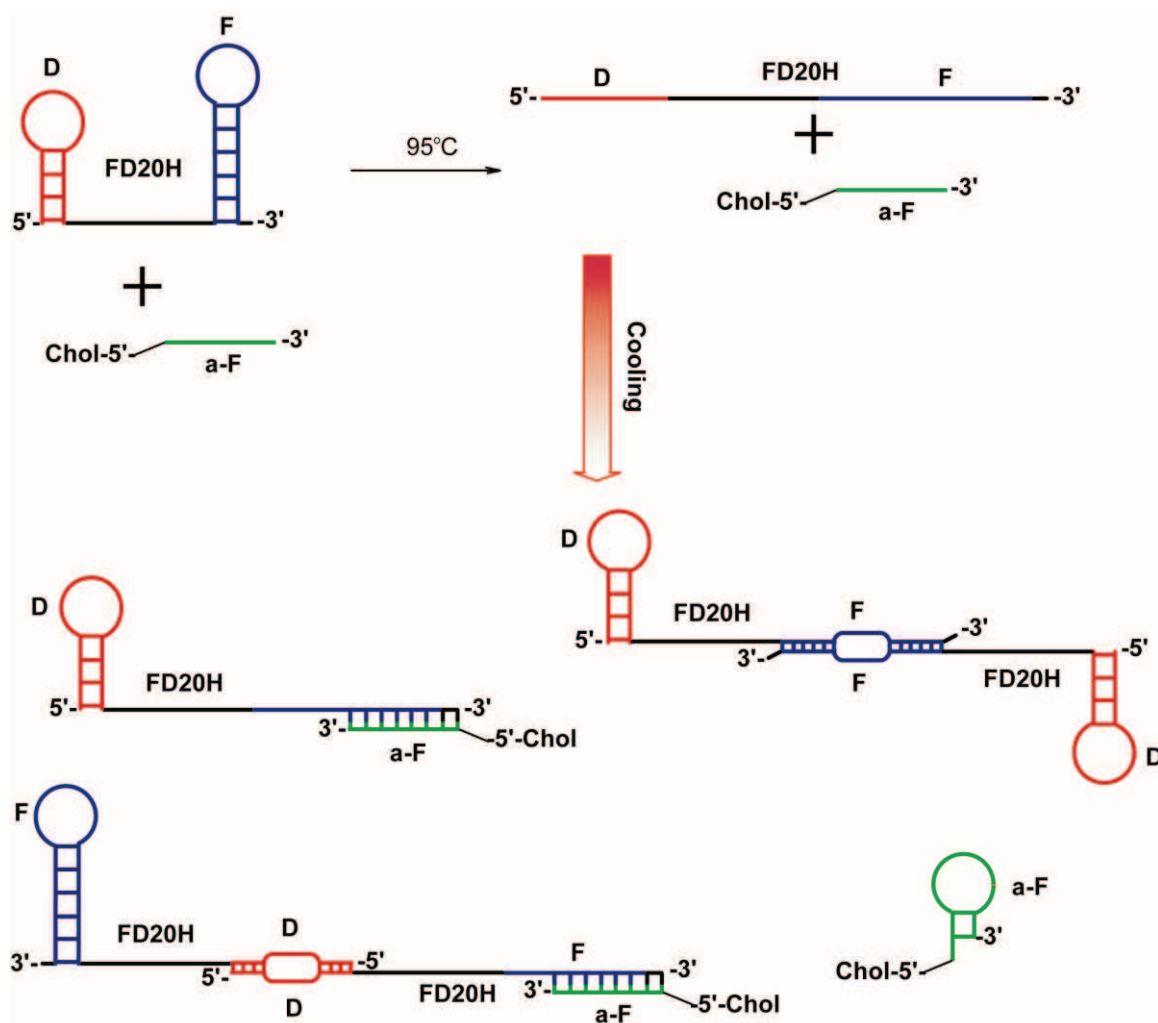
Figure 15. Scheme of FD20H/a-F annealing. Possible reaction products are shown.

To increase the probability of DNA/RNA annealing, we modeled various RNA-DNA duplexes and analyzed their thermodynamic parameters: entropy, enthalpy, Gibbs free energy and temperature of melting (Table 3).

Table 3. Thermodynamic parameters for duplexes formed by FD20H and DNA-probes.

DNA-probe	ΔH, kcal/mol	ΔS, cal/(mol*K)	ΔG$_{37}$, kcal/mol	T$_{m}$,^{o}C
a-F 1	-113.9	-311.5	-17.3	63
a-F 2	-129.6	-357	-18.62	64
a-F 3	-132.5	-357.9	-21.5	70
a-F 4	-141.8	-381.1	-23.6	73
a-D	-166.5	-455.7	-25.2	71.5

Based on these data, we synthesized 3'- and 5'-cholesterol conjugates of DNA oligonucleotides, for DNA probe "a-D" represents the sequence complementary to RNA D-

arm, another probes designed for F-hairpin can be only partially annealed to this RNA domain (Figure 16 A). The length of "a-F" probes is limited by extremely stable DNA hairpin formation; to solve this problem we synthesized chimeric DNA/2'-OMe-RNA molecule a-F2 (Table 3). For the chemical synthesis of cholesterol conjugated oligonucleotides we used an original approach previously developed in my home laboratory in Novosibirsk, with my participation (**Publication 5**).
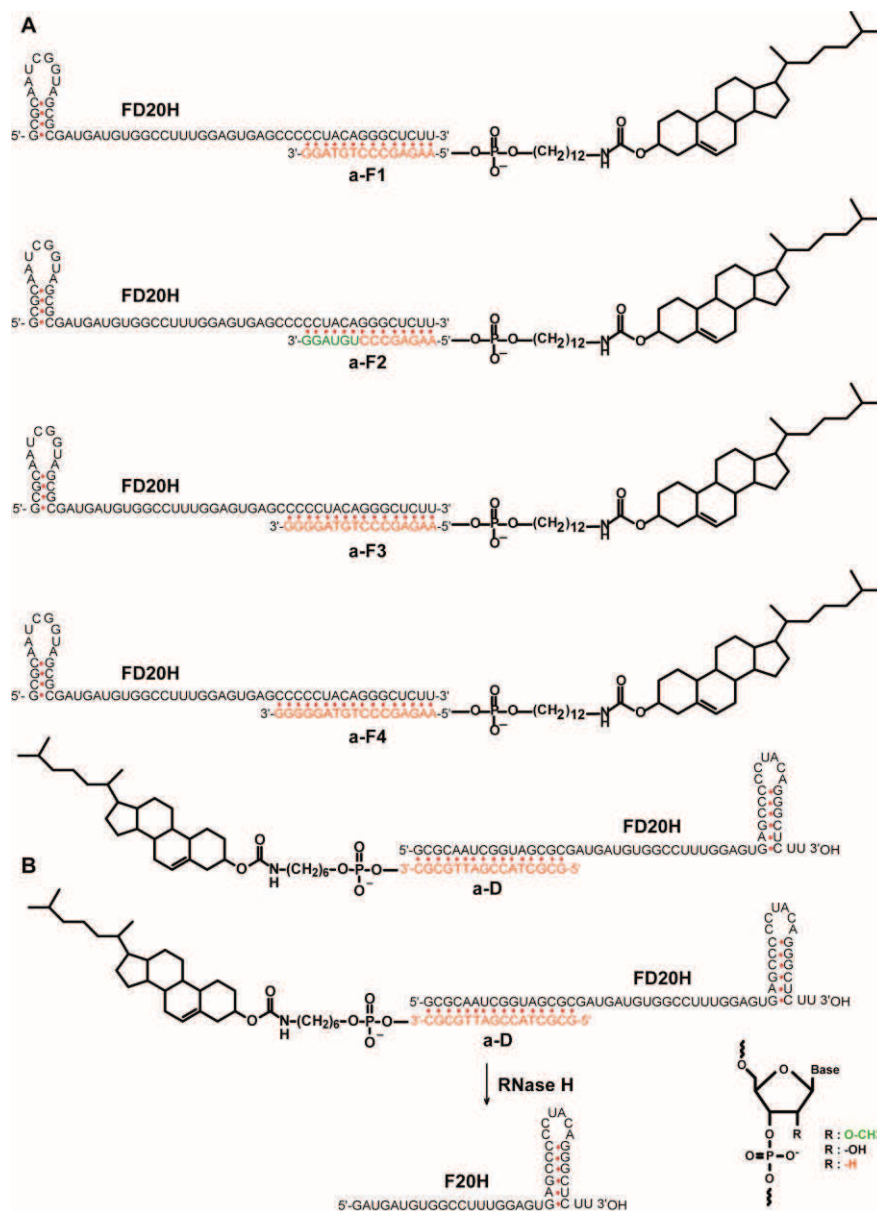
Figure 16. (A) The structure of RNA/DNA conjugates. 2′-OMe nucleotides are shown in green. (B) The cleavage of RNA part annealed with cholesterol containing oligoribonucleotide by RNase H.

We expected that, upon the carrier-free duplex delivery, the cleavage of RNA in the RNA/DNA duplex by cellular RNase H (Evers et al., 2015) (Figure 16 B) will release RNA

bearing antireplicative sequence and import determinant, which will be imported into mitochondria.
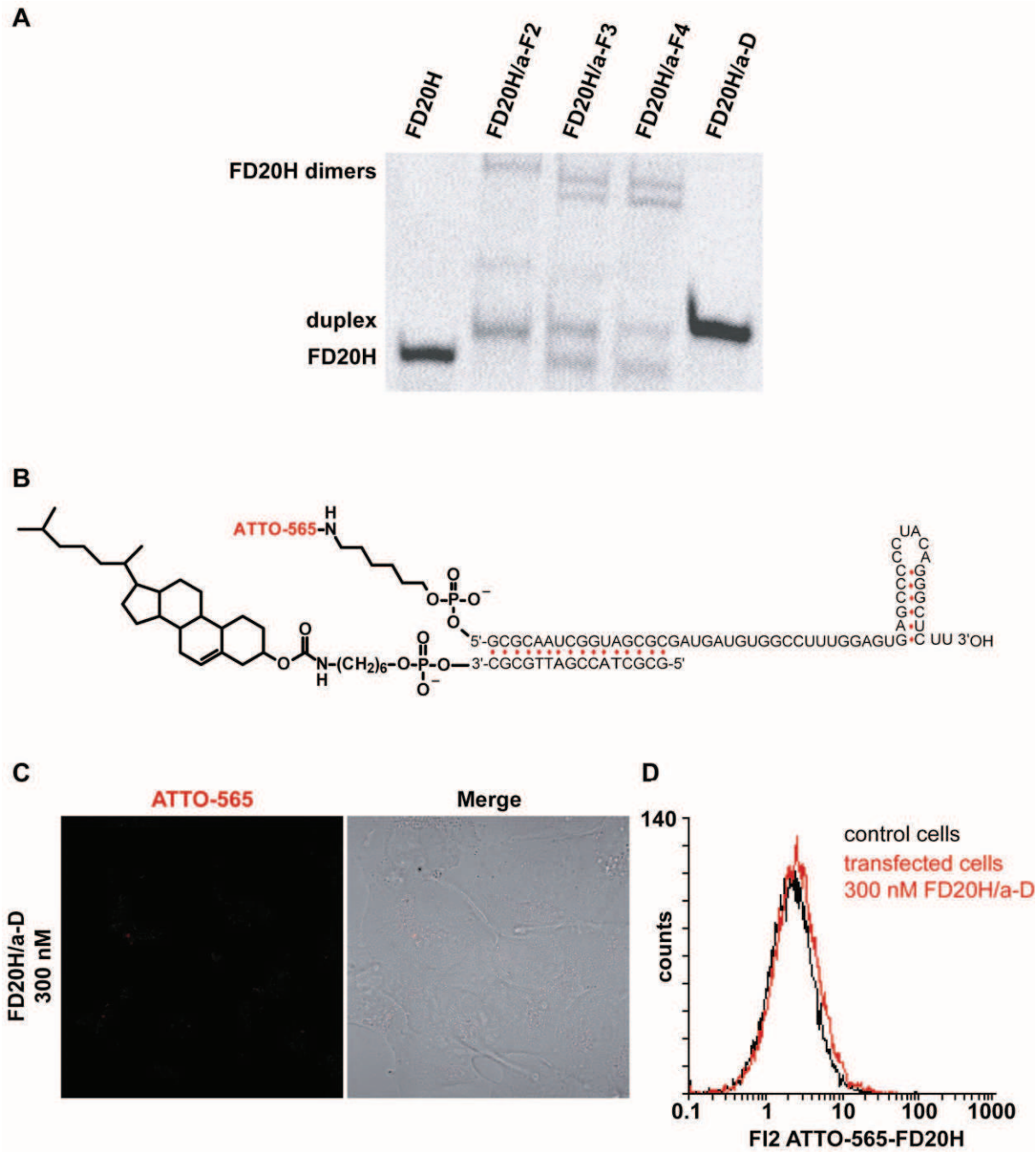
Figure 17. (A) The efficiency of duplex formation after incubation of DNA-probes with FD20H RNA. Native PAGE separation of FD20H RNA annealing with DNA-probes, as indicated above the lanes, RNA:DNA ratio 1:3. (B) Structure of fluorescently labelled RNA/DNA duplex. (C) Confocal image and (D) FACS analysis of 143B cells transiently transfected with 300 nM duplex FD20H/a-D.

The efficiency of duplex formation after incubation of DNA-probes with FD20H RNA was quantified after separation on native PAGE (Figure 17 A). The use of a-D cholesterol

containing conjugate allowed us to obtain high efficiency of duplex formation, contrary to a-F3 and a-F4 DNA-probes which demonstrated low annealing efficiency despite 1:3 RNA:DNA ratio. The methylated version a-F2 was annealed to RNA, however, formation of RNA dimers was also detected. Duplex with a-F1 DNA-probe was not obtained at all (data not shown).

For further experiments we used a-D conjugate. To estimate efficacy of transfection procedure, 143B cells were incubated with fluorescently labeled duplex (ATTO-565-FD20H/a-D, Figure 17 B) at concentrations ranging from 25 to 300 nM. Presence of fluorescence within the cells was analysed by flow cytometry and confocal microscopy. Contrary to our expectations, no transfection could be detected by either method (Figure 17 C and D). This outcome may be explained by: 1) low duplex concentration for carrier-free cell delivery; 2) duplex instability during the transfection procedure; 3) rapid RNA degradation.

3.5.2. Lipophilic conjugates of therapeutic RNA with cleavable bonds: synthesis, cell delivery and mitochondrial targeting.

Since transfection with RNA/DNA duplex was not successful, we designed small antireplicative RNAs covalently conjugated with cholesterol residue. Taking into account the possibility of cholesterol binding to lipid bilayers of intracellular membranes, we introduced biodegradable bonds between the oligoribonucleotide and cholesterol; these included either reducible disulfide bond (construct referred to as D20HssCh) or acid-cleavable hydrazone bond (D20HcnCh). I have synthesised and characterised by NMR spectroscopy all cholesterol derivatives in my home laboratory in Novosibirsk. For the chemical synthesis of oligoribonucleotides conjugated with cholesterol residue through hydrazone bond, a new method has been developed. We also optimised synthesis of fluorescently labelled RNA conjugates (**Publication 3**).

For both constructs (D20HssCh and D20HcnCh), we estimated *in vitro* stability of linkers. For RNA conjugated with cholesterol through hydrazone bond, we tested the acid lability of conjugates by at various pH, and analyzed cleavage products was by gel electroforesis (see **Fig. 3 in Publ. 3**). At neutral pH, cholesterol containing conjugate demonstrated rather high stability (30% of molecules were hydrolized after 24 hours), contrary to a quick hydrolysis at pH<6 (50% and 90% of molecules were hydrolyzed in 2.5 hours at pH 6 and 5.6, respectively).

Stability test for the conjugate with disulfide bond was performed in the presence of glutation tripeptide (GSH), which should reduce the disulfide bond in the cytoplasm. The

antireplicative RNA conjugated with cholesterol were incubated in buffers containing two concentrations of GSH: in millimolar range (corresponding to cytosolic concentration of GSH) and in micromolar range (corresponding to concentration of GSH in blood and transfection media). Products of reaction were analyzed by gel electroforesis (**Fig. 2 in Publ. 3).** After 3h incubation in 5 mM GSH solution, S-S bond reduction was detected in 50% of molecules, whereas < 3 % of molecules were cleaved in micromolar GSH solution. Thus, we demonstrated that both conjugated molecules can be used for transfection, since they should be stable during cell transfection procedure and quickly cleaved, releasing the cholesterol part after internalisation.

In the next step, both molecules were tested for cell transfection ability using 143B human cell line. Cells were incubated with fluorescently labeled RNA conjugates for 15 hours. The efficacy of cell transfection procedure was estimated by cytofluorometry. Hydrazone bond containing conjugate demonstrated rather high efficacy, after incubation with 70 nM D20HcnCh approximately 90% of cells were transfected. In contrast, the disulfide containing conjugate showed lower efficacy of transfection: up to 10% of transfected cells were detected at 110 nM concentration of D20HssCh. Cytofluorometry results were confirmed by confocal microscopy (**Fig. 4, 5 in Publ. 3**).

Further experiments were performed with cells transfected with D20HcnCh conjugates. For molecules containing hydrazone bond, we analysed kinetics of their accumulation. Cells were transfected by fluorescently labeled D20HcnCh, and its accumulation was estimated by FACS. We found that the efficient time of transfection for 70 nM concentration of RNA is 12-15h. In the optimized conditions for the carrier-free cell transfection with D20HcnCh conjugate (15h of incubation with 70 nM D20HcnCh), we used scaning laser confocal microscopy to demonstrate that fluorescently labeled RNA internalized by cells can be partially targeted into mitochondria. In this instance , D20HcnCh was labeled with fluorescein (FITC) at 3'-end, FITC was chosen due to its low affinity to lipid bilayer (Table 2).

Treatment of transfected cells with lysosomotropic agent chloroquine (Varkouhi et al., 2011) impeded RNA co-localisation with mitochondrial network. Chloroquine treatment prevents endosomal acidification (Rutz et al., 2004), thus affecting the D20HcnCh hydrazone bond cleavage. This should result in the decreased amount of D20H RNA molecules released from the membrane-bound conjugate with cholesterol and therefore accessible for the mitochondrial targeting (**Fig. 6 in Publ. 3**).

The RNA component of D20HcnCh conjugate represents an anti-replicative RNA D20H targeting a point mutation in ND5 gene, previously demonstrated to be imported into

mitochondria and able to decrease the heteroplasmy level in human cybrid cells and patient fibroblasts (**Publication 2**). To prove that the released D20H RNA molecules still possess the anti-replicative activity inside the mitochondria, we performed the carrier-free transfection of patient fibroblasts bearing the pathogenic point mutation in ND5 gene of mtDNA, and a small but reliable shift of heteroplasmy level has been observed (**Fig. 7 in Publ. 3**).

Minor impact on heteroplasmy level can be explained by rapid degradation of non-protected RNA in cells and mitochondria, and can be improved by further optimization of the structure and stability of the RNA component of the conjugates. Nevertheless, even the small decrease of heteroplasmy level can be sufficient to obtain a curative effect of mitochondrial dysfunctions in human cells, since only high levels of mutations in human mtDNA become pathogenic (Wallace, 2010). Our data indicate that the conjugation with cholesterol through cleavable bonds may represent a useful and promising approach for a carrier-free delivery of therapeutic anti-replicative RNA molecules into mitochondria of human cells.

3.6. Publication 3.

Ilya Dovydenko, Ivan Tarassov, Alya Venyaminova, Nina Entelis. Method of carrier-free delivery of therapeutic RNA importable into human mitochondria: lipophilic conjugates with cleavable bonds.
Submitted.

Method of carrier-free delivery of therapeutic RNA importable into human mitochondria: lipophilic conjugates with cleavable bonds.

Ilya Dovydenko[1,2], Ivan Tarassov [1], Alya Venyaminova[2], Nina Entelis [1]*

[1] Department of Molecular and Cellular Genetics, UMR Génétique Moléculaire, Génomique, Microbiologie (GMGM), Strasbourg University - CNRS , Strasbourg 67084 France;
[2] Laboratory of RNA Chemistry, Institute of Chemical Biology and Fundamental Medicine, Siberian Branch of Russian Acadadmy of Sciences, Novosibirsk Russia

*Corresponding author, UMR 7156, 4, Allée Konrad Roentgen 67081 STRASBOURG Cedex , France; n.entelis@unistra.fr

ABSTRACT

Defects in mitochondrial DNA often cause neuromuscular pathologies, for which no efficient therapy has yet been developed. MtDNA targeting nucleic acids might therefore be promising therapeutic candidates. Nevertheless, mitochondrial gene therapy has never been achieved because DNA molecules can not penetrate inside mitochondria *in vivo*. In contrast, some small non-coding RNAs are imported into mitochondrial matrix, and we recently designed mitochondrial RNA vectors that can be used to address therapeutic oligoribonucleotides into human mitochondria. Here we describe an approach of carrier-free targeting of the mitochondrially importable RNA into living human cells. For this purpose, we developed the protocol of chemical synthesis of oligoribonucleotides conjugated with cholesterol residue through cleavable covalent bonds. Conjugates containing pH-triggered hydrazone bond were stable during the cell transfection procedure and rapidly cleaved in acidic endosomal cellular compartments. RNAs conjugated to cholesterol through a hydrazone bond were characterized by efficient carrier-free cellular uptake and partial co-localisation with mitochondrial network. Moreover, the imported oligoribonucleotide designed to target a pathogenic point mutation in mitochondrial DNA was able to induce a decrease in the proportion of mutant mitochondrial genomes. This newly developed approach can be useful for a carrier-free delivery of therapeutic RNA into mitochondria of living human cells.

Keywords: cell delivery; RNA therapeutics; RNA conjugates; mitochondrial drug delivery; mitochondrial diseases; antireplicative RNA.

Introduction

Small RNA molecules are increasingly used in clinical applications. RNA-based therapeutics include inhibitors of mRNA translation, agents of RNA interference, ribozymes and aptamers binding various molecular targets [1, 2]. Recently, we developed mitochondrial RNA vectors that can be used to address therapeutic oligoribonucleotides into human mitochondria [3, 4]. To date, >250 human diseases, mostly neuromuscular and neurodegenerative, were shown to be caused by defects in mitochondrial DNA (mtDNA) [5]. The majority of these mutations are heteroplasmic, meaning that mtDNA coexists in two forms, wild type and mutated, in the same cell. The occurrence and severity of pathologic effects depend on the heteroplasmy

level, therefore, the shift in proportion between two types of mitochondrial genome could restore mitochondrial functions [6, 7]. Anti-replicative strategy aims to decrease the heteroplasmy level by targeting into mitochondria the RNA molecules able to affect the replication of mutant mtDNA. Recently, we demonstrated that small RNAs containing structural determinants for mitochondrial import (hairpin domains responsible for RNA mitochondrial targeting) and 20-nucleotide sequence corresponding to the mutated region of mtDNA, are able to anneal selectively to the mutated mitochondrial genomes. Capable to penetrate into mitochondria of cultured human cells, these RNAs induced a decrease of the proportion of mtDNA bearing pathogenic mutations [4, 8].

A factor that significantly limits biomedical application of RNAs is their inefficient delivery to target cells and tissues [9]. Delivery of therapeutic RNAs in the complexes with commercial cationic lipids has been characterized by high toxicity and inefficiency *in vivo* [10]. The conjugation of RNA with the ligands which can be internalized by natural transport mechanisms is a promising approach to overcome this problem [11].

To decrease the toxicity of cell transfection procedure and create an approach of targeting various anti-replicative RNAs into living human cells, we designed conjugates containing a cholesterol residue. Cholesterol is a natural lipid and an essential structural component of animal cell membranes, its efficiency as a transporter molecule and low toxicity were demonstrated by several research groups [12-14]. Nevertheless, cholesterol could stall the mitochondrial import of therapeutic anti-replicative RNA due to attachment to the mitochondrial membranes. To address this problem, we synthesized RNA molecules conjugated with cholesterol through biocleavable covalent bonds. These linkages have been previously used to release drugs under specific conditions: cleavage of disulfide bonds is triggered by a mildly reducing intracellular environment; hydrazone bonds are pH - triggered linkers releasing the drug in acidic conditions of endosomes [15]. Here we describe the synthesis of oligoribonucleotides conjugated with cholesterol through cleavable covalent bonds and show that this approach can be used for a carrier-free transfection of human cells with anti-replicative RNA molecules addressing mtDNA mutations.

Materials and Methods

Chemical compounds

Thiol-Modifier C6 S-S, 5'-Aldehyde-Modifier C2, RNA phosphoramidites and solid supports for oligoribonucleotide synthesis were obtained from Glen Research; cholesteryl chloroformate, 6-aminohexanoic acid, cysteamine, chloroquine diphosphate salt and FITC

isomer I were purchased from Sigma-Aldrich; hydrazine hydrate - from Fluka; ATTO 565 N-succinimidyl ester from ATTO-TEC. Other chemicals were supplied by Merck, Acros and TCI. Solvents were supplied from Panreac.

Synthesis of chemical compounds

6-(Cholesteryloxycarbonylamino)-hexanoic acid (1)

Compound (1) (Fig. 1A, step i) was synthesized as described in [16] with modifications. 6-Aminohexanoic acid (0.9 g, 6.6 mmol) was suspended in dry pyridine (15 ml), then chlorotrimethylsilane (3.3 ml, 26.4 mmol) was added dropwise at 0°C. The mixture was stirred until the solution became clear, then cholesteryl chloroformate (1 g, 2.2 mmol) was added and the reaction mixture was stirred for 3 h at room temperature. Pyridine was evaporated under reduced pressure, the residue was dissolved in dichloromethane (100 ml), washed with 0.7 M hydrochloric acid (50 ml) and saturated aqueous NaCl (50 ml). The organic phase was dried under anhydrous Na_2SO_4 and evaporated under reduced pressure. The residue was purified by Silica gel, pore size 60 Å, 230–400 mesh (Sigma) column chromatography (CH_2Cl_2/EtOH, 0-30%) to obtain (1) with a yield 0.95 g (80%). ^{1}H NMR spectra were recorded on a Bruker AV-400 spectrometer with tetramethylsilane as an internal standard. H[1]-NMR (400 MHz, $CDCl_3$, δ, ppm): 0.69 (s, 3H, H-18/19 cholesterol); 0.87 (d, 3H, H-26/27 cholesterol); 0.89 (d, 3H, H-26/27 cholesterol); 0.93 (d, 3H, H-21 cholesterol); 1.025 (s, 3H, H-18/19 cholesterol); 2.33 (t, 2H, -C$\underline{H}_2$-COOH); 3.35 (dd, 2H, -C$\underline{H}_2$-NH-,); 4.51 (m, 1H, H-3 cholesterol); 4.88 (t, 1H, -NH-,); 5.4 (d, 1H, H-6 cholesterol).

Methyl 6-(cholesteryloxycarbonylamino)hexanoate (2)

Compound (1) (0.2 g, 0.37 mmol) was dissolved in dry dichloromethane (5 ml), phosphorus trichloride (13 µl, 0.149 mmol) was added (Fig. 1A step ii), the reaction mixture was stirred for 3h under argon at 50°C, then absolute methanol (1 ml) was added. The mixture was diluted by dichloromethane (45 ml) and washed with saturated aqueous $NaHCO_3$ (50 ml) and twice by water (50 ml). The organic phase was dried under anhydrous Na_2SO_4 and evaporated to oily residue. The product (2) was purified by Silica gel column chromatography (CH_2Cl_2/EtOH, 0-2.5%) (yield 0.165 g, 80%).

H[1]-NMR (400 MHz, $CDCl_3$, δ, ppm): 0.69 (s, 3H, H-18/19 cholesterol); 0.87 (d, 3H, H-26/27 cholesterol); 0.89 (d, 3H, H-26/27 cholesterol); 0.93 (d, 3H, H-21 cholesterol); 1.025 (s, 3H, H-18/19 cholesterol); 2.29 (t, 2H, -C$\underline{H}_2$-C(O)OCH$_3$,); 3.35 (dd, 2H, -C$\underline{H}_2$-NH-,); 3.65 (s, 3H, -CH$_2$-C(O)OC$\underline{H}_3$,): 4.51 (m, 1H, H-3 cholesterol); 4.88 (t, 1H, -NH-,); 5.4 (d, 1H, H-6 cholesterol).

Hydrazine 6-(cholesteryloxycarbonylamino)hexanoate (3)

Hydrazine derivative (**3**) was synthesized by analogy with [17]. Compound (**2**) (0.1 g, 0.18 mmol) was dissolved in methanol (5 ml). Hydrazine monohydrate (1.25 mL, 49 mmol) was added dropwise (**Fig. 1A step iii**), and the reaction mixture was left for 8 h at room temperature. Compound (**3**) was precipitated in cold water (100 ml), the precipitate was filtered off, washed with water and dried (yield, 0.089 g, 89%). H^1-NMR (400 MHz, CDCl$_3$, δ, ppm): 0.69 (s, 3H, H-18/19 cholesterol); 0.87 (d, 3H, H-26/27 cholesterol); 0.89 (d, 3H, H-26/27 cholesterol); 0.93 (d, 3H, H-21 cholesterol); 1.025 (s, 3H, H-18/19 cholesterol); 2.13 (t, 2H, -C$\underline{H}_2$-C(O)NH-NH$_2$,); 3.35 (dd, 2H, -C$\underline{H}_2$-NH-,); 3.85 (s, 2H, -CH$_2$-C(O)NH-N$\underline{H}_2$,): 4.51 (m, 1H, H-3 cholesterol); 4.88 (t, 1H, -NH-,); 5.4 (d, 1H, H-6 cholesterol); 6.75 (s, H, -CH$_2$-C(O)N$\underline{H}$-NH$_2$).

2-(Pyridyldithio)-ethylamine (4)

Compound (**4**) (**Fig. 1B step i**) was synthesized as described in [18] with some modifications. The reaction was kept under argon atmosphere. Cysteamine (0.23g, 2 mmol) was dissolved in methanol (5 ml) and added dropwise to a stirred solution of 2,2'-dipyridyl disulfide (0.88g, 4 mmol) in methanol/acetic acid (1:25; 4 ml). The mixture was stirred at room temperature for 48 h and then evaporated to oily residue. The product (**4**) was precipitated by cold diethyl ether (20 ml), suspension was filtered and the precipitation step was repeated three times. H^1-NMR (400 MHz, D$_2$O, δ, ppm) 3.1 (m, 2H, NH$_2$-C$\underline{H}_2$-CH$_2$-S-); 3.29 (t, 2H, NH$_2$-CH$_2$-C$\underline{H}_2$-S-); 7.3 (m, 1H, 3'-H, pyridyl); 7.74 (m, 1H, 4 '/ 5'-H, pyridyl), 7.81 (m, 1H, 4' / 5'-H, pyridyl); 8.4 (m, 1H, 6'-H, pyridyl).

Cholesteryl N-[2-(2-pyridyldisulfonyl)ethyl]carbamate (5)

Synthesis of (**5**) was carried out as described in [19] with some modifications (**Fig. 1B step ii**). To the cholesteryl chloroformate solution (0.4 g, 0.9 mmol) in dry dichloromethane (4 ml), were added the suspension of (**4**) (0.1 g, 0.45 mmol) in dioxane (2 ml) and triethylamine (0.15 mL, 1.1 mmol). The reaction mixture was stirred for 48 h under argon at room temperature. After addition of dichloromethane (20 ml), reaction mixture was washed twice with saturated aqueous NaHCO$_3$ (20 mL) and water (20 mL). The organic phase was dried under anhydrous Na$_2$SO$_4$ and evaporated to oily residue. The product (**5**) was purified by Silica gel column chromatography (hexane/ethyl acetate, 0-30%) (yield 0.19 g, 71%). H^1-NMR (400 MHz, CDCl$_3$, δ, ppm): 0.69 (s, 3H, H-18/19 cholesterol); 0.87 (d, 3H, H-26/27 cholesterol); 0.89 (d, 3H, H-26/27 cholesterol); 0.93 (d, 3H, H-21 cholesterol); 1.025 (s, 3H, H-18/19 cholesterol); 2.92 (dd, 2H, -NH-C$\underline{H}_2$-CH2-S-,); 3.44 (m, 2H, -NH-CH$_2$-C$\underline{H}$2-S-,): 4.47 (m, 1H, H-3

cholesterol); 4.88 (t, 1H, -NH-,); 5.35 (d, 1H, H-6 cholesterol); 7.1 (m, 1H, 3'-H, pyridyl); 7.51 (m, 1H, 4 '/ 5'-H, pyridyl), 7.59 (m, 1H, 4' / 5'-H, pyridyl); 8.51 (m, 1H, 6'-H, pyridyl).

Oligonucleotide synthesis

Oligoribonucleotide D20H (**Fig. 1C)** was synthesized on an automatic DNA/RNA ASM-800 synthesizer (Biosset) at 0.4 μmol scale using 2′-O-TBDMS-protected phosphoramidites and solid phase phosphoramidite synthesis protocols [20] optimized for the instrument. Synthesis of 3'-amino modified oligoribonucleotide (N-D20H) was carried out using 3'-PT-Amino-Modifier C6 CPG (Glen Research). At the final step of the synthesis, Thiol-Modifier C6 SS or 5'-Aldehyde-Modifier C2 phosphoramidites were used. Cleavage of oligoribonucleotides from the support and removal of 2′-O-silyl and nucleobase exocyclic amine protecting groups were carried out as described previously [13].

Synthesis of lipophilic conjugates with hydrazone bond (D20HcnCh and N-D20HcnCh)

Modified with 5'-O-Aldehyde-Modifier C2 phosphoramidite oligoribonucleotides D20H and N-D20H were incubated in 80% acetic acid 1h at room temperature to remove the acetal protecting group, then oligoribonucleotides were precipitated by addition of 2% $NaClO_4$ in acetone and isolated via preparative electrophoresis in 12% polyacrylamide/8M urea gel (acrylamide:N,N′-methylenebisacrylamide 30:0.5, TBE buffer, 10 V/cm) followed by elution with 0.3 M NaOAc (pH 5.2)/0.1% SDS solution and precipitation with ethanol. Purified oligoribonucleotides D20H-CHO and N-D20H-CHO were conjugated with compound (**3**) (**Fig. 1A steps iv, v**). For this, the oligoribonucleotides (5 units A_{260}) dissolved in 50μl of 0.1 M NaOAc pH 5.0 were mixed with the same volume of (**3**) (3 mg, 5,2 μmol) in dioxane and incubated 12h at room temperature with permanent stirring. Yield of the products D20HcnCh and N-D20HcnCh was estimated by gel electrophoresis and ethidium bromide staining as a ratio between signals corresponding to product (D20HcnCh or N-D20HcnCh) and initial compound (D20H-CHO or N-D20H-CHO). Cholesterol-conjugated oligoribonucleotides D20HcnCh and N-D20HcnCh were characterized by ESI-TOF-MS analysis (theoretical mass 12405.8 Da, measured mass 12405.2 Da) performed by the Proteomics Platform of Esplanade, Strasbourg, France.

Synthesis of lipophilic conjugates with disulfide bond (D20HssCh and N-D20HssCh)

Modified with Thiol-Modifier C6 S-S phosphoramidite (Glen Research) oligonucleotides D20H and N-D20H (5 units A_{260}) were treated with 50 mM DTT, 25 mM HEPES-NaOH, pH 8.5 at room temperature for 30 min with permanent stirring, precipitated with 2% $NaClO_4$ in acetone, the pellet was washed with acetone and dried. The reduced 5'-thiol containing

oligonucleotide derivatives D20H-SH and N-D20H-SH (**Fig. 1C**) were purified using Bio-Rad P6 column in 100 mM HEPES-NaOH, pH 8.5, for complete elimination of DTT.
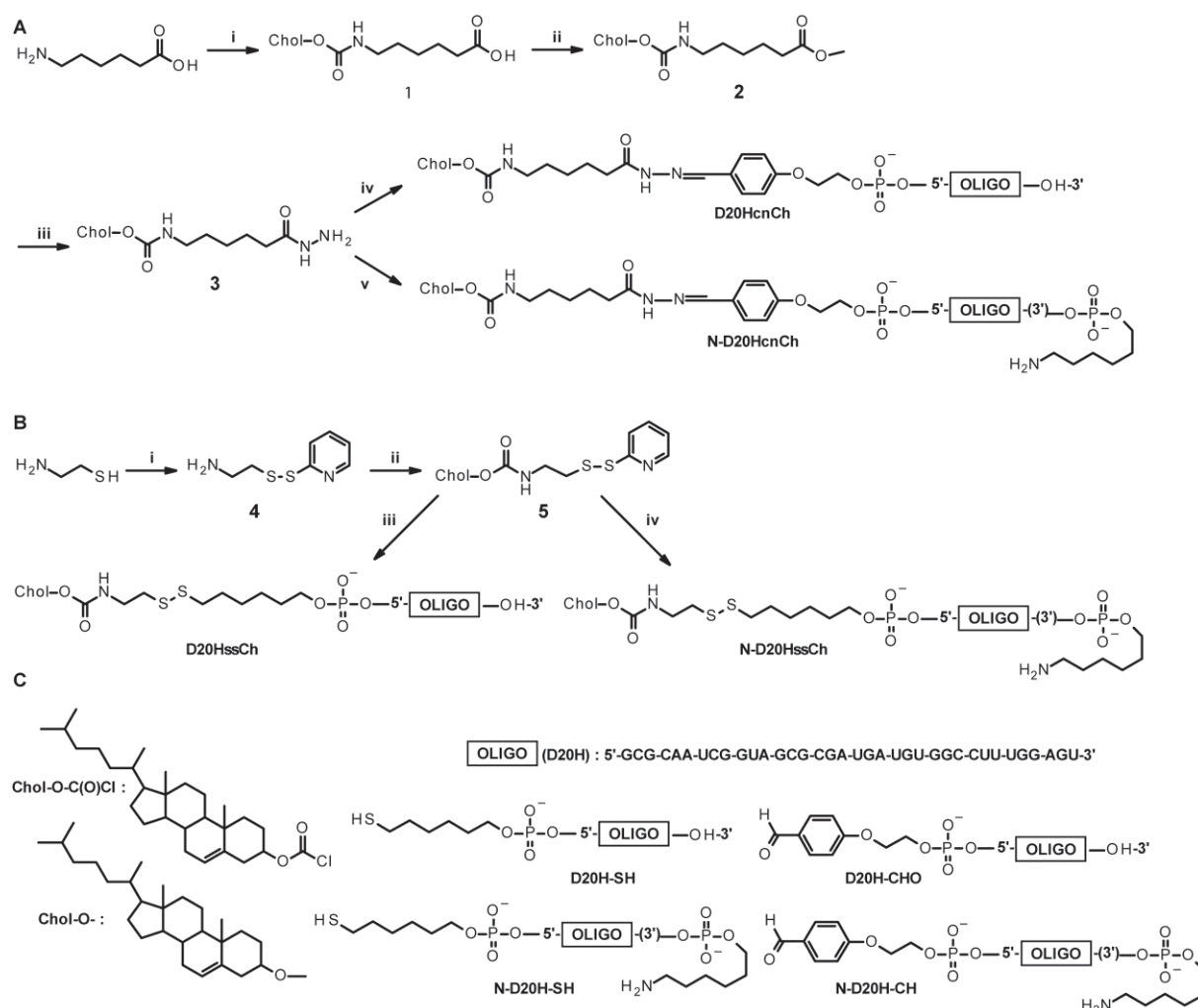
Figure 1. Synthesis of oligoribonucleotides conjugated with cholesterol through cleavable covalent hydrazone (**A**) and disulfide (**B**) bonds. Reagents: **A**, i) $(CH_3)_3SiCl$, Py, $4^{O}C$; CholOC(O)Cl, Py, r.t.; H_3O+; ii) PCl_3, CH_2Cl_2, argon, $50^{O}C$; $MeOH_{abs}$, r.t.; iii) $NH_2NH_2 \cdot H_2O$, MeOH, r.t.; iv)D20H-CHO, 0.1M NaOAc, pH 5.0/dioxane, r.t.; v) N-D20H-CHO, 0.1M NaOAc, pH 5.0/dioxane, r.t.; **B**. i) $(PyS)_2$, MeOH/AcOH, r.t.; ii) CholOC(O)Cl, CH_2Cl_2/dioxane/Et_3N, argon, r.t.; iii) D20H-SH, dioxane, r.t.; iv) N-D20H-SH, dioxane, r.t. **C**. Structure of compounds used for the synthesis.

Compound (**5**) (2 mg, 3,3 µmol) in dioxane (0.2 ml) was added to 5'-thiol oligonucleotide and incubated overnight at room temperature with permanent stirring (**Fig. 1B steps iii, iv**), followed by precipitation with 2% $NaClO_4$ in acetone. Cholesterol-conjugated oligoribonucleotides D20HssCh (yield 30%) and N-D20HssCh (yield 45%) (yields were estimated as described above) were isolated via preparative electrophoresis in 12% polyacrylamide/8M urea gel, followed by elution with 0.3 M NaOAc (pH 5.2)/0.1% SDS

solution and precipitation with ethanol. The purified D20HssCh and N-D20HssCh were characterized by ESI-TOF-MS analysis (theoretical mass – 12320,4 Da, measured mass – 12321,0 Da).

Synthesis of fluorescently labeled conjugates

Labeling of lipophilic conjugates with ATTO-565 or FITC was carried out as described previously [21]. Briefly, the conjugate containing 3′-terminal aminolinker (N-D20HssCh or N-D20HcnCh) (5 units A_{260}) dissolved in 85 µL of 0.1 M HEPES-NaOH, pH 8.5 was mixed with 15 µL of *N*-succinimidyl ester of ATTO-565 in dry DMSO (5 mg/ml); or (N-D20HcnCh) (1 unit A_{260}) in 30 µL of 0.1 M HEPES-NaOH, pH 8.5 was mixed with 30 µL of FITC dissolved in dry DMSO (10 mg/ml). Reaction mixture was incubated overnight at room temperature with permanent stirring. The conjugates were precipitated with ethanol as Na+ salts.

Test of the lipophilic conjugates stability

To test the lipophilic conjugates stability in Opti-MEM Reduced Serum Medium (Gibco), 20 ng of ATTO-565 labeled D20HcnCh or D20HssCh conjugates were incubated 3 h at 37°C in 25 µl of OptiMem medium. To test the hydrazone bond stability, 100 ng of D20HcnCh conjugate was incubated for 2.5, 4, 6, 8 and 24 h at 37°C in 20mM Na-acetate buffer pH 4.6; 5.2 or 5.6 or Na-phosphate buffer pH 6.0; 6.6 or 7.4. Stability of D20HssCh was tested in 20 mM Hepes-NaOH, pH 7.4 containing 5mM glutathion (GSH) 3h at 37°C. For complete reduction of the disulfide bond, the conjugate was incubated with 20 mM β–mercaptoethanol 15 min at room temperature.

Reaction products were separated on 8M urea – 12% PAGE (AA/bisAA 30:0.5), TBE, stained with ethidium bromide and quantified using G-box and GeneTools analysis software (Syngene) or PhosphorImager (Typhoon-Trio, GE Healthcare).

Cell culture and transfection

Homo sapiens osteosarcoma 143B cells and primary skin fibroblasts from a patient, bearing mtDNA point mutation in the *ND5* gene (A13514G) at 30% heteroplasmy level [8], were cultivated at 37°C and 5% CO_2 in MEM (Sigma) containing 1 g/l glucose, supplemented with 10% fetal calf serum (Gibco), 100 U/ml penicillin, 100 µg/ml streptomycin, uridine (50 mg/l) and fungizone (2.5 mg/l) (Gibco). For carrier-free transfection with the lipophilic conjugates labeled with ATTO-565, cells (2 cm^2) were washed with PBS, Opti-MEM Reduced Serum Medium (Gibco) containing conjugates at 10 – 100 nM final concentration was added and cell were cultivated 15h at 37°C and 5% CO_2, then the medium was changed to MEM. Transfection procedure did not lead to detectable decrease of viability of the cells. Efficiency

of transfection was evaluated by flow cytometry using CyFlow® Space (*Partec*), ATTO-565 labeled conjugates were excited at 488nm, and fluorescence emitted at 592 nm. More than 10,000 cells from each sample were analyzed using Flowing Software 2.5.1 (Perttu Terho, Turku Centre for Biotechnology).

Fluorescent confocal microscopy

For confocal microscopy, cybrids cells cultivated in 2 cm² chambers slide (Lab-Tek) were transfected with ATTO-565 or FITC labelled RNA-cholesterol conjugates. At different time periods after transfections, living cells were stained with 100 nM MitoTracker Green or Deep Red correspondingly for 30 min at 37°C, washed and imaged in MEM without red phenol. For chloroquine treatment, transfected cells were cultivated in MEM containing 100 μM chloroquine for 5h, then the medium was changed to MEM. LSM 780 confocal microscope (Zeiss) was used in conjunction with Zen imaging software and images acquired with a Zeiss 63x /1,40 oil immersion objective. The excitation/ emission laser wavelengths were 488 nm (green channel) and 555 nm (red channel). Images were analysed using ImageJ [22] and MosaicSuit plug-in [23].

Heteroplasmy test

Patient fibroblasts were transfected with 1 μM D20HcnCh conjugate for 15h, cultivated 2 days in MEM, then a second transfection was performed in the same conditions. In various post-transfection time periods, cellular DNA was isolated, and heteroplasmy level analysis was performed as described previously [8], using fluorescently labelled primer 5'-FITC-CATACCTCTCACTTCAACCTCC-3' (Eurogentec). Briefly, the heteroplasmy level was analyzed by restriction fragment length polymorphism on a 125-bp PCR fragment where A13514G mutation creates an HaeIII-specific cleavage site. The HaeIII-digested fragments were separated on a 10% PAGE and quantified using PhosphorImager (Typhoon-Trio, GE Healthcare).

Statistical analysis

Results of mitochondrial uptake and heteroplasmy test were statistically processed using the one-way ANOVA, followed by the Duncan's test. values of $p \leq 0.05$ (*), $p \leq 0.001$ (***) were considered to be statistically significant. IBM SPSS software v.22 has been used for analysis. Data are expressed as mean ±S.D. for at least 3 independent experiments.

Results

Lipophilic conjugates of oligoribonucleotides

To establish a carrier-free transfection of human cells with small RNA molecules, we used an anti-replicative RNA (referred to as D20H) targeting a point mutation in ND5 gene, previously demonstrated to be imported into mitochondria and able to decrease the heteroplasmy level in human cybrid cells and patient fibroblasts [8]. This small RNA was conjugated with cholesterol through a biodegradable disulfide bond (D20HssCh, **Fig**. **1**). For this, oligoribonucleotides synthesized according to the phosphoramidite method were 5'-O-thiol-modified and conjugated with cholesteryl N-[2-(2-pyridyldisulfonyl)ethyl]carbamate (compound **5, Fig. 1B**). Since the length of the linker between the RNA and lipophilic residue significantly influenced the cellular accumulation of siRNA conjugates [13], we designed a molecule containing 6 carbon atoms, S-S bridge and another two carbon atoms between 5'-nucleotide of RNA and cholesterol residue (**Fig. 2A**). Purified lipophilic oligoribonucleotide was analyzed by ESI-TOF mass spectrometry. The calculated molecular weight was in agreement with the measured value, confirming the structure of the isolated product.
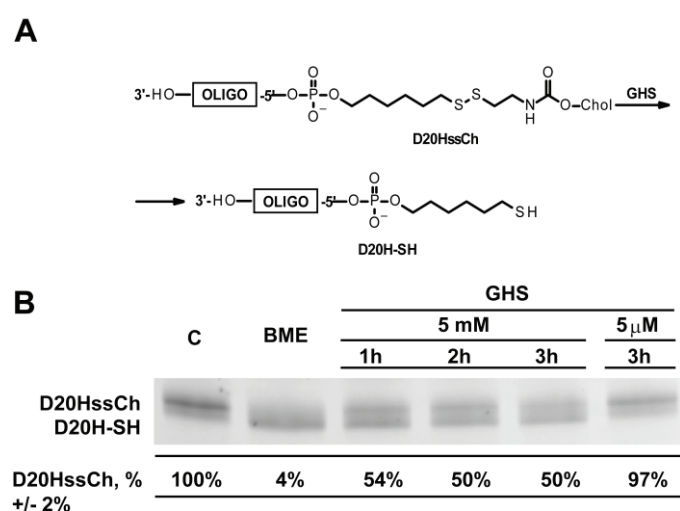
Figure 2. Cleavage of disulfide bond in D20HssCh conjugate in presence of glutathion (GSH). **A**, Structure of D20HssCh conjugate and its reduced form D20H-SH. **B**, Gel electrophoresis analysis of the conjugate treated with GSH as indicated above the panel. Quantification of the portion of D20ssCh (upper band) expressed as mean ±S.D. for 3 independent experiments is shown below the lanes.

Cleavage of the S-S bond by glutathion (GSH) treatment can be detected by separation of molecules bearing or not a cholesterol residue by denaturating PAGE (**Fig. 2B**). After 3h incubation at 37° in buffer containing 5 μM GSH (corresponding to GSH concentration in blood), the S-S bond was not significantly cleaved (**Fig. 2B**). Upon the increase of GSH concentration up to 5 mM (corresponding to GSH concentration in cytosol of mammalian cells [24]), S-S bond reduction was detected in 50% of molecules, indicating that the conjugate of oligoribonucleotide with cholesterol through a disulfide bond should be rapidly cleaved after delivery into cytoplasm.

Another type of biodegradable linker is a hydrazone bond, which can be cleaved in acid conditions of certain cellular compartments including endosomes [15]. To obtain an optimal balance between the hydrazone bond lability under acidic conditions and stability under neutral conditions, we used the combination of an aromatic aldehyde with an aliphatic acyl hydrazide [15] (**Fig. 1A**). We designed a linker containing 2 carbon atoms, hydrazone bridge and another 6 carbon atoms between 5'-nucleotide of RNA and cholesterol residue (**Fig. 3A**)
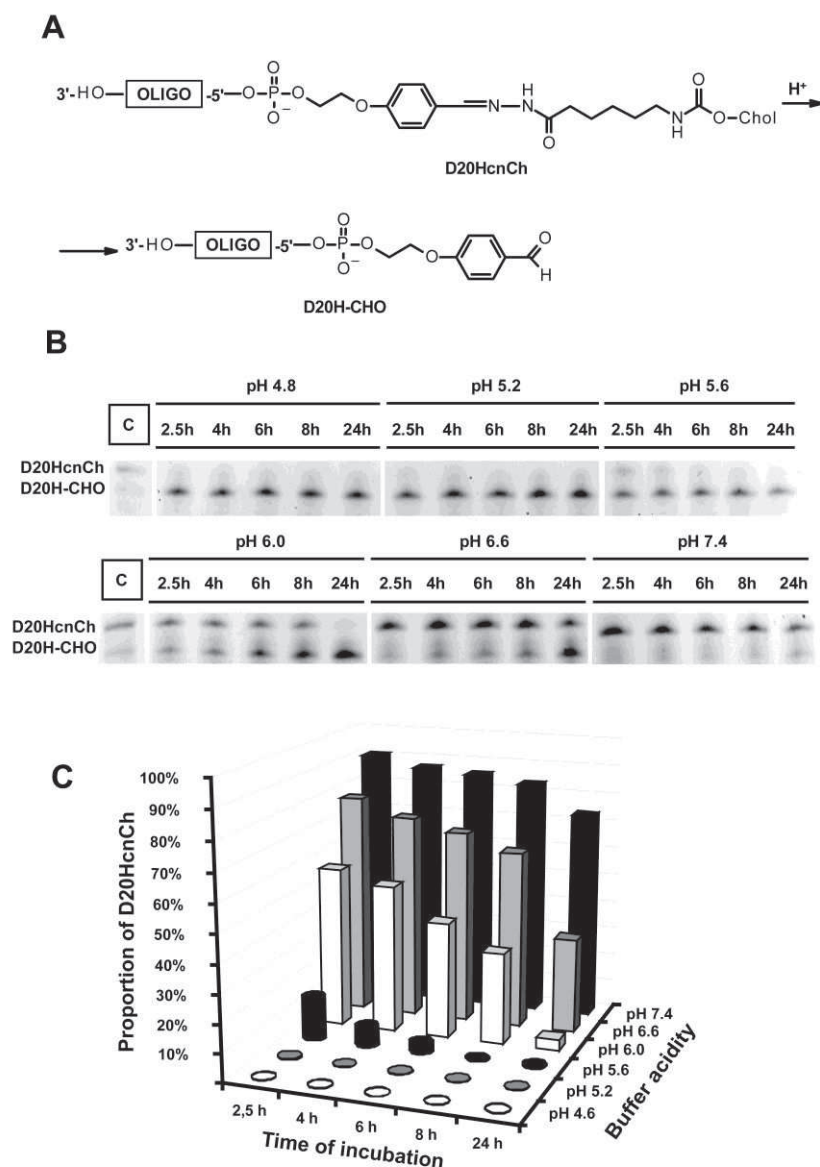
Figure 3. Hydrazone bond cleavage in D20HcnCh conjugate. **A**, Structure of D20HcnCh conjugate and its cleaved form D20H-CHO. **B**, Gel electrophoresis analysis of the hydrolysis products after incubation of the conjugate at various pH during 2.5, 4, 6, 8 and 24 hours (as indicated above the panels). Bands corresponding to the full size conjugate (upper band) and the product of its acid hydrolysis (lower band) are indicated at the left. **C**, Quantification of the full size conjugate (%, axis Y) depending on pH and the time of incubation.

For this, hydrazino 6- (cholesteryloxycarbonylamino) hexanoate (compound **3, Fig. 1A**) was synthesized and conjugated to D20H RNA. Lability of the resulted hydrazone bond was tested

at various pH conditions, demonstrating that the hydrazone link is stable at pH 6.6 and above, while at pH 6.0 it was completely cleaved in 24h. At more acidic pH (5.6 and below), cholesterol residue was quickly cut from oligoribonucleotide (50% and 90% of molecules were hydrolyzed in 2.5 hours at pH 6 and 5.6 respectively) (**Fig. 3**). Therefore, the conjugate of oligoribonucleotide with cholesterol through a hydrazone bond (referred to as D20HcnCh) should be stable during the cell transfection procedure (pH 7.4), and then would be cleaved inside the endosomes, thus facilitating the release and further mitochondrial import of the RNA moiety.

Cellular uptake of lipophilic conjugates

To detect and quantify the cellular uptake of RNA conjugated with cholesterol, 3'-end of the oligoribonucleotide was labeled with fluorescent compound ATTO-565. Carrier-free transfection of cultured human cells was performed by incubation of cells with increasing concentrations of RNA conjugated with cholesterol. Efficiency of transfection was measured using cytofluorometry (**Fig. 4 A,B**).
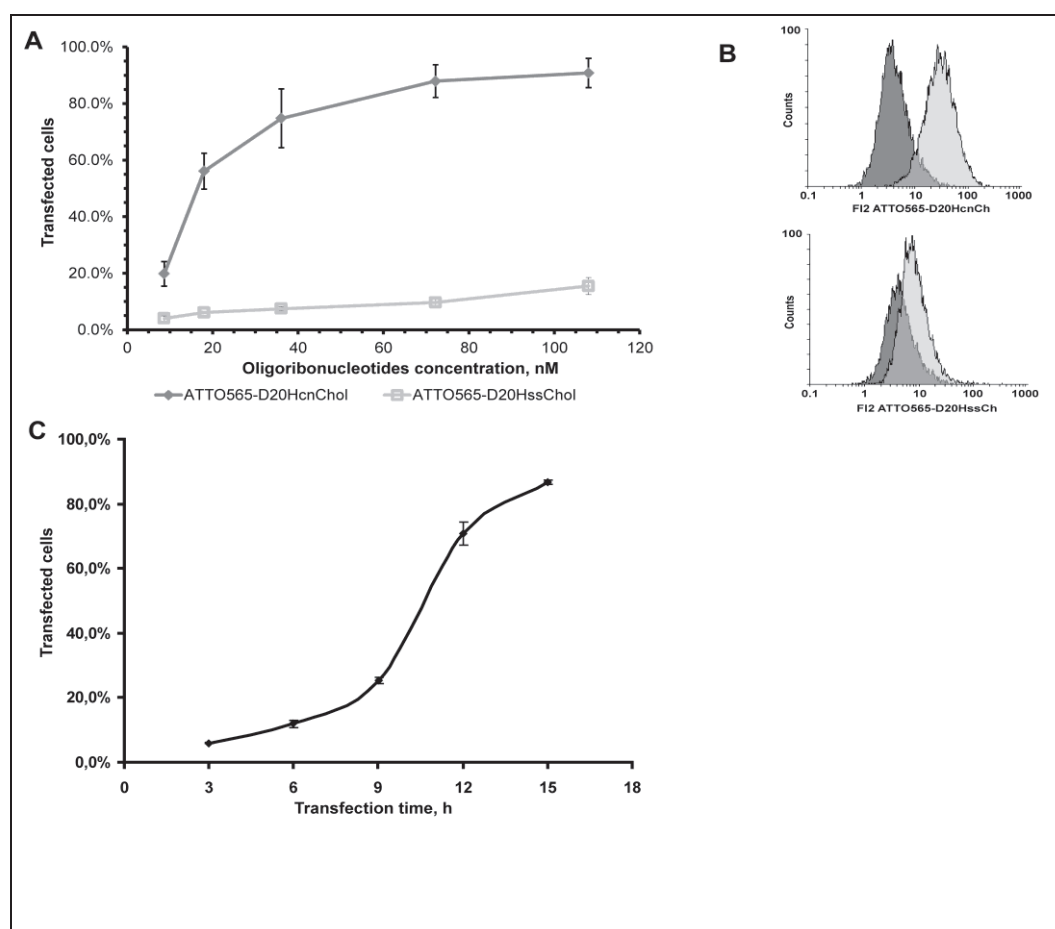
Figure 4. Cellular uptake of ATTO-labeled lipophilic conjugates estimated by flow cytometry. **A**, percentage of ATTO-positive cells in the population after 15h incubation

with increased concentrations of conjugates (indicated below). **B**, an example of flow cytometry analysis, cells were incubated 15h with 70 nM ATTO-D20HcnCh (above) or ATTO-D20HssCh (lower panel). In dark gray, signal corresponding to auto-fluorescence of non-transfected cells. **C**, the percentage of ATTO-positive cells in the population after incubation with 70 nM D20HcnCh during various periods of time (indicated below). More than ten thousand events were counted in each sample; mean values from three independent experiments are presented.

Cellular delivery of RNA conjugated with cholesterol through a disulfide bond (D20HssCh) was rather inefficient, the fluorescence exceeding the maximum level of cell auto-fluorescence was detected in less than 10% of cells. In contrast to poor uptake obtained for D20HssCh, D20H RNA conjugated through a hydrazone bond (D20HcnCh) was rather efficiently internalized by cells. Percentage of transfected cells reached a plateau of 90±2% after 15h of incubation with 70 nM D20HcnCh (**Fig. 4C**). Fluorescent confocal microscopy images also demonstrated a very low internalization of D20HssCh molecules and efficient accumulation of D20HcnCh in the cytoplasm of transfected cells (**Fig**. **5**).
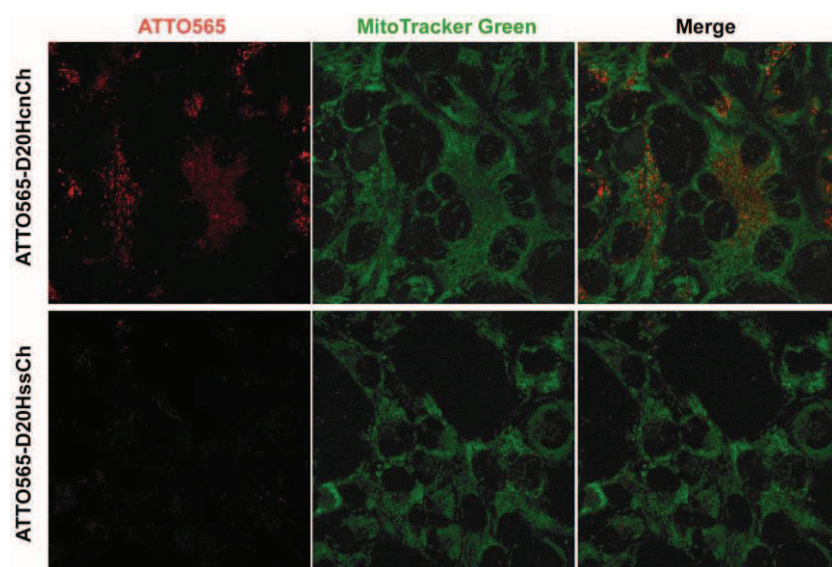
Figure 5. Cellular uptake of ATTO-labeled lipophilic conjugates analyzed by fluorescent confocal microscopy after 15h incubation with ATTO-D20HcnCh or ATTO-D20HssCh as indicated at the left. Mitochondria were stained with MitoTracker Green (indicated above the panel).

To explain the low level of D20HssCh delivery, we tested the stability of the both conjugates in conditions used for cells transfection and could not detect a significant degradation (data not shown). Thus, a cause of low efficacy of transfection with RNA conjugate containing disulfide bond remains unclear. Further experiments were performed with cells transfected with D20HcnCh conjugate.

Mitochondrial targeting and anti-replicative capacity of D20H RNA

We used optimized conditions for the carrier-free cell transfection with D20HcnCh conjugate (15h of incubation with 70 nM D20HcnCh) to check if the RNA-component of the internalized conjugate can be targeted to mitochondria. For this, we used confocal laser scanning microscopy of living cells. D20HcnCh was labeled with fluorescein (FITC) at 3'-end, mitochondrial network stained by MitoTracker Deep Red, and co-localization of fluorescent signals had been quantified and statistically analyzed (**Fig. 6**). The data clearly show that the FITC-labeled molecules were partially (13 ± 3 % of the cellular pool) addressed to mitochondria 20-45h post-transfection, then the co-localization level has been significantly decreased, probably indicating on the RNA degradation in the mitochondrial matrix (**Fig. 6 A, B**). Control experiments with FITC only did not demonstrate significant co-localization with mitochondria (1-2%, not shown).
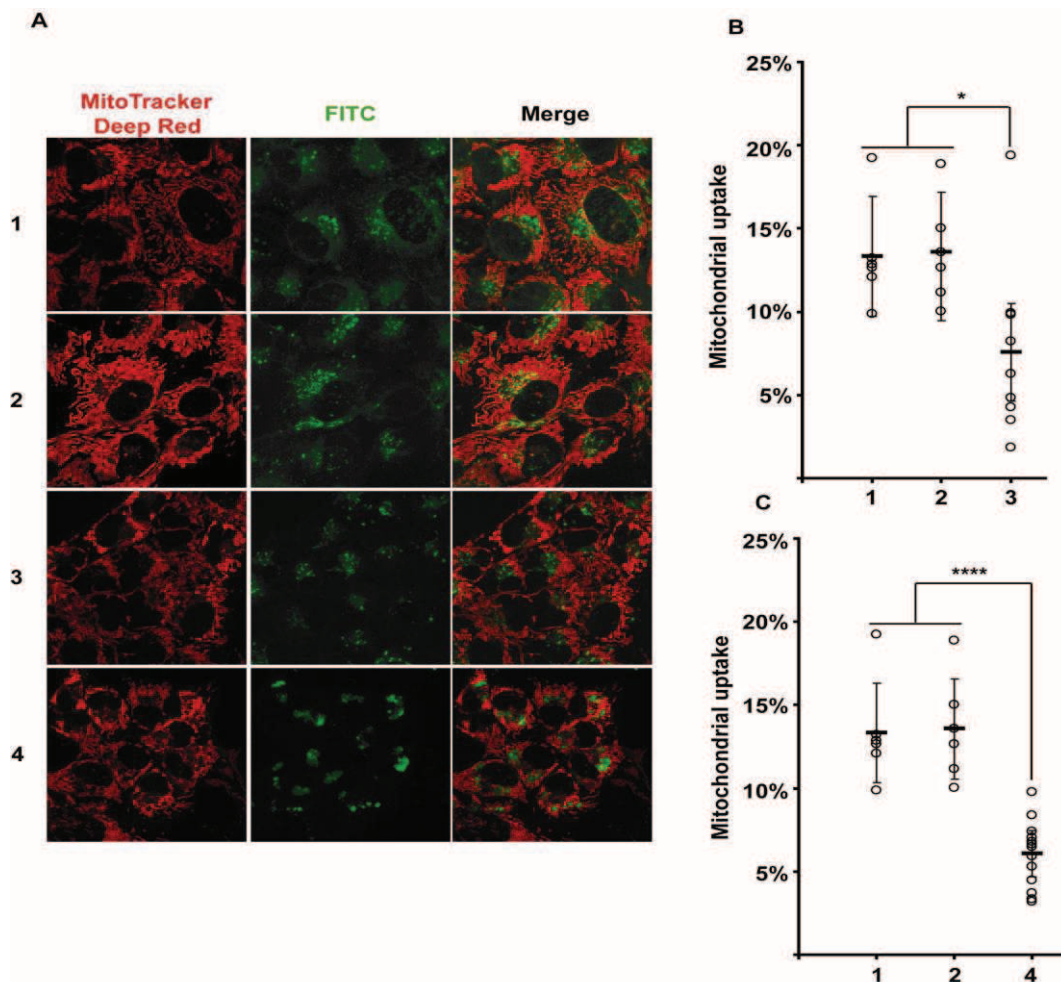
Figure 6. Mitochondrial targeting of D20H RNA evaluated by fluorescent confocal microscopy. **A**, confocal microscopy images of 143B cells incubated with FITC-D20HcnCh (green signal), 20h (**1**), 45h (**2**) and 70h (**3**) post-transfection; (**4**), cells were incubated with FITC-D20HcnCh for 15h, treated with chloroquine for 5h and analyzed 45h post-transfection. Mitochondrial network was visualized by

MitoTracker DeepRed staining. **B** and **C**, quantification of RNA co-localization with mitochondria, estimated as the percentage of green fluorescence signal co-localized with red fluorescence for 6–14 optical sections. The data were statistically processed using the one-way ANOVA, followed by the Duncan's test. Significant differences between cells: *, $p < 0.05$; ****, $p < 0.001$.

To check the impact of the hydrazone bond cleavage, which was anticipated to occur in acid conditions inside the endosomes, facilitating the release and mitochondrial import of RNA, we treated the transfected cells with chloroquine, an agent that prevents endosomal acidification, commonly used to study the role of endosomal pH in cellular processes [25]. After 5h of chloroquine treatment, the level of D20H co-localisation with mitochondria was significantly decreased (**Fig. 6 A,C**). This indicates that the increased endosomal pH, preventing the D20HcnCh hydrazone bond cleavage, resulted in the decreased amount of D20H RNA molecules released from the membrane-bound conjugate with cholesterol and therefore accessible for the mitochondrial targeting.

To prove that the released D20H RNA still possessed the anti-replicative activity inside the mitochondria, we performed the carrier-free transfection of patient fibroblasts bearing the pathogenic point mutation in ND5 gene of mtDNA [8]. In various post-transfection time periods, cellular DNA was isolated, and the proportion between normal and mutant mitochondrial genomes (so called heteroplasmy level) was measured by cleavage of the PCR amplicon (**Fig. 7**). A small but significant decrease of the mutant mtDNA proportion has been detected in the transfected fibroblasts, but not in the control cells cultivated in the same conditions. These data indicate that the conjugation with cholesterol can be useful for a carrier-free delivery of therapeutic anti-replicative RNA into mitochondria of human cells.
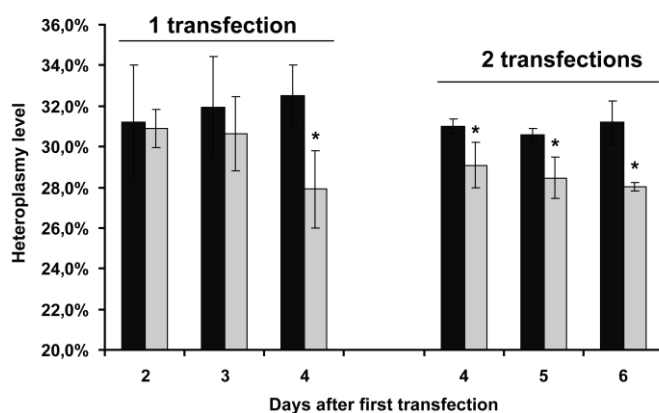
Figure 7. The effect of D20HcnCh on heteroplasmy level in transfected patient fibroblasts bearing A13514G mutation in mtDNA. Time dependence of heteroplasmy level during 6 days (as indicated below the graphs) after one or two consecutive transfections with D20HcnCh conjugate (shown in gray) or in the control cells cultivated in the same conditions without transfection (in black). Data are expressed as mean ±S.D. for 3–4 independent experiments. Significant differences between control and transfected cells were calculated by one-way ANOVA, followed by Duncan's test (*, $p < 0.05$).

14

Discussion

RNA therapeutics is an emerging class of innovative medicine. In recent years, significant progress has been made to overcome some of the obstacles associated with *in vivo* delivery of RNA [25]. Lipid nanoparticles represent one of the most advanced technological platforms [26], together with the rapidly developing approach of molecular conjugates, as triple acetyl-galactosamine conjugates and combination of backbone neutralization with cell-penetrating peptides [27], or lipophilic conjugates [12, 28]. A variety of lipophilic moieties can be conjugated to siRNAs to improve the *in vivo* uptake, the best studied one is cholesterol. Mechanistically, cholesterol-modified siRNAs interact with serum lipoprotein particles and the uptake is dependent upon cellular lipoprotein and other *trans*membrane receptors [12]. Recently reported data demonstrate that the adsorption of siRNA lipophilic conjugates on the cell surface and their subsequent transport into the cells could occur *via* the mechanism of endocytosis. It was suggested that two main factors might determine the efficacy of adsorption of the conjugates on the cell surface: the hydrophobicity of the conjugates and the distance between negatively charged cellular membrane and anionic siRNA [13]. The long aliphatic linker in the conjugate structure provides an optimal distance between the cellular membrane and siRNA moiety, along with an increase of the hydrophobicity of the conjugates. Taking into account these data, we synthesized mitochondrially imported RNAs conjugated to cholesterol through the linker containing 8 aliphatic -CH2- units.

Another important point is that chemical modifications introduced into RNA molecules should not interfere with their sub-cellular localisation and therapeutic function. In case of siRNA duplexes, lipophilic residue can be conjugated to the sense strand, which is destroyed upon the cell delivery by RISC complex. For anti-replicative RNAs, expected to be mitochondrially targeted and to interact with mutant mitochondrial genomes stalling their replication [4], the cholesterol residue, improving the cellular uptake, can also create an obstacle for the mitochondrial import. In fact, human mitochondria possess a system facilitating the transport of cholesterol from the outer mitochondrial membrane to the inner one. This transport is necessary for cholesterol metabolization to pregnenolone, the precursor of all steroid hormones [29]. Translocator protein of the outer mitochondrial membrane TSPO consists of five *trans*membrane helices forming a channel-like structure that may accommodate the import of lipophilic molecules into mitochondria and contains a recognition motif with high affinity to cholesterol [30]. Therefore, the cholesterol residue can be recognized by TSPO and translocated through the outer mitochondrial membrane. In this case, RNA molecule conjugated with cholesterol would be trapped on the outer membrane

15

and, probably, could not be addressed into mitochondrial matrix. To avoid this problem, we introduced a cleavable linker between RNA and cholesterol residue. We expected that the linkers (disulfide or hydrazone bonds) should be stable during cell transfection procedure and cleaved upon internalizing of the conjugate in the cytoplasm [15]. Mammalian cells uptake of extracellular macromolecules proceeds through endocytosis, leading (for the most of endocytosis pathways) to formation of vesicle-like structures that fuse with early endosomes characterised by a reduced pH (6.0–6.6, compared to a physiological pH 7.2–7.4) [31]. The pH drops further during endosomal processing, reaching 5.0 at the late endosomal stage. Therefore, we supposed that the hydrazone bond between RNA and cholesterol moieties would be cleaved inside the endosome, while the disulfide bond should be cleaved after release of the conjugate into the cytoplasm. In both cases, this should permit the mitochondrial targeting of the therapeutic RNA.

Unexpectedly, our data revealed a very low level of cellular uptake for RNA conjugated with cholesterol through a disulfide bond (D20HssCh) compared to RNA conjugated through a hydrazone bond (D20HcnCh). The cause of low efficacy of transfection with RNA conjugate containing disulfide bond remains unclear. It had been demonstrated that siRNAs conjugated through disulfide bond were rather efficient in knockdown [32], however, the level of cell transfection had not been estimated. As a possible explanation of low transfection, we can hypothesize a self-assembling of conjugates into micelle-like particles where cholesterol residue and the linker form hydrophobic core which is shelled by water-soluble RNA. Soft micellar nanoparticles assembly from DNA-cholesterol conjugates have been recently described [33]. Cholesterol residues shielded inside the particles could not bind the cell surface receptors and, therefore, penetrate the cells.

Hydrazone bonds demonstrated an improved stability in the transfection media, thus assuring an efficient carrier-free cellular uptake of the conjugated molecule D20HcnCh. The level of its consequent co-localisation with mitochondria was estimated as 13±3 % of the D20H cellular pool (**Fig. 6**). We suppose that this value is limited by the endosomal escape of the D20H RNA after the hydrazone bond cleavage in acidic conditions. However, the treatment of transfected cell with chloroquine, one of the endosomal escape agents, which was supposed to facilitate the disruption of the endosomal membrane due to proton sponge mechanism [34], in fact decreased the mitochondrial targeting of D20H RNA (**Fig. 6**). This results indicate that the conjugated molecules D20HcnCh were anchored in the endosomal membranes by the cholesterol residue. Since the endosomal pH has been increased by the chloroquine treatment, the hydrazone bond between the cholesterol and RNA components

was not cleaved, and RNA could not be released into cytoplasm even after the disruption of endosomes.

Noteworthy, the moderate mitochondrial import of D20H RNA still allowed detection of its anti-replicative activity. Even the small decrease of heteroplasmy level (**Fig. 7**) can be important to obtain a curative effect of mitochondrial dysfunctions in human cells, since only high levels of mutations in human mtDNA become pathogenic [6], while a small reduction of the mutant DNA load can provide significant clinical improvement [35]. We believe that the present study represents a further step towards the development of RNA therapeutics against incurable mitochondrial diseases.

Acknowledgements

References
1. Burnett, JC, and Rossi, JJ (2012). RNA-based therapeutics: current progress and future prospects. *Chemistry & biology* **19**: 60-71.
2. Tavernier, G, Andries, O, Demeester, J, Sanders, NN, De Smedt, SC, and Rejman, J (2011). mRNA as gene therapeutic: how to control protein expression. *J Control Release* **150**: 238-247.
3. Kolesnikova, O*, et al.* (2010). Selection of RNA aptamers imported into yeast and human mitochondria. *RNA* **16**: 926-941.
4. Comte, C*, et al.* (2013). Mitochondrial targeting of recombinant RNAs modulates the level of a heteroplasmic mutation in human mitochondrial DNA associated with Kearns Sayre Syndrome. *Nucleic Acids Res* **41**: 418-433.
5. Ruiz-Pesini, E*, et al.* (2007). An enhanced MITOMAP with a global mtDNA mutational phylogeny. *Nucleic Acids Res* **35**: D823-828.
6. Wallace, DC (2010). Mitochondrial DNA mutations in disease and aging. *Environmental and molecular mutagenesis* **51**: 440-450.
7. Taylor, RW, and Turnbull, DM (2005). Mitochondrial DNA mutations in human disease. *Nat Rev Genet* **6**: 389-402.
8. Tonin, Y*, et al.* (2014). Modeling of antigenomic therapy of mitochondrial diseases by mitochondrially addressed RNA targeting a pathogenic point mutation in mitochondrial DNA. *J Biol Chem* **289**: 13323-13334.

9. Zhou, J, Shum, KT, Burnett, JC, and Rossi, JJ (2013). Nanoparticle-Based Delivery of RNAi Therapeutics: Progress and Challenges. *Pharmaceuticals (Basel, Switzerland)* **6**: 85-107.

10. Lv, H, Zhang, S, Wang, B, Cui, S, and Yan, J (2006). Toxicity of cationic lipids and cationic polymers in gene delivery. *J Control Release* **114**: 100-109.

11. Winkler, J (2013). Oligonucleotide conjugates for therapeutic applications. *Ther Deliv* **4**: 791-809.

12. Wolfrum, C*, et al.* (2007). Mechanisms and optimization of in vivo delivery of lipophilic siRNAs. *Nat Biotechnol* **25**: 1149-1157.

13. Petrova, NS*, et al.* (2012). Carrier-free cellular uptake and the gene-silencing activity of the lipophilic siRNAs is strongly affected by the length of the linker between siRNA and lipophilic group. *Nucleic Acids Res* **40**: 2330-2344.

14. Letsinger, RL, Zhang, GR, Sun, DK, Ikeuchi, T, and Sarin, PS (1989). Cholesteryl-conjugated oligonucleotides: synthesis, properties, and activity as inhibitors of replication of human immunodeficiency virus in cell culture. *Proc Natl Acad Sci U S A* **86**: 6553-6556.

15. West, KR, and Otto, S (2005). Reversible covalent chemistry in drug delivery. *Curr Drug Discov Technol* **2**: 123-160.

16. Yamada, C, Khvorova, A, Kaiser, R, Anderson, E, and Leake, D (2013). Duplex oligonucleotide complexes and methods for gene silencing by RNA interference. Google Patents.

17. Tognolini, M*, et al.* (2012). Structure-activity relationships and mechanism of action of Eph-ephrin antagonists: interaction of cholanic acid with the EphA2 receptor. *ChemMedChem* **7**: 1071-1083.

18. Zugates, GT, Anderson, DG, Little, SR, Lawhorn, IE, and Langer, R (2006). Synthesis of poly(beta-amino ester)s with thiol-reactive side chains for DNA delivery. *J Am Chem Soc* **128**: 12726-12734.

19. Sugahara, M, Uragami, M, Yan, X, and Regen, SL (2001). The structural role of cholesterol in biological membranes. *J Am Chem Soc* **123**: 7939-7940.

20. Bellon, L (2001). Oligoribonucleotides with 2'-O-(tert-butyldimethylsilyl) groups. *Curr Protoc Nucleic Acid Chem* **Chapter 3**: Unit 3 6.

21. Dovydenko, I*, et al.* (2015). Mitochondrial targeting of recombinant RNA. *Methods Mol Biol* **1265**: 209-225.

22. Schneider, CA, Rasband, WS, and Eliceiri, KW (2012). NIH Image to ImageJ: 25 years of image analysis. *Nat Methods* **9**: 671-675.

23. Rizk, A*, et al.* (2014). Segmentation and quantification of subcellular structures in fluorescence microscopy images using Squassh. *Nature protocols* **9**: 586-596.

24. Hwang, C, Sinskey, AJ, and Lodish, HF (1992). Oxidized redox state of glutathione in the endoplasmic reticulum. *Science* **257**: 1496-1502.

25. de Fougerolles, AR (2008). Delivery vehicles for small interfering RNA in vivo. *Hum Gene Ther* **19**: 125-132.

26. Hope, MJ (2014). Enhancing siRNA delivery by employing lipid nanoparticles. *Ther Deliv* **5**: 663-673.

27. Meade, BR*, et al.* (2014). Efficient delivery of RNAi prodrugs containing reversible charge-neutralizing phosphotriester backbone modifications. *Nat Biotechnol* **32**: 1256-1261.

28. Raouane, M, Desmaele, D, Urbinati, G, Massaad-Massade, L, and Couvreur, P (2012). Lipid conjugated oligonucleotides: a useful strategy for delivery. *Bioconjug Chem* **23**: 1091-1104.

29. Miller, WL, and Bose, HS (2011). Early steps in steroidogenesis: intracellular cholesterol trafficking. *J Lipid Res* **52**: 2111-2135.
30. Jaremko, L, Jaremko, M, Giller, K, Becker, S, and Zweckstetter, M (2014). Structure of the mitochondrial translocator protein in complex with a diagnostic ligand. *Science* **343**: 1363-1366.
31. De Haes, W, Van Mol, G, Merlin, C, De Smedt, SC, Vanham, G, and Rejman, J (2012). Internalization of mRNA lipoplexes by dendritic cells. *Mol Pharm* **9**: 2942-2949.
32. Chen, Q*, et al.* (2010). Lipophilic siRNAs mediate efficient gene silencing in oligodendrocytes with direct CNS delivery. *J Control Release* **144**: 227-232.
33. Magnusson, JP, Fernandez-Trillo, F, Sicilia, G, Spain, SG, and Alexander, C (2014). Programmed assembly of polymer-DNA conjugate nanoparticles with optical readout and sequence-specific activation of biorecognition. *Nanoscale* **6**: 2368-2374.
34. Varkouhi, AK, Scholte, M, Storm, G, and Haisma, HJ (2011). Endosomal escape pathways for delivery of biologicals. *J Control Release* **151**: 220-228.
35. Picard, M*, et al.* (2014). Progressive increase in mtDNA 3243A>G heteroplasmy causes abrupt transcriptional reprogramming. *Proc Natl Acad Sci U S A* **111**: E4033-4042.

CONCLUSIONS AND PERSPECTIVES

Conclusions and perspectives

My PhD study addressed the problem of carrier-free cell delivery, stability and mitochondrial targeting of therapeutic anti-replicative RNA molecules.

The main results and conclusions of my work are:

1. Synthesis of the various versions of antireplicative RNA imported into human mitochondria bearing modifications of sugar ring and 3'-terminus (2'-deoxy; 2'-OMe, 2'-F, 3'-3'-Thymidine), analysis of their stability, mitochondrial targeting and the effect on heteroplasmy in human cybrid cells in culture. Most of the versions were characterized by increased intracellular stability, but did not cause a significant effect on the heteroplasmy level in transfected *trans*mitochondrial cybrid cells bearing a pathogenic mtDNA deletion, proving to be less efficient than non-modified antireplicative RNA molecules.

2. Design and synthesis of molecules, including RNA-DNA chimera, targeting a pathogenic point mutation in ND5 gene of mtDNA, analysis of their mitochondrial targeting by the laser scanning confocal microscopy. Synthetic oligonucleotides containing mitochondrial targeting determinants and a 20-nucleotide sequence corresponding to the mutated region of mtDNA were imported into mitochondria of cultured *trans*mitochondrial human cells; RNA (but not RNA-DNA chimeras) significantly decreased the proportion of mtDNA molecules bearing a point mutation.

3. Development and optimization of methods for the chemical synthesis of antireplicative RNA conjugated with cholesterol through cleavable bonds; analysis of stability, carrier-free cellular uptake and mitochondrial targeting of conjugated molecules.

4. RNA conjugated to cholesterol through a hydrazone bond was characterized by efficient internalization, partial import into mitochondria and capacity to induce a moderate but significant decrease of the mutant mtDNA proportion in the transfected patient fibroblasts bearing the pathogenic point mutation in ND5 gene of mtDNA.

My PhD project was focused on the creation of small RNA molecules, which should be stable, non-toxic, capable of penetrating human cells without additional agents, to be addressed into mitochondria and to reduce the proportion of mutant mitochondrial genomes. First, I participated in the studies on the design and stabilisation of the antireplicative RNAs, then, I synthesized conjugates of a selected RNA version with cholesterol residue. It had been

demonstrated that cholesterol conjugates can be used for targeting of oligonucleotides to different tissues such as liver, lung, kidney, heart, intestine, fat, skin, bone marrow, muscle, ovaries and adrenal glands (Krutzfeldt et al., 2005) with low toxicity (Moschos et al., 2007; Petrova et al., 2011), therefore, cholesterol can be considered as a universal vector for targeting of synthetic oligonucleotides for systemic delivery. Silencing of the targeted genes detected after delivery of cholesterol conjugated with siRNAs (Moschos et al., 2007) indirectly demonstrated the ability of conjugates to self-release from endosomes.

We designed an antireplicative RNA capable to be targeted into mitochondria due to presence of a structural determinant for mitochondrial import, and the covalently bound cholesterol residue could prevent or decrease the efficiency of its mitochondrial import for several reasons. First, high hydrophobicity of cholesterol can lead to undesirable binding with organelle membranes, thus, the anchored RNA conjugate would not be able to penetrate into mitochondrial matrix. Another problem is potential impact of cholesterol residue on the assembling of RNA-protein import complex. Unfortunately, the mechanism of antireplicative RNA import into mitochondria of mammalian cells is still poorly understood, and all participants of the import machinery are not yet identified, but the implication of several protein factors have been clearly demonstrated (Baleva et al., 2015; Gowher et al., 2013). For preventing these troubleshooting, cholesterol residue was conjugated to RNA through cleavable linkers.

If we, once again, consider the pathway of RNA targeting to mitochondria: after internalisation, RNA accumulates in early endosomes, which then mature into late endosomes and, finally, fuse with a lysosome and form the endolysosome, in which active degradation takes place. Therefore, the fate of the internalised molecules is to be released from endosomes into cytoplasm, where RNA can continue its way to mitochondria, or to be degraded. Cholesterol residue can be detached from oligonucleotide inside the endosomes or in the cytoplasm before antireplicative RNA will be imported into mitochondria. For release of RNA from cholesterol in cytoplasm, we designed two types of conjugated molecules: RNA/DNA duplexes, formed by antireplicative RNA and cholesterol containing oligonucleotide, and antireplicative RNA covalently linked with cholesterol through disulfide bond. Surprisingly, these constructs did not show significant efficiency of cell transfection. The absence of transfection with the duplex can be explained by low stability of the duplex during cell transfection procedure, while the cause of low efficacy of transfection with RNA conjugate containing disulfide bond remains unclear. Previously it had been demonstrated that siRNAs conjugates containing cleavable disulfide bond were rather efficient in knockdown

(Chen et al., 2010), however, the level of cell transfection had not been estimated. As a possible explanation of low transfection, we can hypothesize a self-assembling of conjugates into micelle-like particles where cholesterol residue and the linker form hydrophobic core which is shielded by water-soluble RNA (see p. 14, Fig. 3). Soft micellar nanoparticles assembly from DNA-cholesterol conjugates have been recently described (Magnusson et al., 2014). Cholesterol residue sequestered inside the particles could not bind the cell surface receptors and, therefore, penetrate the cells. In perspective, supramolecular unpacking can be achieved by addition of unsaturated carbon-carbon bonds in linker backbone.

Another cholesterol-conjugated molecule, designed for release of RNA in the endosomal compartments, was RNA conjugated with cholesterol through hydrazone bond. This is a very new type of cholesterol conjugates, containing pH-triggered hydrazone bond, has been developed during my PhD project and characterized by high efficiency of transfection. If we assume the formation of self-assembling micelle-like particles for conjugate with disulfide bond, why hydrazone containing conjugate does not form the particles? The only difference between two molecules is a structure of the linker used for conjugation of RNA with cholesterol. We suppose that, in case of hydrazone containing conjugate, the proportion between the hydrophobic and hydrophilic parts of the molecules should be more significant than in case of disulfide linker, thus preventing the probable self-assembling of conjugates into micelle-like particles and increasing the amount of molecules available for cell delivery.

RNA conjugates containing hydrazone bond were also characterized by the ability of self-release from endosomes, which was confirmed by its partial colocalisation with mitochondria. A possible mechanism of their endosomal escape could be the destabilization of endosomal lipid bilayer by hydrazine 6-(cholesteryloxycarbonylamino)hexanoate, which is formed in process of conjugate hydrolysis. The cholesterol derivative containing free hydrazide group should be positively charged, by analogy with hexane hydrazide (pKa=13.5), which suggests the same mechanism of endosomal escape as the one demonstrated for cationic lipids (Rehman et al., 2013).

Thereby, the cholesterol conjugate with antireplicative oligonucleotide through hydrazone bond, designed and synthetized in the frame of my PhD project, is capable to penetrate human cells in carrier-free way, to be addressed into mitochondria and to reduce the proportion of mutant mitochondrial genomes, thus fitting the criteria for a therapeutic molecule which can be used, in perspective, for treatment of mitochondrial diseases caused by heteroplasmic mutations in mtDNA. It is evident that many parameters are still to be thoroughly optimized, essentially concerning the stability of the molecules, efficiency of the mitochondrial import

and of the antireplication effect. An interesting possibility would be to optimize the disulfide bridged conjugates structures by altering mutual positions of the import determinant and cholesterol residue. To increase the efficiency of chemically stabilized antireplicative molecules, one can also propose to use a new set of modifications, as inter-nucleotide link modifications, and to introduce them not into the anti-replicative part of the molecule, but into the loop structures of the import determinants.

At long term, after being tested on cultures of immortalized human cells and primary patients cell cultures, these molecules can be exploited in other models (for example mouse stem cells or embryos) and, ultimately, for the pharmacological treatment of patients with mitochondrial disease caused by mutations in mtDNA. To be therapeutically applicable, many additional questions concerning *in vivo* delivery must be solved, but these issues are inherent to any gene therapy approach, while our main objective was to create and test tools specifically applicable to mitochondrial diseases.

On a fundamental level, our new modified RNA molecules would be interesting to use as an investigative tool to understand in more details their mode of action and the molecular mechanism of their targeting in the mitochondria.

4. Materials and Methods

4.1. Materials

5'-dimethoxytrityl-N-benzoyl-adenosine,2'-O-methyl,3'-[(2-cyanoethyl)-(N,N-diisopropyl)]-phosphoramidite, 5'-dimethoxytrityl-N-acetyl-cytidine,2'-O-methyl,3'-[(2-cyanoethyl)-(N,N-diisopropyl)]-phosphoramidite, 5'-dimethoxytrityl-N-isobutyryl-guanosine,2'-O-methyl,3'-[(2-cyanoethyl)-(N,N-diisopropyl)]-phosphoramidite, 5'-dimethoxytrityl-uridine,2'-O-methyl,3'-[(2-cyanoethyl)-(N,N-diisopropyl)]-phosphoramidite, 5'-dimethoxytrityl-N-benzoyl-deoxyadenosine, 2'-fluoro-3'-[(2-cyanoethyl)-(N,N-diisopropyl)]-phosphoramidite, 5'-dimethoxytrityl-N-acetyl-deoxycytidine,2'-fluoro-3'-[(2-cyanoethyl)-(N,N-diisopropyl)]-phosphoramidite, 5'-dimethoxytrityl-N-isobutyryl-deoxyguanosine, 2'-fluoro-3'-[(2-cyanoethyl)-(N,N-diisopropyl)]-phosphoramidite, 5'-dimethoxytrityl-deoxyUridine, 2'-fluoro-3'-[(2-cyanoethyl)-(N,N-diisopropyl)]-phosphoramidite, 5'-Dimethoxytrityl-N-benzoyl-2'-deoxyAdenosine,3'-[(2-cyanoethyl)-(N,N-diisopropyl)]-phosphoramidite, 5'-Dimethoxytrityl-N-acetyl-2'-deoxyCytidine,3'-[(2-cyanoethyl)-(N,N-diisopropyl)]-phosphoramidite, 5'-Dimethoxytrityl-N-isobutyryl-2'-deoxyGuanosine,3'-[(2-cyanoethyl)-(N,N-diisopropyl)]-phosphoramidite, 5'-Dimethoxytrityl-2'-deoxyThymidine,3'-[(2-cyanoethyl)-(N,N-diisopropyl)]-phosphoramidite, Thiol-Modifier C6 S-S, 5'-Aldehyde-Modifier C2, RNA phosphoramidites and solid supports for oligoribonucleotide synthesis were obtained from Glen Research; cholesteryl chloroformate, 6-aminohexanoic acid, cysteamine, chloroquine diphisphate salt and FITC isomer I were purchased from Sigma-Aldrich; hydrazine hydrate - from Fluka; ATTO 565 N-succinimidyl ester from ATTO-TEC, Alexa-488 N-succinimidyl ester from Invitrogen. Other chemicals were supplied by Merck, Acros and TCI. Solvents were supplied from Panreac.

4.2. Methods

4.2.1. Synthesis of cholesterol derivatives

Synthesis of cholesterol-3-(carboxyaminododecan-12-ol) and its H-phosphonate derivative described in details in **Publication 5**. Synthesis of 6-(cholesteryloxycarbonylamino)-hexanoic acid, methyl 6-(cholesteryloxycarbonylamino)hexanoate, hydrazino 6-(cholesteryloxycarbonylamino)hexanoate, 2-(pyridyldithio)-ethylamine, cholesteryl N-[2-(2-pyridyldisulfonyl) ethyl] carbamate described in details in **Publication 3**.

4.2.2. Oligonucleotide synthesis

Oligonucleotides used in work (**Publication 1-3**) were synthesized on an automatic ASM-800 synthesizer at 0.4 µmol scale using solid phase phosphoramidite synthesis protocols (Bellon, 2001) optimized for the instrument, with a 10 min coupling step for 2′-O-TBDMS-protected RNA phosphoramidites (0.1M in acetonitrile), 6 min coupling step for 2′-OMe-pyrimidine RNA phosphoramidites (0.05M in acetonitrile) and for 2′-F-pyrimidine RNA phosphoramidites (0.05M in acetonitrile), 5 min coupling step for 2'-deoxy DNA phosphoramidites (0.05M in acetonitrile) and 25 min coupling step for Thiol-Modifier C6 S-S phosphoramidite (0.1M in acetonitrile) and for 5'-Aldehyde-Modifier C2 phosphoramidite (0.1M in acetonitrile), 5-ethylthio-H-tetrazole (0.25M in acetonitrile) as an activating agent. A mixture of acetic anhydride with 2,6-lutidine in THF and N-methylimidazole in THF were utilized as capping reagents. The oxidizing agent was 0.02M iodine in pyridine/water/THF (1/9/90). Dichloroacetic acid (3%) in dichloromethane was usedas a detritylating reagent. The oligoribonucleotides after synthesis were cleaved from the support and deprotected by 40% methylamine in water at 65_C for 15 min, after that water mix was evaporated under the reduced presure. For 2'-O-Silyl groups deprotection step removed from solid support oligonucleotides were treated with a mixture of NMP/TEA·3HF/TEA (150/100/75) at 65°C for 1.5 h. Unreacted HF was eliminated by trimethoxysilane, and oligonucleotides were precipitated by diethyl ester and dried. Deprotected oligonucleotides were used in the follow steps of modification or were purified by preparative electrophoresis in 12% polyacrylamide/8M urea gel (acrylamide:N,N′-methylenebisacrylamide 30:0.5, TBE buffer, 10 V/cm) followed by elution with 0.3 M NaOAc (pH 5.2)/0.1% SDS solution and precipitation with ethanol.

4.2.3. Synthesis of lipophilic conjugates

Synthesis of oligoribinucleotides conjugated with cholesterol through a biodegradable linker containing hydrazone or disulfide bond described in details in **Publication 3**. Synthesis of lipophilic conjugates through dodecan-linker described in **Publication 5**.

4.2.4. Synthesis of 3'-terminus lipophilic conjugates

Derivative of a-D oligonucleotide containing 3'-terminus aminohexanoic linker (5 OU_{260}) was dissolved in 50 µl of water, then cholesteryl chloformiate (1mg, 2.2 µmol) in 100 µl of absolute dioxane and 5µl of triethylamine were added. The mixture was stirred at 37°C for 12

h, oligoribonucleotide conjugate was precipitated by addition 1.5 ml of diethyl ester/2% LiClO$_4$ in acetone (1:1), the pellet was washed with acetone and dried. Yield of the cholesterol conjugated oligonucleotide was estimated by gel electrophoresis and ethidium bromine staining as a ratio between intensity of signals corresponding to the reaction product containing cholesterol and the initial amino modified oligonucleotide (yield 70%). Cholesterol containing product was isolated via preparative electrophoresis in 12% polyacrylamide gel (30:0.5)/8M urea, TBE, followed by elution with 0.3 M NaOAc (pH 5.2)/0.1% SDS solution and precipitation with ethanol. The purified a-D conjugate was characterized by ESI-TOF-MS analysis (theoretical mass – 5779.0 Da, measured mass – 5780.0 Da).

4.2.5. DNA/RNA duplex formation

Duplexes were formed in a 25 μL final volume containing FD20H RNA (1 μg, 55 pmol), 10 μL annealing buffer (500 mM KOAc, 150 mM HEPES-KOH pH 7.4, 10 mM MgAc) and DNA-cholesterol conjugates (a-F 1-4 and a-D) to RNA:DNA molar ratios at 1:1, 1:2 and 1:3. After mixing, samples were heated 3 min at 95°C and left to cool down to 25°C during 1 hour. The duplex formation was analysed by gel electroforesis in 10% native polyacrylamide gel (30:0.5) in TBE buffer and Ethidium Bromine staining.

4.2.6. Test of the lipophilic conjugates stability

To test of the lipophilic conjugates stability in OptiMem, 100 ng (8.6 pmol) of D20HcnCh or D20HssCh conjugates were incubated 3 h at 37°C in 25 μl of OptiMem reduced serum medium. To test the hydrazon bond stability, 100 ng of D20HcnCh conjugate was incubated 2.5, 4, 6, 8 and 24 h at 37°C in 20mM Na-acetate buffer pH 4.6; 5.2 or 5.6 or Na-phosphate buffer pH 6.0; 6.6 or 7.4. Stability of D20HssCh was tested in 20 mM Hepes-NaOH pH 7.4 containing 5mM Glutathion (GHS) 3h at 37°C. For complete reduction of the disulfide bond, 20 mM β–mercaptoethanol was added for 15 min at room temperature.

Reaction products were separated on 8M urea – 12% PAGE (AA/bisAA 30:0.5), TBE, stained with Ethidium Bromide and quantified using G-box and GeneTools analysis software (Syngene) (**Publication 3**).

4.2.7. Radioactive labeling of oligonucleotides probes

The oligonucleotides probes (50 pmol) were incubated at 37°C for 45 min in a mixture of 20 μl containing 2 μl of 10X buffer (Promega), 1-2 μl γ-ATP (10 mCi/ml, 5000Ci/mmole), 1U of Polynucleotide Kinase (Promega). Ureacted γ-ATP was eliminated by gel filtration on Micro Bio-Spin Chromatography Column P-6 (Bio-Rad). The labelled oligonucleotides were diluted by 1 M STE (10 mM Tris-HCl pH 7.5, 1 M NaCl, 1 mM EDTA)/prehybridization buffer (6xSSC, 10X Denhardt solution, 0.2% SDS) and either used for hybridisation or stored at -20°C.

4.2.8. Cell culture

Human bone osteosarcoma 143B cells, *trans*-mitochondrial cybrid cells and primary skin fibroblasts from a patient were cultivated at 37°C and 5% CO_2 in MEM (Sigma) containing 1 g/l glucose, supplemented with fetal calf serum (Gibco), 100 U/ml penicillin, 100 μg/ml streptomycin, uridine (50 mg/l) and fungizone (2,50 mg/l) (Gibco).

To check the cell culture contamination by *Mycoplasma:*

In two days of cells cultivation, 2 ml of cell growing medium was harvested and centrifuged 5 min 600xg. The supernatant was centrifuged 10 min at 16000 xg. The pellet was re-suspended in 50 μl of water. Bacterial and mycoplasma contaminations were determined by PCR, reaction mix 25 μl contained 2 μl of suspension, 0.25 μl of primer 3 (100 μM), 0.25 μl of primer 5 (100 μM), 0.25 μl of primer UNI (10 μM), 1.25 μl of dNTPs (2.5 mM), 5 μl of buffer HF, 0.5 μl of high fidelity polymerase Phusion (Thermo Fisher Scientific). Cycling parameters were one step of 30 sec at 98°C; 30 cycles of 30 sec at 98°C, 90 sec at 61°C and 90 sec at 72°C and one final extension step of 10 min at 72°C, products were analysed in 1.5% agarose gels stained with ethidium bromide. Product with size 772 bp indicates on mycoplasma contamination, product 1055 bp indicates on non-specific bacterial contamination (Dussurget and Roulland-Dussoix, 1994). Primers used in test: primer 3 (5'-ACGAGCTGACGACAACCATGCAC-3'), primer 5 (5'-AGAGTTTGATCCTGGCTCAGGA-3'), UNI (5'-TAATCCTGTTTGCTCCCCAC-3').

4.2.9. Carrier-free cell transfection

Transient transfection of cells with DNA/RNA duplex: 143B cells (2 cm^2) were cultivated 24 h before cell transfection procedure in MEM supplemented with fetal calf serum as

described above. For carrier-free transfection with fluorescently labeled duplex FD20H/a-D, cells were washed with PBS, and Opti-MEM Reduced Serum medium (Gibco) containing 10 – 300 nM final concentration of duplex was added. Cells were cultivated 15 h at 37°C and 5% CO_2, then the medium was changed to MEM.

Transient transfection of cells with lipophilic conjugates is described in **Publication 3**.

4.2.10. Isolation of total RNA and RNA stability test

Total cellular RNA were isolated with TRIzol reagent (Invitrogen). Stability of synthetic RNA molecules were analysed by Northern hybridisation of total and mitochondrial RNA with ^{32}P-labelled oligonucleotide probes against synthetic RNAs or against control cytosolic RNA. The following probes were used: D-loop (5'-GAGTCATACGCGCTACCGATTGCGCCAACAAGGC-3') ; 5,8S (5'-GGCCGCAAGTGCGTTCGAAG-3') ; 5S (5'-CATCCAAGTACTACCAGGCCC-3') ; tRNA^{Thr} (5'-TCTCCGGTTTACAAGAC-3') ; KSS part (5'-GCTAAGTAAGCACTGTA-3'). To compare the stability of different recombinant RNA, relative concentration (R_0, …, R_t) of each RNA in various time period (t) after transfection was calculated as a ratio between the specific probe signal and the signal for 5S rRNA probe. The half-life period of RNA was calculated as $t_{1/2}=\ln2/k$, where the degradation constant k can be estimated according to the formula: $\ln R_t/R_0=kt$. (**Publication 1**).

4.2.11. Cytofluorometry

Transfected cells (2 cm^2) were washed by MEM supplemented with fetal calf serum (Gibco) to eliminate non-internalised oligonucleotides from the cells surface, cells were trypsinized and centrifuged 10 min 600xg. The pellet was resuspended in ice cold PBS and kept protected from light. Efficiency of transfection was evaluated by flow cytometry using CyFlow® Space (Partec), ATTO-565 labeled conjugates was excited at 488nm, and fluorescence emitted at 592 nm. More than 10,000 cells from each sample were analyzed using Flowing Software 2.5.1 (Perttu Terho, Turku Centre for Biotechnology).

4.2.12. Isolation of total DNA and Heteroplasmy test

Isolation of total cellular DNA was performed as described previously (Comte et al., 2013). Heteroplasmy level for KSS deletion in mtDNA was measured by real-time PCR using SYBR Green (iCycler, MyiQ^{TM} Real-Time Detection System, BioRad) as described in **Publication 1**. Two pairs of primers were used: (1) amplifying the 210 bp fragment of 12S rRNA gene

region (nucleotides 1095-1305 in mtDNA) not touched by the KSS deletion as a value showing all mtDNA molecules, and (2) amplifying the 164 bp fragment of the deleted region (nucleotides 11614-11778) as a value showing wild type mtDNA molecules. All reactions were performed in a 20 μl volume in triplicates. PCR using water instead of template was used as a negative control. PCR was performed by initial denaturation at 95° C for 10 min, followed by 40 cycles of 30 sec at 95°C, 30 sec at 60°C, and 30 sec at 72°C. Specificity was verified by melting curve analysis and gel electrophoresis.

Heteroplasmy level for A13514G mutation was measured as described in **Publication 2 and 3**. Briefly, the heteroplasmy level was analyzed by restriction fragment length polymorphism on a 125-bp PCR fragment where A13514G mutation creates an HaeIII-specific cleavage site. The HaeIII-digested fragments were separated on a 10% PAGE and quantified using PhosphorImager (Typhoon-Trio, GE Healthcare).

In **Publication 4,** we provide detailed protocols for transfection of cultured human cells with small recombinant RNA molecules by use of Lipofectamine 2000 and describe two approaches useful to demonstrate their import into mitochondria : (1) isolation of RNA from purified mitochondria and quantitative hybridization analysis and (2) confocal microscopy of cells transfected with fluorescently labelled RNA and co-localisation analysis. We also describe *in vitro* synthesis of fluorescently labelled RNA transcripts and end-labeling of RNA with fluorescent dyes.

4.3. Publication 4

Dovydenko I., Heckel A. M., Tonin Y., Gowher A., Venyaminova A., Tarassov I., Entelis N. Mitochondrial targeting of recombinant RNA. Methods Mol Biol. (2015) 1265, 209-2.

Mitochondrial Targeting of Recombinant RNA

Ilya Dovydenko, Anne-Marie Heckel, Yann Tonin, Ali Gowher, Alya Venyaminova, Ivan Tarassov, and Nina Entelis

Abstract

Mitochondrial import of small noncoding RNA is found in a large variety of species. In mammalian cells, this pathway can be used for therapeutic purpose, to restore the mitochondrial functions affected by pathogenic mutations. Recently, we developed mitochondrial RNA vectors able to address therapeutic oligoribonucleotides into human mitochondria. Here we provide the protocol for transfection of cultured human cells with small recombinant RNA molecules and describe two approaches useful to demonstrate their import into mitochondria: (1) isolation of RNA from purified mitochondria and quantitative hybridization analysis and (2) confocal microscopy of cells transfected with fluorescently labeled RNA. These protocols can be used in combination with overexpression or downregulation of protein import factors to detect and to evaluate their influence on the mitochondrial import of various RNAs.

Key words Mammalian cells transfection, RNA mitochondrial import, Mitochondria isolation, Northern hybridization, RNA labeling, Fluorescent microscopy

1 Introduction

RNA is increasingly used in therapeutic applications, including the agents of RNA interference, catalytically active RNA molecules, and RNA aptamers, which bind proteins and other ligands (reviewed in ref. 1, 2). We use RNA molecules targeted (imported) into human mitochondria to suppress negative effects of pathogenic mutations in mitochondrial DNA (mtDNA). Human mtDNA is a circular molecule of 16.5 kb able to replicate autonomously and encoding only 13 polypeptides, 2 ribosomal RNAs (12S and 16S), and 22 tRNAs, the vast majority of mitochondrial proteins and several RNAs being encoded in the nucleus and imported from the cytoplasm. In animal cells, no tRNA import was found in vivo, although other small RNAs, namely, 5S rRNA, RNA components of RNase P and MRP endonuclease, and probably some miRNAs, are imported (reviewed in ref. 3).

In yeast *Saccharomyces cerevisiae*, cytosolic tRNA$^{Lys}_{CUU}$ (further referred to as tRK1) is transcribed from nuclear genes and then unequally redistributed between the cytosol (97–98 %) and mitochondria (2–3 %) [4]. The mitochondrial targeting of tRK1 in yeast was shown to depend on the cytosolic precursor of mitochondrial lysyl-tRNA synthetase, which serves as a carrier [5, 6], and the glycolytic enzyme enolase (Eno2p) [7, 8]. Analysis of conformational rearrangements in the RNA by *in-gel* FRET approach [9] permitted to demonstrate that binding of protein factors and subsequent RNA import require formation of an alternative structure, different from a classic L-form tRNA model (Fig. 1a). Exploiting these data, a set of small RNA molecules with significantly improved efficiency of import not only into yeast but also into human mitochondria has been constructed (Fig. 1b). These small recombinant RNAs, based on the import determinants identified in tRK1 structures, can be used as vectors to deliver oligonucleotides with potential therapeutic capacities into human mitochondria [10].

Multiple alterations may occur in the mitochondrial genome (deletions, duplications, point mutations) resulting in a severe impact on cellular respiration and therefore leading to many diseases, essentially muscular and neurodegenerative disorders. To date, more than 250 pathologies were shown to be caused by defects in mtDNA [11]. Various strategies have been proposed to address these pathologies; unfortunately for the vast majority of cases, no efficient treatment is currently available. In some cases, defects may be rescued by targeting into mitochondria nuclear DNA-expressed counterparts of the affected molecules, an approach called allotopic strategy [12, 13]. We have exploited RNA mitochondrial import pathway, which is the only known natural mechanism of nucleic acid delivery into mitochondria [3], to develop two successful models of such allotopic rescue of a mtDNA mutation by targeting recombinant tRNA into mitochondria [14, 15]. More recently, we demonstrated that the replication of mtDNA containing a pathogenic mutation may be specifically affected by RNA molecules bearing oligonucleotide stretches complementary to the mutant region [10].

Here we provide the protocol of cultured cells transfection with such therapeutical small recombinant RNA molecules and describe how to detect their import into mitochondria.

2   Materials

2.1 Transfection of Human Cultured Cells for RNA Mitochondrial Import Analysis

1. Recombinant RNA molecules, obtained by T7-transcription or chemically synthesized. SiRNA (synthetic RNA–RNA duplexes 20–21 bases long); control non-silencing siRNA (Ref: SR-CL000-005, Eurogentec).
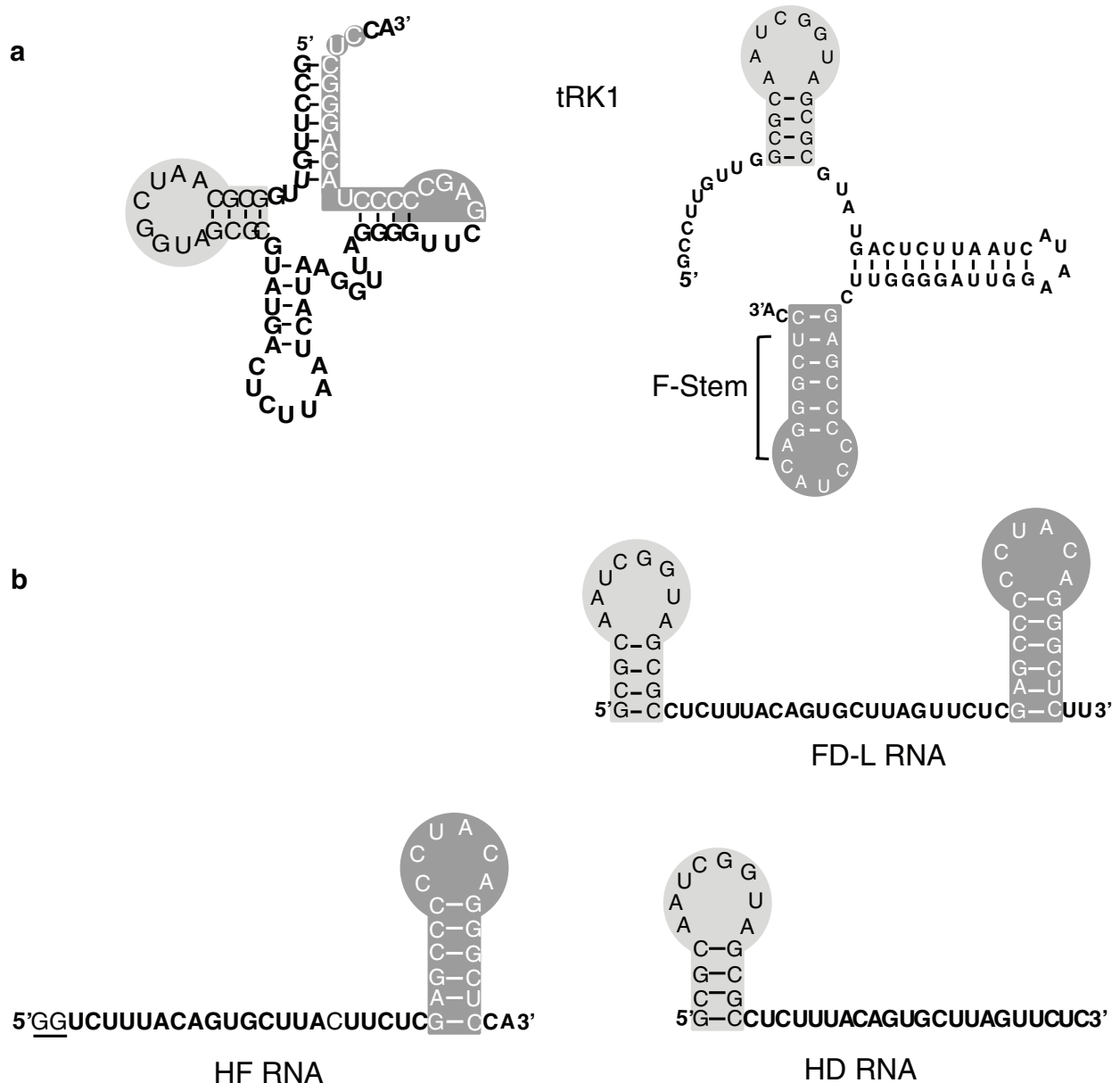
Fig. 1 Predicted secondary structures of the yeast tRNA$^{Lys}_{CUU}$ (tRK1) and small RNAs importable into human mitochondria. (**a**) Two alternative structures of tRK1 [9]. The cloverleaf structure is shown at the *left* and the alternative F-structure at the *right*. (**b**) Secondary structures of recombinant RNAs composed of the tRK1 D-arm (highlighted with a *light gray*) and/or the F helix-loop structure (highlighted with a *dark gray*) [10]. The nucleotides added to the 5′-end of HF RNA to improve T7-transcription are *underlined*

2. Plasmids based on pCMV6 vectors for transient overexpression of the protein import factors in human cells under the control of CMV promoter.

3. Transfection reagents Lipofectamine 2000 and RNAiMax (Invitrogen).

4. Opti-MEM Reduced Serum medium for transfection (GIBCO).

5. Cultured human cells: HeLa, HepG2, HEK293T, 143B, or human skin fibroblasts.

6. Dulbecco's modified Eagle's medium (DMEM) with 4.5 mg/mL glucose, sodium pyruvate (110 mg/L), and L-glutamine.

7. EMEM (essential modified Eagle's medium) with 1 mM pyruvate and 5 mg/mL uridine.

8. PBS, Dulbecco's phosphate-buffered saline without $CaCl_2$.

9. PBS-EDTA: Sterile 1× PBS solution containing 1 mM EDTA.

10. FBS, fetal bovine serum.

11. Streptomycin, penicillin, Fungizone, 100× solutions.

2.2 Mitochondria Purification and Quantitative Analysis of RNA Import

1. Mito Buffer with or without bovine serum albumin (BSA): 0.44 M sorbitol, 1 mM ethylenediaminetetraacetic acid (EDTA), 10 mM HEPES-NaOH pH 6.7, 0.1 % (w/v) BSA (to add before use).

2. Ribonuclease A from bovine pancreas 2× RNase A solution: 10 µg/mL RNase A (*see* **Note 1**), 4 mM $MgCl_2$.

3. Digitonin, freshly prepared solution 1 mg/mL, preheated for 1 min at 90 °C to avoid the micelle formation.

4. TRIzol reagent (Invitrogen).

5. Chloroform (HPLC), isopropanol, ethanol absolute (*see* **Note 2**).

6. Standard equipment for polyacrylamide gel electrophoresis and blotting.

7. Ethidium bromide solution (1 µg/mL), UV-transilluminator.

8. 10× Tris borate EDTA (TBE) electrode buffer: 0.89 M Tris base, 0.89 M boric acid, 20 mM EDTA, pH 8.4.

9. Acrylamide solution (methylene-bisacrylamide:acrylamide 1:19).

10. RNA loading buffer: deionized formamide (Genomic Grade) 98 %, 0.01 % Bromophenol blue, 0.01 % Xylene cyanol.

11. Hybond-N membrane (Amersham-Pharmacia).

12. Equipment for hybridization: rotating oven, ultraviolet (UV) cross-linking chamber.

13. 20× SSC solution: 3 M NaCl, 0.3 M sodium citrate, 1 mM EDTA.

14. 100× Denhardt solution: 2 % (w/v) BSA, 2 % (w/v) Ficoll, 2 % (w/v) polyvinylpyrrolidone.

15. Equipment for phosphoimaging and corresponding software.

16. 5′-^{32}P-labeled synthetic oligonucleotides (hybridization probes).

2.3 Fluorescent Confocal Microscopy

2.3.1 In Vitro Synthesis of Fluorescently Labeled RNA Transcripts

1. Alexa Fluor 488-5-UTP (Molecular Probes).

2. DNA template (PCR amplificate); T7 RNA polymerase HC (Promega); transcription optimized 5× buffer (Promega); NTP 10 mM; DTT 100 mM; RNaseOUT (Invitrogen) 40 u/µL.

3. RQ1 RNAse-Free DNAse (Promega).

4. NanoDrop spectrophotometer (Thermo Fisher Scientific).

2.3.2 End-Labeling of RNA with Fluorescent Dyes

1. Synthetic oligoribonucleotide (RNA) containing 5′- or 3′-terminus aminolinker.

2. *N*-succinimidyl ester of Alexa-488 (Invitrogen), *N*-succinimidyl ester of ATTO-546 (ATTO-TEC).

3. DMSO ≥99.9 %.

4. Buffer HEPES-NaOH 0.1 M pH = 8.5.

5. 2 % solution of lithium perchlorate in acetone.

6. Micro Bio-Spin Chromatography Column P-6 (Bio-Rad).

2.3.3 Transfection of Human Cells with Fluorescent RNA and Confocal Microscopy

1. Lipofectamine™ 2000 (Invitrogen).

2. Opti-MEM Reduced Serum medium for transfection.

3. Dulbecco's modified Eagle's medium (DMEM) without red phenol. Glucose, sodium pyruvate, and L-glutamine should be added before sterilization.

4. Tetramethylrhodamine methyl ester (TMRM) (Invitrogen); MitoTracker Green FM (Molecular Probes). Both dyes can be dissolved in dimethyl sulfoxide (DMSO) at 100 μM concentration, aliquoted, and stored at –20 °C.

3   Methods

3.1   Transfection of Human Cultured Cells for RNA Mitochondrial Import Analysis

Here we provide a general protocol for transfection of human cultured cells with recombinant RNA (synthetic or obtained by T7-transcription) for subsequent analysis of its mitochondrial import (Subheading 3.1.1). This approach can be used in combination with overexpression or downregulation of protein import factors to detect their influence on the mitochondrial import of various RNAs [16]. To overexpress the protein of interest, the cells can be transiently transfected with plasmid DNA, containing corresponding gene under the control of CMV promoter in one of commercial mammalian expression vectors, as pcDNA versions or pCMV6 (Subheading 3.1.2). To downregulate the protein of interest, the cells can be transiently transfected with interference synthetic RNA–RNA duplexes 20–21 bases long (Subheading 3.1.3).

3.1.1 Transfection of Human Cultured Cells with RNA

1. Grow the cells in DMEM or EMEM medium with 10 % FBS, penicillin, streptomycin, and Fungizone to the confluence of 60–80 %, depending on the line, in 75 cm² flask for cell culture in a CO_2 incubator (at 37 °C, 5 % CO_2).

2. Wash the cells with 1× PBS, add 9 mL of Opti-MEM, put into incubator for 2 h.

3. Prepare RNA-Lipofectamine mixture: 3 μg RNA in small volume of water (5–10 μL) add to 100 μL of Opti-MEM. In another tube,

dilute 20 μL of Lipofectamine in 80 μL of Opti-MEM, incubate for 5 min at 20 °C.

4. Mix diluted RNA and diluted Lipofectamine and incubate for 20 min at 20 °C.

5. Add the RNA-Lipofectamine mixture to the cells in the flask, gently mix, and incubate at 37 °C in a CO_2 incubator for 6–12 h.

6. Remove the medium with RNA-Lipofectamine complexes, add prewarmed (37 °C) DMEM medium; continue incubation for 24–48 h. Detach the cells with PBS-EDTA for mitochondria purification.

3.1.2 Transfection of Human Cultured Cells with RNA and Plasmid DNA

1. Perform **steps 1–3** of the previous protocol.

2. Prepare DNA-Lipofectamine mixture: 7.5 μg of plasmid DNA in small volume of water (5–10 μL) add to 100 μL of Opti-MEM. Dilute 20 μL of Lipofectamine in 80 μL of Opti-MEM, incubate for 5 min at 20 °C. Mix diluted DNA and diluted Lipofectamine and incubate for 20 min at room temperature.

3. Add the RNA-Lipofectamine and DNA-Lipofectamine mixtures to the cells in the flask, gently mix, and incubate at 37 °C in a CO_2 incubator for 6–12 h.

4. Remove the medium with Lipofectamine complexes, replace it by prewarmed DMEM medium; continue incubation for 24–48 h. Detach the cells with PBS-EDTA for mitochondria purification. Pellet 1/50 of cells (equivalent of 1.5 cm² confluent cells) separately to check the protein expression level by Western immunodecoration (*see* **Note 3**).

3.1.3 Transfection of Human Cultured Cells with Recombinant RNA and siRNA

Our optimized protocol for downregulation of the proteins influencing RNA import consists of two subsequent transfections: firstly, cells were transfected in suspension with 40 nM of each siRNA using RNAiMax transfection reagent. 24 h later, the cells form a monolayer and should be transfected again using Lipofectamine 2000.

1. Prepare the siRNA-Lipofectamine RNAiMax mixture: dilute siRNA (0.3–0.4 nmol, 3–4 μL of 100 μM stock solution) in 100 μL of Opti-MEM. Mix 35 μL of Lipofectamine (RNAiMax) with 100 μL of Opti-MEM; incubate for 5 min at 20 °C. Mix diluted RNA and diluted Lipofectamine, mix gently, and incubate for 20 min at 20 °C. As a negative control, use a non-silencing siRNA.

2. During these 20 min, detach the cells from the flasks with PBS-EDTA.

3. Centrifuge the cells at $600 \times g$ for 10 min; resuspend the pellet in 2 mL of Opti-MEM.

4. Add the cells suspension to 75 cm² flask containing 9 mL of Opti-MEM. Add the siRNA-Lipofectamine mix to the cells, mix gently, and incubate for 6 h.

5. Carefully remove the Opti-MEM and add DMEM medium.

6. 24 h later, the cells formed a monolayer and should be transfected again with 0.4 nmol of each siRNA using Lipofectamine 2000. 24–40 h after the second siRNA transfection (to be optimized for each siRNA), the cells can be transfected with a recombinant RNA (Subheading 3.1.1).

7. In 1–3 days, detach the cells with PBS-EDTA; analyze the protein downregulation by western blotting and RNA import by mitochondria purification and northern hybridization (Subheading 3.2).

3.2 Mitochondria Purification and Quantitative Analysis of RNA Import

3.2.1 Mitochondria Isolation and Purification

1. Detach the cells with PBS-EDTA, centrifuge 10 min at $600 \times g$, and resuspend the pellet in 1.5 mL of Mito Buffer containing BSA.

2. Pellet 1/10 of cells separately to isolate total cellular RNA by TRIzol extraction (Subheading 3.2.2).

3. Disrupt the cell by 25–30 passages through 2 mL syringe, needle No23G (Terumo), on ice.

4. Centrifuge two times 5 min at $1,500 \times g$, 4 °C, collecting the supernatant in a fresh tube on ice.

5. Centrifuge the supernatant 20 min at $15,000 \times g$, 4 °C (Tabletop Eppendorf centrifuge) and resuspend the mitochondrial pellet in 300 μL of Mito Buffer without BSA, on ice.

6. Add 300 μL of 2× RNase A solution and keep at room temperature for 10 min.

7. Stop RNase A by adding 500 μL of Mito Buffer containing 4 mM EDTA.

8. Centrifuge the mitochondria 10 min at $15,000 \times g$, 4 °C and wash the pellet three times with cold Mito Buffer.

9. Resuspend the mitochondria in 300 μL of Mito Buffer.

10. Add 20 μL of Digitonin (1 mg/mL) and keep at room temperature for 7 min. Dilute with 700 μL of cold Mito Buffer.

11. Centrifuge 10 min at $15,000 \times g$, 4 °C, discard the supernatant, and wash the pellet of mitoplasts with 500 μL of cold Mito Buffer.

12. Resuspend the pellet in 500 μL of TRIzol reagent (Invitrogen), and then the suspension can be frozen and kept at –80 °C, or treated immediately.

3.3 Quantitative Analysis of RNA Import by Northern Hybridization

1. Thaw the suspension of cells or mitoplasts in TRIzol (if frozen) at room temperature, incubate 5 min, add 100 μL of chloroform, mix well 15 s, and incubate at room temperature for 10 min.

2. Centrifuge at $12,000 \times g$ for 10 min at 4 °C.

3. Precipitate RNA from the upper (water) phase by adding 0.35 mL of isopropanol (*see* **Note 4**) and keep at –20 °C for at least 2 h (or overnight).

4. Centrifuge at $13,000 \times g$ for 30 min at 4 °C, discard supernatant, and wash the pellet with 0.5 mL of 80 % ethanol and then with 0.5 mL of absolute ethanol.

5. Dry the pellet, add 10–15 μL of water, solubilize by vortexing, and keep on ice.

6. Add the same volume of RNA loading buffer, heat at 95 °C for 3 min, and load on 8–12 % PAAG (depending on the length of recombinant RNA molecules) containing 8 M urea and TBE buffer.

7. After migration in TBE buffer, stain the gel with ethidium bromide 5 min at room temperature, and then take a picture using any kind of UV-transilluminator. Wash the gel for 15 min with 0.5×TBE buffer and perform electrotransfer onto Hybond-N membrane in a wet transfer camera in the same buffer at 4 °C, 10–12 V for 6–12 h.

8. Fix RNAs on the membrane by irradiation in a cross-linking UV chamber (Amersham Life Science), 3 min at each side of the membrane at constant energy $1,500 \times 100$ μJ/cm^2.

9. Prehybridize the membrane by rotating in a hybridization oven in 6× SSC, 0.1 % SDS, 10× Denhardt solution for 1 h at 65 °C.

10. Discard the prehybridization solution; add the hybridization solution, consisting of one volume of prehybridization buffer and one volume of 5′-^{32}P-labeled oligonucleotide probe in 1 M NaCl (purified before use on a small DEAE-cellulose column).

11. Hybridize overnight at appropriate temperature (depending on the probe, the hybridization temperature normally used is 5 °C below the melting point).

12. Remove hybridization solution and wash the membrane three times for 10 min in 2× SSC and 0.1 % SDS at room temperature; seal the wet membrane between two polyethylene sheets and expose on the phosphoimager screen for 6–12 h.

13. Take a picture of the hybridization signals. Wash out the hybrids three times for 10 min in 100 mL of 0.02× SSC and 0.1 % SDS at 80 °C in a water bath with slow agitation.
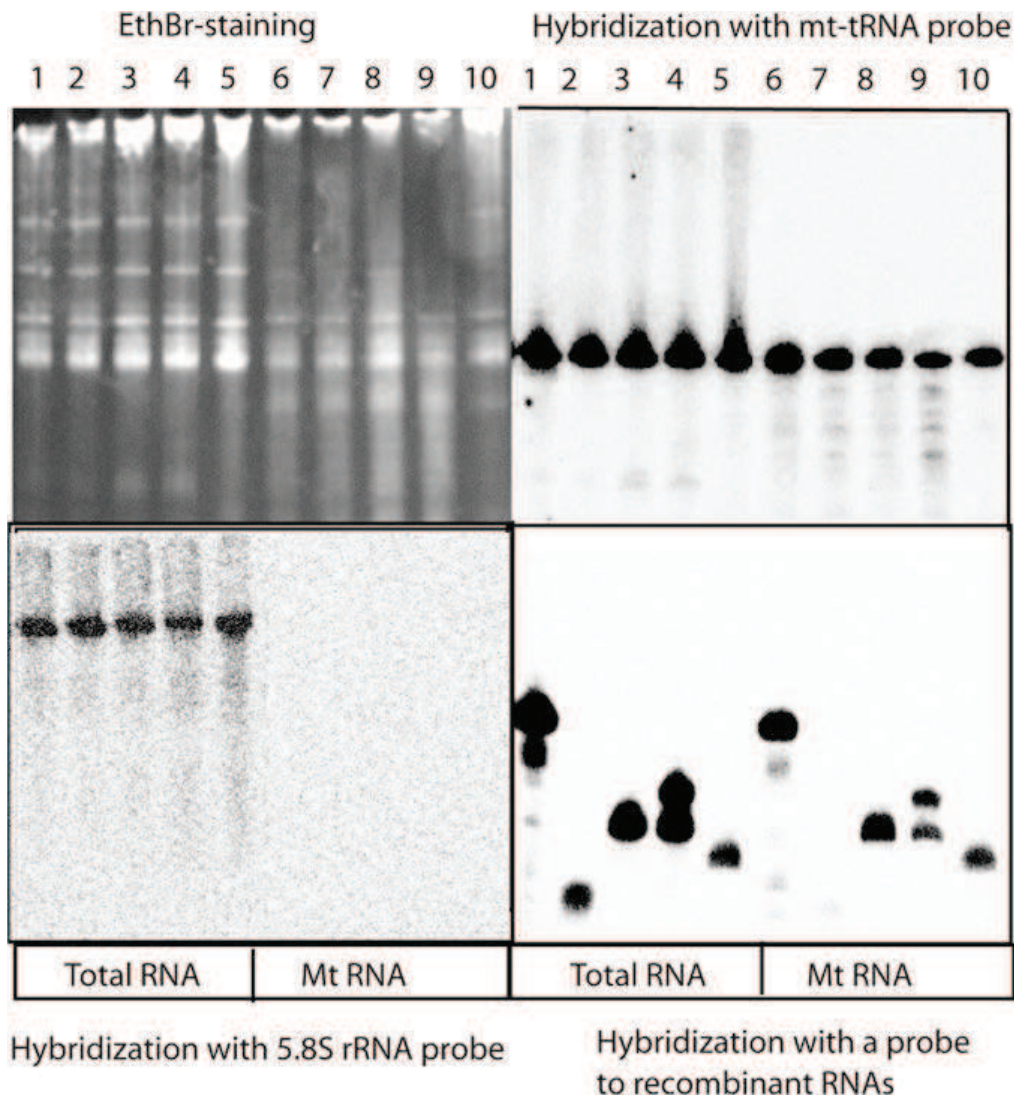
Fig. 2 Mitochondrial import of recombinant RNAs in transiently transfected cells. An example of urea-PAGE separation (*left upper panel*) and hybridization analysis of RNA isolated from cells (Total RNA, *lanes 1–5*) or purified mitoplasts (Mt RNA, *lanes 6–10*) 2 days after transfection with the following RNAs: yeast tRK1 (*lanes 1, 6*); control RNA, which is not imported into mitochondria (*lanes 2, 7*); various imported recombinant RNAs (*lanes 3–5* and *8–10*). The signals obtained with the probe to mt-tRNA are weaker in the mitochondrial fraction comparing to the total RNA, indicating on the partial mtRNA degradation during the mitochondria isolation and purification (Adapted from ref. 10)

14. Hybridize the same membrane with other 5′-³²P-labeled oligo-nucleotide probes (*see* **Note 5**) to obtain the series of hybridization pictures (Fig. 2).

15. After quantification using Typhoon-Trio scanner, the relative efficiency of RNA import into mitochondria can be calculated as a ratio between the signal obtained with a probe specific for recombinant RNA used for cell transfection (e.g., a probe against D-loop, Fig. 1) and that obtained with the probe against the host mitochondrial tRNA^Val (*see* **Note 6**).

To calculate the absolute import efficiencies for various RNA, the total level of RNA in the transfected cell was taken into account. For this the relative import efficiencies were divided by the ratios calculated in the same way but for total RNA preparations [10, 17]. To quantify the effect of the overexpression or downregulation of protein import factors, the efficiency of RNA import in control cells can be taken as 1 (Fig. 3).
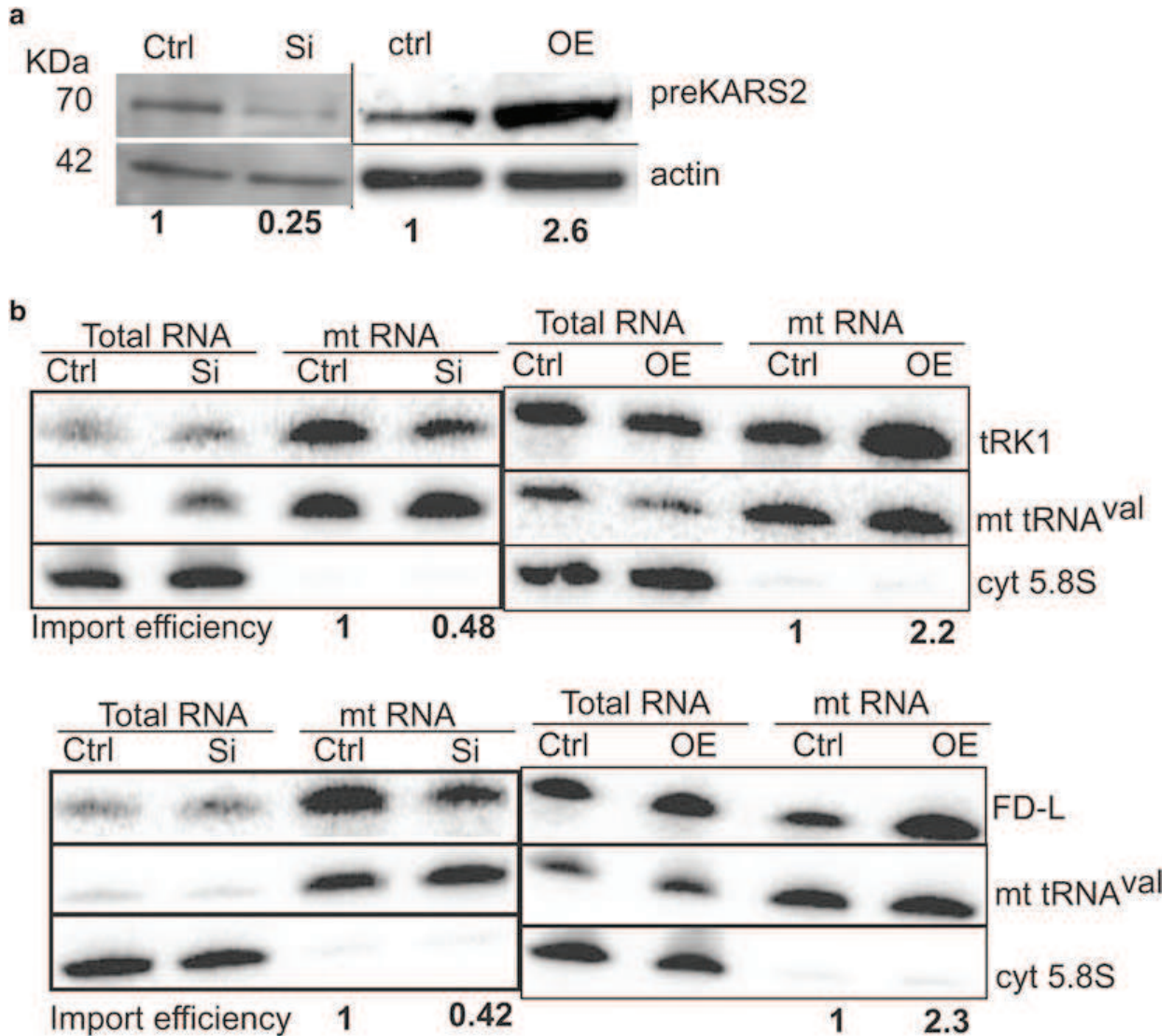
Fig. 3 Implication of precursor of human mitochondrial lysyl-tRNA synthetase (preKARS2) in the RNA mitochondrial import in vivo. (**a**) Western blot analysis of an import factor (preKARS2) downregulation by RNA interference (Si, *left panel*) or its overexpression (OE, *right panel*). The relative levels of the protein are indicated below the panels. Ctrl, control cells transfected with an empty vector. The antibodies used for immunodecoration are shown on the *right*. (**b**) Northern blot hybridization of the total or purified mitochondrial (mtRNA) RNAs isolated from the control cells (Ctrl), cells transfected with siRNAs against preKARS2 (Si), and the preKARS2-overexpressing cells (OE), after transfection with RNA. The hybridization probes are shown on the *right*. The relative RNA import efficiencies, taken as 1 for the control cells, are shown below each panel (Adapted from ref. 16)

3.4 Fluorescent Confocal Microscopy

Alexa Fluor 488-5-UTP can be incorporated into recombinant RNA by in vitro transcription using T7-RNA polymerase.

3.4.1 In Vitro Synthesis of Fluorescently Labeled RNA Transcripts

1. Make a reaction mixture in a black tube, final volume 20 μL:

    0.5 μg of DNA template (PCR-fragment containing T7 promoter and sequence of recombinant RNA starting with at least one G).

    0.5 mM of ATP, 0.5 mM CTP, 0.5 mM GTP, 0.37 mM UTP.

    0.125 mM Alexa Fluor 488-5-UTP.

    10 mM DTT.

    40 u of RNaseOUT.

    Transcription Optimized Buffer.

    80 u of T7 RNA polymerase HC.

2. Incubate at 37 °C for 6–12 h.

3. Add 1 μL of RQ1 RNAse-Free DNAse, incubate 15 min at 37 °C.

4. Purify RNA on Micro Bio-Spin Chromatography Column P-6.

5. To check the incorporation of the label in purified transcript, compare the dye absorbance at 492 nm and the nitrous bases absorbance at 260 nm using NanoDrop Microarray Program. The efficiency of labeling is calculated according to the following formula:

$$\text{Base} : \text{Dye} = \left(A_{\text{base}} \times \varepsilon_{\text{dye}} \right) / \left(A_{\text{dye}} \times \varepsilon_{\text{base}} \right)$$

where ε_{dye} is the extinction coefficient for the fluorescent dye, and is equal to 62,000 cm^{-1} M^{-1}, and $\varepsilon_{\text{base}}$ is the average extinction coefficient for a base in RNA, and is equal to 8,250 cm^{-1} M^{-1}. A_{base} is calculated as $A_{\text{base}} = A_{260} - (A_{\text{dye}} \times \text{CF}_{260})$, where CF_{260} is a correction factor equal to 0.3. The efficiency of labeling is normally about 1-2 labeled UTP per RNA molecule of 50 nucleotides.

3.4.2 End-Labeling of RNA with Fluorescent Dyes

1. Dry DMSO using Molecular Sieves 3A.

2. Dissolve 1 mg N-succinimidyl ester of fluorescent dye in 200 μL of anhydrous DMSO.

3. Dissolve five optical units of aminomodified RNA in 10 μL of water.

4. Mix 10 μL of RNA solution and 75 μL of HEPES-NaOH 0.1 M pH = 8.5.

5. Add 15 μL of N-succinimidyl ester Alexa-488 or N-succinimidyl ester of ATTO-546 dissolved in DMSO. Use black tubes; avoid the bright light during all the manipulations with the fluorescent dyes and labeled RNA.

6. Incubate the reaction mixture overnight at room temperature with permanent shaking (Eppendorf MixMate, 800 rpm).

7. Add 1 mL of 2 % $LiClO_4$ in acetone, mix, and keep at −20 °C for 30 min.

8. Centrifuge at $15,000 \times g$ for 15 min at 4 °C.

9. Discard the supernatant and wash the pellet with 1 mL of acetone.

10. Centrifuge at $15,000 \times g$ for 10 min at 4 °C and aspirate acetone.

11. Dry the pellet (in the dark).

12. Dissolve the pellet of fluorescently labeled RNA in 20 μL of water.

13. Purify RNA on Micro Bio-Spin Chromatography Column P-6.

14. The efficiency of labeling can be estimated by spectrophotometry (Subheading 3.3.1, **step 5**) or by PAGE separation of RNA on 12 % polyacrylamide gel (methylene-bisacrylamide: acrylamide 1:37.5) with 8 M urea (Fig. 4a).

3.4.3 Transfection of Human Cells with Fluorescent RNA and Confocal Microscopy

1. Grow the cells in 0.5–0.9 mL of DMEM medium with penicillin, streptomycin, and Fungizone on chambered cover glass for microscopy with 4 wells (2 cm²) (Lab-Tek) in a CO_2 incubator (at 37 °C, 5 % CO_2) to the confluence of 60–70 %.

2. Aspirate DMEM, wash cells gently with phosphate-buffered saline (PBS), and add 900 μL of Opti-MEM.

3. Mix 0.3 μg of fluorescently labeled RNA obtained by T7 transcription or 0.6 μg of end-labeled fluorescent RNA with 50 μL Opti-MEM.

4. Mix 1 μL of Lipofectamine™ 2000 with 50 μL Opti-MEM medium, and incubate for 5 min at room temperature.

5. Combine RNA mix and Lipofectamine™ 2000 mix, incubate for 30 min at room temperature, and then add to cells. All the manipulations with RNA and transfected cells carry out in the twilight to avoid the bleaching of the fluorescence.

6. Incubate cells with RNA 10 h, remove medium, wash cells with PBS, and add 0.5–0.9 mL of DMEM medium.

7. Cultivate cells for 1–4 days before microscopy (*see* **Note 7**), keeping them in the dark and changing the medium each 2 days.

8. Replace the medium with 0.5–0.9 mL of DMEM containing TMRM (or MitoTracker Green) at final concentration 100 nM, and incubate for 15 min in a CO_2 incubator at 37 °C.

9. Aspirate medium and wash cells gently three times with PBS, add 0.5–0.9 mL of DMEM without red phenol. Image cells
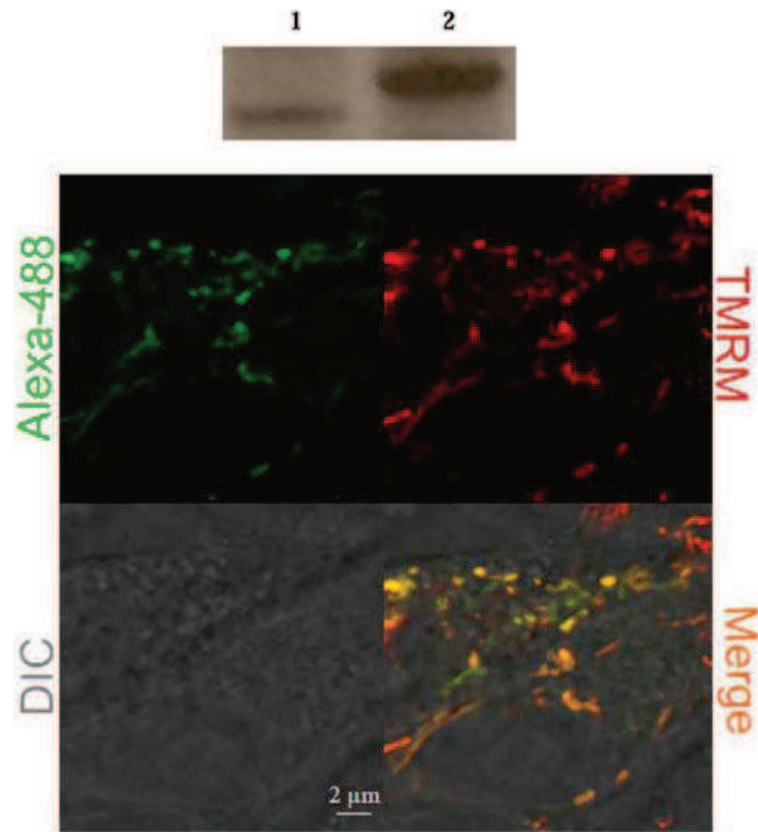
Fig. 4 Fluorescent confocal microscopy. (**a**) An example of urea-PAGE separation of aminomodified RNA (*lane 1*) and ATTO-546-labeled RNA (*lane 2*), EtBr staining. (**b**) Confocal microscopy images of 143B cells 3 days post transfection with fluorescently labeled RNA (Alexa-488, *green signal*) importable into mitochondria. Mitochondria are stained with TMRM (*red signal*). Quantitative co-localization analysis: Pearson's coefficient = 0.6; Manders' coefficients, M1 = 0.9 (fraction of Alexa-488 overlapping TMRM), M2 = 0.6 (fraction of TMRM overlapping Alexa-488)

using a confocal laser scanning microscope (Fig. 4b). We use the LSM 700 confocal microscope (Zeiss) in conjunction with Zen imaging software and a Zeiss 63×/1.40 oil immersion objective. The excitation/emission laser wavelengths were 488 nm (green channel) and 555 nm (red channel). For co-localization analysis, use ImageJ software and JACoP plugin to calculate Pearson's and Manders' coefficients (*see* **Note 8**).

4   Notes

1. Concentration of RNase should be optimized for each new stock of the enzyme, since some preparations may contain contaminants disrupting mitochondrial membranes, which lead to degradation of all the mitochondrial RNA. RNase treatment should completely degrade cytosolic RNA (as 5.8S

rRNA), but affect only in a minor extent the transcripts of mitochondrial DNA (Fig. 2).

2. Organic solvents should be of high quality, stored in a dark place. If RNA pellet obtained after TRIzol extraction and iso-propanol purification turns yellow, the isopropanol and/or chloroform stock should be replaced by a fresh one.

3. To check the protein expression level by Western immunodec-oration, add to the pellet of cells (equivalent of 1.5 cm² conflu-ent cells) 20 µL of loading Laemmli buffer (50 mM Tris–HCl pH 6.8, 2 % SDS, 0.1 % β-mercaptoethanol, 0.01 % Bromophenol blue and 10 % Glycerol), sonicate 10 s, heat for 5–10 min at 90 °C (at 40 °C for membrane protein analysis), and separate proteins by 10 % SDS-PAGE before electroblot-ting and probing with antibodies.

4. To precipitate completely the small-sized RNA, we add glyco-gen as a carrier. Stock solution of 20 mg/mL in water can be stored frozen at –20 °C. Add this solution to the water phase obtained after TRIzol extraction to final concentration 0.1 mg/mL, and then add isopropanol.

5. We use the hybridization probes in following order:

    (a) "D-loop" probe specific for recombinant molecules (*see* Fig. 1), 5′-GAG TCA TAC GCG CTA CCG ATT GCG CCA ACA AGG C-3′.

    (b) Probe against the mitochondrial tRNAVal, 5′-GAA CCT CTG ACT GTA AAG-3′.

    (c) Cytosolic 5.8S rRNA probe, 5′-GGC CGC AAG TGC GTT CGA AG-3′.

    (d) Probe against the nuclear snRNA U3, 5′-CGC TAC CTC TCT TCC TCG TGG-3′.

    Probes (c) and (d) are useful to demonstrate the absence of nuclear and cytosolic contaminations in the fraction of mitochondrial RNA. The signal for nuclear snRNA in mitochondrial fraction indicates that the mito-chondrial pellet (Subheading 3.2.1, **step 5**) contained nuclei. This can be avoided by several low-speed centrifu-gations (aimed to pellet the unbroken cells and nuclei) after the disruption of cells. The hybridization signal cor-responding to cytosolic RNA contamination indicates that the external RNAs were not completely degraded by RNase (Subheading 3.2.1, **step 6**) and/or that the outer mitochondrial membranes were not disrupted by digito-nin treatment (Subheading 3.2.1, **step 10**). In this case, the fresh (or more concentrated) solutions of RNase A and digitonin should be used.

Because it is rather difficult to normalize exactly the amount of mitoplasts isolated from various cell lines, we load on gels mitochondrial RNA isolated from the same number of cells, and then use the hybridization signals, corresponding to mitochondrial valine tRNA, as a loading control. Thus, we take into account not the absolute intensity of hybridization signals but only ratios between signals corresponding to imported RNA and to the host mitochondrial valine tRNA gene transcript.

6. Normally, our protocol allows to obtain mitochondria completely devoid of nuclear and cytosolic RNA contamination, including 5,8S ribosomal RNA, which can copurify with mitochondria (as a part of cytosolic ribosomes associated with the outer mitochondrial membrane). However, during the RNase and digitonin treatment and multiple repurification of organelles by centrifugation, an important part of mitochondria can be partially disrupted, and thus mitochondrial RNA can be partially lost and/or degraded. In fact, we recover only 10–50 % of intact mtRNA, and this yield may vary in different experiments. That is why we normally do not detect a clear enrichment of mitochondrial valine tRNA nor imported RNAs in the mitoplast fractions (Fig. 2). The weaker (or comparable) hybridization signals corresponding to mitochondrial probe (mt-tRNA^{Val}) obtained for mitochondrial RNA comparing to total cellular RNA indicates on the partial mtRNA degradation.

7. We detect significant accumulation of RNA in the mitochondria 2 days after cells transfection. The explanation would be that RNA is released from the Lipofectamine vesicles, which occurs gradually and then becomes available for internalization by mitochondria. We suppose that some critical concentration of importable RNA in the cytoplasm might be needed for interaction with the protein factors of RNA mitochondrial targeting [16], and a rather important concentration of RNA in the mitochondrial matrix would be necessary for detection of the fluorescent signal.

8. Pearson's correlation coefficient evaluates the correlation of the signal intensity distribution between different channels. Its values are highly dependent on the variation in fluorescence intensities, and in this case, the overlap coefficient according to Manders would be more suitable. This coefficient indicates the overlap of the signals and represents the true degree of co-localization [18]. Therefore, the M1 value of 0.9 (Fig. 4b) indicates that in 3 days post transfection, approximately 90 % of green fluorescence (RNA) is co-localized with the red one (mitochondria). Coefficient M2 value, representing the percentage of the red fluorescence (mitochondria) overlapping with the green one

(RNA), indicates that 60 % of mitochondria contain RNA. This degree can be increased in 4 days up to 70–80 % probably due to the mitochondrial dynamic events, fusion and fission, resulting in more homogenous RNA distribution.

Acknowledgements

References

1. Burnett JC, Rossi JJ, Tiemann K (2011) Current progress of siRNA/shRNA therapeutics in clinical trials. Biotechnol J 6: 1130–1146

2. Burnett JC, Rossi JJ (2012) RNA-based therapeutics: current progress and future prospects. Chem Biol 19:60–71

3. Schneider A (2011) Mitochondrial tRNA import and its consequences for mitochondrial translation. Annu Rev Biochem 80:1033–1053

4. Martin R, Schneller JM, Stahl A et al (1979) Import of nuclear deoxyribonucleic acid coded lysine-accepting transfer ribonucleic acid (anti-codon C-U-U) into yeast mitochondria. Biochemistry 18:4600–4605

5. Tarassov I, Entelis N, Martin R (1995) Mitochondrial import of a cytoplasmic lysine-tRNA in yeast is mediated by cooperation of cytoplasmic and mitochondrial lysyl-tRNA synthetases. EMBO J 14:3461–3471

6. Kamenski P, Smirnova E, Kolesnikova O et al (2010) tRNA mitochondrial import in yeast: Mapping of the import determinants in the carrier protein, the precursor of mitochondrial lysyl-tRNA synthetase. Mitochondrion 10:284–293

7. Entelis N, Brandina I, Kamenski P et al (2006) A glycolytic enzyme, enolase, is recruited as a cofactor of tRNA targeting toward mitochondria in Saccharomyces cerevisiae. Genes Dev 20:1609–1620

8. Brandina I, Graham J, Lemaitre-Guillier C et al (2006) Enolase takes part in a macromolecular complex associated to mitochondria in yeast. Biochim Biophys Acta 1757: 1217–1228

9. Kolesnikova O, Kazakova H, Comte C et al (2010) Selection of RNA aptamers imported into yeast and human mitochondria. RNA 16:926–941

10. Comte C, Tonin Y, Heckel-Mager AM et al (2013) Mitochondrial targeting of recombinant RNAs modulates the level of a heteroplasmic mutation in human mitochondrial DNA associated with Kearns Sayre syndrome. Nucleic Acids Res 41:418–433

11. Ruiz-Pesini E, Lott MT, Procaccio V et al (2007) An enhanced MITOMAP with a global mtDNA mutational phylogeny. Nucleic Acids Res 35:D823–D828

12. Rustin P, Jacobs H, Dietrich A et al (2007) Targeting allotopic material to the mitochondrial compartment: new tools for better understanding mitochondrial physiology and prospect for therapy. Med Sci (Paris) 23: 519–525

13. Manfredi G, Fu J, Ojaimi J et al (2002) Rescue of a deficiency in ATP synthesis by transfer of MTATP6, a mitochondrial DNA-encoded gene, to the nucleus. Nat Genet 30:394–399

14. Karicheva OZ, Kolesnikova OA, Schirtz T et al (2011) Correction of the consequences of mitochondrial 3243A>G mutation in the MT-TL1 gene causing the MELAS syndrome by tRNA import into mitochondria. Nucleic Acids Res 39:8173–8186

15. Kolesnikova OA, Entelis NS, Jacquin-Becker C et al (2004) Nuclear DNA-encoded tRNAs targeted into mitochondria can rescue a mitochondrial DNA mutation associated with the MERRF syndrome in cultured human cells. Hum Mol Genet 13:2519–2534

16. Gowher A, Smirnov A, Tarassov I et al (2013) Induced tRNA import into human mitochondria: implication of a host aminoacyl-tRNA-synthetase. PLoS One 8:e66228

17. Smirnov A, Tarassov I, Mager-Heckel AM et al (2008) Two distinct structural elements of 5S rRNA are needed for its import into human mitochondria. RNA 14:749–759

18. Zinchuk V, Zinchuk O, Okada T (2007) Quantitative colocalization analysis of multi-color confocal immunofluorescence microscopy images: pushing pixels to explore biological phenomena. Acta Histochem Cytochem 40:101–111

BIBLIOGRAPHY

Bibliography

Akita, H., Kudo, A., Minoura, A., Yamaguti, M., Khalil, I.A., Moriguchi, R., Masuda, T., Danev, R., Nagayama, K., Kogure, K., *et al.* (2009). Multi-layered nanoparticles for penetrating the endosome and nuclear membrane via a step-wise membrane fusion process. Biomaterials *30*, 2940-2949.

Alexeyev, M.F., Venediktova, N., Pastukh, V., Shokolenko, I., Bonilla, G., and Wilson, G.L. (2008). Selective elimination of mutant mitochondrial genomes as therapeutic strategy for the treatment of NARP and MILS syndromes. Gene therapy *15*, 516-523.

Amar-Lewis, E., Azagury, A., Chintakunta, R., Goldbart, R., Traitel, T., Prestwood, J., Landesman-Milo, D., Peer, D., and Kost, J. (2014). Quaternized starch-based carrier for siRNA delivery: from cellular uptake to gene silencing. J Control Release *185*, 109-120.

Angelini, C., Bello, L., Spinazzi, M., and Ferrati, C. (2009). Mitochondrial disorders of the nuclear genome. Acta Myol *28*, 16-23.

Bacman, S.R., Williams, S.L., Pinto, M., Peralta, S., and Moraes, C.T. (2012). Specific elimination of mutant mitochondrial genomes in patient-derived cells by mitoTALENs. Nature medicine *19*, 1111-1113.

Balazs, D.A., and Godbey, W. (2011). Liposomes for use in gene delivery. Journal of drug delivery *2011*, 326497.

Baleva, M., Gowher, A., Kamenski, P., Tarassov, I., Entelis, N., and Masquida, B. (2015). A Moonlighting Human Protein Is Involved in Mitochondrial Import of tRNA. International journal of molecular sciences *16*, 9354-9367.

Bangham, A.D., Standish, M.M., and Watkins, J.C. (1965). Diffusion of univalent ions across the lamellae of swollen phospholipids. Journal of molecular biology *13*, 238-252.

Bartlett, D.W., and Davis, M.E. (2008). Impact of tumor-specific targeting and dosing schedule on tumor growth inhibition after intravenous administration of siRNA-containing nanoparticles. Biotechnology and bioengineering *99*, 975-985.

Becker, T., Bottinger, L., and Pfanner, N. (2012). Mitochondrial protein import: from transport pathways to an integrated network. Trends in biochemical sciences *37*, 85-91.

Behr, J.P. (1997). The proton sponge: A trick to enter cells the viruses did not exploit. Chimia *51*, 34−36.

Bellon, L. (2001). Oligoribonucleotides with 2'-O-(tert-butyldimethylsilyl) groups. Current protocols in nucleic acid chemistry / edited by Serge L Beaucage [et al *Chapter 3*, Unit 3 6.

Bennett, C.F., and Swayze, E.E. (2010). RNA targeting therapeutics: molecular mechanisms of antisense oligonucleotides as a therapeutic platform. Annual review of pharmacology and toxicology *50*, 259-293.

Bhat, B., Balow, G., Guzaev, A., Cook, P.D., and Manoharan, M. (1999). Synthesis of fully protected nucleoside- folic acid conjugated phosphoramidites and their incorporation into antisense oligonucleotides. Nucleosides Nucleotides *18*, 1471-1472.

Bianco, A., Kostarelos, K., and Prato, M. (2005). Applications of carbon nanotubes in drug delivery. Current opinion in chemical biology *9*, 674-679.

Biessen, E.A., Vietsch, H., Rump, E.T., Fluiter, K., Kuiper, J., Bijsterbosch, M.K., and van Berkel, T.J. (1999). Targeted delivery of oligodeoxynucleotides to parenchymal liver cells in vivo. The Biochemical journal *340 (Pt 3)*, 783-792.

Bikram, M., Lee, M., Chang, C.W., Janat-Amsbury, M.M., Kern, S.E., and Kim, S.W. (2005). Long-circulating DNA-complexed biodegradable multiblock copolymers for gene delivery: degradation profiles and evidence of dysopsonization. J Control Release *103*, 221-233.

Boisguerin, P., Deshayes, S., Gait, M.J., O'Donovan, L., Godfrey, C., Betts, C.A., Wood, M.J., and Lebleu, B. (2015). Delivery of therapeutic oligonucleotides with cell penetrating peptides. Advanced drug delivery reviews *87*, 52-67.

Bonnet, C., Augustin, S., Ellouze, S., Benit, P., Bouaita, A., Rustin, P., Sahel, J.A., and Corral-Debrinski, M. (2008). The optimized allotopic expression of ND1 or ND4 genes restores respiratory chain complex I activity in fibroblasts harboring mutations in these genes. Biochimica et biophysica acta *1783*, 1707-1717.

Boussif, O., Lezoualc'h, F., Zanta, M.A., Mergny, M.D., Scherman, D., Demeneix, B., and Behr, J.P. (1995). A versatile vector for gene and oligonucleotide transfer into cells in culture and in vivo: polyethylenimine. Proceedings of the National Academy of Sciences of the United States of America *92*, 7297-7301.

Boutorine, A.S., and Kostina, E.V. (1993). Reversible covalent attachment of cholesterol to oligodeoxyribonucleotides for studies of the mechanisms of their penetration into eucaryotic cells. Biochimie *75*, 35-41.

Boyer, P.D., Cross, R.L., and Momsen, W. (1973). A new concept for energy coupling in oxidative phosphorylation based on a molecular explanation of the oxygen exchange reactions. Proceedings of the National Academy of Sciences of the United States of America *70*, 2837-2839.

Campbell, M.A., and Wengel, J. (2011). Locked vs. unlocked nucleic acids (LNA vs. UNA): contrasting structures work towards common therapeutic goals. Chemical Society reviews *40*, 5680-5689.

Cesarone, G., Edupuganti, O.P., Chen, C.P., and Wickstrom, E. (2007). Insulin receptor substrate 1 knockdown in human MCF7 ER+ breast cancer cells by nuclease-resistant IRS1 siRNA conjugated to a disulfide-bridged D-peptide analogue of insulin-like growth factor 1. Bioconjugate chemistry *18*, 1831-1840.

Chaltin, P., Margineanu, A., Marchand, D., Van Aerschot, A., Rozenski, J., De Schryver, F., Herrmann, A., Mullen, K., Juliano, R., Fisher, M.H.*, et al.* (2005). Delivery of antisense oligonucleotides using cholesterol-modified sense dendrimers and cationic lipids. Bioconjugate chemistry *16*, 827-836.

Chen, Q., Butler, D., Querbes, W., Pandey, R.K., Ge, P., Maier, M.A., Zhang, L., Rajeev, K.G., Nechev, L., Kotelianski, V.*, et al.* (2010). Lipophilic siRNAs mediate efficient gene silencing in oligodendrocytes with direct CNS delivery. J Control Release *144*, 227-232.

Chinnery, P.F., Johnson, M.A., Wardell, T.M., Singh-Kler, R., Hayes, C., Brown, D.T., Taylor, R.W., Bindoff, L.A., and Turnbull, D.M. (2000). The epidemiology of pathogenic mitochondrial DNA mutations. Annals of neurology *48*, 188-193.

Cho, Y.W., Kim, J.D., and Park, K. (2003). Polycation gene delivery systems: escape from endosomes to cytosol. The Journal of pharmacy and pharmacology *55*, 721-734.

Comte, C., Tonin, Y., Heckel-Mager, A.M., Boucheham, A., Smirnov, A., Aure, K., Lombes, A., Martin, R.P., Entelis, N., and Tarassov, I. (2013). Mitochondrial targeting of recombinant RNAs modulates the level of a heteroplasmic mutation in human mitochondrial DNA associated with Kearns Sayre Syndrome. Nucleic acids research *41*, 418-433.

D'Souza, G.G., Boddapati, S.V., and Weissig, V. (2005). Mitochondrial leader sequence--plasmid DNA conjugates delivered into mammalian cells by DQAsomes co-localize with mitochondria. Mitochondrion *5*, 352-358.

D'Souza, G.G., Rammohan, R., Cheng, S.M., Torchilin, V.P., and Weissig, V. (2003). DQAsome-mediated delivery of plasmid DNA toward mitochondria in living cells. J Control Release *92*, 189-197.

Davis, M.E. (2009). The first targeted delivery of siRNA in humans via a self-assembling, cyclodextrin polymer-based nanoparticle: from concept to clinic. Molecular pharmaceutics *6*, 659-668.

De Haes, W., Van Mol, G., Merlin, C., De Smedt, S.C., Vanham, G., and Rejman, J. (2012). Internalization of mRNA lipoplexes by dendritic cells. Molecular pharmaceutics *9*, 2942-2949.

De Mesmaeker, A., Lebreton, J., Waldner, A., Fritsch, V., and Wolf, R.M. (1994). Replacement of the phosphodiester linkage in oligonucleotides: comparison of two structural amide isomers. Bioorg Med Chem Lett *4*, 873–878.

DiFiglia, M., Sena-Esteves, M., Chase, K., Sapp, E., Pfister, E., Sass, M., Yoder, J., Reeves, P., Pandey, R.K., Rajeev, K.G., *et al.* (2007). Therapeutic silencing of mutant huntingtin with siRNA attenuates striatal and cortical neuropathology and behavioral deficits. Proceedings of the National Academy of Sciences of the United States of America *104*, 17204-17209.

Ding, Y., Jiang, Z., Saha, K., Kim, C.S., Kim, S.T., Landis, R.F., and Rotello, V.M. (2014). Gold nanoparticles for nucleic acid delivery. Mol Ther *22*, 1075-1083.

Dizaj, S.M., Jafari, S., and Khosroushahi, A.Y. (2014). A sight on the current nanoparticle-based gene delivery vectors. Nanoscale research letters *9*, 252.

Dussurget, O., and Roulland-Dussoix, D. (1994). Rapid, sensitive PCR-based detection of mycoplasmas in simulated samples of animal sera. Applied and environmental microbiology *60*, 953-959.

El-Sayed, A., Khalil, I.A., Kogure, K., Futaki, S., and Harashima, H. (2008). Octaarginine- and octalysine-modified nanoparticles have different modes of endosomal escape. The Journal of biological chemistry *283*, 23450-23461.

Entelis, N.S., Kolesnikova, O.A., Martin, R.P., and Tarassov, I.A. (2001). RNA delivery into mitochondria. Advanced drug delivery reviews *49*, 199-215.

Ernster, L., and Schatz, G. (1981). Mitochondria: a historical review. The Journal of cell biology *91*, 227s-255s.

Evers, M.M., Toonen, L.J., and van Roon-Mom, W.M. (2015). Antisense oligonucleotides in therapy for neurodegenerative disorders. Advanced drug delivery reviews *87*, 90-103.

Farhood, H., Bottega, R., Epand, R.M., and Huang, L. (1992). Effect of cationic cholesterol derivatives on gene transfer and protein kinase C activity. Biochimica et biophysica acta *1111*, 239-246.

Felgner, P.L., Gadek, T.R., Holm, M., Roman, R., Chan, H.W., Wenz, M., Northrop, J.P., Ringold, G.M., and Danielsen, M. (1987). Lipofection: a highly efficient, lipid-mediated DNA-transfection procedure. Proceedings of the National Academy of Sciences of the United States of America *84*, 7413-7417.

Fletcher, S., Ahmad, A., Perouzel, E., Heron, A., Miller, A.D., and Jorgensen, M.R. (2006). In vivo studies of dialkynoyl analogues of DOTAP demonstrate improved gene transfer efficiency of cationic liposomes in mouse lung. Journal of medicinal chemistry *49*, 349-357.

Flierl, A., Jackson, C., Cottrell, B., Murdock, D., Seibel, P., and Wallace, D.C. (2003). Targeted delivery of DNA to the mitochondrial compartment via import sequence-conjugated peptide nucleic acid. Mol Ther *7*, 550-557.

Fraley, R., Subramani, S., Berg, P., and Papahadjopoulos, D. (1980). Introduction of liposome-encapsulated SV40 DNA into cells. The Journal of biological chemistry *255*, 10431-10435.

Freedland, S.J., Malone, R.W., Borchers, H.M., Zadourian, Z., Malone, J.G., Bennett, M.J., Nantz, M.H., Li, J.H., Gumerlock, P.H., and Erickson, K.L. (1996). Toxicity of cationic lipid-ribozyme complexes in human prostate tumor cells can mimic ribozyme activity. Biochemical and molecular medicine *59*, 144-153.

Furukawa, R., Yamada, Y., Kawamura, E., and Harashima, H. (2015). Mitochondrial delivery of antisense RNA by MITO-Porter results in mitochondrial RNA knockdown, and has a functional impact on mitochondria. Biomaterials *57*, 107-115.

Gebhart, C.L., and Kabanov, A.V. (2001). Evaluation of polyplexes as gene transfer agents. J Control Release *73*, 401-416.

Ginn, S.L., Alexander, I.E., Edelstein, M.L., Abedi, M.R., and Wixon, J. (2013). Gene therapy clinical trials worldwide to 2012 - an update. The journal of gene medicine *15*, 65-77.

Glodde, M., Sirsi, S.R., and Lutz, G.J. (2006). Physiochemical properties of low and high molecular weight poly(ethylene glycol)-grafted poly(ethylene imine) copolymers and their complexes with oligonucleotides. Biomacromolecules *7*, 347-356.

Gowher, A., Smirnov, A., Tarassov, I., and Entelis, N. (2013). Induced tRNA import into human mitochondria: implication of a host aminoacyl-tRNA-synthetase. PloS one *8*, e66228.

Grayson, A.C., Doody, A.M., and Putnam, D. (2006). Biophysical and structural characterization of polyethylenimine-mediated siRNA delivery in vitro. Pharmaceutical research *23*, 1868-1876.

Green, J.J., Zhou, B.Y., Mitalipova, M.M., Beard, C., Langer, R., Jaenisch, R., and Anderson, D.G. (2008). Nanoparticles for Gene Transfer to Human Embryonic Stem Cell Colonies. Nano Letters *8*, 3126-3130.

Gryaznov, S.M., Lloyd, D.H., Chen, J.K., Schultz, R.G., DeDionisio, L.A., Ratmeyer, L., and Wilson, W.D. (1995). Oligonucleotide N3'-->P5' phosphoramidates. Proceedings of the National Academy of Sciences of the United States of America *92*, 5798-5802.

Guy, J., Qi, X., Pallotti, F., Schon, E.A., Manfredi, G., Carelli, V., Martinuzzi, A., Hauswirth, W.W., and Lewin, A.S. (2002). Rescue of a mitochondrial deficiency causing Leber Hereditary Optic Neuropathy. Annals of neurology *52*, 534-542.

Hall, A.H., Wan, J., Shaughnessy, E.E., Ramsay Shaw, B., and Alexander, K.A. (2004). RNA interference using boranophosphate siRNAs: structure-activity relationships. Nucleic acids research *32*, 5991-6000.

Heidel, J.D., Yu, Z., Liu, J.Y., Rele, S.M., Liang, Y., Zeidan, R.K., Kornbrust, D.J., and Davis, M.E. (2007). Administration in non-human primates of escalating intravenous doses of targeted nanoparticles containing ribonucleotide reductase subunit M2 siRNA. Proceedings of the National Academy of Sciences of the United States of America *104*, 5715-5721.

Heidenreich, O., Gryaznov, S., and Nerenberg, M. (1997). RNase H-independent antisense activity of oligonucleotide N3 '--> P5 ' phosphoramidates. Nucleic acids research *25*, 776-780.

Herdewijn, P. (2000). Heterocyclic modifications of oligonucleotides and antisense technology. Antisense & nucleic acid drug development *10*, 297-310.

Hope, M.J. (2014). Enhancing siRNA delivery by employing lipid nanoparticles. Therapeutic delivery *5*, 663-673.

Hughes, L.D., Rawle, R.J., and Boxer, S.G. (2014). Choose your label wisely: water-soluble fluorophores often interact with lipid bilayers. PloS one *9*, e87649.

Hunter, A.C. (2006). Molecular hurdles in polyfectin design and mechanistic background to polycation induced cytotoxicity. Advanced drug delivery reviews *58*, 1523-1531.

Huotari, J., and Helenius, A. (2011). Endosome maturation. The EMBO journal *30*, 3481-3500.

Iyer, S., Xiao, E., Alsayegh, K., Eroshenko, N., Riggs, M.J., Bennett, J.P., Jr., and Rao, R.R. (2011). Mitochondrial gene replacement in human pluripotent stem cell-derived neural progenitors. Gene therapy *19*, 469-475.

Jager, M., Schubert, S., Ochrimenko, S., Fischer, D., and Schubert, U.S. (2012). Branched and linear poly(ethylene imine)-based conjugates: synthetic modification, characterization, and application. Chemical Society reviews *41*, 4755-4767.

Jiang, H.L., Kim, T.H., Kim, Y.K., Park, I.Y., Cho, M.H., and Cho, C.S. (2008). Efficient gene delivery using chitosan-polyethylenimine hybrid systems. Biomedical materials (Bristol, England) *3*, 025013.

Juliano, R., Alam, M.R., Dixit, V., and Kang, H. (2008). Mechanisms and strategies for effective delivery of antisense and siRNA oligonucleotides. Nucleic acids research *36*, 4158-4171.

Juliano, R., Bauman, J., Kang, H., and Ming, X. (2009). Biological barriers to therapy with antisense and siRNA oligonucleotides. Molecular pharmaceutics *6*, 686-695.

Juliano, R.L., Carver, K., Cao, C., and Ming, X. (2013). Receptors, endocytosis, and trafficking: the biological basis of targeted delivery of antisense and siRNA oligonucleotides. Journal of drug targeting *21*, 27-43.

Kaltimbacher, V., Bonnet, C., Lecoeuvre, G., Forster, V., Sahel, J.A., and Corral-Debrinski, M. (2006). mRNA localization to the mitochondrial surface allows the efficient translocation inside the organelle of a nuclear recoded ATP6 protein. RNA (New York, NY *12*, 1408-1417.

Karicheva, O.Z., Kolesnikova, O.A., Schirtz, T., Vysokikh, M.Y., Mager-Heckel, A.M., Lombes, A., Boucheham, A., Krasheninnikov, I.A., Martin, R.P., Entelis, N*., et al.* (2011). Correction of the consequences of mitochondrial 3243A>G mutation in the MT-TL1 gene causing the MELAS syndrome by tRNA import into mitochondria. Nucleic acids research *39*, 8173-8186.

Kawasaki, A.M., Casper, M.D., Freier, S.M., Lesnik, E.A., Zounes, M.C., Cummins, L.L., Gonzalez, C., and Cook, P.D. (1993). Uniformly modified 2'-deoxy-2'-fluoro phosphorothioate oligonucleotides as nuclease-resistant antisense compounds with high affinity and specificity for RNA targets. Journal of medicinal chemistry *36*, 831-841.

Kay, M.A. (2011). State-of-the-art gene-based therapies: the road ahead. Nat Rev Genet *12*, 316-328.

Keeney, P.M., Quigley, C.K., Dunham, L.D., Papageorge, C.M., Iyer, S., Thomas, R.R., Schwarz, K.M., Trimmer, P.A., Khan, S.M., Portell, F.R*., et al.* (2009). Mitochondrial gene therapy augments mitochondrial physiology in a Parkinson's disease cell model. Human gene therapy *20*, 897-907.

Khan, S.M., and Bennett, J.P., Jr. (2004). Development of mitochondrial gene replacement therapy. Journal of bioenergetics and biomembranes *36*, 387-393.

Kolesnikova, O., Entelis, N., Kazakova, H., Brandina, I., Martin, R.P., and Tarassov, I. (2002). Targeting of tRNA into yeast and human mitochondria: the role of anticodon nucleotides. Mitochondrion *2*, 95-107.

Kolesnikova, O., Kazakova, H., Comte, C., Steinberg, S., Kamenski, P., Martin, R.P., Tarassov, I., and Entelis, N. (2011). Selection of RNA aptamers imported into yeast and human mitochondria. RNA (New York, NY *16*, 926-941.

Kolesnikova, O.A., Entelis, N.S., Jacquin-Becker, C., Goltzene, F., Chrzanowska-Lightowlers, Z.M., Lightowlers, R.N., Martin, R.P., and Tarassov, I. (2004). Nuclear DNA-encoded tRNAs targeted into mitochondria can rescue a mitochondrial DNA mutation associated with the MERRF syndrome in cultured human cells. Human molecular genetics *13*, 2519-2534.

Kolesnikova, O.A., Entelis, N.S., Mireau, H., Fox, T.D., Martin, R.P., and Tarassov, I.A. (2000). Suppression of mutations in mitochondrial DNA by tRNAs imported from the cytoplasm. Science (New York, NY *289*, 1931-1933.

Koopman, W.J., Willems, P.H., and Smeitink, J.A. (2012). Monogenic mitochondrial disorders. The New England journal of medicine *366*, 1132-1141.

Koshkin, A.A., Singha S.K., Nielsen, P., Rajwanshi, V.K., Kumar, R., Meldgaard, M., Olsen, C.E., and Wengel, J. (1998). LNA (Locked Nucleic Acids): Synthesis of the adenine, cytosine, guanine, 5-methylcytosine, thymine and uracil bicyclonucleoside monomers, oligomerisation, and unprecedented nucleic acid recognition. Tetrahedron *54*, 3607-3630.

Krutzfeldt, J., Rajewsky, N., Braich, R., Rajeev, K.G., Tuschl, T., Manoharan, M., and Stoffel, M. (2005). Silencing of microRNAs in vivo with 'antagomirs'. Nature *438*, 685-689.

Kubo, T., Zhelev, Z., Ohba, H., and Bakalova, R. (2007). Modified 27-nt dsRNAs with dramatically enhanced stability in serum and long-term RNAi activity. Oligonucleotides *17*, 445-464.

Lechauve, C., Augustin, S., Cwerman-Thibault, H., Reboussin, E., Roussel, D., Lai-Kuen, R., Saubamea, B., Sahel, J.A., Debeir, T., and Corral-Debrinski, M. (2014). Neuroglobin gene therapy prevents optic atrophy and preserves durably visual function in Harlequin mice. Mol Ther *22*, 1096-1109.

Lee, M., Choi, J.S., Choi, M.J., Pak, Y.K., Rhee, B.D., and Ko, K.S. (2007). DNA delivery to the mitochondria sites using mitochondrial leader peptide conjugated polyethylenimine. Journal of drug targeting *15*, 115-122.

Lee, R.J., and Huang, L. (1996). Folate-targeted, anionic liposome-entrapped polylysine-condensed DNA for tumor cell-specific gene transfer. The Journal of biological chemistry *271*, 8481-8487.

Letsinger, R.L., Zhang, G.R., Sun, D.K., Ikeuchi, T., and Sarin, P.S. (1989). Cholesteryl-conjugated oligonucleotides: synthesis, properties, and activity as inhibitors of replication of human immunodeficiency virus in cell culture. Proceedings of the National Academy of Sciences of the United States of America *86*, 6553-6556.

Leventis, R., and Silvius, J.R. (1990). Interactions of mammalian cells with lipid dispersions containing novel metabolizable cationic amphiphiles. Biochimica et biophysica acta *1023*, 124-132.

Li, S., Deshmukh, H.M., and Huang, L. (1998). Folate-mediated targeting of antisense oligodeoxynucleotides to ovarian cancer cells. Pharmaceutical research *15*, 1540-1545.

Li, W., and Szoka, F.C., Jr. (2007). Lipid-based nanoparticles for nucleic acid delivery. Pharmaceutical research *24*, 438-449.

Liu, D., Qiao, W., Li, Z., Chen, Y., Cui, X., Li, K., Yu, L., Yan, K., Zhu, L., Guo, Y.*, et al.* (2008). Structure-function relationship research of glycerol backbone-based cationic lipids for gene delivery. Chemical biology & drug design *71*, 336-344.

Lorenz, C., Hadwiger, P., John, M., Vornlocher, H.P., and Unverzagt, C. (2004). Steroid and lipid conjugates of siRNAs to enhance cellular uptake and gene silencing in liver cells. Bioorganic & medicinal chemistry letters *14*, 4975-4977.

Lv, H., Zhang, S., Wang, B., Cui, S., and Yan, J. (2006). Toxicity of cationic lipids and cationic polymers in gene delivery. J Control Release *114*, 100-109.

MacKellar, C., Graham, D., Will, D.W., Burgess, S., and Brown, T. (1992). Synthesis and physical properties of anti-HIV antisense oligonucleotides bearing terminal lipophilic groups. Nucleic acids research *20*, 3411-3417.

Magnusson, J.P., Fernandez-Trillo, F., Sicilia, G., Spain, S.G., and Alexander, C. (2014). Programmed assembly of polymer-DNA conjugate nanoparticles with optical readout and sequence-specific activation of biorecognition. Nanoscale *6*, 2368-2374.

Mahato, B., Jash, S., and Adhya, S. (2011). RNA-mediated restoration of mitochondrial function in cells harboring a Kearns Sayre Syndrome mutation. Mitochondrion *11*, 564-574.

Manfredi, G., Fu, J., Ojaimi, J., Sadlock, J.E., Kwong, J.Q., Guy, J., and Schon, E.A. (2002). Rescue of a deficiency in ATP synthesis by transfer of MTATP6, a mitochondrial DNA-encoded gene, to the nucleus. Nature genetics *30*, 394-399.

Manoharan, M., Kesavan, V., and Rajeev, K.G. (2005). Modified iRNA agents. In Fish and Richardson Paper Corporation Boston MA (USA, 20050107325 A1), pp. 245.

Maxfield, F.R., and Wustner, D. Analysis of cholesterol trafficking with fluorescent probes. Methods in cell biology *108*, 367-393.

Maxfield, F.R., and Wustner, D. (2013). Analysis of cholesterol trafficking with fluorescent probes. Methods in cell biology *108*, 367-393.

McGuire, M.J., Gray, B.P., Li, S., Cupka, D., Byers, L.A., Wu, L., Rezaie, S., Liu, Y.H., Pattisapu, N., Issac, J.*, et al.* (2014). Identification and characterization of a suite of tumor targeting peptides for non-small cell lung cancer. Scientific reports *4*, 4480.

Meade, B.R., Gogoi, K., Hamil, A.S., Palm-Apergi, C., van den Berg, A., Hagopian, J.C., Springer, A.D., Eguchi, A., Kacsinta, A.D., Dowdy, C.F.*, et al.* (2014). Efficient delivery of RNAi prodrugs containing reversible charge-neutralizing phosphotriester backbone modifications. Nature biotechnology *32*, 1256-1261.

Milligan, J.F., Matteucci, M.D., and Martin, J.C. (1993). Current concepts in antisense drug design. Journal of medicinal chemistry *36*, 1923-1937.

Minczuk, M., Papworth, M.A., Miller, J.C., Murphy, M.P., and Klug, A. (2008). Development of a single-chain, quasi-dimeric zinc-finger nuclease for the selective degradation of mutated human mitochondrial DNA. Nucleic acids research *36*, 3926-3938.

Ming, X., Alam, M.R., Fisher, M., Yan, Y., Chen, X., and Juliano, R.L. (2010). Intracellular delivery of an antisense oligonucleotide via endocytosis of a G protein-coupled receptor. Nucleic acids research *38*, 6567-6576.

Mislick, K.A., and Baldeschwieler, J.D. (1996). Evidence for the role of proteoglycans in cation-mediated gene transfer. Proceedings of the National Academy of Sciences of the United States of America *93*, 12349-12354.

Miyata, K., Nishiyama, N., and Kataoka, K. (2012). Rational design of smart supramolecular assemblies for gene delivery: chemical challenges in the creation of artificial viruses. Chemical Society reviews *41*, 2562-2574.

Moschos, S.A., Jones, S.W., Perry, M.M., Williams, A.E., Erjefalt, J.S., Turner, J.J., Barnes, P.J., Sproat, B.S., Gait, M.J., and Lindsay, M.A. (2007). Lung delivery studies using siRNA conjugated to TAT(48-60) and penetratin reveal peptide induced reduction in gene expression and induction of innate immunity. Bioconjugate chemistry *18*, 1450-1459.

Movahedi, F., Hu, R.G., Becker, D.L., and Xu, C. (2015). Stimuli-responsive liposomes for the delivery of nucleic acid therapeutics. Nanomedicine *11*, 1575-1584.

Muratovska, A., Lightowlers, R.N., Taylor, R.W., Turnbull, D.M., Smith, R.A., Wilce, J.A., Martin, S.W., and Murphy, M.P. (2001). Targeting peptide nucleic acid (PNA) oligomers to mitochondria within cells by conjugation to lipophilic cations: implications for mitochondrial DNA replication, expression and disease. Nucleic acids research *29*, 1852-1863.

Mutisya, D., Selvam, C., Lunstad, B.D., Pallan, P.S., Haas, A., Leake, D., Egli, M., and Rozners, E. (2014). Amides are excellent mimics of phosphate internucleoside linkages and are well tolerated in short interfering RNAs. Nucleic acids research *42*, 6542-6551.

Nagley, P., Farrell, L.B., Gearing, D.P., Nero, D., Meltzer, S., and Devenish, R.J. (1988). Assembly of functional proton-translocating ATPase complex in yeast mitochondria with cytoplasmically synthesized subunit 8, a polypeptide normally encoded within the organelle. Proceedings of the National Academy of Sciences of the United States of America *85*, 2091-2095.

Nair, J.K., Willoughby, J.L., Chan, A., Charisse, K., Alam, M.R., Wang, Q., Hoekstra, M., Kandasamy, P., Kel'in, A.V., Milstein, S.*, et al.* (2014). Multivalent N-acetylgalactosamine-conjugated siRNA localizes in hepatocytes and elicits robust RNAi-mediated gene silencing. Journal of the American Chemical Society *136*, 16958-16961.

Nijtmans, L.G., Ugalde, C., van den Heuvel, L.P., and Smeitink, J.A. (2004). Function and dysfunction of the oxidative phosphorylation system. In Mitochondrial Function and Biogenesis (Springer Berlin Heidelberg), pp. 149-176.

Oberhauser, B., and Wagner, E. (1992). Effective incorporation of 2'-O-methyl-oligoribonucleotides into liposomes and enhanced cell association through modification with thiocholesterol. Nucleic acids research *20*, 533-538.

Oupicky, D., and Li, J. (2014). Bioreducible polycations in nucleic acid delivery: past, present, and future trends. Macromolecular bioscience *14*, 908-922.

Palade, G.E. (1952). The fine structure of mitochondria. The Anatomical record *114*, 427-451.

Palade, G.E. (1953). An electron microscope study of the mitochondrial structure. J Histochem Cytochem *1*, 188-211.

Peng, X.H., Qian, X., Mao, H., Wang, A.Y., Chen, Z.G., Nie, S., and Shin, D.M. (2008). Targeted magnetic iron oxide nanoparticles for tumor imaging and therapy. International journal of nanomedicine *3*, 311-321.

Petrova, N.S., Chernikov, I.V., Meschaninova, M.I., Dovydenko, I.S., Venyaminova, A.G., Zenkova, M.A., Vlassov, V.V., and Chernolovskaya, E.L. (2011). Carrier-free cellular uptake and the gene-silencing activity of the lipophilic siRNAs is strongly affected by the length of the linker between siRNA and lipophilic group. Nucleic acids research *40*, 2330-2344.

Pinto, M., and Moraes, C.T. (2014). Mitochondrial genome changes and neurodegenerative diseases. Biochimica et biophysica acta *1842*, 1198-1207.

Poopeiko, N.E., Dahl, B.M., and Wengel, J. (2003). xylo-configured oligonucleotides (XNA, xylo nucleic acids): synthesis and hybridization studies. Nucleosides, nucleotides & nucleic acids *22*, 1147-1149.

Prakash, T.P., Graham, M.J., Yu, J., Carty, R., Low, A., Chappell, A., Schmidt, K., Zhao, C., Aghajan, M., Murray, H.F*., et al.* (2014). Targeted delivery of antisense oligonucleotides to hepatocytes using triantennary N-acetyl galactosamine improves potency 10-fold in mice. Nucleic acids research *42*, 8796-8807.

Raouane, M., Desmaele, D., Urbinati, G., Massaad-Massade, L., and Couvreur, P. (2012). Lipid conjugated oligonucleotides: a useful strategy for delivery. Bioconjugate chemistry *23*, 1091-1104.

Reddy, P., Ocampo, A., Suzuki, K., Luo, J., Bacman, S.R., Williams, S.L., Sugawara, A., Okamura, D., Tsunekawa, Y., Wu, J*., et al.* (2015). Selective elimination of mitochondrial mutations in the germline by genome editing. Cell *161*, 459-469.

Reed, M.W., Adams, A.D., Nelson, J.S., and Meyer, R.B., Jr. (1991). Acridine- and cholesterol-derivatized solid supports for improved synthesis of 3'-modified oligonucleotides. Bioconjugate chemistry *2*, 217-225.

Rehman, Z., Zuhorn, I.S., and Hoekstra, D. (2013). How cationic lipids transfer nucleic acids into cells and across cellular membranes: recent advances. J Control Release *166*, 46-56.

Rhee, W.J., and Bao, G. (2010). Slow non-specific accumulation of 2'-deoxy and 2'-O-methyl oligonucleotide probes at mitochondria in live cells. Nucleic acids research *38*, e109.

Rolland, A. (1999). Advanced Gene Delivery: From Concepts to Pharmaceutical Products. (Amsterdam, Harwood).

Rubio, M.A., Rinehart, J.J., Krett, B., Duvezin-Caubet, S., Reichert, A.S., Soll, D., and Alfonzo, J.D. (2008). Mammalian mitochondria have the innate ability to import tRNAs by a mechanism distinct from protein import. Proceedings of the National Academy of Sciences of the United States of America *105*, 9186-9191.

Rump, E.T., de Vrueh, R.L., Sliedregt, L.A., Biessen, E.A., van Berkel, T.J., and Bijsterbosch, M.K. (1998). Preparation of conjugates of oligodeoxynucleotides and lipid structures and their interaction with low-density lipoprotein. Bioconjugate chemistry *9*, 341-349.

Ruponen, M., Honkakoski, P., Tammi, M., and Urtti, A. (2004). Cell-surface glycosaminoglycans inhibit cation-mediated gene transfer. The journal of gene medicine *6*, 405-414.

Rutz, M., Metzger, J., Gellert, T., Luppa, P., Lipford, G.B., Wagner, H., and Bauer, S. (2004). Toll-like receptor 9 binds single-stranded CpG-DNA in a sequence- and pH-dependent manner. European journal of immunology *34*, 2541-2550.

Salinas, T., Duchene, A.M., and Marechal-Drouard, L. (2008). Recent advances in tRNA mitochondrial import. Trends in biochemical sciences *33*, 320-329.

Schon, E.A., DiMauro, S., and Hirano, M. (2012). Human mitochondrial DNA: roles of inherited and somatic mutations. Nat Rev Genet *13*, 878-890.

Seibel, P., Trappe, J., Villani, G., Klopstock, T., Papa, S., and Reichmann, H. (1995). Transfection of mitochondria: strategy towards a gene therapy of mitochondrial DNA diseases. Nucleic acids research *23*, 10-17.

Seo, B.B., Nakamaru-Ogiso, E., Flotte, T.R., Matsuno-Yagi, A., and Yagi, T. (2006a). In vivo complementation of complex I by the yeast Ndi1 enzyme. Possible application for treatment of Parkinson disease. The Journal of biological chemistry *281*, 14250-14255.

Seo, Y.J., Jeong, H.S., Bang, E.K., Hwang, G.T., Jung, J.H., Jang, S.K., and Kim, B.H. (2006b). Cholesterol-linked fluorescent molecular beacons with enhanced cell permeability. Bioconjugate chemistry *17*, 1151-1155.

Shabi, S., Sajjad, K., and Arif, A. (2006). Peptide nucleic acid (PNA) – a review. J Chem Technol Biotechnol *81*, 892–899.

Sheehan, D., Lunstad, B., Yamada, C.M., Stell, B.G., Caruthers, M.H., and Dellinger, D.J. (2003). Biochemical properties of phosphonoacetate and thiophosphonoacetate oligodeoxyribonucleotides. Nucleic acids research *31*, 4109-4118.

Shim, M.S., and Kwon, Y.J. (2009). Acid-responsive linear polyethylenimine for efficient, specific, and biocompatible siRNA delivery. Bioconjugate chemistry *20*, 488-499.

Sjostrand, F.S. (1953). Electron microscopy of mitochondria and cytoplasmic double membranes. Nature *171*, 30-32.

Smirnov, A., Comte, C., Mager-Heckel, A.M., Addis, V., Krasheninnikov, I.A., Martin, R.P., Entelis, N., and Tarassov, I. (2010). Mitochondrial enzyme rhodanese is essential for 5 S ribosomal RNA import into human mitochondria. The Journal of biological chemistry *285*, 30792-30803.

Smirnov, A., Entelis, N., Martin, R.P., and Tarassov, I. (2011). Biological significance of 5S rRNA import into human mitochondria: role of ribosomal protein MRP-L18. Genes & development *25*, 1289-1305.

Smirnov, A., Tarassov, I., Mager-Heckel, A.M., Letzelter, M., Martin, R.P., Krasheninnikov, I.A., and Entelis, N. (2008). Two distinct structural elements of 5S rRNA are needed for its import into human mitochondria. RNA (New York, NY *14*, 749-759.

Soutschek, J., Akinc, A., Bramlage, B., Charisse, K., Constien, R., Donoghue, M., Elbashir, S., Geick, A., Hadwiger, P., Harborth, J., *et al.* (2004). Therapeutic silencing of an endogenous gene by systemic administration of modified siRNAs. Nature *432*, 173-178.

Srivastava, S., and Moraes, C.T. (2001). Manipulating mitochondrial DNA heteroplasmy by a mitochondrially targeted restriction endonuclease. Human molecular genetics *10*, 3093-3099.

Stetsenko, D.A., and Gait, M.J. (2001). A convenient solid-phase method for synthesis of 3'-conjugates of oligonucleotides. Bioconjugate chemistry *12*, 576-586.

Stockert, R.J. (1995). The asialoglycoprotein receptor: relationships between structure, function, and expression. Physiological reviews *75*, 591-609.

Summerton, J., and Weller, D. (1997). Morpholino antisense oligomers: design, preparation, and properties. Antisense & nucleic acid drug development *7*, 187-195.

Tan, W., Wang, H., Chen, Y., Zhang, X., Zhu, H., Yang, C., Yang, R., and Liu, C. (2011). Molecular aptamers for drug delivery. Trends in biotechnology *29*, 634-640.

Tanaka, M., Borgeld, H.J., Zhang, J., Muramatsu, S., Gong, J.S., Yoneda, M., Maruyama, W., Naoi, M., Ibi, T., Sahashi, K., *et al.* (2002). Gene therapy for mitochondrial disease by delivering restriction endonuclease SmaI into mitochondria. Journal of biomedical science *9*, 534-541.

Tang, Z., Zhou, Y., Sun, H., Li, D., and Zhou, S. (2014). Biodegradable magnetic calcium phosphate nanoformulation for cancer therapy. Eur J Pharm Biopharm *87*, 90-100.

Tarassov, I., Chicherin, I., Tonin, Y., Smirnov, A., Kamenski, P., and Entelis, N. (2013). Mitocondrial Targeting of RNA and Mitochondrial Translation. In Translation in Mitochondria and Other Organels, A.M. Duchene, ed. (Springer Heidelberg), pp. 85-109.

Taylor, R.W., Chinnery, P.F., Turnbull, D.M., and Lightowlers, R.N. (1997). Selective inhibition of mutant human mitochondrial DNA replication in vitro by peptide nucleic acids. Nature genetics *15*, 212-215.

Thomas, C.E., Ehrhardt, A., and Kay, M.A. (2003). Progress and problems with the use of viral vectors for gene therapy. Nat Rev Genet *4*, 346-358.

Torchilin, V.P. (2005). Recent advances with liposomes as pharmaceutical carriers. Nature reviews *4*, 145-160.

Tuerk, C., and Gold, L. (1990). Systematic evolution of ligands by exponential enrichment: RNA ligands to bacteriophage T4 DNA polymerase. Science (New York, NY *249*, 505-510.

Uckun, F.M., Qazi, S., Dibirdik, I., and Myers, D.E. (2013). Rational design of an immunoconjugate for selective knock-down of leukemia-specific E2A-PBX1 fusion gene expression in human Pre-B leukemia. Integr Biol (Camb) *5*, 122-132.

Ueno, Y., Kawada, K., Naito, T., Shibata, A., Yoshikawa, K., Kim, H.S., Wataya, Y., and Kitade, Y. (2008). Synthesis and silencing properties of siRNAs possessing lipophilic groups at their 3'-termini. Bioorganic & medicinal chemistry *16*, 7698-7704.

Varkouhi, A.K., Scholte, M., Storm, G., and Haisma, H.J. (2011). Endosomal escape pathways for delivery of biologicals. J Control Release *151*, 220-228.

Vestweber, D., and Schatz, G. (1989). DNA-protein conjugates can enter mitochondria via the protein import pathway. Nature *338*, 170-172.

Vives, E., Schmidt, J., and Pelegrin, A. (2008). Cell-penetrating and cell-targeting peptides in drug delivery. Biochimica et biophysica acta *1786*, 126-138.

Volkov, A.A., Kruglova, N.S., Meschaninova, M.I., Venyaminova, A.G., Zenkova, M.A., Vlassov, V.V., and Chernolovskaya, E.L. (2009). Selective protection of nuclease-sensitive sites in siRNA prolongs silencing effect. Oligonucleotides *19*, 191-202.

Vu, H., Singh, P., Joyce, N., Hogan, M.E., and Jayaraman, K. (1993). Synthesis of cholesteryl supports and phosphoramidites containing a novel peptidyl linker for automated synthesis of triple-helix forming oligonucleotides (TFOs). Nucleic acids symposium series, 19-20.

Wallace, D.C. (2010). Mitochondrial DNA mutations in disease and aging. Environmental and molecular mutagenesis *51*, 440-450.

Walther, W., and Stein, U. (2000). Viral vectors for gene transfer: a review of their use in the treatment of human diseases. Drugs *60*, 249-271.

Wang, G., Shimada, E., Zhang, J., Hong, J.S., Smith, G.M., Teitell, M.A., and Koehler, C.M. (2012). Correcting human mitochondrial mutations with targeted RNA import. Proceedings of the National Academy of Sciences of the United States of America *109*, 4840-4845.

Wanrooij, S., and Falkenberg, M. (2010). The human mitochondrial replication fork in health and disease. Biochimica et biophysica acta *1797*, 1378-1388.

Weecharangsan, W., Opanasopit, P., and Lee, R.J. (2007). In vitro gene transfer using cationic vectors, electroporation and their combination. Anticancer research *27*, 309-313.

Weissig, V. (2011). From serendipity to mitochondria-targeted nanocarriers. Pharmaceutical research *28*, 2657-2668.

Weissig, V., D'Souza, G.G., and Torchilin, V.P. (2001). DQAsome/DNA complexes release DNA upon contact with isolated mouse liver mitochondria. J Control Release *75*, 401-408.

Weissig, V., Lasch, J., Erdos, G., Meyer, H.W., Rowe, T.C., and Hughes, J. (1998). DQAsomes: a novel potential drug and gene delivery system made from Dequalinium. Pharmaceutical research *15*, 334-337.

Westermann, B. (2012). Bioenergetic role of mitochondrial fusion and fission. Biochimica et biophysica acta *1817*, 1833-1838.

Winkler, J. (2013). Oligonucleotide conjugates for therapeutic applications. Therapeutic delivery *4*, 791-809.

Wolfrum, C., Shi, S., Jayaprakash, K.N., Jayaraman, M., Wang, G., Pandey, R.K., Rajeev, K.G., Nakayama, T., Charrise, K., Ndungo, E.M.*, et al.* (2007). Mechanisms and optimization of in vivo delivery of lipophilic siRNAs. Nature biotechnology *25*, 1149-1157.

Xua, Z.P., Zengb, Q.H., Lua G.Q., and BingYub, A. (2006). Inorganic nanoparticles as carriers for efficient cellular delivery. Chemical Engineering Science *61*, 1027 – 1040.

Yamada, Y., Akita, H., and Harashima, H. (2012a). Multifunctional envelope-type nano device (MEND) for organelle targeting via a stepwise membrane fusion process. Methods in enzymology *509*, 301-326.

Yamada, Y., Akita, H., Kamiya, H., Kogure, K., Yamamoto, T., Shinohara, Y., Yamashita, K., Kobayashi, H., Kikuchi, H., and Harashima, H. (2008). MITO-Porter: A liposome-based carrier system for delivery of macromolecules into mitochondria via membrane fusion. Biochimica et biophysica acta *1778*, 423-432.

Yamada, Y., Kawamura, E., and Harashima, H. (2012b). Mitochondrial-targeted DNA delivery using a DF-MITO-Porter, an innovative nano carrier with cytoplasmic and mitochondrial fusogenic envelopes. Journal of Nanoparticle Research *14*.

Yamanouchi, D., Wu, J., Lazar, A.N., Kent, K.C., Chu, C.C., and Liu, B. (2008). Biodegradable arginine-based poly(ester-amide)s as non-viral gene delivery reagents. Biomaterials *29*, 3269-3277.

ANNEX

Other studies.

During my master training course performed in the Laboratory of RNA Chemistry, Institute of Chemical Biology and Fundamental Medicine SB RAS, Novosibirsk, Russia under supervision of Dr. A. G. Venyaminova, I have participated in a study of the carrier-free cellular uptake of nuclease-resistant anti-MDR1 siRNA equipped with lipophilic residues (cholesterol, lithocholic acid, oleyl alcohol and litocholic acid oleylamide) attached to the 5'-end of the sense strand via aliphatic linker of various length. My contribution to this study consisted in the chemical synthesis and NMR characterization of various lipophilic precursors and in the synthesis of 5'-lipophilic conjugates of siRNAs by combination of H-phosphonate and phosphoramidite methods. Detailed description of the synthesis protocols are provided in the following **Publication 5**.

In a parallel with the main theme of my thesis, I have also participated in a study performed in the Institute of Chemical Biology and Fundamental Medicine SB RAS, Novosibirsk, Russia devoted to investigation of the effect of selectively 2'-O-methyl-modified 42 and 63 bp anti-MDR1-siRNAs on the innate immune response induction and silencing activity (**Publication 6**). My contribution to this study consisted in the chemical synthesis, purification and MALDI-TOF mass spectrometry characterization of long (42 and 63 b) oligoribonucleotides containing 2'-O-methyl analogues of ribonucleotides in the nuclease sensitive sites CpA, UpA and UpG.

Experience acquired during these studies helped me to optimize the protocols of chemical synthesis used in my Thesis project.

Publication 5.

Petrova N.S., Chernikov I.V., Meschaninova M.I., Dovydenko I.S., Venyaminova A.G., Zenkova M.A., Vlassov V.V., Chernolovskaya E.L. Carrier-free cellular uptake and the gene-silencing activity of the lipophilic siRNAs is strongly affected by the length of the linker between siRNA and lipophilic group. Nucleic Acids Res. 2012. V.40. N.5. P.2330-2344.

Carrier-free cellular uptake and the gene-silencing activity of the lipophilic siRNAs is strongly affected by the length of the linker between siRNA and lipophilic group

Natalya S. Petrova, Ivan V. Chernikov, Mariya I. Meschaninova[1], Ilya S. Dovydenko[1], Aliya G. Venyaminova[1], Marina A. Zenkova, Valentin V. Vlassov and Elena L. Chernolovskaya*

Laboratory of Nucleic Acids Biochemistry and [1]Labotarory of RNA Chemistry, Institute of Chemical Biology and Fundamental Medicine, SB RAS, Lavrentiev ave., 8, Novosibirsk 630090, Russia

ABSTRACT

The conjugation of siRNA to molecules, which can be internalized into the cell via natural transport mechanisms, can result in the enhancement of siRNA cellular uptake. Herein, the carrier-free cellular uptake of nuclease-resistant anti-*MDR1* siRNA equipped with lipophilic residues (cholesterol, lithocholic acid, oleyl alcohol and litocholic acid oleylamide) attached to the 5′-end of the sense strand via oligomethylene linker of various length was investigated. A convenient combination of H-phosphonate and phosphoramidite methods was developed for the synthesis of 5′-lipophilic conjugates of siRNAs. It was found that lipophilic siRNA are able to effectively penetrate into HEK293, HepG2 and KB-8-5 cancer cells when used in a micromolar concentration range. The efficiency of the uptake is dependent upon the type of lipophilic moiety, the length of the linker between the moiety and the siRNA and cell type. Among all the conjugates tested, the cholesterol-conjugated siRNAs with linkers containing from 6 to 10 carbon atoms demonstrate the optimal uptake and gene silencing properties: the shortening of the linker reduces the efficiency of the cellular uptake of siRNA conjugates, whereas the lengthening of the linker facilitates the uptake but retards the gene silencing effect and decreases the efficiency of the silencing.

INTRODUCTION

Small interfering RNAs (siRNAs) (1–3) have broad application within molecular biology and experimental pharmacology, being widely used for the control of gene expression (4–6). Currently, siRNAs are used successfully for the validation of potent drug targets for anti-cancer therapy (7,8). A factor that significantly limits their biomedical application, are the challenges associated with the inefficient delivery of siRNAs to target cells and tissues. Various approaches have been developed in an attempt to overcome this problem. These different approaches can be assigned to one of two major groups: viral (9,10) and non-viral (11–13) methods. Viral-based RNAi provides an efficient and long-lasting silencing in cultured cells and in laboratory animals systems; however, immunogenicity, in the case of adenoviral vectors, is a factor that limits their biomedical application (14). Furthermore, the potential tumorogenicity as a result of the integration into the host genome, in the case of lenti- and retroviral vectors is an additional limiting factor (15–17). Non-viral approaches include the following groups of methods: firstly, high-pressure intravenous injections (18–20); secondly, the delivery of siRNA in the complexes with cationic lipids, polymers and different types of particles; thirdly, the covalent conjugation of siRNAs with different carrier molecules (11,21,22). The first approach can be applied only to laboratory animals, since it often results in organ damage and immune activation. The second group of methods is a member of a quickly developing field of science; however, the toxicity of lipids and polymers (23) and the

*To whom correspondence should be addressed. Tel: +7 383 3635161; Fax: +7 383 3635153; Email: elena_ch@niboch.nsc.ru

insufficient transfection efficacy *in vivo* (11), severely limits the application of available up-to-date formulations. The conjugation of siRNA to the molecules, which can be internalized into the cell by natural transport mechanisms, is an approach that shows considerable promise in the attempt to overcome the problem of toxicity and target delivery (22,24). Steroids and other hydrophobic lipid groups can be attached to siRNA, thereby extending the siRNA circulation time and enhancing the direct cellular uptake (25–27). The potential of cholesterol (26,27), α-tocopherol (28), aptamers (29–31), antibodies (32–34) and cell-penetrating peptides (35–38) in the alteration of the bioavailability and distribution of siRNAs has been described; however, the silencing efficacy of different conjugates varies substantially and the optimization of the composition and structure of the conjugates is required.

Within this study, we investigated the carrier-free cellular accumulation and silencing activity of various lipophilic conjugates of the nuclease-resistant anti-*MDR1* siRNA. The following lipophilic moieties: cholesterol, oleyl alcohol, lithocholic acid and oleylamide of lithocholic acid, were attached to the 5′-end of the sense strand of siRNA directly or via aliphatic amino-propyl-, -hexyl-, -octyl-, -decyl- and -dodecyl- linker. It was ascertained that the efficiency of cellular accumulation is dependent upon the type of lipophilic residues, the type of the target cells and the length of the linker between siRNA and lipophilic residue.

MATERIALS AND METHODS

General remarks

RNA phosphoramidites, 2′-O-methylphosphoramidites and other reagents for the oligonucleotide synthesis were obtained from Glen Research (USA). 3-Aminopropan-1-ol, 6-aminohexan-1-ol, cholesterol, cholesteryl chloroformate and lithocholic acid were purchased from Sigma-Aldrich (USA), oleylamine and oleyl alcohol were supplied from Acros (Belgium) and 8-aminooctan-1-ol, 10-aminodecan-1-ol, 12-aminododecan-1-ol were acquired from TCI (Belgium). Other chemicals were supplied by Merck (Germany) and Fluka (Switzerland). Solvents were supplied from Panreac (Spain).

Column chromatography was performed with Silica gel 60 Å 230–400 mesh (Sigma), and thin-layer chromatography (TLC) was performed on Silica gel 60 F_{254} aluminum sheets (Merck) in CH_3OH/CH_2Cl_2 5/95. ^1H and ^{31}P NMR spectra were recorded on a Bruker AV-300 spectrometer with tetramethylsilane as an internal standard, or 85% phosphoric acid as an external standard, respectively. RNA synthesis (0.4 μmol scale) was performed on the automatic ASM-800 DNA/RNA synthesizer (Biosset, Russia). Preparative reverse phase high performance liquid chromatography (RP-HPLC) was performed on an Alliance chromatographic system (Waters, USA) equipped with XBridge C18 column, 2.5 μm, 4.6 × 50 mm (Waters, USA) at 50°C. The flow rate was 1 ml/min (buffer A, 0.05 M $NaClO_4$; buffer B, 0.05 M $NaClO_4$/90% CH_3CN); the

gradient was as follows: (i) 0.00 min, 0.0% buffer B; 35.00 min, 90.0% buffer B for the conjugated siRNAs; (ii) 0.00 min, 0.0% buffer B; 35.00 min, 20.0% buffer B for the non-conjugated siRNAs. The oligonucleotide-containing fractions were evaporated in Speedvac concentrator (SVC-100 H, Savant, USA) and precipitated as Na^+ salts. The preparative PAGE was performed using denaturing 12% polyacrylamide gel (acrylamide:N,N′-methylenebisacrylamide (30:0.5), 8 M urea, 89 mM Tris–borate, pH 8.3, 2 mM Na_2EDTA, 20 V/cm). After electrophoretic separation, oligonucleotide material was visualized by UV shadowing, extracted from the gel with 0.3 M NaOAc (pH 5.2) containing 0.1% sodium dodecyl sulfate (SDS), followed by precipitation with ethanol. LC-ESI and MALDI-TOF mass-spectra were obtained with an ESI MS/MSD XCT (Agilent Technologies, USA) and a autoflex III (Bruker Daltonics, Germany) mass spectrometer.

Synthesis

Cholesterol-3-(carboxyaminopropan-3-ol) (**2**), *cholesterol-3-(carboxyaminohexan-6-ol)* (**3**), *cholesterol-3-(carboxy aminooctan-8-ol)* (**4**), *cholesterol-3-(carboxyaminodecan-10-ol)* (**5**) and *cholesterol-3-(carboxyaminododecan-12-ol)* (**6**) were synthesized by analogy with (39). Cholesteryl chloroformate (**1**, 0.5 g, 1.1 mmol) and dry triethanolamine (TEA, 0.15 ml, 1.1 mmol) were dissolved in dry dichloromethane (4 ml) and added to anhydrous aminoalcohol (1.1 mmol). The mixture was stirred at room temperature for 2 h (TLC, AcOEt/hexane 50/50), following this dichloromethane (20 ml) was added, and the resulting solution was then washed with saturated aqueous (sat. aq.) $NaHCO_3$ (20 ml × 2) and water (20 ml), dried over Na_2SO_4, and then filtered and evaporated under reduced pressure. The residue was dissolved in AcOEt/hexane (10/90) and purified via silica gel column chromatography (elution with AcOEt/hexane 10/90 to 50/50). The characteristics of **2** to **6** are presented in the Supplementary Materials.

3α-(Acetoxy)-5β-cholanic acid (**8**). Lithocholic acid (**7**, 0.5 g, 1.3 mmol) was dissolved in dry pyridine (10 ml) under argon and cooled to 0°C. 4-Dimethylaminopyridine (0.02 g, 0.13 mmol) and acetyl chloride (1.1 ml, 16 mmol) were added to the solution. After the mixture was stirred at room temperature for 1 h (under TLC control), water (3 ml) was added and the solution was evaporated under reduced pressure. Dichloromethane (15 ml) was used to dissolve the residue, which was subsequently washed with sat. aq. NaCl (20 ml) and water (15 ml). The organic phase was dried over Na_2SO_4, then filtered and evaporated to dryness. The crude product was co-evaporated with toluene (10 ml × 2), ethanol (10 ml × 2), acetonitrile (10 ml × 2) and dichloromethane (10 ml × 2) in order to remove the traces of pyridine and purified by silica gel chromatography (elution with CH_3OH/CH_2Cl_2 0/100 to 5/95). The characteristics of **8** are presented in Supplementary Methods.

3α-(Acetoxy)-5β-cholanic acid pentafluorophenyl ester (**9**) was synthesized by analogy with (40). Compound

8 (0.4 g, 1.0 mmol) was dissolved in dry dichloromethane (13 ml) under argon and cooled to 0°C. N,N-Dicyclohexylcarbodiimide (0.25 g, 1.2 mmol) was added to the solution. The mixture was stirred for 30 min at 0°C. Following this, pentafluorophenol (0.2 g, 1.1 mmol) in dichloromethane (1 ml) was added and the stirring was then continued at room temperature for an additional 20 h (under TLC control). The precipitated N,N-dicyclohexylurea was filtered off and washed with cold dichloromethane; combined filtrates were evaporated under reduced pressure. The oily residue obtained was then diluted with dichloromethane (15 ml) and washed with sat. aq. NaCl (20 ml) and water (15 ml). The organic phase was dried over Na_2SO_4, filtered and evaporated until complete dryness had been achieved. Compound **9** (0.55 g, 98%) thus obtained was directly used for the next step without purification. R_f (TLC, CH_3OH/CH_2Cl_2 5/95): 0.8.

3α-(Acetoxy)-5β-cholanic acid 3-hydroxypropylamide **(10)** and *3α-(acetoxy)-5β-cholanic acid 6-hydroxy-hexylamide* **(11)**. Aminoalcohol (1.3 mmol) was co-evaporated with dry pyridine (3 ml × 3), dissolved in dry dichloromethane (1 ml) and added to the mixture of compound **6** (0.5 g, 0.9 mmol) and TEA (three equiv) in dry dichloromethane (20 ml) cooled to 0°C. The reaction mixture was stirred at room temperature under argon for 40 min (under TLC control) and washed with sat. aq. NaCl (50 ml × 2) and water (50 ml). The organic phase was dried over Na_2SO_4. Following this, it was filtered and evaporated to dryness. The crude product was then purified via silica gel column chromatography (elution with $CH_3OH/hexane/CH_2Cl_2$ 0/50/50 to 8/46/46) in order to afford the compounds **10** and **11** as white solids. The characteristics of **10** and **11** are presented in the Supplementary Materials.

3α-(Hydroxy)-5β-cholanic acid pentafluorophenyl ester **(12)** was synthesized by analogy with (41). Lithocholic acid **(7)** (0.5 g, 1.35 mmol) was dissolved in dry dichloromethane (13 ml) and then cooled to 0°C. Following this N,N-dicyclohexylcarbodiimide (0.34 g, 1.65 mmol) was added to the solution. After stirring for 30 min at 0°C, pentafluorophenol (0.27 g, 1.5 mmol) in dichloromethane (1 ml) was added; the stirring was then continued at room temperature under argon for an additional 20 h (under TLC control). The precipitated N,N-dicyclohexylurea was filtered off and washed with cold dichloromethane. Combined filtrates were then evaporated under reduced pressure. The oily residue obtained was then diluted with dichloromethane (15 ml) and washed with sat. aq. NaCl (20 ml) and water (15 ml). The organic phase was dried over Na_2SO_4, filtered and evaporated to dryness. The obtained compound **12** (0.7 g, 96%), was directly used for the next step without purification. R_f (TLC, CH_3OH/CH_2Cl_2 5/95): 0.8.

3α-(Hydroxy)-5β-cholanic acid oleylamide **(13)**. Compound **12** (0.7 g, 1.3 mmol) was dissolved in dry dichloromethane (30 ml) and then cooled to 0°C. A cold mixture of oleylamine (0.65 ml, 2.0 mmol) and TEA (0.55 ml, 4.0 mmol) in dichloromethane (2 ml) was added to the resulting solution. The reaction mixture was stirred at room temperature for an additional 1 h (under TLC control) and washed with sat. aq. NaCl (50 ml × 2) and water (50 ml). The organic phase was dried over Na_2SO_4 and filtered. In order to afford the compound **13** as a white solid, the crude product was purified via silica gel column chromatography (elution with $CH_3OH/hexane/CH_2Cl_2$ 0/50/50 to 4/48/48) following the evaporation of solvents. The characteristics of **13** are presented in the Supplementary Materials.

3α-(Succinimidyloxycarbonyl)-5β-cholanic acid oleylamide **(14)** was synthesized by analogy with (40). The amide **13** (0.45 g, 0.72 mmol) was dissolved in dry dichloromethane (6 ml). N,N′-disuccinimidyl carbonate (0.55 g, 2.1 mmol), dry TEA (0.5 ml) and dry acetonitrile (3 ml) were added to the solution. The reaction mixture was stirred at room temperature under argon for 24 h (under TLC control) and was then evaporated until dryness had been achieved. The residue was dissolved in dichloromethane (20 ml), washed with sat. aq. $NaHCO_3$ (20 ml × 2), dried over Na_2SO_4, filtered and then evaporated under reduced pressure. Compound **14** (0.54 g, 98%) was obtained as a colorless powder, which was directly used for the next step in the absence of further purification. R_f (TLC, CH_3OH/CH_2Cl_2 5/95): 0.2.

3α-(Carboxyaminopropan-3-ol)-5β-cholanic acid oleylamide **(15)** and *3α-(carboxyaminohexan-6-ol)-5β-cholanic acid oleylamide* **(16)** were synthesized via analogy with (40). Aminoalcohol (0.7 mmol) was dried via co-evaporation with dry pyridine (3 ml × 3), dissolved in dry pyridine (0.8 ml) and subsequently added to the solution of compound **14** (0.54 g, 0.7 mmol) in dry dichloromethane (4 ml). The resulting mixture was then cooled to 0°C. Following stirring at room temperature under argon for 20 h (under TLC control), the reaction mixture was evaporated to dryness, dissolved in dichloromethane (20 ml), washed with sat. aq. $NaHCO_3$ (20 ml × 2) and water (20 ml); dried over Na_2SO_4 and then evaporated under reduced pressure. The residue was purified via silica gel column chromatography (elution with CH_3OH/CH_2Cl_2 0/100 to 4/96) to afford **15** and **16**. The characteristics of **15** and **16** are shown in the Supplementary Materials.

Synthesis of lipophilic H-phosphonates **(17–28)**. H-Phosphonates of lipophilic compounds were synthesized via analogy with (42). Imidazole (1 g, 14.5 mmol) was dissolved in dry acetonitrile (20 ml) and then cooled to 0°C. TEA (2 ml, 14.0 mmol) and PCl_3 (0.4 ml, 4.5 mmol) were added to this solution and subsequently stirred for 25 min at 0°C. Lipophylic compound (1 mmol) was dissolved separately in dry dichloromethane (10 ml) and added drop-wise into the mixture for 40 min under argon. The reaction mixture was then stirred for an additional 1 h at room temperature (under TLC control) followed by the addition of water (3 ml) and subsequent evaporation. The residue was dissolved in dichloromethane (30 ml), washed with water (20 ml × 2), dried over Na_2SO_4, filtered and then evaporated under reduced pressure. The crude product was dissolved in CH_3OH/CH_2Cl_2 (10/90) and was then subjected to silica gel chromatography (elution with CH_3OH/CH_2Cl_2 10/90 to 70/30 with 0.1% TEA), in order to afford the

corresponding H-phosphonate. The characteristics of H-phosphonates (**17–28**) are shown in the Supplementary Materials.

Synthesis of siRNA

Oligoribonucleotides were synthesized on an automatic ASM-800 synthesizer at 0.4 µmol scale using solid phase phosphoramidite synthesis protocols (43) optimized for the instrument, with a 10 min coupling step for 2′-O-TBDMS-protected phosphoramidites (0.1 M in acetonitrile), 6 min coupling step for 2′-O-methylated phosphoramidites (0.05 M in acetonitrile) and 5-ethylthio-H-tetrazole (0.25 M in acetonitrile) as an activating agent. A mixture of acetic anhydride with 2,6-lutidine in THF and N-methylimidazole in THF were utilized as capping reagents. The oxidizing agent was 0.02 M iodine in pyridine/water/THF (1/9/90). Dichloroacetic acid (3%) in dichloromethane was used as a detritylating reagent. The 3′-end of the antisense strand of siRNA used in the uptake assay was labeled by fluorescein (FITC) as described in (44).

Synthesis of lipophilic conjugates of oligonucleotides

Conjugates were prepared via analogy with (42). Each H-phosphonate of the lipophilic compound (**17–28**) (4.5 µmol) was dissolved in dichloromethane (150 µl). The 5′-O-detritylated, support-bound oligonucleotide (15 mg, 0.45 µmol) was then transferred from the synthesis column to a 0.6 ml screw top glass vial and subsequently blended with a solution of the corresponding H-phosphonate (50 µl), followed by treatment with pivaloyl chloride (1.3 µl, 12.5 µmol in 150 µl pyridine/acetonitrile, 2/1) for 5 min. In order to remove an uncoupled lipophilic compound, the support-bound conjugate was washed with acetonitrile. In order to increase the yield of the conjugates the condensation was repeated twice. The conjugate-containing support was then washed with acetonitrile, treated with I_2 (0.2 ml of 0.1 M solution in pyridine/water, 98/2) for 20 min, washed with acetonitrile, acetone and diethyl ether, and then subsequently dried.

Deprotection, purification and annealing of siRNAs and lipophilic analogs

The oligoribonucleotides (Table 1) and their conjugates (Table 2) were cleaved from the support and deprotected by 40% methylamine in water at 65°C for 15 min. 2′-O-Silyl groups were removed upon treatment with a mixture of NMP/TEA·3HF/TEA (150/100/75) at 65°C for 1.5 h. Deprotected oligoribonucleotides and conjugates were isolated by RP-HPLC and precipitated with ethanol as Na$^+$ salts. Alternatively, they were isolated via preparative electrophoresis in 12% polyacrylamide/8 M urea gel, followed by elution from the gel with 0.3 M NaOAc (pH 5.2)/0.1% SDS solution and precipitated with ethanol as Na$^+$ salts. The purified oligoribonucleotides were characterized by electrophoretic mobility in 12% dPAAG, MALDI-TOF-MS and LC-ESI-MS (Table 2). siRNA duplexes were annealed at 10 µM in 30 mM HEPES-KOH, pH 7.4, 100 mM potassium acetate, 2 mM magnesium acetate and stored at −20°C.

Table 1. Sequences of oligoribonucleotides

Designation	Sequence[a] (5′–3′)
ON1 (sense strand of siMDR)	GGCUUGACAAGUUGUAUAUGG
ON2 (antisense strand of siMDR)	AUAUACAACUUGUCAAGCCAA
ON3 (sense strand of siScr)	CAAGUCUCGUAUGUAGUGGUU
ON4 (antisense strand of siScr)	CCACUACAUACGAGACUUGUU

[a]2′-O-methyl-modified nucleotides are underlined.

Table 2. 5′-lipophilic conjugates of the sense strands of siRNAs

No.	Conjugate	Yield[a] (%)	Mass found	Mass calculated
29	Ch0-ON1	8/88[b]	7286.3[c]	7285.8
30	Ch3-ON1	9/89[b]	7386.5[c]	7386.8
31	Ch6-ON1	7/87.5[b]	7428.7[c]	7428.8
32	Ch8-ON1	9.5/89.3[d]	7456.5[e]	7456.8
33	Ch10-ON1	10/89.5[d]	7485.3[c]	7484.8
34	Ch12-ON1	9.5/89.3[d]	7513.2[e]	7512.8
35	Lt3-ON1	8.5/88.4[b]	7332.8[c]	7332.7
36	Lt6-ON1	11/90[b]	7374.8[e]	7374.7
37	Ol-ON1	7/87.5[b]	7167.2[e]	7167.7
38	OlLt0-ON1	7/87.5[d]	7524.7[c]	7525.2
39	OlLt3-ON1	9/89[d]	7625.7[c]	7626.2
40	OlLt6-ON1	8.5/88.4[d]	7667.7[c]	7668.2
41	Ch0-ON3	11/90[b]	7208.5[e]	7208.7
42	Ch3-ON3	9/89[b]	7308.9[e]	7309.7
43	Ch6-ON3	10/89.5[b]	7351.2[e]	7351.7
44	Ch8-ON3	10/89.5[d]	7380.1[e]	7379.7
45	Ch10-ON3	11/90[d]	7407.8[e]	7407.7
46	Ch12-ON3	10.5/89.8[d]	7436.2[e]	7435.7
47	Lt3-ON3	11/90[b]	7255.1[e]	7255.6
48	Lt6-ON3	11/90[b]	7297.4[e]	7297.6
49	OlLt0-ON3	9/89[d]	7448.4[e]	7448.1
50	OlLt3-ON3	9/89[d]	7549.2[e]	7549.1
51	OlLt6-ON3	9/89[d]	7590.5[e]	7591.1

[a]Overall yield/coupling yield (per support-bound starting nucleoside) after isolation.
[b]Overall yield/coupling yield (per support-bound starting nucleoside) after isolation by RP-HPLC.
[c]LC-ESI-MS (ESI MS/MSD XCT, Agilent Technologies, USA).
[d]Overall yield/coupling yield (per support-bound starting nucleoside) after isolation by PAGE.
[e]MALDI-TOF-MS (autoflex III, Bruker Daltonics, Germany).

Cell cultures

Human HEK293 and HepG2 cell lines were obtained from the Institute of Cytology RAS, St. Petersburg, Russia. Multiple drug resistant human cell line KB-8-5 growing in the presence of 300 nM vinblastine was generously provided by Prof. M. Gottesman (National Institutes of Health, USA). The cells were grown in Dulbecco modified Eagle's medium (DMEM) supplemented with 10% fetal bovine serum (FBS), 100 U/ml penicillin, 100 µg/ml streptomycin and 0.25 µg/ml amphotericin at 37°C in a humidified atmosphere containing 5% CO_2/95% air.

Cellular accumulation assay

One day before the experiment KB-8-5, HepG2 and HEK 293 cells in the exponential phase of growth were plated

in 24-well plates at a density of 1.7×10^5 cells/well. The growth medium was then replaced by fresh DMEM (200 µl/well) without FBS. Each of the FITC-labeled lipophilic siRNAs was added to the cells in 50 µl of Opti-Mem to give the final concentration varying from 0.2 to 5 µM. Four hours post-transfection cells were trypsinized and fixed in 2% formaldehyde in phosphate-buffered saline (PBS). In the case of KB-8-5 cells, the accumulation of conjugates was estimated 1, 2, 4, 8 and 24 h post-transfection. Cells were analyzed using Cytomics FC 500 (Beckman Coulter, USA) flow cytometer (excitation wave length 488 nm, emission 530 ± 30 nm). Of cells, 10 000 from each sample were analyzed. The percentage of FITC positive cells with green fluorescence exceeded the level of the auto-fluorescence of untreated cells (here and after referred to as 'transfected cells'). The mean values of cell fluorescence intensity normalized to this value of untreated cells were used for data presentation.

Confocal microscopy

In order to prove the intracellular localization of the lipophilic siRNAs, the confocal fluorescent microscopy was utilized. KB-8-5 cells in the exponential phase of growth were plated on the glass coverslips in 24-well plates at a density of 1.3×10^5 cells/well one day before the experiment. FITC-labeled cholesterol-containing siRNAs were then added to the cells to final concentration 2 µM. Following 8 h of incubation the cells were washed with PBS, fixed in 4% formaldehyde/PBS at 37°C for 20 min, permeabilized in 0.5% saponin/PBS for 10 min and stained with Rhodamine Phalloidin (Millipore, USA) and dissolved in PBS for 15 min for cytoskeleton (ß-actin) visualization. The cells on the coverslips were then washed with PBS and mounted on the object-plate in DAPI/Antifade solution (Millipore, USA). The analysis of lipophilic siRNA localization was performed using a confocal fluorescent microscope LSM 510 Meta (Carl Zeiss, Germany) at 100× magnification using optical filters BP 420–480 nm, BP 505–530 nm and LP 560 nm.

MTT Assay

In order to determine the number of living cells a colorimetric assay was used, based on the reduction of the dye 3-[4,5-dimethylthiazol-2-yl]-2,5-diphenyltetrazolium bromide (MTT) in mitochondria (45). Exponentially growing KB-8-5 cells were plated in 96-well plates (2.5×10^3 cells/well) in a vinblastine-free medium one day before the experiment. Following this lipophilic conjugates of siRNA (1–5 µM) were added to the cells. After 24 h of incubation, the vinblastine was added to the cells to the final concentration of 300 nM. After 4, 5 and 6 days of incubation the MTT assay was then performed according to the procedure described in (45). The relative number of living cells normalized to the number of living cells in control was used for data presentation.

Western blotting

The level of P-glycoprotein (P-gp) in KB-8-5 cells was evaluated in a vinblastine-free medium. The cells in the exponential phase of growth were plated in 48-well plates (7×10^3–10^4 cells/well). After 24 h had elapsed, cholesterol-containing siRNAs (5 µM) were added to the cells as previously described. Alternatively, the cells were transfected with non-modified siRNA (0.2 µM) using Lipofectamine 2000 (Invitrogene, Carlsbad, CA) (0.8 µl per well) according to the manufacturer's protocol. The cells were then cultured for 3–8 days. During this incubation period cells were re-plated after 4 and 5 days of incubation into 48-well plates (2×10^4 cells/well) for the time points: 6 and 8 days, respectively. The cells were lysed in 40 µl of sample buffer (Sigma-Aldrich, USA) at the time points 3, 4, 5, 6 and 8 days of incubation. Of each sample, 20 µl was loaded on a 10% SDS/polyacrylamide gel and then separated at 60 mA for 1 h. The proteins were transferred from PAAG to PVDF membrane (Millipore, USA) using SemiPhor (Hoefer, USA) and the membrane was then blocked overnight in 0.5% non-fat dried milk in 0.05 M Tris–HCl, 0.15 M NaCl, 0.1% Tween-20 pH 7.5. The membranes were incubated with monoclonal anti-P-gp and anti-β-actin antibodies (Sigma-Aldrich, USA) at 1:3000 and 1:6000 dilutions, respectively for 1 h. After the membranes were washed in buffer B, they were subsequently incubated for 30 min with secondary rabbit anti-mouse antibodies conjugated with alkaline phosphatase (Invitrogen, USA). Chromogenic detection was then performed using Western Blue Stabilized Substrate for alkaline phosphatase (Promega, USA). The reaction was stopped via rinsing with water. The human β-actin protein was used as an internal control. Data were analyzed using GelPro 4.0. software (Media Cybernetics, USA).

RESULTS

The sequence of siRNA (Table 1) targeted to 557–577 nt of the human *MDR1* mRNA (here and after siMDR) was selected in our previous study (46). It was demonstrated that siMDR has the ability to inhibit the *MDR1* expression both at the level of mRNA and P-gp. Furtermore, siMDR is capable of reversing the multiple drug resistance of cancer cells. siRNA that has no significant homology to any known mRNA sequences from mouse, rat or human was used as a negative control (here and after referred to as 'siScr', Table 1). These siRNAs contained 2′-O-methyl modifications in CpA, UpA and UpG motives, earlier identified as the primary sites of nuclease attack (47). 5′-Hydroxyl-position of the sense strands of siRNAs was used for the introduction of the lipophilic moieties since the modification of this position is better tolerated by RNAi machinery than the modification of the antisense or both strands (25,48,49).

Synthesis of lipophilic siRNAs

A combination of H-phosphonate and phosphoramidite methods was applied to the synthesis of 5′-lipophilic conjugates of siRNAs. The modified lipophilic synthons were then synthesized, beginning with cholesterol, cholesteryl chloroformate (**1**) and lithocholic acid (**7**) (Figure 1). Lithocholic acid was selected due to the fact that both
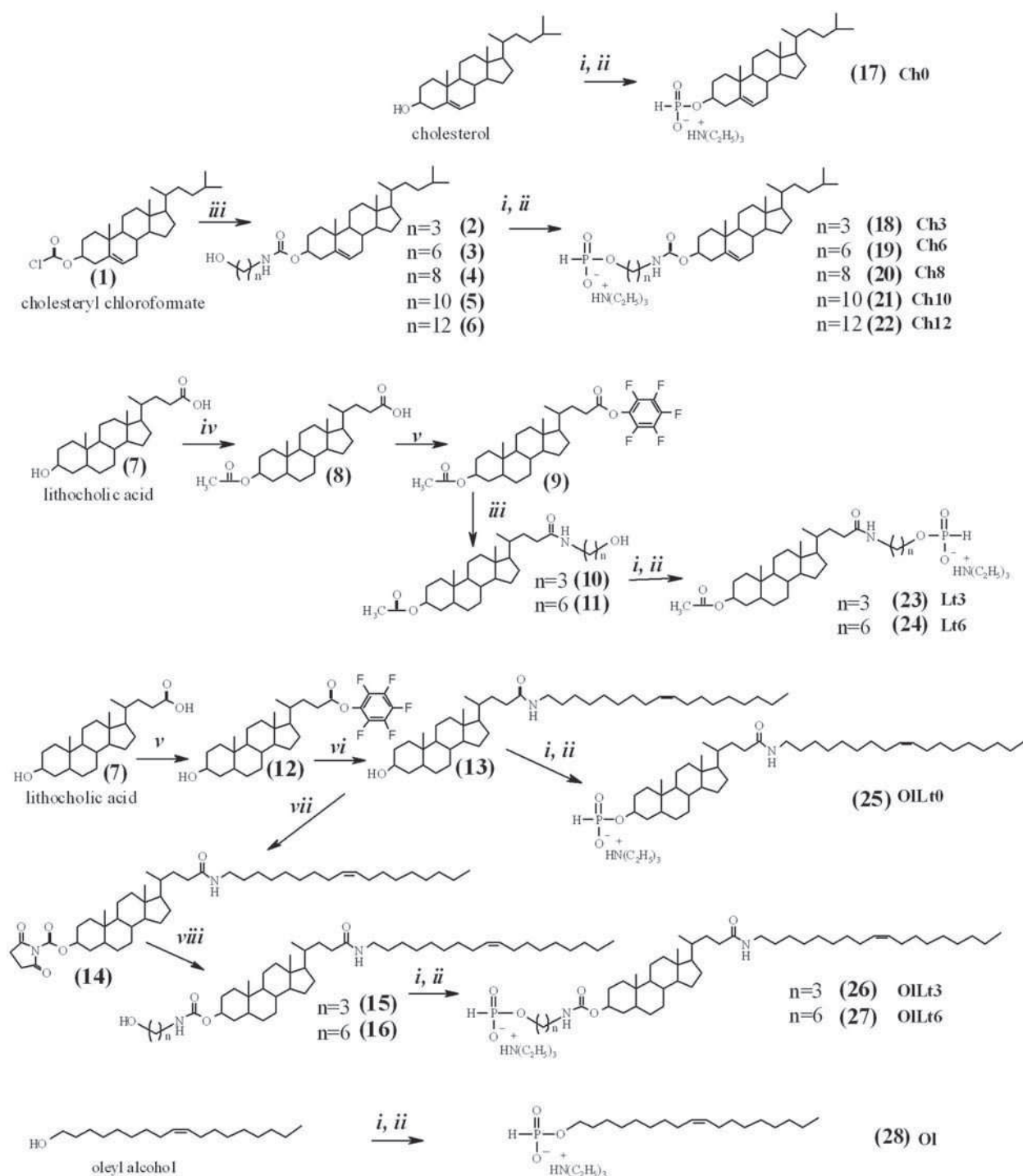
Figure 1. Synthesis of lipophilic H-phosphonates **17–28**. Reagents: (i) PCl₃, imidazole, TEA; (ii) H₂O; (iii) aminopropanol, aminohexanol, aminooctanol, aminodecanol or aminododecanol, TEA; (iv) acetyl chloride, DMAP; (v) DCC, pentafluorophenol; (vi) oleylamide, TEA; (vii) N,N'-disuccinimidyl carbonate, TEA; (viii) aminopropanol or aminohexanol.

carboxylic and hydroxyl groups are presented in one molecule and can be used for attachment to siRNAs or esterification with fatty acids. The lipophilicity of the lithocholic acid was enhanced via introduction of the oleylamine residue giving compounds **13**, **15** and **16**.

The lipophilic compounds **1**, **7** and their derivatives bearing linkers of various lengths were transformed into the corresponding H-phosphonates via interaction with phosphorus triimidazolide followed by hydrolysis (Figure 1). This reaction gives H-phosphonates **17–28**

with high yield (41–94%). Structures of H-phosphonates and their precursors were confirmed by NMR and MS methods (see Supplementary Materials for details).

The sense and antisense strands of siRNAs were synthesized according to the phosphoramidite method. Support-bound 5′-hydroxyl-containing sense strands of siRNA were used for the condensation with H-phosphonates **17–28** in the presence of pivaloyl chloride. The lipophilic conjugates obtained were fully deprotected according to the standard procedures, using methylamine and TEA·3HF (43).

Isolation of the oligoribonucleotides conjugated with cholesterol (**29–34**, **41–46**), lithocholic acid (**35**, **36**, **47**, **48**) and oleyl alcohol (**37**) from reaction mixtures was accomplished via reverse-phase HPLC. With regards to the conventional oligoribonucleotides, the retention time increased from 5 min to 15–23 min for lipophilic oligoribonucleotides depending on the nature of the lipophilic component and the linker length (Supplementary Figure S1). Purification of the oligoribonucleotides conjugated with the litocholic acid oleylamide (**38–40**, **49–51**) via RP-HPLC resulted in the loss of oligonucleotide material because of their high lipophilicity. Preparative PAGE was used followed by conjugates precipitation as Na$^+$ salts, in order to overcome these obstacles. The overall yield of the lipophilic oligoribonucleotides purified by HPLC or PAGE methods was 8-12% (per support-bound starting nucleoside) (Table 2).

All purified lipophilic oligoribonucleotides were analyzed by LC-ESI and MALDI-TOF mass spectrometry. The calculated molecular weights were in agreement with the measured values, thereby confirming the structures of the isolated products (Table 1).

Carrier-free cellular uptake of lipophilic siRNAs

The accumulation of the FITC-labeled siRNA and its lipophilic conjugates into KB-8-5, HepG2 and HEK 293 cells was measured using flow cytometry after 4 h of incubation with the corresponding siRNA. Two parameters reflecting the efficiency of the process were used for the comparison: the transfection efficiency (here and after referred to as 'TE') estimated as a percentage of cells with green fluorescence exceeding the maximum level of cell auto-fluorescence and the normalized mean value of the intensity of the green fluorescence of the cell measured in relative fluorescent units (here and after referred to as "RFU") normalized to that of untreated cells. The data show that the efficacy of cellular accumulation is dependent upon the type of cell line; however, all conjugates of siRNA with cholesterol or with oleylamide of lithocholic acid accumulated in all cells under study, with a higher degree of effectiveness than other conjugates (Figure 1). The 100% transfection of KB-8-5 cells was observed after the incubation of the cells with these conjugates at 2 and 5 μM concentrations (Figure 2A); conversely, the same level of transfection was achieved at the concentrations of the conjugates 0.2 and 1 μM, respectively for HepG2 and HEK293 cells (Figure 2C and E). Non-modified siRNA and conjugates of siRNA and lithocholic acid did not penetrate in KB-8-5 and HepG2 cells (Figure 2A

and C), whereas the TE of HEK293 with these conjugates reached 90% at 5 μM concentration (Figure 2E). The accumulation of the siRNA conjugated with oleic alcohol in the cells was insignificant. The comparison of mean values of the cell fluorescence intensity revealed a substantial preference of cholesterol-conjugated siRNA in comparison with other conjugates (Figure 2B, D and F). The cholesterol residue conjugated to siRNA via aminohexyl and aminododecyl linkers enabled a 4–5-fold higher accumulation of siRNA in KB-8-5 cells at a 5 μM concentration of the conjugates, in comparison with that of oleylamide of lithocholic acid conjugated to siRNA (Figure 2B). Similar results were obtained in HepG2 cells. The differences between cellular accumulation of the conjugates in HEK293 cells were less pronounced, but still substantial (Figure 2).

It was discovered that the length of the linker between the siRNA and lipophilic residue significantly influences the cellular accumulation. The conjugates containing linkers of 6-12 carbon atoms accumulated in all tested cells more efficiently than conjugates in which the lipophilic residue was attached to siRNA directly or via a shorter linker (Figure 2). The estimation of TE at the lower concentrations of the conjugates (0.2–1 μM) revealed that the percentage of transfected cells increased with the increase of the linker length (Figure 2A, C and E). TE of HEK293 cells was 0, 20, 50 and 70% for the siRNA with cholesterol tethered directly (without linker) or via the aminopropyl, aminohexyl and aminododecyl linkers, respectively (Figure 2E). This tendency can evidently be observed via comparison of the mean fluorescence values (Figure 2B, D and F). For instance, the lengthening of the linker from 0 to 12 carbon atoms increased the mean fluorescence intensity from 5 to 110 RFU for KB-8-5 cells, from 10 to 117 RFU for HepG2 cells and from 20 to 90 RFU for HEK293 cells, when the conjugates were used at concentration 5 μM (Figure 2B, D and F).

Kinetics of accumulation of lipophilic siRNAs in KB-8-5 cells

The time course of the accumulation of lipophilic siRNAs in KB-8-5 cells was monitored for 1–24 h. FITC-labeled conjugates Ch6-siMDR, Ch12-siMDR and OlLt6-siMDR were selected for these experiments since they demonstrated an efficient accumulation in all cell types (Figure 2). The maximal mean fluorescence of the cells was observed at 8 h for all tested conjugates (Figure 3). Cellular accumulation of cholesterol-containing siRNAs was 2.5–3-fold higher than this value for OlLt6-siMDR. After 24 h of incubation with the lipophilic siRNAs the mean values of the cell fluorescence was substantially reduced (Figure 3).

The localization of FITC-labeled Ch6-siMDR and Ch12-siMDR in KB-8-5 cells was studied by confocal fluorescent microscopy (Figure 4) in order to prove the accumulation of the lipophilic siRNAs inside the cells. Non-modified siRNA did not penetrate into the cells (Figure 4A), whereas cholesterol-containing siRNAs accumulated inside the cells effectively after 8 h of incubation (Figure 4B and C). The green signal corresponding
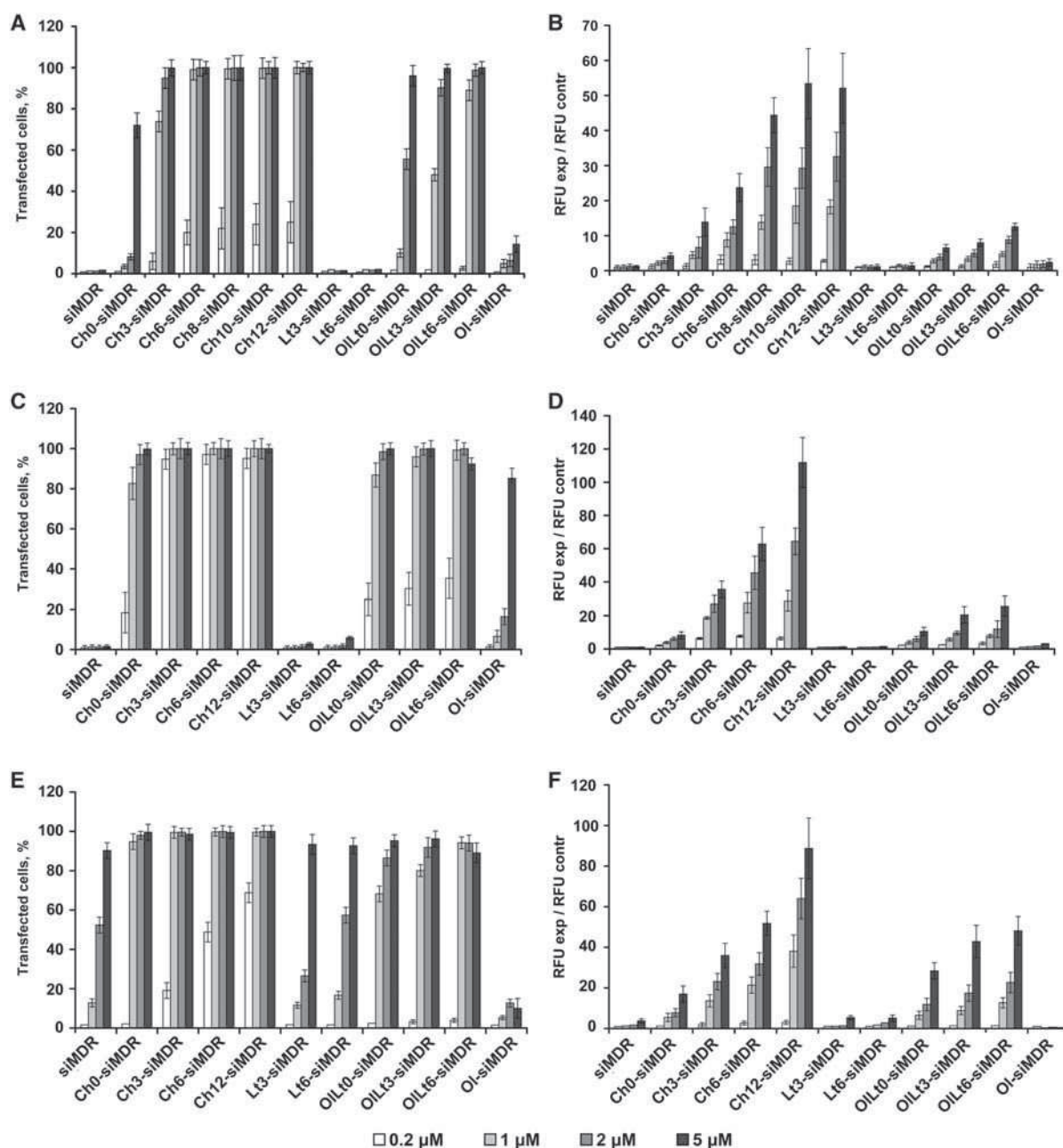
Figure 2. Cellular accumulation of FITC-labeled lipophilic siRNAs. The percentage of FITC-positive cells in the population (%) **(A**, **C** and **E)** and the normalized mean value of the cell fluorescence (RFU exp/RFU contr) **(B**, **D** and **F)** after incubation of KB-8-5 (A and B), HepG2 (C and D) and HEK293 (E and F) cells in the presence of corresponding siRNAs are shown. Data were obtained via flow cytometry. Fifteen thousand events were counted in each sample. Mean values ($\pm$SD) from three independent experiments are presented.

to FITC-labeled siRNAs is located in the cytoplasm of the cells as small discrete granules, and the granules are concentrated around the nuclei. Consequently, cholesterol-conjugated siRNA do accumulate in the cell cytoplasm.

Kinetics of *MDR1* gene silencing by cholesterol-containing siMDR

The silencing activity of the cholesterol-conjugated siMDR was investigated using drug resistant KB-8-5

cells. These cells are capable of growing in the presence of 300 nM vinblastine, due to the over-expression of the *MDR1* gene. The level of the *MDR1* gene product–P-gp was estimated by western blotting after 3–8 days of incubation of cells with 5 μM conjugates in the absence of cytostatic in order to avoid the negative selection of living cells. The start time point (3 days) was chosen taking into account the half-life time of P-gp: 48–72 h (50). The level of β-actin in the same samples was used as an internal standard. Scrambled siRNA (siScr) and its
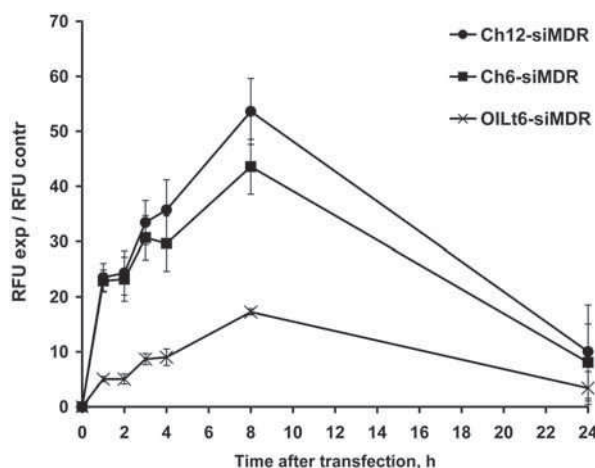
Figure 3. The time course of lipophilic siRNA accumulation in KB-8-5 cells. The incubation time after carrier-free transfection of cholesterol-conjugated siMDR with hexyl (Ch6-siMDR) or dodecyl (Ch12-siMDR) amino-linkers and siMDR conjugated to oleylamide of lithocholic acid moiety (OlLt6-siMDR) varied from 1 to 24 h. The efficacy of cellular uptake was estimated as the mean value of the cell fluorescence intensity (RFU). Data were obtained via flow cytometry, in each sample 10 000 events were counted. Mean values ($\pm$ SD) from three independent experiments are presented.

lipophilic analogs were used as controls of specificity. The levels of P-gp were normalized to the levels of β-actin for data presentation (Figure 5A and B). It was found that the efficiency of the *MDR1* gene silencing increased when the linker length augmented from 0 to 6-10 carbon atoms and correlated with the efficacy of cellular accumulation of the lipophilic siRNAs. The further increase of linker length, to aminododecyl, resulted in a decrease of the silencing activity and retardation of P-gp level reduction (Figure 5A). The 40% P-gp suppression was observed at Day 4 after addition of Ch6-siMDR to the cells, the action of Ch8-, Ch10- and Ch12-siMDR was less pronounced (30, 25 and 18% reduction of P-gp level, respectively) and was detected at the same time point, the levels of the P-gp in the cells incubated with Ch0- and Ch3-siMDR did not differ from the controls. The maximum levels of P-gp silencing were detected in the cells incubated with cholesterol-containing siMDRs with linkers of 3–10 carbon atoms for 5 days (60% for Ch6-, Ch8- and Ch10-siMDRs and 50% for Ch3-siMDR) (Figure 5). It is noteworthy that there is no statistically relevant difference between the silencing activities of conjugates containing linkers with 3-10 carbon atoms; whereas Ch3-siMDR has a tendency to be less efficient than others. Ch12-siMDR was reliably less efficient than Ch6-, Ch8- and Ch10-siMDRs: this conjugate induced only 30% reduction of the P-gp level after 4 days of incubation ($P < 0.02$, Ch12-siMDR versus Ch6-, Ch8- or Ch10-siMDR). At Day 6 of incubation the silencing activities of Ch6-, Ch8- and Ch10-siMDRs were similar (Figure 5A). In contrast, the silencing activity of Ch12-siMDR increased to 57% and did not differ to a reliable degree from the activity of Ch3-, Ch6- and

Ch10-siMDRs at Day 6, the activity of Ch8-siMDR was slightly higher ($P < 0.05$, Ch8-siMDR versus Ch12-siMDR). The silencing effect decreased at days 7–8 and did not exceed 15–20% for these conjugates (Figure 5A). Ch0-siMDR was inactive. Hence, the linker length between cholesterol residue and siRNA is critical for the biological activity of the conjugates.

The comparison of P-gp levels after carrier-free uptake of the conjugates with P-gp levels observed after Lipofectamine 2000 mediated delivery of siRNA revealed the difference in the kinetics of the silencing process: in the first case the level of P-gp at Day 3 of incubation of the cells with the conjugates virtually did not change in comparison with the controls (Figure 5A), whereas in the second case (Lipofectamine 2000 mediated transfection) 65% reduction of the P-gp level was observed. At Days 5 and 6, the inhibitory effects of conventional siMDR (200 nM) transfected with Lipofectamine 2000 was similar to the effects of Ch3-, Ch6-, Ch8-, Ch10- and Ch12-siMDRs (5 μM) entering into the cells in a carrier-free mode.

Reversion of multiple drug resistance phenotype of cancer cells

The ability of cholesterol-containing siMDRs to reverse MDR phenotype of KB-8-5 cells was subjected to comparison. After 6 days of cell incubation in the presence of lipophilic siRNAs (1–5 μM) and 300 nM vinblastine, a number of living cells was assayed via an MTT-test. siScr and its lipophilic analogs were used as controls. The obtained results (Figure 6) demonstrate that control siRNAs (Ch0-, Ch3-, Ch6-, Ch8-, Ch10- and Ch12-siScr) did not affect the resistance of the cell to the cytostatic. Incubation of the cells with non-modified siMDR or with Ch0-siMDR also did not alter the cells viability, thereby verifying that the cholesterol-containing siRNAs are not toxic for the cells. Quite conversely, the number of living cells incubated with Ch6-siMDR (5 μM) decreased to 45% as compared to the controls, whereas Ch3-siMDR and Ch12-siMDR (5 μM) were less active: ~65–70% of the cells survived in their presence. The results on the number of living cells at Day 6 of incubation obtained in these experiments correlates well with the data on P-gp suppression levels at Day 6 of incubation (Figures 5 and 6).

DISCUSSION

MDR1 gene encodes P-gp, the transmembrane pump that effluxes a number of various compounds including cytostatics out of the cells (51,52). Over-expression of this gene is one of the main origins for multiple drug resistance of the cells impeding the chemotherapy of oncological diseases (53). Temporal silencing of *MDR1* gene expression by siRNAs decreases the P-gp level and reverses the MDR phenotype. Efficient gene silencing can be achieved only in the case of the efficient delivery of siRNA into the cytoplasm of the cells. However, the negatively charged cellular membrane organized in lipid bilayer is the main barrier on the way of negatively
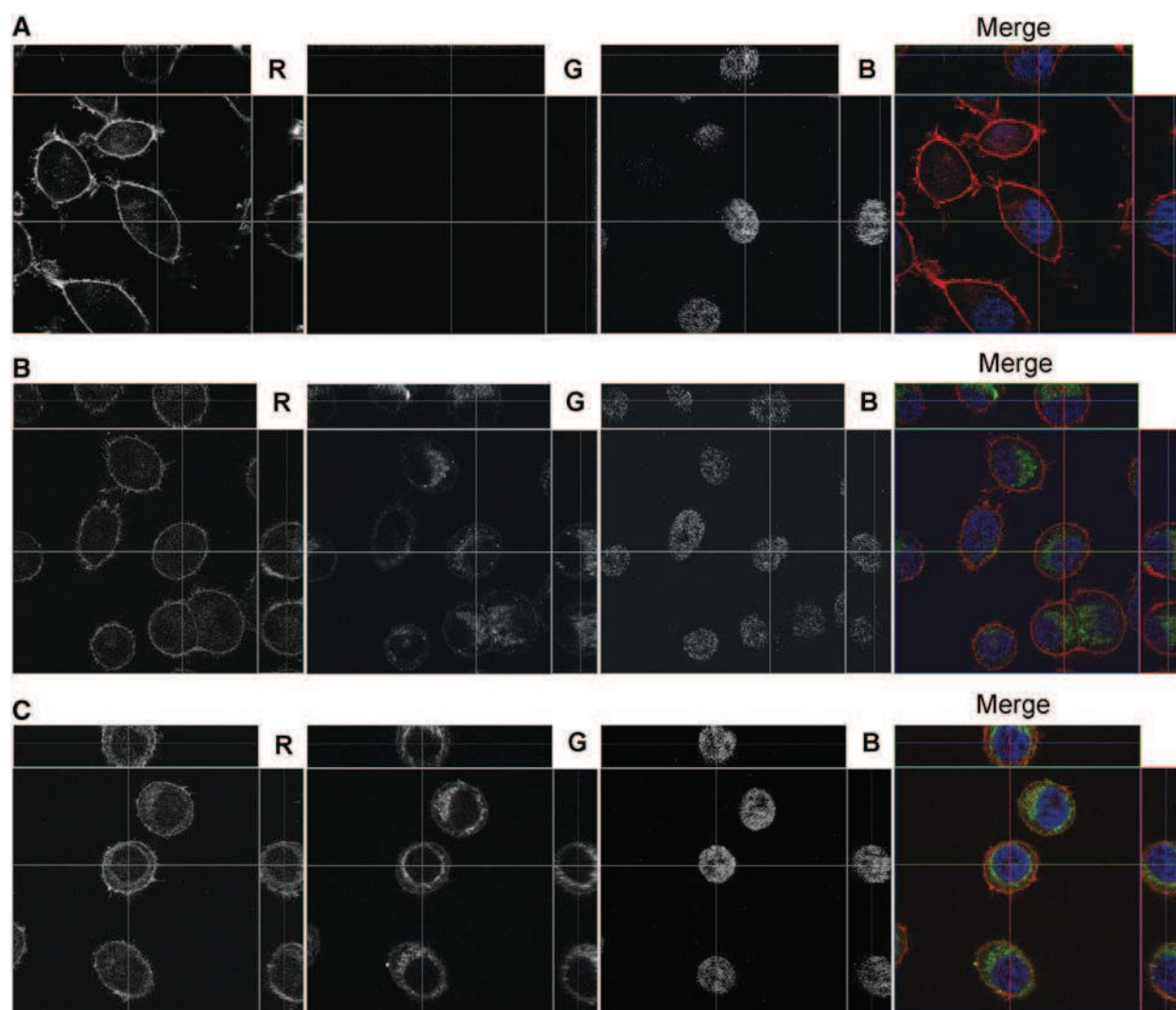
Figure 4. Accumulation of the cholesterol-contaning siRNAs in KB-8-5 cells. The carrier-free transfection of non-modified siMDR (**A**), Ch6-siMDR (**B**) Ch12-siMDR (**C**) was analyzed by confocal fluorescent microscopy at 100× magnification after 8 h of incubation. Three-channel (RGB) pictures were obtained using staining by Rhodamine Phalloidin (R), binding to the actin filaments; FITC (G), attached to cholesterol-modified and non-modified siRNAs and DAPI (B), intercalating in DNA.

charged siRNA to the cellular targets. Conjugation of siRNAs to lipophilic molecules, such as cholesterol, bile and fatty acids, is a promising approach to solving the problem of siRNA delivery *in vivo* (26,27). These modifications improved the bio-distribution of siRNAs (26,37) and significantly increased their cellular uptake (25,27,35). The presence of the cholesterol in siRNA did not however guarantee efficient cellular uptake and gene silencing without the aid of the transfection agent (54). Moreover, the data on the efficiency of carrier-free uptake and the biological effects of lipophilic siRNAs vary significantly in different reports where different synthetic methods for the introduction of lipophilic moieties resulted in the obtaining of the conjugates with different structures (26,37,54).

In this study, we posited a new synthetic scheme for the preparation of lipophilic siRNAs and investigated the influence of the type of lipophilic residue and the length of the aliphatic amino-linker between the lipophilic residue and the siRNA on the efficiency of the carrier-free cellular accumulation and the silencing activity of the conjugates. There exist two approaches to the synthesis of lipophilic conjugates of oligonucleotides, namely the synthesis in solution (41) and the solid phase synthesis (25,27, 39,55–58). At the time of writing, the common method for the chemical modification of siRNA at the 5′-end is the use of lipophilic compounds as phosphoramidite synthons in solid phase chemical synthesis by the phosphoramidite method (25,27). The H-phosphonate method is rarely used for these purposes (55,57,58) in spite of the fact that H-phosphonates have the advantages of stability and readily available compounds. The developed approach gives high coupling yields (87.5–90%) (Table 2, Supplementary Figure S2) in the condensation of lipophilic
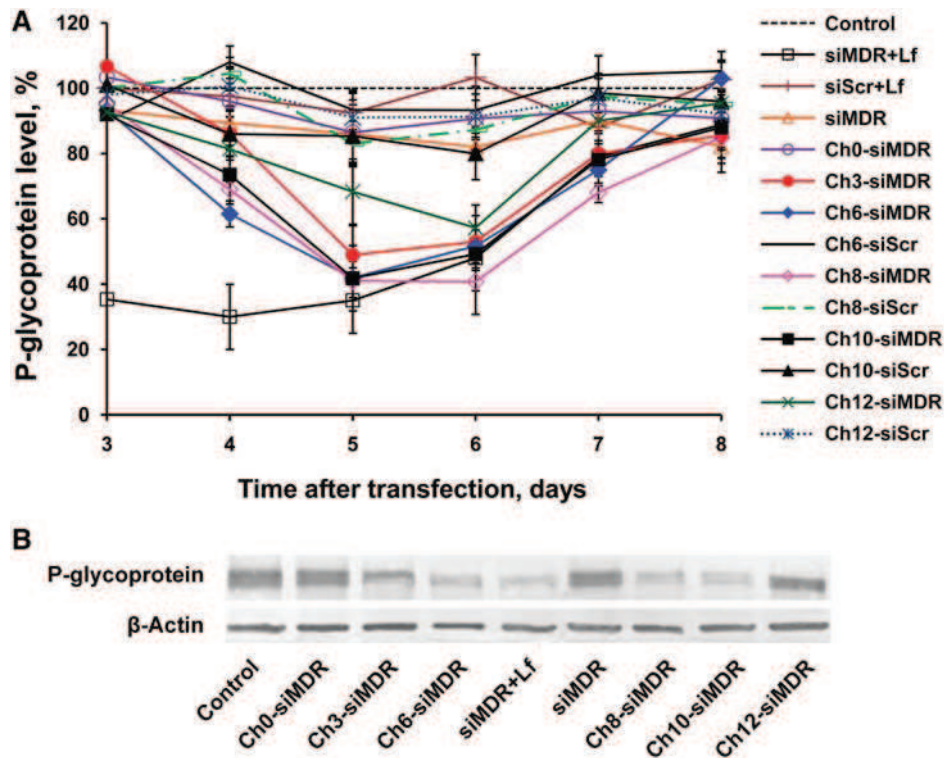
Figure 5. Silencing of P-gp expression in KB-8-5 cells by non-modified or cholesterol-containing siRNAs. (**A**) Kinetics of P-gp level suppression following incubation with cholesterol-modified siRNAs or transfection of siRNA with Lipofectamine 2000. The data were obtained via western blotting carried out after 3–8 days of incubation followed by data quantitative analysis by GelPro 4.0. program (Media Cybernetics, USA). The human β-actin protein was used as an internal standard. Data were normalized to the ratio of the P-gp/β-actin levels in untreated cells (control). Mean values (±SD) from three independent experiments are shown. (**B**) Levels of P-gp in KB-8-5 cells at Day 5 post-transfection. An untreated sample of KB-8-5 cells was taken as a control.
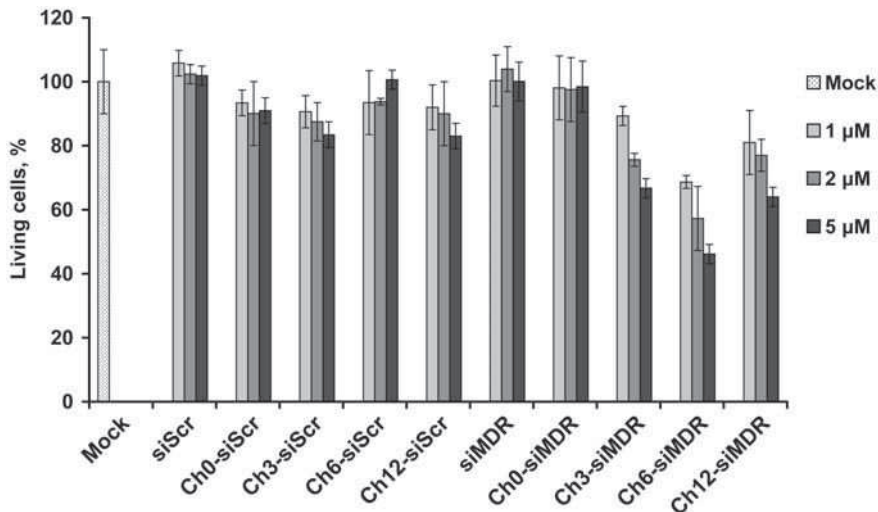
Figure 6. Restoration of KB-8-5 cells sensitivity to vinblastine. The number of living cells (%) in the presence of 300 nM vinblastine was estimated after 6 days of incubation with cholesterol-conjugated siRNAs in the absence of transfection agent. siScr containing the same type of modification were used as controls. Untreated cells are denoted as Mock.

H-phosphonates with 5′-hydroxyl of polymer-bound oligoribonucleotide in the presence of pivaloyl chloride.

The results obtained demonstrate that the efficiency of the carrier-free cellular accumulation of lipophilic siRNAs is dependent upon the type of lipophilic residues, the type of the target cells and the length of the linker connecting the lipophilic residue and siRNA strand. The most efficient accumulation of siRNAs was observed in HepG2

cells, while the accumulation in the drug-resistant cell line KB-8-5 was the least efficient. Among the lipophilic siRNAs tested, the cholesterol-containing siRNAs displayed the best TE in all the cells that were tested. Incubation of the cells with cholesterol-containing siRNAs (1–5 μM) in a serum-free medium leads to the transfection of 100% of cells in the population, siRNAs containing oleylamide of lithocholic acid accumulated a slightly less acutely; whereas the two other types of siRNA, containing both lithocholic acid and oleic alcohol residues displayed very poor cellular accumulation properties. Thus indicating that cholesterol is the promising lipophilic molecule provided carrier-free transport of modified siRNA into cells.

Cholesterol is an important biogenic molecule, which can be internalized into and effluxed out of the cell via natural cellular mechanisms (59,60). It is well known that the majority of cholesterol is transported throughout the blood stream as cholesteryl esters in the form of lipid-protein particles known as low-density lipoproteins (LDL) (61,62). Apolipoprotein B organizes the particle and mediates the specific binding of LDL to cell-surface receptor proteins (61). Hence the internalization of the cholesterol into cells occurs via receptor-mediated endocytosis. It was suggested that LDL receptors could facilitate the cellular uptake of the cholesterol-containing siRNAs *in vivo* via receptor-mediated endocytosis (27). Our data correlates well with the data reported in (27), in which was shown that the efficiency of the interaction of lipophilic siRNA with LDL-particles depends on the hydrophobicity of the lipophilic residue and cholesterol-conjugated siRNAs associate with LDL very efficiently. This fact may explain the superior cellular accumulation of cholesterol-conjugated siRNAs in hepatocytes (HepG2) and embryonic kidney cells (HEK293) expressing a high level of LDL receptors (63–65) (Figure 1C–F). However, it does not explain the accumulation of non-modified siRNA and conjugate of siRNA and lithocholic acid into HEK293 cells, neither does it explain the significantly poor accumulation of the same siRNAs in HepG2 cells (Figure 1C and E). Furthermore, the efficient uptake of lipophilic-siRNA in serum-free condition and the reduction of their accumulation in the presence of serum (data not shown) do not support the participation of LDL receptors in this process.

An alternative hypothesis concerning the mechanism of carrier-free uptake of lipophilic siRNA by the cells puts forward the transmembrane protein SID-1, which was shown to be essential for the systemic RNAi (66) and promotes the transport of lipophilic siRNA conjugates into the cells (27). It is assumed, that SID-1 forms a channel for dsRNA diffusion or mediates dsRNA uptake indirectly. However, the participation of SID-1 also does not explain the obtained data, since the level of SID-1 in kidney cells (HEK293) is very lower whereas the expression of this protein in liver (HepG2) is high (27).

The adsorption of the lipophilic conjugates on the cell surface and their subsequent transport into the cells via the mechanism of adsorption endocytosis/pinocytosis could be the alternative option for their cellular uptake.

In this case, two main factors could determine the efficacy of adsorption of the conjugates on the cell surface: the hydrophobicity of the conjugates and the distance between negatively charged cellular membrane and anionic siRNA. In light of this fact, more hydrophobic siRNAs containing oleylamide of lithocholic acid accumulate in the cells considerably better than less hydrophobic siRNAs containing lithocholic acid (Figure 2). Conversely, the long aliphatic linker in the conjugate structure provides an optimal distance between the cellular membrane and siRNA, along with an increase of the hydrophobicity of the conjugates. As a result, lipophilic siRNAs with amino-linkers of 6-12 carbon atoms exibit the best cellular accumulation (Figures 1–3). The substantial difference between the efficiency of the cellular accumulation of cholesterol-conjugated siRNAs and siRNAs equipped with the lithocholic acid suggests also the role of specific interactions with the cellular membrane (inherent in the binding with the proteins), since the structure of the moieties is similar, with the exception of the presence of the only free hydroxyl group in position 3 of lithocholic acid (Figure 1).

Another important issue coming from the obtained data is retardation in the development of the silencing effect induced by cholesterol-conjugated siRNA following carrier-free cellular accumulation in comparison with that of siRNA delivered into the cells by Lipofectamine 2000 (Figure 4A). It is known that intracellular trafficking of siRNA begins in endocytic vesicles, which subsequently turns into early endosomes, late endosomes (pH 5–6) and lysosome (pH 4.5) (67). siRNA must escape from the endosomes into the cytosol, where it can be incorporated into RISC, since siRNA molecule is extremely unstable in lysosomes. The endosomal escape is one of the key rate-limiting steps in the delivery process. The problem of endosomal trapping has been intensively discussed in literature, with respect to the conjugates of antisense oligonucleotides and cell-penetrating peptides (68–70), when it was found that conjugates containing only stable chemical bonds accumulated readily in the cells, but displays no biological activity. Cholesterol-containing siRNA do escape from the endosomes since high levels of the target gene silencing are observed, but the process of their release into the cytoplasm seems to be rather slow and less efficient than for siRNA/Lipofestamine complexes: maximal level of P-gp silencing was detected at Day 5 for Ch6-, Ch8-, Ch10-siRNA and at Day 2 for siRNA/Lipofectamine 2000 complexes (Figure 5). Hence, the conclusion can be drawn that lipophilic siRNAs are trapped on the endosomes for some time. The obtained data show that the increase of the length of the aliphatic amino-linker between the cholesterol residue and siRNA above 10 carbon atoms impedes the endosomal release of lipophilic siRNA, retards the development of the silencing effect and decreased the efficiency of the silencing: the conjugate with dodecyl amino-linker was less active than the conjugates with the linkers of 6-10 carbon atoms (Figure 6).

The results consistent with the kinetics of P-gp suppression were obtained in the experiments on KB-8-5 cell viability. This cell line is characterized by the over-expression

of the *MDR1* gene. As a result of this, the cells have the ability to grow in the presence of 300 nM vinblastine. Silencing of the *MDR1* gene by siRNAs brings about the death of KB-8-5 cells, at concentrations of vinblastine that were previously tolerated. The pronounced reduction of the number of living cells was observed at Day 6 of cells incubation with cholesterol-containing siMDR (Figure 6). This effect was similar to the effect observed at Day 4 after cell transfection with siMDR/Lipophectamine 2000 (54).

Lipofectamine 2000 contains a fusogenic lipid DOPE (dioleylphosphatidyl-ethanolamine) responsible for endosomal release of siRNA by facilitating the interactions between the lipoplexes and the endosomal membranes (67,71), but this formulation is toxic for cells and is not stable in the presence of blood plasma, and is subsequently is incompatible with regards to therapeutic usage. Unlike Lipophectamine and other commercially available cationic lipid formulations, the conjugates of siRNA with cholesterol that were subjected to study are stable and non-toxic for cells. Furthermore, unlike the conjugates of antisense oligonucleotides, they do release from the endosome with a moderate delay and display a substantial level of biological activity.

Thus, the structure of lipophilic siRNA was optimized by variation of the type of lipophilic moiety and length of the linker between this moiety and siRNA. The designed anti-*MDR1* siRNAs (Ch6-, Ch8- and Ch10-siMDR) were found to penetrate efficiently into the cells in a carrier-free mode, to silence the expression of P-gp and to restore the sensitivity of drug resistant cancer cells to vinblastine. Designed lipoophilic siRNAs are promising agents for *in vivo* applications. For this reason, it is necessary to further investigate the optimization of their structure, in order to facilitate their endosomal release.

SUPPLEMENTARY DATA

Supplementary Data are available at NAR Online: Supplementary Methods and Supplementary Figures S1 and S2.

ACKNOWLEDGEMENTS

FUNDING

Conflict of interest statement. None declared.

REFERENCES

1. Elbashir,S.M., Harborth,J., Lendeckel,W., Yalcin,A., Weber,K. and Tuschl,T. (2001) Duplexes of 21-nucleotide RNAs mediate RNA interference in cultured mammalian cells. *Nature*, **411**, 494–498.
2. Hammond,S.M., Bernstein,E., Beach,D. and Hannon,G.J. (2000) An RNA-directed nuclease mediates post-transcriptional gene silencing in Drosophila cells. *Nature*, **404**, 293–296.
3. Zamore,P.D., Tuschl,T., Sharp,P.A. and Bartel,D.P. (2000) RNAi: double-stranded RNA directs the ATP-dependent cleavage of mRNA at 21 to 23 nucleotide intervals. *Cell*, **101**, 25–33.
4. Chen,S.H. and Zhaori,G. (2010) Potential clinical applications of siRNA technique: benefits and limitations. *Eur. J. Clin. Invest.*, **41**, 221–232.
5. Dorsett,Y. and Tuschl,T. (2004) siRNAs: applications in functional genomics and potential as therapeutics. *Nat. Rev. Drug Discov.*, **3**, 318–329.
6. Lares,M.R., Rossi,J.J. and Ouellet,D.L. (2010) RNAi and small interfering RNAs in human disease therapeutic applications. *Trends Biotechnol.*, **28**, 570–579.
7. Jankovic,R., Radulovic,S. and Brankovic-Magic,M. (2009) siRNA and miRNA for the treatment of cancer. *J. BUON*, **14**, S43–S49.
8. Pirollo,K.F. and Chang,E.H. (2008) Targeted delivery of small interfering RNA: approaching effective cancer therapies. *Cancer Res.*, **68**, 1247–1250.
9. Couto,L.B. and High,K.A. (2010) Viral vector-mediated RNA interference. *Curr. Opin. Pharmacol.*, **10**, 534–542.
10. Mowa,M.B., Crowther,C. and Arbuthnot,P. (2010) Therapeutic potential of adenoviral vectors for delivery of expressed RNAi activators. *Expert Opin. Drug Deliv.*, **7**, 1373–1385.
11. Leng,Q., Woodle,M.C., Lu,P.Y. and Mixson,A.J. (2009) Advances in systemic siRNA delivery. *Drugs Future*, **34**, 721.
12. Posadas,I., Guerra,F.J. and Cena,V. (2010) Nonviral vectors for the delivery of small interfering RNAs to the CNS. *Nanomedicine*, **5**, 1219–1236.
13. Shim,M.S. and Kwon,Y.J. (2010) Efficient and targeted delivery of siRNA in vivo. *FEBS J.*, **277**, 4814–4827.
14. Bessis,N., GarciaCozar,F.J. and Boissier,M.C. (2004) Immune responses to gene therapy vectors: influence on vector function and effector mechanisms. *Gene Ther.*, **11**, S10–S17.
15. Check,E. (2002) A tragic setback. *Nature*, **420**, 116–118.
16. Kaiser,J. (2003) Gene therapy. Seeking the cause of induced leukemias in X-SCID trial. *Science*, **299**, 495.
17. Sinn,P.L., Sauter,S.L. and McCray,P.B. Jr (2005) Gene therapy progress and prospects: development of improved lentiviral and retroviral vectors–design, biosafety, and production. *Gene Ther.*, **12**, 1089–1098.
18. De Souza,A.T., Dai,X., Spencer,A.G., Reppen,T., Menzie,A., Roesch,P.L., He,Y., Caguyong,M.J., Bloomer,S., Herweijer,H. *et al.* (2006) Transcriptional and phenotypic comparisons of Ppara knockout and siRNA knockdown mice. *Nucleic Acids Res.*, **34**, 4486–4494.
19. Song,E., Lee,S.K., Wang,J., Ince,N., Ouyang,N., Min,J., Chen,J., Shankar,P. and Lieberman,J. (2003) RNA interference targeting Fas protects mice from fulminant hepatitis. *Nat. Med.*, **9**, 347–351.
20. Zender,L. and Kubicka,S. (2007) Suppression of apoptosis in the liver by systemic and local delivery of small-interfering RNAs. *Methods Mol. Biol.*, **361**, 217–226.
21. De Paula,D., Bentley,M.V. and Mahato,R.I. (2007) Hydrophobization and bioconjugation for enhanced siRNA delivery and targeting. *RNA*, **13**, 431–456.
22. Jeong,J.H., Mok,H., Oh,Y.K. and Park,T.G. (2009) siRNA conjugate delivery systems. *Bioconjug. Chem.*, **20**, 5–14.

23. Lv,H., Zhang,S., Wang,B., Cui,S. and Yan,J. (2006) Toxicity of cationic lipids and cationic polymers in gene delivery. *J. Control Release*, **114**, 100–109.

24. Thomas,M., Kularatne,S.A., Qi,L., Kleindl,P., Leamon,C.P., Hansen,M.J. and Low,P.S. (2009) Ligand-targeted delivery of small interfering RNAs to malignant cells and tissues. *Ann. NY Acad. Sci.*, **1175**, 32–39.

25. Lorenz,C., Hadwiger,P., John,M., Vornlocher,H.P. and Unverzagt,C. (2004) Steroid and lipid conjugates of siRNAs to enhance cellular uptake and gene silencing in liver cells. *Bioorg. Med. Chem. Lett.*, **14**, 4975–4977.

26. Soutschek,J., Akinc,A., Bramlage,B., Charisse,K., Constien,R., Donoghue,M., Elbashir,S., Geick,A., Hadwiger,P., Harborth,J. *et al.* (2004) Therapeutic silencing of an endogenous gene by systemic administration of modified siRNAs. *Nature*, **432**, 173–178.

27. Wolfrum,C., Shi,S., Jayaprakash,K.N., Jayaraman,M., Wang,G., Pandey,R.K., Rajeev,K.G., Nakayama,T., Charrise,K., Ndungo,E.M. *et al.* (2007) Mechanisms and optimization of in vivo delivery of lipophilic siRNAs. *Nat. Biotechnol.*, **25**, 1149–1157.

28. Nishina,K., Unno,T., Uno,Y., Kubodera,T., Kanouchi,T., Mizusawa,H. and Yokota,T. (2008) Efficient in vivo delivery of siRNA to the liver by conjugation of alpha-tocopherol. *Mol. Ther.*, **16**, 734–740.

29. Chu,T.C., Twu,K.Y., Ellington,A.D. and Levy,M. (2006) Aptamer mediated siRNA delivery. *Nucleic Acids Res.*, **34**, e73.

30. Hicke,B.J. and Stephens,A.W. (2000) Escort aptamers: a delivery service for diagnosis and therapy. *J. Clin. Invest.*, **106**, 923–928.

31. McNamara,J.O. II, Andrechek,E.R., Wang,Y., Viles,K.D., Rempel,R.E., Gilboa,E., Sullenger,B.A. and Giangrande,P.H. (2006) Cell type-specific delivery of siRNAs with aptamer-siRNA chimeras. *Nat. Biotechnol.*, **24**, 1005–1015.

32. Dassie,J.P., Liu,X.Y., Thomas,G.S., Whitaker,R.M., Thiel,K.W., Stockdale,K.R., Meyerholz,D.K., McCaffrey,A.P., McNamara,J.O. II and Giangrande,P.H. (2009) Systemic administration of optimized aptamer-siRNA chimeras promotes regression of PSMA-expressing tumors. *Nat. Biotechnol.*, **27**, 839–849.

33. Song,E., Zhu,P., Lee,S.K., Chowdhury,D., Kussman,S., Dykxhoorn,D.M., Feng,Y., Palliser,D., Weiner,D.B., Shankar,P. *et al.* (2005) Antibody mediated in vivo delivery of small interfering RNAs via cell-surface receptors. *Nat. Biotechnol.*, **23**, 709–717.

34. Xia,C.F., Boado,R.J. and Pardridge,W.M. (2009) Antibody-mediated targeting of siRNA via the human insulin receptor using avidin-biotin technology. *Mol. Pharm.*, **6**, 747–751.

35. Chiu,Y.L., Ali,A., Chu,C.Y., Cao,H. and Rana,T.M. (2004) Visualizing a correlation between siRNA localization, cellular uptake, and RNAi in living cells. *Chem. Biol.*, **11**, 1165–1175.

36. Endoh,T. and Ohtsuki,T. (2009) Cellular siRNA delivery using cell-penetrating peptides modified for endosomal escape. *Adv. Drug Deliv. Rev.*, **61**, 704–709.

37. Moschos,S.A., Jones,S.W., Perry,M.M., Williams,A.E., Erjefalt,J.S., Turner,J.J., Barnes,P.J., Sproat,B.S., Gait,M.J. and Lindsay,M.A. (2007) Lung delivery studies using siRNA conjugated to TAT(48-60) and penetratin reveal peptide induced reduction in gene expression and induction of innate immunity. *Bioconjug. Chem.*, **18**, 1450–1459.

38. Muratovska,A. and Eccles,M.R. (2004) Conjugate for efficient delivery of short interfering RNA (siRNA) into mammalian cells. *FEBS Lett.*, **558**, 63–68.

39. MacKellar,C., Graham,D., Will,D.W., Burgess,S. and Brown,T. (1992) Synthesis and physical properties of anti-HIV antisense oligonucleotides bearing terminal lipophilic groups. *Nucleic Acids Res.*, **20**, 3411–3417.

40. Manoharan,M., Kesavan,V. and Rajeev,K.G. (2005), US Patent 20050107325 A1.

41. Rump,E.T., de Vrueh,R.L., Sliedregt,L.A., Biessen,E.A., van Berkel,T.J. and Bijsterbosch,M.K. (1998) Preparation of conjugates of oligodeoxynucleotides and lipid structures and their interaction with low-density lipoprotein. *Bioconjugate Chem.*, **9**, 341–349.

42. Sergeeva,Z.A., Lokhov,S.G. and Ven'yaminova,A.G. (1996) Oligo(2′-O-methylribonucleotides) and their derivatives. II. Synthesis and properties of oligo(2'-O-methylribonucleotides) modified with N-(2-hydroxyethyl)phenazinium and steroid groups at the 5'-terminus. *Bioorgan. Khim.*, **22**, 916–922.

43. Bellon,L. (2001) Oligoribonucleotides with 2'-O-(tert-butyldimethylsilyl) groups. *Curr. Protoc. Nucleic Acid Chem.*, doi: 10.1002/0471142700.nc0306s01.

44. Proudnikov,D. and Mirzabekov,A. (1996) Chemical methods of DNA and RNA fluorescent labeling. *Nucleic Acids Res.*, **24**, 4535–4542.

45. Carmichael,J., DeGraff,W.G., Gazdar,A.F., Minna,J.D. and Mitchell,J.B. (1987) Evaluation of a tetrazolium-based semiautomated colorimetric assay: assessment of radiosensitivity. *Cancer Res.*, **47**, 943–946.

46. Logashenko,E.B., Vladimirova,A.V., Repkova,M.N., Venyaminova,A.G., Chernolovskaya,E.L. and Vlassov,V.V. (2004) Silencing of MDR 1 gene in cancer cells by siRNA. *Nucleosides Nucleotides Nucleic Acids.*, **23**, 861–866.

47. Volkov,A.A., Kruglova,N.S., Meschaninova,M.I., Venyaminova,A.G., Zenkova,M.A., Vlassov,V.V. and Chernolovskaya,E.L. (2009) Selective protection of nuclease-sensitive sites in siRNA prolongs silencing effect. *Oligonucleotides.*, **19**, 191–202.

48. Chiu,Y.L. and Rana,T.M. (2003) siRNA function in RNAi: a 115 chemical modification analysis. *RNA*, **9**, 1034–1048.

49. de Fougerolles,A., Vornlocher,H.P., Maraganore,J. and Lieberman,J. (2003) Interfering with disease: a progress report on siRNA-based therapeutics. *Nat. Rev. Drug Discov.*, **6**, 443–453.

50. Richert,N.D., Aldwin,L., Nitecki,D., Gottesman,M.M. and Pastan,I. (1988) Stability and covalent modification of P-glycoprotein in multidrug-resistant KB cells. *Biochemistry*, **27**, 7607–7613.

51. Anthony,V. and Skach,W.R. (2002) Molecular mechanism of P-glycoprotein assembly into cellular membranes. *Curr. Protein Pept. Sci.*, **3**, 485–501.

52. Juliano,R.L. and Ling,V. (1976) A surface glycoprotein modulating drug permeability in Chinese hamster ovary cell mutants. *Biochim. Biophys. Acta*, **455**, 152–162.

53. Gottesman,M.M. and Pastan,I. (1989) Clinical trials of agents that reverse multidrug-resistance. *J. Clin. Oncol.*, **7**, 409–411.

54. Kruglova,N.S., Meshchaninova,M.I., Ven'iaminova,A.G., Zenkova,M.A., Vlasov,V.V. and Chernolovskaia,E.L. (2010) Cholesterol-modified anti-MDR1 small interfering RNA: uptake and biological activity. *Mol. Biol.*, **44**, 284–293.

55. Krieg,A.M., Tonkinson,J., Matson,S., Zhao,Q., Saxon,M., Zhang,L.M., Bhanja,U., Yakubov,L. and Stein,C.A. (1993) Modification of antisense phosphodiester oligodeoxynucleotides by a 5′-cholesteryl moiety increases cellular association and improves efficacy. *PNAS*, **90**, 1048–1052.

56. Manoharan,M., Tivel,K.L. and Cook,P.D. (1995) Lipidic nucleic acids. *Tetrahedron Lett.*, **36**, 3651–3654.

57. Stein,C.A., Pal,R., DeVico,A.L., Hoke,G., Mumbauer,S., Kinstler,O., Sarngadharan,M.G. and Letsinger,R.L. (1991) Mode of action of 5 -linked cholesteryl phosphorothioate oligodeoxynucleotides in inhibiting syncytia formation and infection by HIV-1 and HIV-2 in vitro. *Biochemistry.*, **30**, 2439–2444.

58. Venyaminova,A.G., Sergeyeva,Z.A. and Bashirova,V.Z. (1991) H-Phosphonates of hydroxysterols as new key compounds for the synthesis of sterol derivatives of mono-, oligonucleotides and their analogues. *Bioorgan. Khim.*, **17**, 1294–1296.

59. Brown,M.S. and Goldstein,J.L. (1997) The SREBP pathway: regulation of cholesterol metabolism by proteolysis of a membrane-bound transcription factor. *Cell*, **89**, 331–340.

60. Plosch,T., Kosters,A., Groen,A.K. and Kuipers,F. (2005) The ABC of hepatic and intestinal cholesterol transport. *Handb. Exp. Pharmacol.*, 465–482.

61. Burnett,J.R. and Barrett,P.H. (2002) Apolipoprotein B metabolism: tracer kinetics, models, and metabolic studies. *Crit. Rev. Clin. Lab. Sci.*, **39**, 89–137.

62. Deckelbaum,R.J., Shipley,G.G. and Small,D.M. (1977) Structure and interactions of lipids in human plasma low density lipoproteins. *J. Biol. Chem.*, **252**, 744–754.

63. Havekes,L.M., De Wit,E.C.M. and Princen,H.M.G. (1987) Cellular free cholesterol in Hep G2 cells is only partially available for down-regulation of low-density-lipoprotein receptor activity. *Biochem. J.*, **247**, 739–746.

64. Kambouris,A.M., Roach,P.D., Calvert,G.D. and Nestel,P.J. (1990) Retroendocytosis of high density lipoproteins by the human hepatoma cell line, HepG2. *Arteriosclerosis*, **10**, 582–590.

65. Marsche,G., Frank,S., Raynes,J.G., Kozarsky,K.F., Sattler,W. and Malle,E. (2007) The lipidation status of acute-phase protein serum amyloid A determines cholesterol mobilization via scavenger receptor class B, type I. *Biochem. J.*, **402**, 117–124.

66. Feinberg,E.H. and Hunter,C.P. (2003) Transport of dsRNA into cells by the transmembrane protein SID-1. *Science*, **301**, 1545–1547.

67. Dominska,M. and Dykxhoorn,D.M. (2010) Breaking down the barriers: siRNA delivery and endosome escape. *J. Cell Sci.*, **123**, 1183–1189.

68. Turner,J.J., Arzumanov,A.A. and Gait,M.J. (2005) Synthesis, cellular uptake and HIV-1 Tat-dependent trans-activation inhibition activity of oligonucleotide analogues disulphide-conjugated to cell-penetrating peptides. *Nucleic Acids Res.*, **33**, 27–42.

69. Turner,J.J., Fabani,M., Arzumanov,A.A., Ivanova,G. and Gait,M.J. (2006) Targeting the HIV-1 RNA leader sequence with synthetic oligonucleotides and siRNA: chemistry and cell delivery. *Biochim. Biophys. Acta*, **1758**, 290–300.

70. Turner,J.J., Ivanova,G.D., Verbeure,B., Williams,D., Arzumanov,A.A., Abes,S., Lebleu,B. and Gait,M.J. (2005) Cell-penetrating peptide conjugates of peptide nucleic acids (PNA) as inhibitors of HIV-1 Tat-dependent trans-activation in cells. *Nucleic Acids Res.*, **33**, 6837–6849.

71. Farhood,H., Serbina,N. and Huang,L. (1995) The role of dioleoyl phosphatidylethanolamine in cationic liposome mediated gene transfer. *Biochim. Biophys. Acta.*, **1235**, 289–295.

Supplementary Materials and Methods

Characteristics of precursor compounds (2 - 6, 8, 10, 11, 13, 15, 16)

Cholesterol-3-(carboxyaminopropan-3-ol) **(2)** (0.45 g, 84%).R_f(TLC, AcOEt/hexane 50/50): 0.14. ^{1}H NMR (300 MHz, CDCl$_3$, δ, ppm):0.69 (s, 3H, H-18/19, cholesterol); 0.87 (d, 3H, H-26/27, cholesterol); 0.89 (d, 3H, H-26/27, cholesterol); 0.93 (d, 3H, H-21, cholesterol); 1.025 (s, 3H, H-18/19, cholesterol); 1.73 (m, 2H, -CH$_2$-C$\underline{H}_2$-CH$_2$-, linker); 3.35 (dd, 2H, -C$\underline{H}_2$-NH-, linker); 3.68 (t, 2H, -C$\underline{H}_2$-OH, linker); 4.51 (m, 1H, H-3, cholesterol); 4.88 (t, 1H, -NH-, linker); 5.4 (d, 1H, H-6, cholesterol).

Cholesterol-3-(carboxyaminohexan-6-ol) **(3)** (0.54 g, 92%).R_f(TLC, AcOEt/hexane 50/50): 0.2. ^{1}H NMR (300 MHz, CDCl$_3$, δ, ppm):0.69 (s, 3H, H-18/19, cholesterol); 0.87 (d, 3H, H-26/27, cholesterol); 0.89 (d, 3H, H-26/27, cholesterol); 0.93 (d, 3H, H-21, cholesterol); 1.025 (s, 3H, H-18/19, cholesterol); 3.19 (dd, 2H, -C$\underline{H}_2$-NH-, linker); 3.67 (t, 1H, -C$\underline{H}_2$-OH, linker); 4.52 (m, 1H, H-3, cholesterol); 4.62 (t, 1H, -NH-, linker); 5.4 (d, 1H, H-6, cholesterol).

Cholesterol-3-(carboxyaminooctan-8-ol) **(4)** (0.44 g, 71%).R_f(TLC, AcOEt/hexane 50/50): 0.43. ^{1}H NMR (300 MHz, CDCl$_3$, δ, ppm):0.65 (s, 3H, H-18/19, cholesterol); 0.83 (d, 3H, H-26/27, cholesterol); 0.86 (d, 3H, H-26/27, cholesterol); 0.89 (d, 3H, H-21, cholesterol); 0.98 (s, 3H, H-18/19, cholesterol); 3.10 (dd, 2H, -C$\underline{H}_2$-NH-, linker); 3.61 (t, 1H, -C$\underline{H}_2$-OH, linker); 4.46 (m, 1H, H-3, cholesterol); 4.55 (t, 1H, -NH-, linker); 5.34 (d, 1H, H-6, cholesterol).

Cholesterol-3-(carboxyaminodecan-10-ol) **(5)** (0.43 g, 67%).R_f(TLC, AcOEt/hexane 50/50): 0.46. ^{1}H NMR (300 MHz, CDCl$_3$, δ, ppm):0.65 (s, 3H, H-18/19, cholesterol); 0.83 (d, 3H, H-26/27, cholesterol); 0.85 (d, 3H, H-26/27, cholesterol); 0.89 (d, 3H, H-21, cholesterol); 0.98 (s, 3H, H-18/19, cholesterol); 3.10 (dd, 2H, -C$\underline{H}_2$-NH-, linker); 3.62 (t, 1H, -C$\underline{H}_2$-OH, linker); 4.46 (m, 1H, H-3, cholesterol); 4.55 (t, 1H, -NH-, linker); 5.35 (d, 1H, H-6, cholesterol).

Cholesterol-3-(carboxyaminododecan-12-ol) **(6)** (0.5g, 75%).R_f(TLC, AcOEt/hexane 50/50): 0.53. ^{1}H NMR (300 MHz, CDCl$_3$, δ, ppm):0.65 (s, 3H, H-18/19, cholesterol); 0.83 (d, 3H, H-26/27, cholesterol); 0.84 (d, 3H, H-26/27, cholesterol); 0.89 (d, 3H, H-21, cholesterol); 0.98 (s, 3H, H-18/19, cholesterol); 3.07 (dd, 2H, -C$\underline{H}_2$-NH-, linker); 3.61 (t, 1H, -C$\underline{H}_2$-OH, linker); 4.46 (m, 1H, H-3, cholesterol); 4.55 (t, 1H, -NH-, linker); 5.35 (d, 1H, H-6, cholesterol).

3 -(Acetoxy)-5 -cholanic acid **(8)** was obtained as a foamy white solid (0.5 g, 90%). R_f (TLC, CH$_3$OH/CH$_2$Cl$_2$ 5/95): 0.4. ^{1}H NMR (300 MHz, CDCl$_3$, δ, ppm):0.67 (s, 3H, H-18/19, cholane); 0.94 (m, 6H, H-18/19,21, cholane); 2.05 (s, 3H, -CH$_3$, Ac); 4.75 (m, 1H, H-3, cholane).

3 -(Acetoxy)-5 -cholanic acid 3-hydroxypropylamide **(10)** (0.25 g, 58%).R_f (TLC, CH$_3$OH/CH$_2$Cl$_2$ 5/95): 0.3. ^{1}H NMR (300 MHz, CDCl$_3$, δ, ppm):0.67 (s, 3H, H-18/19, cholane); 0.95 (m, 6H, H-18/19,21, cholane); 2.05 (s, 3H, -CH$_3$, Ac); 3.44 (dd, 2H, -C$\underline{H}_2$-NH-, linker); 3.65 (t, 2H, -C$\underline{H}_2$-OH, linker); 4.74 (m, 1H, H-3, cholane); 5.8 (t, 1H, -NH-, linker).

3 -(Acetoxy)-5 -cholanic acid 6-hydroxyhexylamide **(11)** (0.19 g, 40%).R_f (TLC, CH_3OH/CH_2Cl_2 5/95): 0.4. ^1H NMR (300 MHz, $CDCl_3$, δ, ppm):0.62 (s, 3H, H-18/19, cholane); 0.92 (m, 6H, H-18/19,21, cholane); 2.02 (s, 3H, -CH_3, Ac); 3.2 (dd, 2H, -C$\underline{H}_2$-NH-, linker); 3.6 (t, 2H, -C$\underline{H}_2$-OH, linker); 4.69 (m, 1H, H-3, cholane), 5.45 (t, 1H, -NH-, linker).

3 -(Hydroxy)-5 -cholanic acid oleylamide **(13)**(0.71g; 87%).R_f(TLC, CH_3OH/CH_2Cl_2 5/95): 0.2. ^1H NMR (300 MHz, $CDCl_3$, δ, ppm):0.61 (s, 3H, H-18/19, cholane); 3.2 (dd, 2H, -C$\underline{H}_2$-NH-, oleylamine); 3.6 (m, 1H, H-3, cholane); 5.35 (m, 3H, -CH=CH-, -NH-,oleylamine).

3 -(Carboxyaminopropan-3-ol)-5 -cholanic acid oleylamide **(15)**(0.41 g,80%).R_f(TLC, CH_3OH/CH_2Cl_2 5/95): 0.7. ^1H NMR (300 MHz, $CDCl_3$, δ, ppm):0.61 (s, 3H, H-18/19, cholane); 2.9-3.1 (m, 4H, -C$\underline{H}_2$-NH-, oleylamine, -C$\underline{H}_2$-NH- linker); 3.58 (t, 2H, -C$\underline{H}_2$-OH, linker); 4.38 (m, 2H, H-3, cholane, -NH-, linker); 5.32 (m, 3H, -CH=CH-, -NH-, oleylamine).

3 -(Carboxyaminohexan-6-ol)-5 -cholanic acid oleylamide **(16)** (0.41 g, 76%). R_f(TLC, CH_3OH/CH_2Cl_2 5/95): 0.3. ^1H NMR (300 MHz, $CDCl_3$, δ, ppm):0.61 (s, 3H, H-18/19, cholane); 3.1-3.3 (m, 4H, -C$\underline{H}_2$-NH-, oleylamine, -C$\underline{H}_2$-NH-, linker); 3.62 (t, 2H, -C$\underline{H}_2$-OH, linker); 4.56 (m, 2H, H-3, cholane, -NH-, linker); 5.35 (m, 3H, -CH=CH-, -NH-, oleylamine).

Characteristics of lipophilic H-phosphonates (17 - 28)

H-Phosphonate of cholesterol **(17)** (triethylammonium salt). Yield 94%. R_f(TLC, CH_3OH/CH_2Cl_2 50/50): 0.19. ^{31}P NMR (300 MHz, $CDCl_3$, δ, ppm):2.2 (J_{P-H} 621.5 Hz). ESI-MS: calcd. for $C_{33}H_{63}PO_3N$ [M+H]$^+$: 552.6; found: 552.0.

H-Phosphonate of cholesterol-3-(carboxyaminopropan-3-ol) **(18)** (triethylammonium salt). Yield 41%. R_f(TLC, CH_3OH/CH_2Cl_2 50/50): 0.21. ^{31}P NMR(300 MHz, $CDCl_3$, δ, ppm):3.2 (J_{P-H} 616.0 Hz). ESI-MS: calcd. for $C_{37}H_{70}PO_5N$[M+H]$^+$: 653.6; found: 653.3.

H-Phosphonate of cholesterol-3-(carboxyaminohexan-6-ol) **(19)** (triethylammoniumsalt). Yield 83%. R_f(TLC, $CH_3OH/CH_2Cl_2$50/50): 0.24. ^{31}P NMR(300 MHz, $CDCl_3$, δ, ppm):5.0 (J_{P-H} 628.5 Hz). ESI-MS: calcd. for $C_{40}H_{76}PO_5N$ [M+H]$^+$: 695.6; found: 695.0.

H-Phosphonate of cholesterol-3-(carboxyaminooctan-8-ol) **(20)** (triethylammonium salt). Yield 71%. R_f(TLC, $CH_3OH/CH2Cl2$ 50/50): 0.26. ^{31}P NMR(300 MHz, $CDCl_3$, δ, ppm):5.1 (J_{P-H} 617.9 Hz). MALDI-TOF-MS:calcd. for$C_{42}H_{80}PO_5N$[M+H]$^+$: 723.6; found: 723.55.

H-Phosphonate of cholesterol-3-(carboxyaminodecan-10-ol) **(21)** (triethylammonium salt). Yield 68%. R_f(TLC, $CH_3OH/CH2Cl2$ 50/50): 0.27. ^{31}P NMR(300 MHz, $CDCl_3$, δ, ppm):5.0 (J_{P-H} 617.3 Hz). MALDI-TOF-MS:calcd. for $C_{44}H_{84}PO_5N$ [M+H]$^+$: 751.6; found: 751.56.

H-Phosphonate of cholesterol-3-(carboxyaminododecan-12-ol) **(22)** (triethylammonium salt). Yield 75%. R_f(TLC, CH_3OH/CH_2Cl_2 50/50): 0.29. ^{31}P NMR(300 MHz, $CDCl_3$, δ, ppm):5.1 (J_{P-H} 625.6 Hz). MALDI-TOF-MS:calcd. for $C_{46}H_{88}PO_5N$ $[M+H]^+$: 779.6; found: 779.61.

H-Phosphonate of 3 -(acetoxy)-5 -cholanic acid 3-hydroxypropylamide **(23)** (triethylammonium salt). Yield 56%. R_f(TLC, CH_3OH/CH_2Cl_2 50/50): 0.21. ^{31}P NMR(300 MHz, $CDCl_3$, δ, ppm):4.4 (J_{P-H} 620.0 Hz).ESI-MS: calcd. for $C_{35}H_{66}PO_6N_2$ $[M+H]^+$: 642.6; found: 641.2.

H-Phosphonate of 3 -(acetoxy)-5 -cholanic acid 6-hydroxyhexylamide **(24)** (triethylammonium salt). Yield 85%. R_f(TLC, CH_3OH/CH_2Cl_2 50/50): 0.21. ^{31}P NMR(300 MHz, $CDCl_3$, δ, ppm):4.8 (J_{P-H} 619.0 Hz).ESI-MS: calcd. for $C_{38}H_{72}PO_6N_2$ $[M+H]^+$: 683.6; found: 683.0.

H-Phosphonate of 3 -(hydroxy)-5 -cholanic acid oleylamide **(25)** (triethylammonium salt). Yield 79%. R_f(TLC, $CH_3OH/CH_2Cl_2$50/50): 0.27. ^{31}P NMR(300 MHz, $CDCl_3$, δ, ppm):0.75 (J_{P-H} 627.0 Hz). ESI-MS: calcd. for $C_{48}H_{91}PO_4N_2$ $[M+H]^+$: 791.5; found: 790.9.

H-Phosphonate of 3 -(carboxyaminopropan-3-ol)-5 -cholanic acid oleylamide **(26)** (triethylammonium salt). Yield 67%. R_f(TLC, CH_3OH/CH_2Cl_2 50/50): 0.30. ^{31}P NMR(300 MHz, $CDCl_3$, δ, ppm):4.8 (J_{P-H} 628.5 Hz). ESI-MS: calcd. for $C_{52}H_{98}PO_6N_3$ $[M+H]^+$: 892.5; found: 892.3.

H-Phosphonate of 3 -(carboxyaminohexan-6-ol)-5 -cholanic acid oleylamide **(27)** (triethylammonium salt). Yield 83%. R_f(TLC, CH_3OH/CH_2Cl_2 50/50): 0.33. ^{31}P NMR(300 MHz, $CDCl_3$, δ, ppm):5.0 (J_{P-H} 623.0 Hz). ESI-MS: calcd. for $C_{55}H_{104}PO_6N_3$ $[M+H]^+$: 934.6; found: 935.0.

H-Phosphonate of oleyl alcohol **(28)** (triethylammonium salt). Yield 54%. R_f(TLC, CH_3OH/CH_2Cl_2 50/50): 0.24. ^{31}P NMR(300 MHz, $CDCl_3$, δ, ppm):3.1 (J_{P-H} 630.0 Hz).ESI-MS: calcd. for $C_{24}H_{53}PO_3N$ $[M+H]^+$: 434.0; found: 434.0.

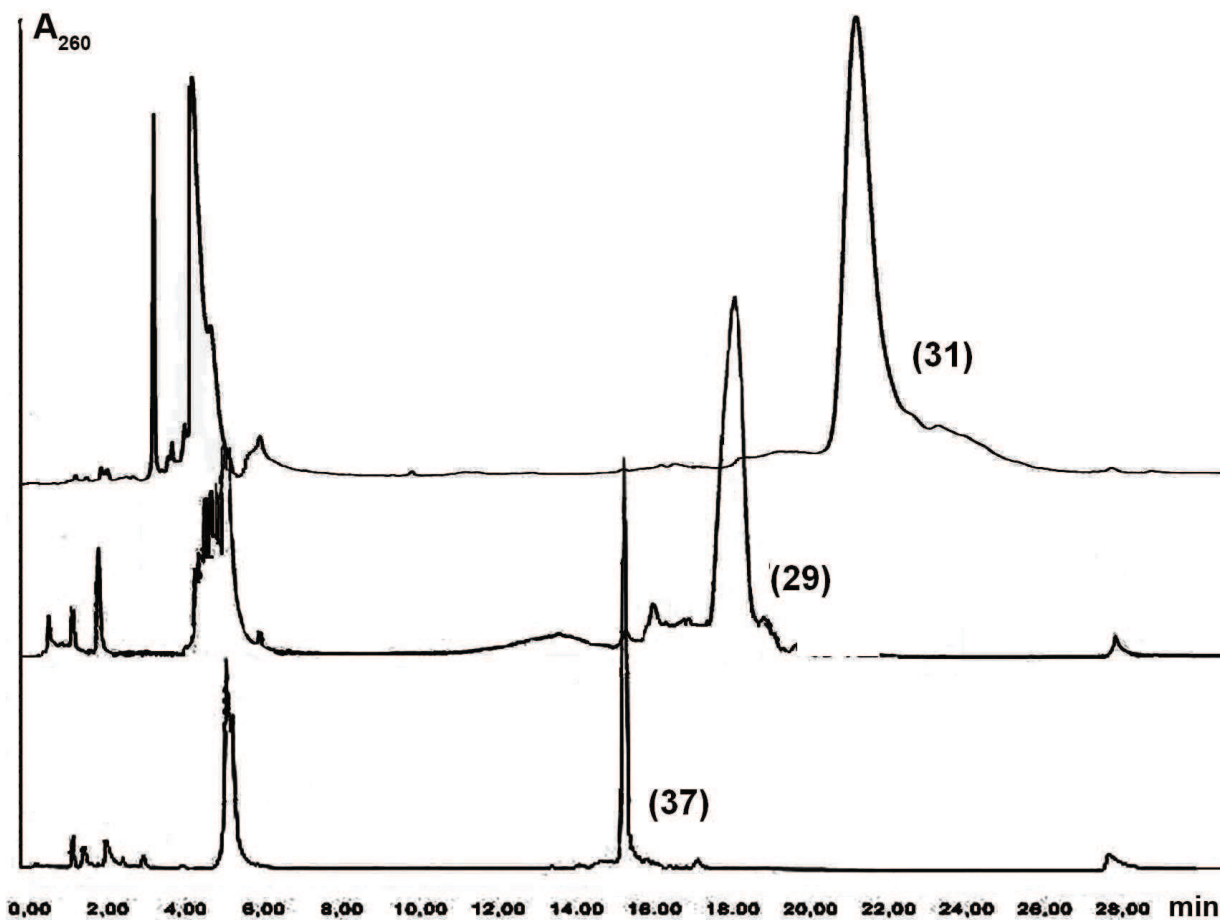## Supplementary Figures

Figure S1. RP-HPLC of crude reaction mixtures of Ch0-ON1 (**29**), Ch6-ON1 (**31**) and Ol-ON1 (**37**) performed using Alliance Waters chromatographic system with a XBridge C18 column (2.5 µm, 4.6 x50 мм) at $50^{O}C$. Flow rate 1 ml/min; buffer A,0.05 M NaClO$_4$; buffer B, 0.05 NaClO$_4$/90% CH$_3$CN).
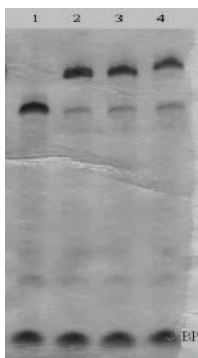

Figure S2. Electrophoretic analysis of crude reaction mixtures of siRNA sense strand conjugates: lane 1, ON1; lane 2, OlLt0-ON1 (**38**); lane 3, OlLt3-ON1 (**39**); lane 4, OlLt6-ON1 (**40**) (12% polyacrylamide gel: acrylamide:N,N'-methylenebisacrylamide (30:0.5), 8 urea, 89 m Tris-borate, pH 8.3, 2 m Na$_2$EDTA). Oligonucleotides were visualized by Stains-All. BP-bromophenol blue.

Publication 6.

Gvozdeva O.V., Dovydenko I.S., Venyaminova A.G., Zenkova M.A., Vlassov V.V., Chernolovskaya E.L. 42- and 63-bp anti-MDR1-siRNAs bearing 2'-OMe modifications in nuclease-sensitive sites induce specific and potent gene silencing. FEBS Lett., 2014. V. 588(6)., P.1037-43.

FEBS *Letters*

42- and 63-bp anti-MDR1-siRNAs bearing 2′-OMe modifications in nuclease-sensitive sites induce specific and potent gene silencing

Olga V. Gvozdeva, Ilya S. Dovydenko, Alya G. Venyaminova, Marina A. Zenkova, Valentin V. Vlassov, Elena L. Chernolovskaya *

Institute of Chemical Biology and Fundamental Medicine SB RAS, 8, Lavrentiev Avenue, Novosibirsk 630090, Russia

ARTICLE INFO

ABSTRACT

DsRNAs longer than 30 bp induce interferon response and global changes in gene expression profile in mammalians. 21 bp siRNA and 25/27 bp dsiRNA acting via RNA interference mechanism are used for specific gene silencing in this class of organisms. We designed selectively 2′-O-methyl-modified 42 and 63 bp anti-MDR1-siRNAs that silence the expression of P-glycoprotein and restore the sensitivity of drug-resistant cancer cells to cytostatic more efficiently than canonical 21 bp siRNAs. We also show that they act in a Dicer-independent mode and are devoid of immunostimulating properties. Our findings suggest that 42 and 63 bp siRNAs could be used as potential therapeutics.
© 2014 Federation of European Biochemical Societies. Published by Elsevier B.V. All rights reserved.

1. Introduction

RNA interference (RNAi) is an evolutionarily conserved cellular mechanism of sequence-specific gene silencing mediated by diverse classes of double-stranded RNAs [1]. Long dsRNAs inside the cell are cleaved by the RNAse-III class nuclease Dicer into 21–23-bp dsRNAs with 2-base 3′-overhangs and 5′-phosphates, termed short interfering RNA (siRNAs) and assemble into the RNA-induced gene silencing complex (RISC) [2–4]. Because of the outstanding potency and specificity in comparison with other loss-of-function technologies, RNAi has quickly developed into a potent biological tool for the specific inhibition of gene expression.

Long dsRNAs efficiently induce RNAi in non-mammalian eukaryotes, but in mammalian cells, dsRNAs longer than 30 bp activate the innate immunity system and induce global changes in the gene expression profile [5]. Tuschl and colleagues demonstrated that short 21-bp RNA duplexes, mimicking the products of dsRNA processing by Dicer, can be used for specific gene silencing, avoiding non-specific interferon response [3].

Another approach is to use longer synthetic RNA duplexes (typically 25–30 bp) that are substrates for Dicer [6]. These longer duplexes are effectively processed by Dicer into short 21 bp RNA duplexes, enter RISC and trigger RNAi [7]. Recent studies have revealed that longer synthetic RNA duplexes effectively silenced gene expression in many cell types without inducing interferon response, whereas they could trigger an innate immune response in several cell types [8]. The chemical modifications known to prevent the recognition of longer RNA duplexes by the innate immune system without influencing silencing activity have been assumed [6,9]. These chemical modifications can block the immune response and we can suppose that theoretically nothing prevents the use of partly modified dsRNAs of any length. Therefore, we decided to check this theory in our study using various experiments.

In our study, we used selectively modified RNA duplexes 21, 42 and 63 bp in length targeted *MDR1* mRNA and examined their ability to silence the expression of the target gene and the specificity of their action. We showed that 42 and 63 bp siRNAs induced more effective RNAi at lower concentrations than classical 21 bp siRNA without non-specific immune effects. To our surprise, no substantial processing of dsRNAs by Dicer was detected inside the cells. Our results remove the length limits for the design of RNAi effectors, and add another example in the list of novel RNAi-inducing molecules differing from the classical siRNA.

2. Materials and methods

2.1. siRNA synthesis and duplex annealing

Modified siRNAs were synthesised on an automatic ASM-800 DNA/RNA synthesiser (Biosset, Russia) using ribo- and 2′-O-methylribo β-cyanoethyl phosphoramidites (Glen Research, USA). The nuclease-sensitive sites in siRNA were protected by introducing 2′-O-Me-analogues of ribonucleotides. After standard deprotection, oligoribonucleotides were purified by denaturing polyacrylamide gel electrophoresis (PAGE) and isolated as sodium salts. The purified oligoribonucleotides were characterised by MAL-DI-TOF mass spectrometry on PEFLEX III (Bruker Daltonics, Germany). The following siRNAs were used in the present study: a 21 bp monomer (siM) homologous to the mRNA region 557–577 of the *MDR1* gene (sense strand 5′-GGCUUmGACmAAGUUmGUm AUmAUmGG-3′; antisense strand 5′-AUmAUmACmAACUUmGUCm AAGCCmAA-3′), the 42 bp dimer (siMDR-D) and the trimer (siMDR-T), which contain the sequence of the monomer repeated two and three times, respectively. The siRNA-Scr 21 bp monomer (siScr-M), with no significant homology to any known mRNA sequences from mouse, rat or human (sense strand 5′-CmAAGUCUCGUm AUmGUmAGUmGGUU-3′; antisense strand 5′-CCmACUmACmAUm ACGAGACUUmGUU-3′), the 42 bp dimer (siScr-D) and 63 bp trimer (siScr-T), which contain the sequence of the Scr monomer repeated two and three times, respectively, was used as the control. siRNA duplexes were obtained via annealing of the antisense and sense strands at equimolar concentrations in buffer A (15 mM HEPES-KOH pH 7.4, 50 mM potassium acetate, and 1 mM magnesium acetate) and stored at -20 °C.

2.2. Cell culture and transfection

Multiple drug-resistant human cell line KB-8–5 growing in the presence of 300 nM vinblastine was generously provided by Prof M. Gottesman (NIH, USA). The cells were grown in Dulbecco's modified Eagle's medium (DMEM), supplemented with 10% fetal bovine serum (FBS), 100 U/ml penicillin, 100 µg/ml streptomycin and 0.25 µg/ml amphotericin at 37 °C in a humidified atmosphere containing 5% CO_2/95% air. Cells in the exponential phase of growth were plated in 96-well plates at a density of 1×10^3 cells/well, in 24-well plates at a density of 0.4×10^5 cells/well or in 6-well plates at a density of 1.5×10^5 cells/well 1 day before the experiment; 24 h later, cells were transfected with siRNA using Oligofectamine according to the manufacturer's protocol. Untreated cells or those treated with Oligofectamine only were used as controls.

2.3. Real-time reverse transcription PCR (RT-PCR)

KB-8–5 cells were plated in 24-well plates (0.4×105 cells/well) and 24 h later the cells were transfected with siRNA using Oligofectamine. Total RNA was extracted from the cells using the SDS-phenol method 24 and 48 h post-transfection [10]. Quantification of specific mRNAs by RT-PCR was done essentially as described in [11]. The amount of mRNA of each gene was normalized to the amount of *GAPDH* mRNA used as an internal standard. To assess the expression of *GAPDH* gene the following primers were used: GAPDH forward: 5′-GTGAAGGTCGGAGTCAAC-3′ and GAPDH reverse: 5′-TGGAATTTGCCATGGGTG-3′. The relative level of gene expression was calculated using the Bio-Rad iQ5 2.0 software (Bio-Rad Laboratories Inc., United States).

2.4. Western blotting

KB-8–5 cells in an exponential phase of growth were plated in 24-well plates (0.4×10^5 cells/well); 24 h later, the cells were transfected with siRNAs using Oligofectamine. 4 and 6 days post-transfection, the culture medium was removed and the cells were lysed in 60 µl of Sample buffer (Sigma–Aldrich, USA). Western blotting was performed as described with [12] (detailed information in Supplementary material).

2.5. MTT assay

The number of living cells was determined after 120 or 144 h of transfection using the colorimetric method based on the oxidation of 3-[4,5-dimethylthiazol-2-yl]-2,5-diphenyl tetrazolium bromide (MTT) in the mitochondria of living cells as described in [13,14] (detailed information in Supplementary material).

2.6. Northern blotting

KB-8–5 cells in an exponential phase of growth were plated in 6-well plates (1.5×10^5 cells/well); 24 h later, the cells were transfected with siRNAs (200 nM) using Oligofectamine according to the procedure recommended by the manufacturer. After incubation of the cells with siRNAs for 24, 48 and 96 h, the culture medium was removed and the total RNA was extracted from the cells using *mir*Vana miRNA Isolation Kit. Northern blotting was performed via analogy with [15] (detailed information in Supplementary material).

3. Results

3.1. Design of siRNAs

We designed a set of siRNAs with different length (siMDR) targeted to the region 557–577 nt of the human *MDR1* mRNA. Previously, we have demonstrated that 21 bp siRNA targeted to this region has the ability to efficiently inhibit the *MDR1* expression both at the mRNA and protein (P-glycoprotein) levels [16]. Furthermore, this siMDR is capable of reversing the multiple drug resistance phenotype of cancer cells and inducing their death in the presence of earlier tolerable concentrations of cytostatics [16]. Here we constructed longer siRNAs (42 and 63 nt in length) containing the sequence of the previously studied siMDR (here and after siMDR-M or monomer) repeated two and three times, and designated as siMDR-D and siMDR-T or dimer and trimer, respectively. siRNAs with the same lengths: 21 bp siScr-M, 42 bp siScr-D and 63 bp siScr-T, which had no significant homology to any known mRNA sequences from mouse, rat or human, were used as negative controls.

The nuclease sensitive CpA, UpA and UpG sites in siRNAs were protected by introducing 2′-O-methyl analogues of ribonucleotides according to the algorithm, which was described by us earlier [17]. The modifications in the sites of potential Dicer cleavage were omitted.

3.2. Long selectively 2′-O-methylated siRNAs do not trigger interferon response

It is well established that 2′-OMe modifications efficiently prevent the induction of interferon response by 21 bp siRNA containing immunostimulation sequences [18] and 25/27 bp dsiR-NAs [19]. We evaluated the ability of selective 2′-O-methyl modification to prevent the induction of interferon (IFN) response by longer siRNAs. In these experiments, the mRNA levels of two IFN responsive genes, *β-actin* and *protein kinase R* (*PKR*), were used as markers of interferon response and the level of *GAPDH* mRNA was used as internal standard. Poly(I:C), a well-known IFN inducer, was used as a positive control. The data
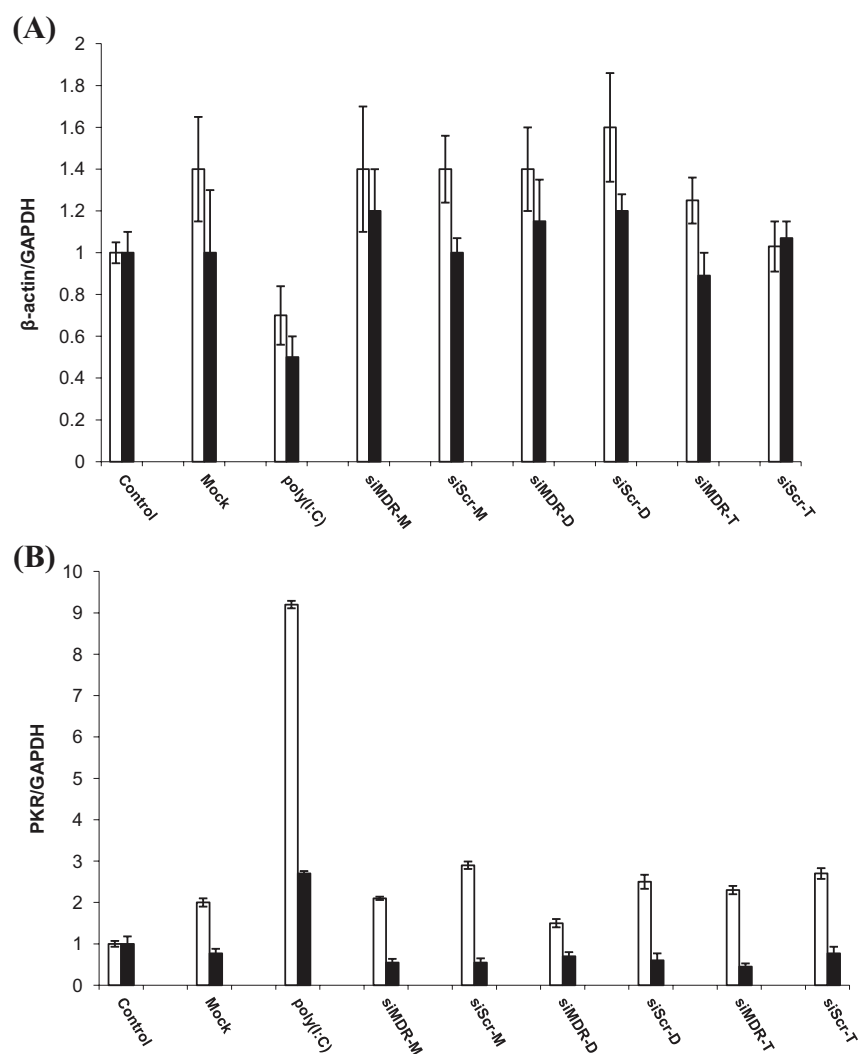
Fig. 1. Expression of interferon response marker genes encoding *β*-actin (A) and PKR (B) measured by RT-PCR 24 h (white bars) and 48 h (black bars) after transfection of KB-8-5 cells with siRNAs (200 nM) or poly (I:C) (250 ng/mL). The level of *GAPDH* mRNA was used as an internal standard. Error bars indicate the standard deviations (SD) of three independent sets of experiments.

obtained (Fig. 1) demonstrated that the level of *PKR* mRNA increased by a factor of 4.5-fold 24 h after and 3-fold 48 h after the transfection of KB-8–5 cells with 250 ng/mL poly(I:C), while the expression level of *β-actin* mRNA was reduced by 2-fold in the same samples. Treatment of the cells with 200 nM siMDR-M, siMDR-D, siMDR-T or siScr-M, siScr-D, siScr-T did not significantly alter the expression of the marker genes. Thus, we can conclude that tested siRNAs do not trigger a non-specific IFN response in the cells.

3.3. siRNA-mediated silencing of P-glycoprotein expression

Silencing activity of the 21-, 42- and 63 bp siRNAs was compared by their ability to reduce the level of P-glycoprotein using Western blot analysis in KB-8–5 cells. Cells were treated with increasing concentrations of siMDR-M (25–200 nM), siMDR-D (12.5–100 nM), siMDr-T (8–66.6 nM) and 200 nM siScr-M, 100 nM siScr-D and 66.6 nM siScr-T. Concentrations of siMDR-D, siMDR-T and siScr-D, siScr-T were selected in such a way in order to keep the equal "dose" of the 21 nucleotide sequence complementary to the target in parallel samples (here and after "dose-equivalent concentrations"), presuming the processing of

siMDR-D and siMDR-T into two and three molecules of siMDR-M, respectively. The P-glycoprotein level was assayed 96 and 144 h after the treatment since the maximum reduction of P-glycoprotein level by siMDR-M was observed at these time points earlier [17]. It was found (Fig. 2) that treatment with specific siRNAs led to a concentration-dependent decrease in the P-glycoprotein level. The silencing effect of siMDR-M (up to 60%) at 96 h after transfection at concentrations of 100–200 nM was similar to that of siMDR-D at the dose-equivalent concentrations. However, when assayed 96 h after transfection, siMDR-D at low concentrations (30–50% silencing) and siMDR-T across the entire range of concentrations (40–20% silencing) induced less pronounced gene silencing than siMDR-M (60% silencing) (Fig. 2). The silencing effect was substantially increased (up to 80%) at 144 h after transfection with 100–200 nM of siMDR-M and was comparable to that of siMDR-D and siMDR-T at dose-equivalent concentrations. It should be noted that siMDR-T at low concentrations (8–16 nM) 144 h after transfection was more active than siMDR-D and siMDR-M: the inhibitory effect was 80%, 62% and 58% for 8 nM concentration, respectively. The P-glycoprotein level in the KB-8–5 cells treated with 200 nM siScr-M, 100 nM siScr-D and 66.6 nM siScr-T remained unaffected.
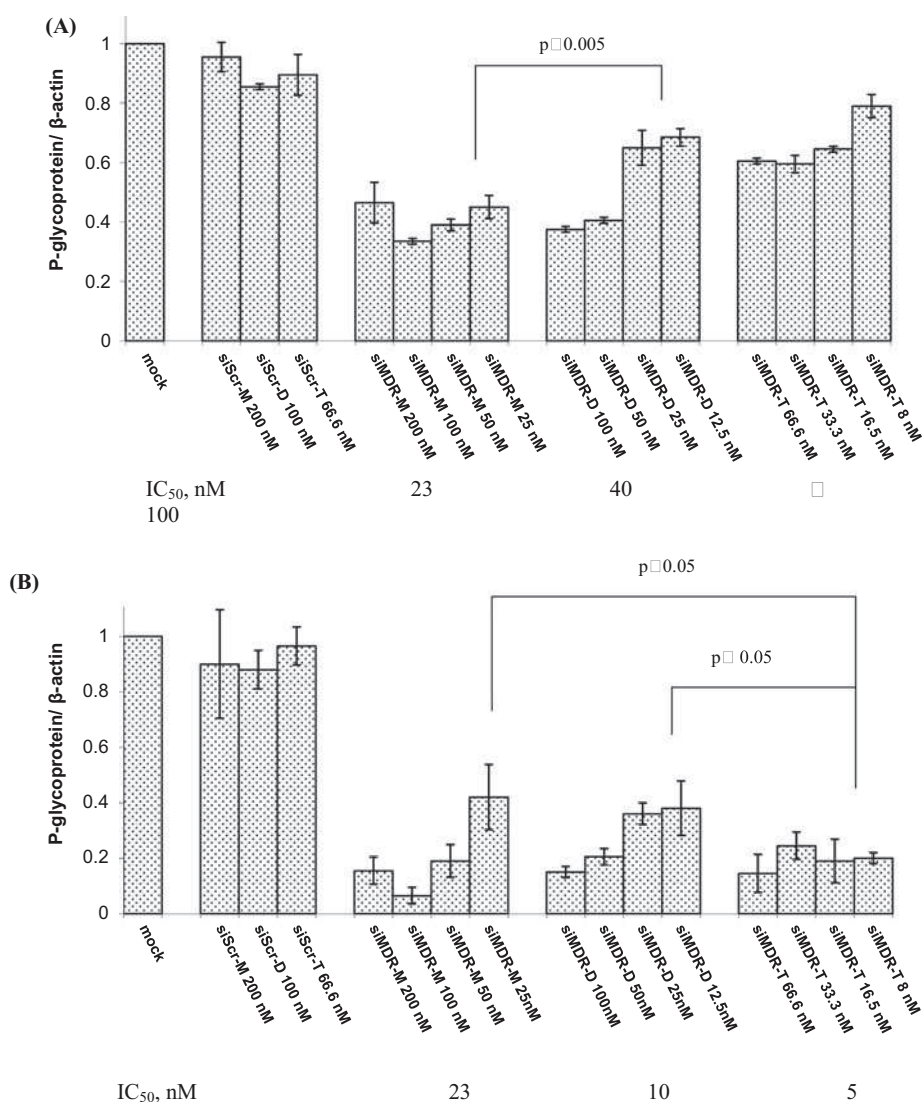
Fig. 2. siRNA-mediated silencing of the P-glycoprotein in KB-8–5 cells. P-glycoprotein levels were determined by Western blot analysis 96 h (A) and 144 h (B) after transfection with different concentrations of siRNAs. The relative P-glycoprotein level was normalised against the level of β-actin protein. Error bars indicate the standard deviations (SD) of three independent sets of experiments.

3.4. Silencing of MDR1 expression by siRNAs revert the multiple drug resistance of cancer cells

Since the therapeutic goal of *MDR1* gene silencing is restoration of the sensitivity of drug-resistant cancer cells to anti-cancer drugs, we examined the ability of anti-MDR siRNAs to decrease a number of living cells in the presence of earlier tolerable concentrations of vinblastine (300 nM) using the MTT assay. Cells were treated with increasing concentrations of siMDR-M (25–200 nM), siMDR-D (12.5–100 nM), siMDR-T (8–66.6 nM) and maximal concentrations of the control siRNAs: 200 nM siScr-M, 100 nM siScr-D and 66.6 nM siScr-T. Amounts of living cells were estimated 122 and 144 h after transfection. The number of cells in the sample treated with transfection reagent only was taken as 100%. The data indicated that treatment with siRNAs led to concentration-dependent cell death (Fig. 3). The treatment of KB-8–5 cells with 200 nM siMDR-M, 100 nM siMDR-D and 66.6 nM siMDR-T caused 50% reduction of viable cells at 122 h and the almost complete disappearance of viable cells at 144 h after transfection. It should be noted that transfection with siMDR-T resulted in the more efficient reduction of viable cell number (up to 75%) at low concentrations

after 144 h of incubation as compared with samples treated with siMDR-D and siMDR-M at dose-equivalent concentrations. siScr-M, siScr-D, and siScr-T had no effect on the cell viability in the presence of 300 nM vinblastine.

3.5. siRNA processing in the cells

dsRNAs longer than 25–30 bp are known to be efficiently processed by the cellular enzyme Dicer when introduced into cells [7]. Modification patterns of 25–27 dsRNAs including alternating 2′-OMe residues that do not span the expected Dicer cut site were found to be compatible with intracellular processing [6]. Here, we investigated whether the longer 42 and 63 bp selectively modified siRNAs are processed in the cells into canonical 21 bp siRNAs and whether the cleavage is necessary for the silencing activity. siMDR-M, siMDR-D and siMDR-T were transfected into KB-8–5 cells and after 4, 24 and 48 h the cells were washed extensively to remove unbound siRNA; the total RNA was isolated from the cells using the SDS-phenol method. Northern blot analysis revealed that siMDR-D and siMDR-T remained intact inside the cells after transfection for a prolonged period of time and the products of their
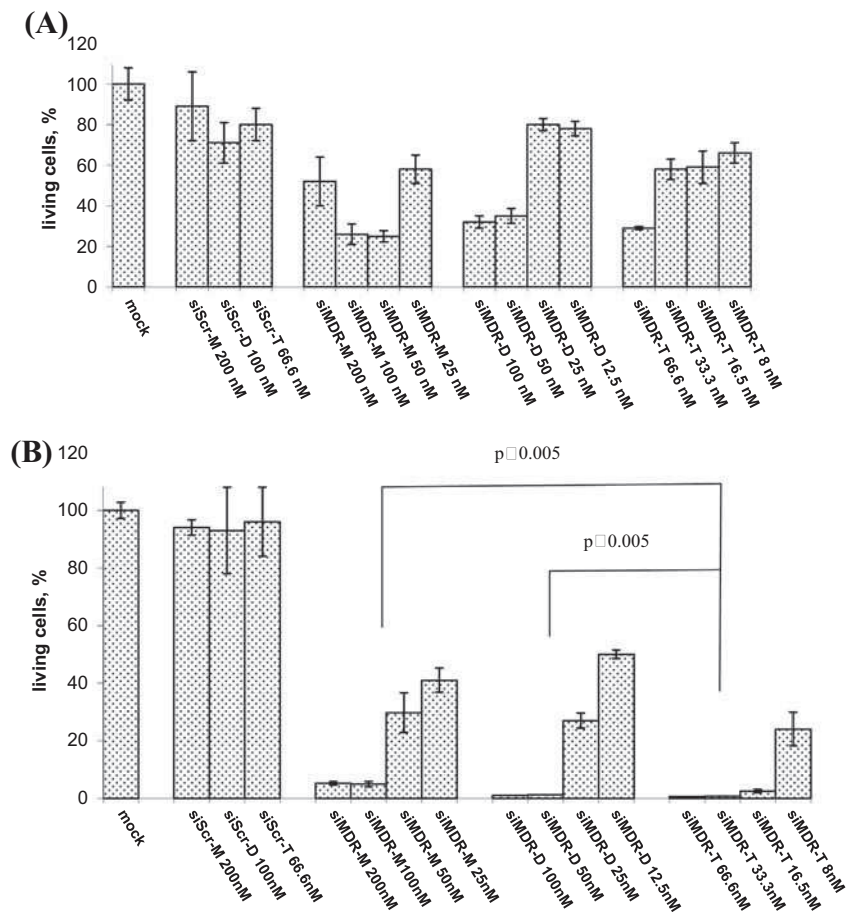
Fig. 3. Amounts of living cells were analysed using MTT-assay 120 h (A) and 144 h (B) after transfection with siRNA and subsequent incubation in the presence of 300 nM vinblastine.
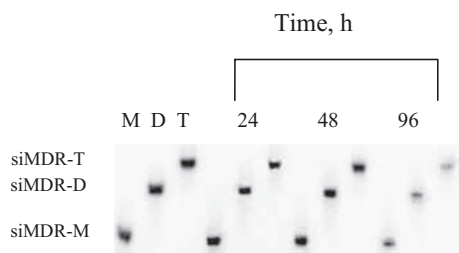

Fig. 4. Northern blot analysis of siMDR-M, siMDR-D and siMDR-T transfected into the KB-8–5 cell line. Sense strands of siMDR-M (M) siMDR-D (D) and siMDR-T (T) were used as controls.

cleavage by Dicer were not detected (Fig. 4). At the same time, these siRNAs showed potent RNAi activity, suggesting that long siMDR-D and siMDR-T duplexes could trigger RNAi in a processing-independent manner.

4. Discussion

Recent reports have proven that longer duplexes (25–30 bp in length) are processed by Dicer into 21 bp siRNAs and loaded into RISC more efficiently than canonical siRNAs and demonstrate better gene silencing [7]. It has been shown that the RNAi effector complex containing Dicer and accessory proteins interacts with an Argonaut protein (Ago) and actively loads the bottom strand of the siRNA into the RISC. Such a model implies an increased

affinity of Dicer and Dicer/TRBP for longer dsRNAs, as Dicer requires a minimum stem length for efficient cleavage [6–8,20]. Moreover, it was recently demonstrated [21] that 25–27 bp dsR-NAs can be directly loaded into Ago2 and show better efficacy as compared with canonical 21 bp siRNAs.

Therefore, in our study, we compared the silencing activity of 21 bp siRNA with the activity of 42 and 63 bp siRNAs containing two and three copies of the same 21 bp sequence, respectively.

The main problem in the application of the long non-modified dsRNAs as mediators of RNAi in mammalian cells and mammalians is the induction of interferon response and the subsequent global changers in gene expression profile [9,22,23]. Chemical modification patterns preventing the activation of innate immunity and compatible with the Dicer cleavage were described for 27/25 bp dsiRNA [19]. Our data revealed that 2′-OMe modification of CpA, UpA and UpG motives in 42 bp and 63 bp siRNAs effectively prevents activation of the innate immunity response and did not change the expression levels of two key interferon response genes, *PKR* and *β-actin,* in KB-8–5 cells. Thus, selectively modified long dsRNAs could be used in mammalian cells for specific gene silencing.

Gene expression assays at the protein level clearly demonstrate the efficacy and specificity of all tested anti-MDR1-siRNAs. Exposure to siRNAs caused a concentration-dependent reduction of the P-glycoprotein level. The concentration-dependent results are consistent with our previous observations using anti-MDR1 siR-NAs, which can effectively inhibit target gene expression at a concentration of 200 nM [24]. To compare the biological activity of siRNAs with different lengths we used concentrations of the equal

"dose" of the 21 nucleotide sequence of siMDR-M repeated two or three times (dose-equivalent concentrations), presuming the processing of siMDR-D and siMDR-T into two or three molecules of siMDR-M, respectively.

We found that siMDR-M (IC_{50} 23 nM) was notably more active than siMDR-D and siMDR-T at 96 h after transfection. The biological activity of siMDR-M exceeded that of siMDR-D (IC_{50} 40 nM) at low concentrations and the biological activity of siMDR-T (IC_{50} was not achieved) at all of the concentrations used.

The data obtained 144 h after transfection showed that the silencing effect of longer siMDR-T (IC_{50} 5 nM) was more pronounced than the effects of siMDR-D (IC_{50} 10 nM) and siMDR-M (IC_{50} 23 nM). The inhibitory effect of siMDR-T at concentrations of 33.3–66.6 nM measured at 144 h after transfection was similar to that of siMDR-D and siMDR-M at dose-equivalent concentrations. However, transfection of siMDR-T at low concentrations (8–16.6 nM) resulted in significantly more efficient reduction of P-glycoprotein level. The siRNA-mediated effect was specific since no effect on the protein levels was observed in cells treated with the same concentrations of siRNA with a scrambled sequence both at 96 and 144 h after transfection.

The results that were consistent with P-glycoprotein suppression data were obtained in the experiments on KB-8–5 cell viability. These cells are characterised by over-expression of the *MDR1* gene, and have the ability to grow in the presence of 300 nM vinblastine. Silencing of the *MDR1* gene by siRNAs induces the death of KB-8–5 cells at concentrations of vinblastine that were previously tolerated by cells. Transfection with 50–25 nM siMDR-M resulted in the more efficient reduction of viable cells (up to 42%) after 122 h of incubation as compared with siMDR-D and siMDR-T at dose-equivalent concentrations. However, siMDR-T was found to be substantially more effective than siMDR-D and siMDR-M 144 h after transfection when used at low concentrations: up to 75% reduction of viable cells was achieved by the samples transfected with 8 nM siMDR-T. This difference in active concentrations of siRNAs is therapeutically relevant and demonstrates the preference of longer selectively modified interfering RNAs.

The slow development of the silencing effect caused by siMDR-D and siMDR-T in comparison with the effect of siMDR-M may be related to the time required for the processing of longer siRNAs or to the difference in the kinetics of Dicer/TRBP-mediated RISC loading and direct Ago2 loading. The potential explanation for the difference in canonical siRNA versus longer siRNA gene silencing potency may be related to the minimum length requirement of siRNA that can be directly loaded into Ago2 leading to bias strand selection towards the guide strand, persistence of the guide strand and improved guide strand gene silencing.

We compared the activity of siRNA at equal 21 bp «dose» concentrations, hypothetically assuming that they will be completely processed into 21 bp duplexes inside the cells. However, the data obtained (Fig. 4) revealed that selectively modified 42 and 63 bp siRNAs were not cleaved by Dicer to yield detectable levels of 21 bp products when transfected into the cells and the intact antisense strands were present in the cells for prolonged periods of time (at least up to 48 h). Despite the fact that the potential sites of cleavage in the tested siRNAs are modification-free, the effect may be connected to the 2′-O-methyl modifications of the flanking regions of these siRNAs, which prevent the formation of degradation products. The direct comparison of our modification patterns with those of Dicer substrates described in [21] shows that besides the cleavage site, the smaller part of dsiRNA, which has to be cut off during processing, does not contain modifications. In our structures, the sequences located after the cleavage site are designed as a copy of interfering RNA and contain modification. We can suppose that modifications in the flanks can reduce the efficiency of cleavage. The observed sequence-specific gene silencing can be

rationalised in at least two ways: firstly, the effect can be induced by the very small quantities of processed siRNA, which are not detectable by the Northern blot in the presence of the majority of non-processed longer species; secondly, the ability of long dsRNA and pre-miRNA to form the direct complexes with Ago2 [21,25] makes Dicer-independent gene silencing possible. The latter suggestion can be supported by the recent study, where a 38 nt-long molecular structure that was not processed by Dicer, but induced efficient gene silencing via the RNAi mechanism, was described [26]. The authors implied that longer dsRNAs can be incorporated into an active RISC complex without Dicer processing. The data on the comparison of the efficiency of siRNA action at different time points are consistent with both explanations: both the need of time for processing and the difference in the kinetics of Dicer/TRBP-mediated RISC loading and direct Ago2 loading could account for the delay in the development of the silencing effect by longer siRNA. However, taking into account the data of Northern Blot analysis we can conclude that the delay in the development of the silencing effect by longer siRNA is related to the difference in the kinetics of Dicer/TRBP-mediated RISC loading and direct Ago2 loading.

In conclusion, we designed selectively modified 42 and 63 bp anti-MDR1 dsRNAs and showed their potent RNAi activity and specificity. These siRNAs were found to silence the expression of P-glycoprotein and restore the sensitivity of drug-resistant cancer cells to vinblastine more efficiently that canonical siRNA with the same sequence. For this reason, we believe that these structures could be used for the development of efficient therapeutics.

Appendix A. Supplementary data

Supplementary data associated with this article can be found, in the online version, at http://dx.doi.org/10.1016/j.febslet.2014.02.015.

References

[1] Fire, A., Xu, S., Montgomery, M.K., Kostas, S.A., Driver, S.E. and Mello, C.C. (1998) Potent and specific genetic interference by double-stranded RNA in *Caenorhabditis elegans*. Nature 391, 806–811.

[2] Bernstein, E., Caudy, A.A., Hammond, S.M. and Hannon, G.J. (2001) Role for a bidentate ribonuclease in the initiation step of RNA interference. Nature 409, 363–366.

[3] Elbashir, S.M., Harborth, M.J., Ledecknel, W. and Tuschl, T. (2001) Duplexes of 21-nucleotide RNAs mediate RNA interference in cultured mammalian cells. Nature 411, 494–498.

[4] Martinez, J., Patkaniowska, A., Urlaub, H., Lührmann, R. and Tuschl, T. (2002) Single-stranded antisense siRNAs guide target RNA cleavage in RNAi. Cell 110, 563–574.

[5] Wang, Q. and Carmichael, G.G. (2004) Effects of length and location on the cellular response to double-stranded RNA. Microbiol. Mol. Biol. Rev. 3, 432–452.

[6] Collingwood, A.M., Rose, D.S., Huang, L., Hiller, C., Amarzguioui, M., Wiiger, M.T., Soifer, H.S., Rossi, J.J. and Behlke, M.A. (2008) Chemical modification patterns compatible with high potency Dicer-substrate small interfering RNAs. Oligonucleotides 18, 187–200.

[7] Kim, D.H., Behlke, M.A., Rose, S.D., Chang, M.S., Choi, S. and Rossi, J.J. (2005) Synthetic dsRNA Dicer substrates enhance RNAi potency and efficacy. Nat. Biotechnol. 23, 222–226.

[8] Reynolds, A., Anderson, E.M., Vermeulen, A., Fedorov, Y., Robinson, K., Leake, D., Karpilow, J., Marshall, W.S. and Khvorova, A. (2006) Induction of the interferon response by siRNA is cell type and duplex length-dependent. RNA 1, 988–993.

[9] Siud, M. and Furset, G. (2006) Molecular basis for the immunostimulatory potency of small interfering RNAs. J. Biomed. Biotechnol. 4, 1–4.

[10] Chattopadhyay, N.R., Godble, K. and Godble, M. (1993) Inexpensive SDS/phenol method for RNA extraction from tissues. Biotechniques 15, 24–26.

[11] Akimov, I.A., Kabilova, T.O., Vlassov, V.V. and Chernolovskaya, E.L. (2009) Inhibition of human cancer-cell proliferation by long double-stranded RNAs. Oligonucleotides 19, 31–40.

[12] Petrova, N.S., Meschaninova, M.I., Venyaminova, A.G., Zenkova, M.A., Vlassov, V.V. and Chernolovskaya, E.L. (2011) Silencing activity of 2′-O-methyl modified anti-MDR1 siRNAs with mismatches in the central part of the duplexes. FEBS let. 585, 2352–2356.

[13] Kabilova, T.O., Vladimirova, A., Chernolovskaya, E.L. and Vlassov, V.V. (2006) Arrest of cancer cell proliferation by dsRNAs. Ann. NY Acad. Sci. 1091, 425–436.

[14] Carmichael, J., Degraff, W.G., Gazdar, A.F., Minna, J.D. and Mitchell, J.B. (1987) Evaluation of a tetrazolium-based semiautomated colorimetric assay: assessment of chemosensitivity testing. Cancer Res. 47, 936–942.

[15] Desnoyers, G. and Massé, E. (2012) Activity of small RNAs on the stability of targeted mRNAs in vivo. Methods Mol. Biol. 905, 245–255.

[16] Logashenko, E.B., Vladimirova, A.V., Repkova, M.N., Venyaminova, A.G., Chernolovskaya, E.L. and Vlassov, V.V. (2004) Silencing of *MDR1* gene in cancer cells by siRNA. Nucleosides, Nucleotides Nucleic Acids 23, 861–866.

[17] Volkov, A.V., Kruglova, N.S., Meschaninova, M.I., Venyaminova, A.G., Zenkova, M.A., Vlassov, V.V. and Chernolovskaya, E.L. (2009) Selective protection of nuclease-sensitive sites in siRNA prolongs silencing effect. Oligonucleotides 19, 191–202.

[18] Hornung, V., Guenthner-Biller, M., Bourquin, C., Ablasser, A., Schlee, M., Uematsu, S., Noronha, A., Manoharan, M., Akira, S., de Fougerolles, A., Endres, S. and Hartmann, G. (2005) Sequence-specific potent induction of IFN-α by short interfering RNA in plasmacytoid dendritic cells through TLR7. Nat. Med. 11, 263–270.

[19] Judge, A.D., Sood, V., Shaw, J.R., Fang, D., Mcclintock, K. and Maclachlan, I. (2005) Sequence-dependent stimulation of the mammalian innate immune response by synthetic siRNA. Nat. Biotechnol. 23, 457–462.

[20] Siolas, D., Lerner, C., Burchard, G.W., Linsley, P.S., Paddison, P.J., Hannon, G.J. and Cleary, M.A. (2005) Synthetic shRNAs as potent RNAi triggers. Nat. Biotechnol. 23, 227–231.

[21] Snead, N.M., Wu, X., Li, A., Cui, Q., Sakurai, K., Burnett, J.C. and Rossi, J.J. (2013) Molecular basis for improved gene silencing by Dicer substrate interfering RNA compared with other siRNA variants. Nucleic Acids Res. 41, 6209–6221.

[22] Wang, Q. and Carmichael, G.G. (2004) Effects of length and location on the cellular response to double-stranded RNA. Microbiol. Mol. Biol. Rev. 68, 432–452.

[23] Manche, L., Green, S.R., Schmedt, C. and Mathews, M.B. (1992) Interactions between double-stranded RNA regulators and the protein kinase DAI. Mol. Cell. Biol. 12, 222–226.

[24] Kruglova, N.S., Meschaninova, M.I., Venyaminova, A.G., Zenkova, M.A., Vlassov, V.V. and Chernolovskaya, E.L. (2010) Cholesterol-modified anti-MDR1 small interfering RNA: uptake and biological activity. Mol. Biol. 44, 254–261.

[25] Salomon, W., Bulock, K., Lapierre, J., Pavco, P., Woolf, T. and Kamens, J. (2010) Modified dsRNAs that are not processed by Dicer maintain potency and are incorporated into the RISC. Nucleic Acids 38, 3771–3779.

[26] Chang, C., Lee, T.Y., Yoo, J.W., Shin, D., Kim, M., Kim, S. and Lee, D. (2012) Branched, tripartite-interfering RNAs silence multiple target genes with long guide strands. Nucleic Acid Ther. 22, 30–39.

Supplementary Data:

Materials and methods

Western blotting: Twenty microliters of each sample was loaded on a 10% sodium dodecyl sulphate (SDS)/acrylamide gel and separated at 60 mA for 1 h. The proteins were transferred from acrylamide gel to PVDF membrane (Millipore, USA) using a Hoeffer TE70 SemiPhor Semi-Dry transfer unit. The membrane was blocked overnight in 0.5% non-fat dried milk in 0.05 M Tris–HCl, 0.15 M NaCl, 0.1% Tween 20, pH 7.5 (buffer B) and incubated with monoclonal anti-P-glycoprotein and anti--actin antibodies (Sigma–Aldrich, USA) at 1:3000 and at 1:6000 dilutions, respectively, in buffer B for 1 h. After washing in buffer B, the membranes were incubated with secondary rabbit anti-mouse antibodies conjugated with alkaline phosphatase (Invitrogen, USA) for 30 min. Chromogenic detection was performed using Western Blue Stabilised Substrate for alkaline phosphatase (Promega, USA). The reaction was stopped by rinsing the membrane with water. Human -actin protein was used as an internal standard. Data were analysed using the Gel-Pro 4.0 program (Media Cybernetics, USA).

MTT assay: KB-8-5 cells in an exponential phase of growth were plated at a density of 1×10^3 cells/well in 96-well plates and transfected with different concentrations of siRNA (25–200 nM). 24 h post-transfection, vinblastine was added at a final concentration of 300 nM. After 120 or 144 hours of incubation at 37°C, MTT was added to a final concentration of 0.5 mg/mL. After 3 h, the culture medium was removed; the resulting formazan crystals were dissolved in dimethyl sulphoxide (100 µl/well), and the optical density of the solution was measured on a Multiscan RC multichannel photometer (Labsystems) at wavelengths of 570 and 620 nm.

Northern blotting: Twenty micrograms of total RNA was heated at 80°C for 5 min, than placed on ice. The samples were loaded on a 12% denaturing polyacrylamide gel and separated at 60 mA for 40 min. The gel was washed with 0.5_X TBE buffer. Total RNA was transferred from acrylamide gel to positively charged nylon membrane (Zeta-probe membrane, Bio- Rad Laboratories Inc., United States) using Hoeffer TE70 SemiPhor Semi-Dry transfer unit for 2 hours. The transferred RNA was cross-linked to the membrane by UV-irradiation for 1 min and baked at 80°C for 30 min. The membrane was pre-incubated at 37°C for 30 min with hybridization solution (50% formamide, 1 M NaCl, 0.2 mg/ mL salmon sperm DNA, 50 mM Tris–HCl pH 7.4, 0.2 x Denhardt solution, 1% SDS) and then incubated in the same solution containing $[\gamma^{32}P]$-labeled probe (5MBq/r) for 1 hour. The membrane was washed with washing solution 1 (2_X SSC, 0.05% SDS) for 30 min and twice with washing solution 2 (0.1_X SSC, 0.1%

SDS) for 15 min. The residual liquid was removed; membrane was covered with saran wrap and analyzed using Pharos FX Plus molecular imager system after 10 h exposition.
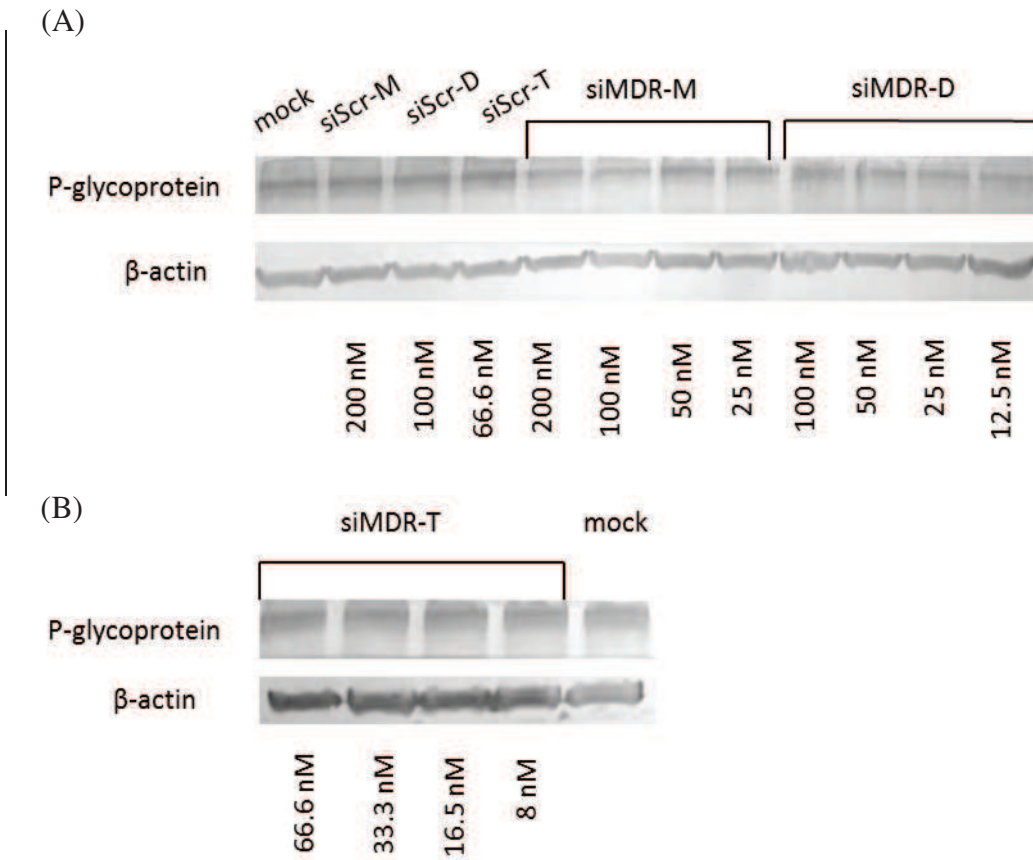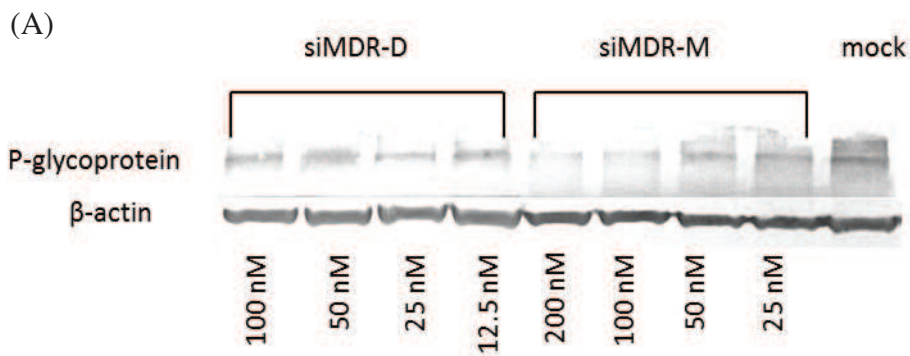
(A)

(B)

Fig. 5. Representative Western Blot analysis 96 h after transfection with different concentrations of siScr, siMDR-M, siMDR-D (A) and siMDR-T (B). Quantitative data is presented in the main text Fig. 2 (A).
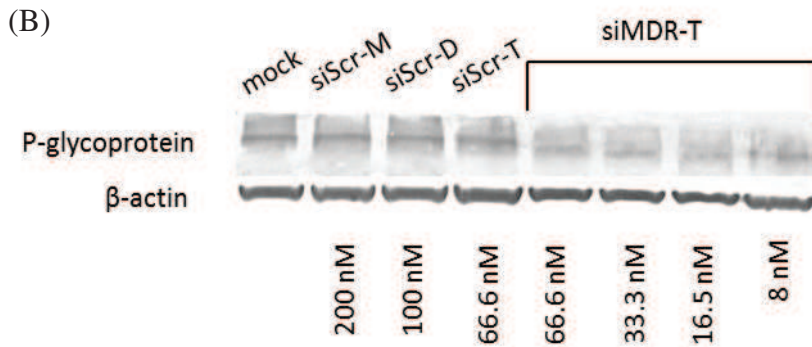
(A)

(B)

Fig. 6. Representative Western Blot analysis 144 h after transfection with different concentrations of siMDR-M, siMDR-D (A) and siScr, siMDR-T (B). Quantitative data is presented in the main text Fig. 2 (B).
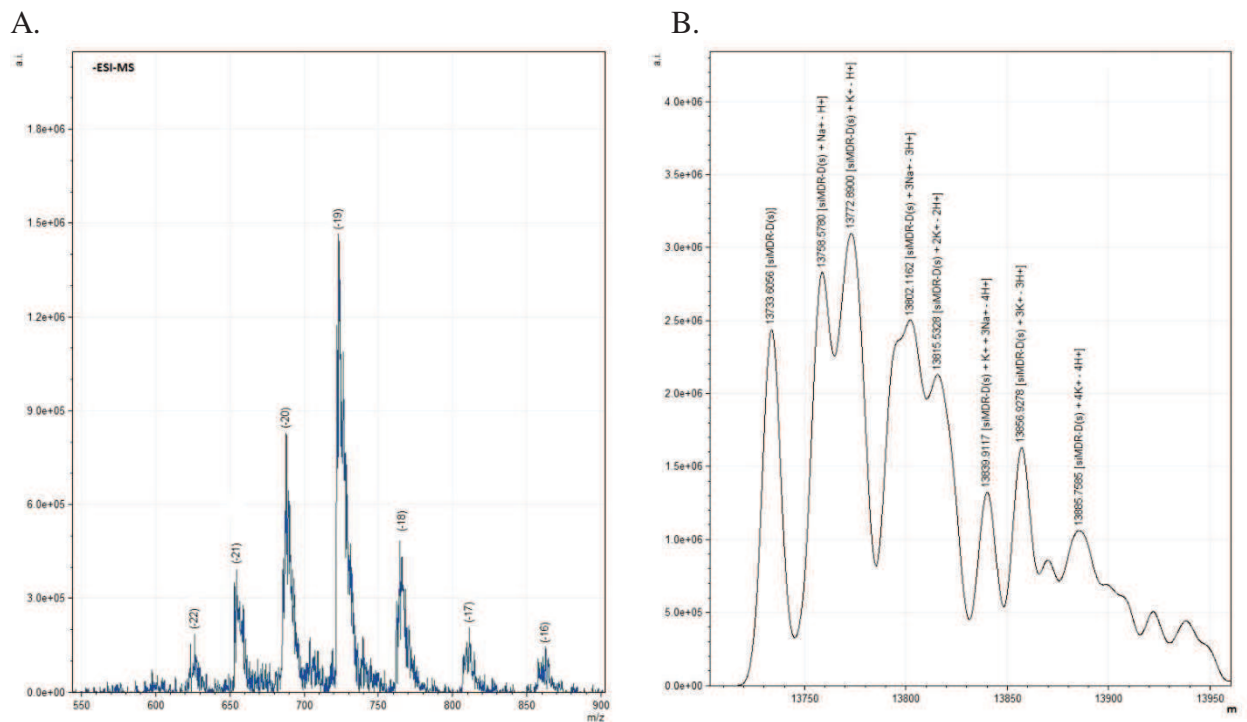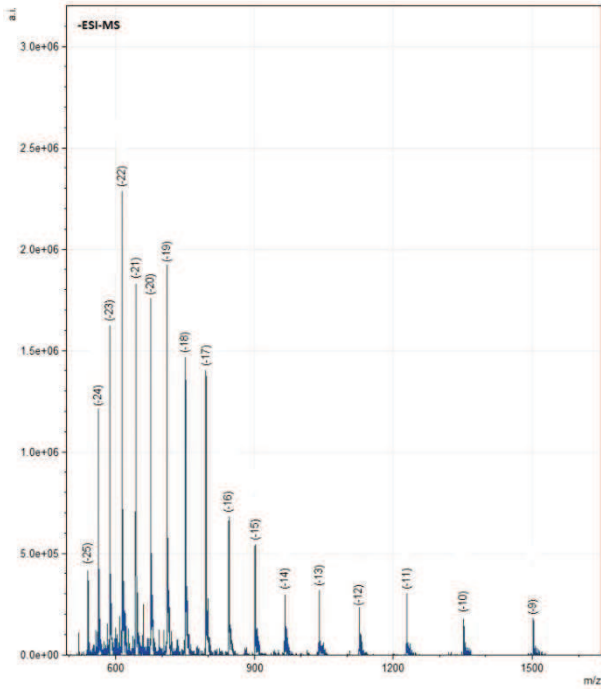
A.

B.

Fig. 7. A. ESI mass spectra of siMDR-D (sense). B. Deconvoluted spectra of siMDR-D (sense): theoretical mass – 13738.4 Da, measured mass – 13733.6 Da. The analysis was performed in the Center of mass-spectrometrical analysis of ICBFM RAS.
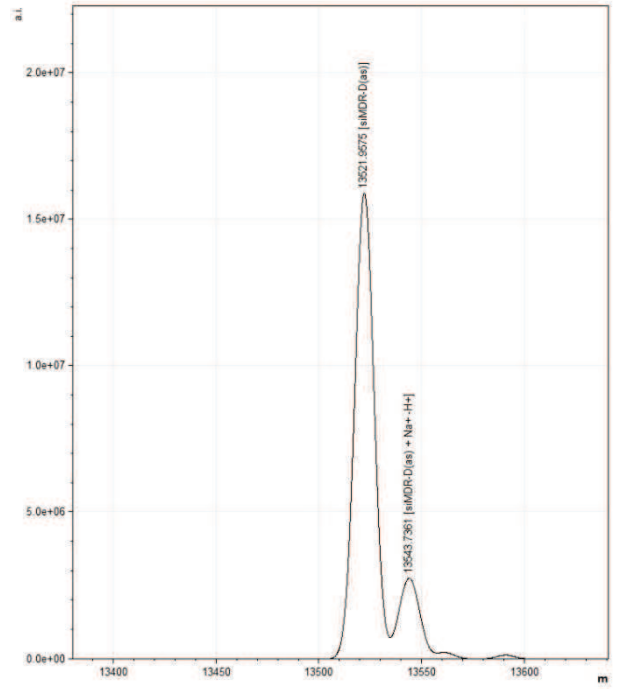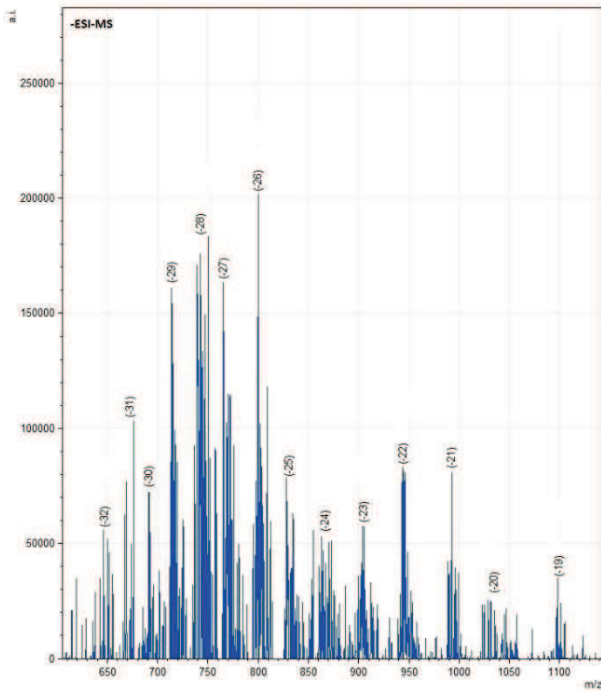
A.

B.

Fig 8. ESI mass spectra of siMDR-D (antisense). Deconvoluted spectra of siMDR-D (antisense): theoretical mass – 13526.4 Da, measured mass – 13521.9 Da.
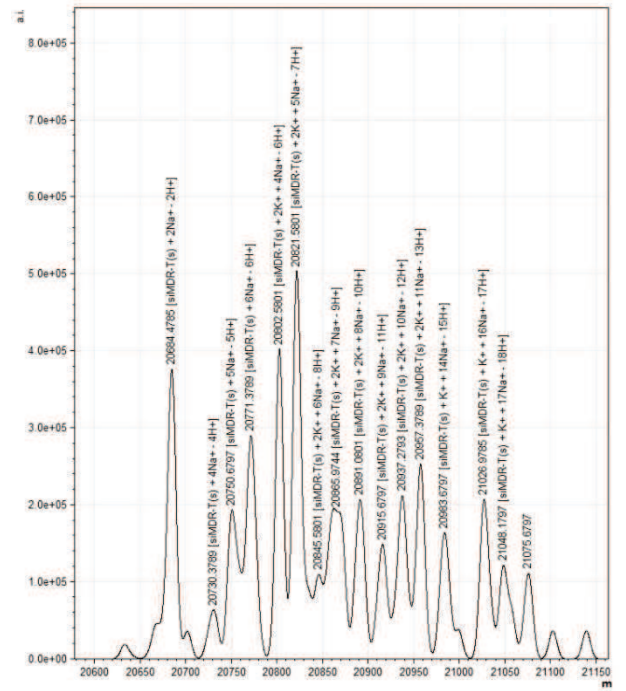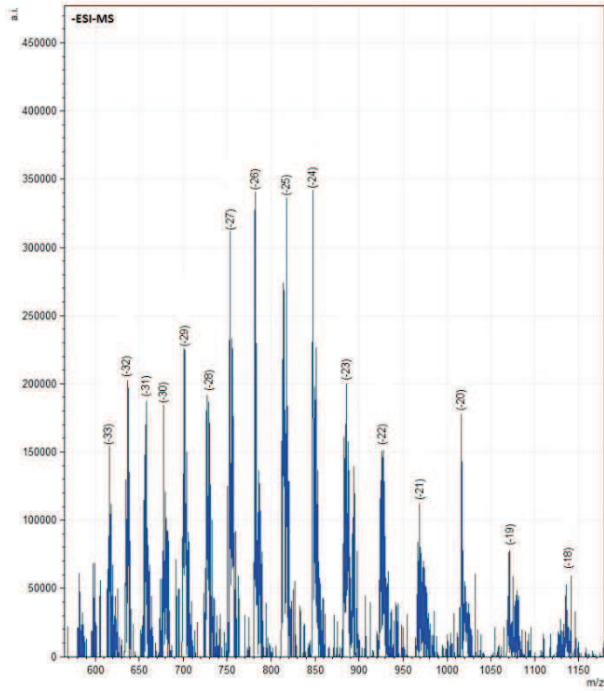
A.

B.

Fig. 9. A. ESI mass spectra of siMDR-T (sense). B. Deconvoluted spectra of siMDR-T (sense): theoretical mass of [siMDR-T(s) +2Na$^+$-2H$^+$] – 20682.5 Da, measured mass of [siMDR-T(s) +2Na$^+$-2H$^+$] – 20684.5 Da.
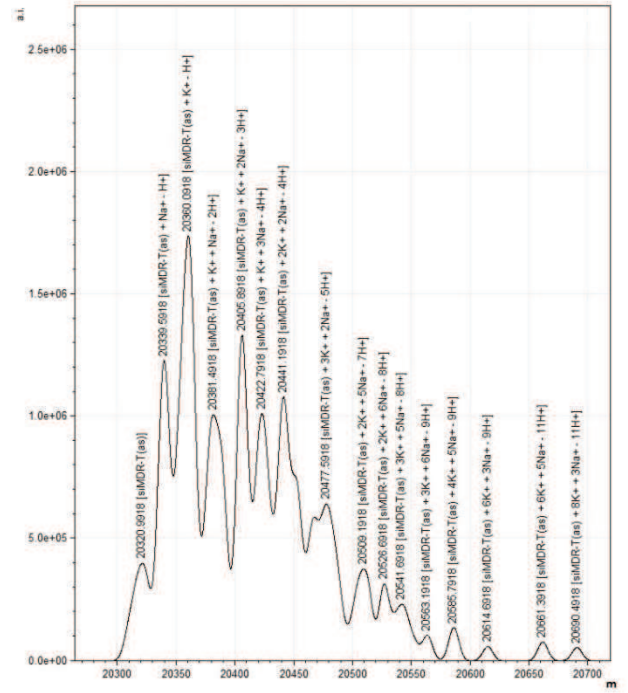
A.

B.

Fig. 10. A. ESI mass spectra of siMDR-T (antisense). B. Deconvoluted spectra of siMDR-T (antisense): theoretical mass – 20320.6 Da, measured mass – 20320.99 Da.
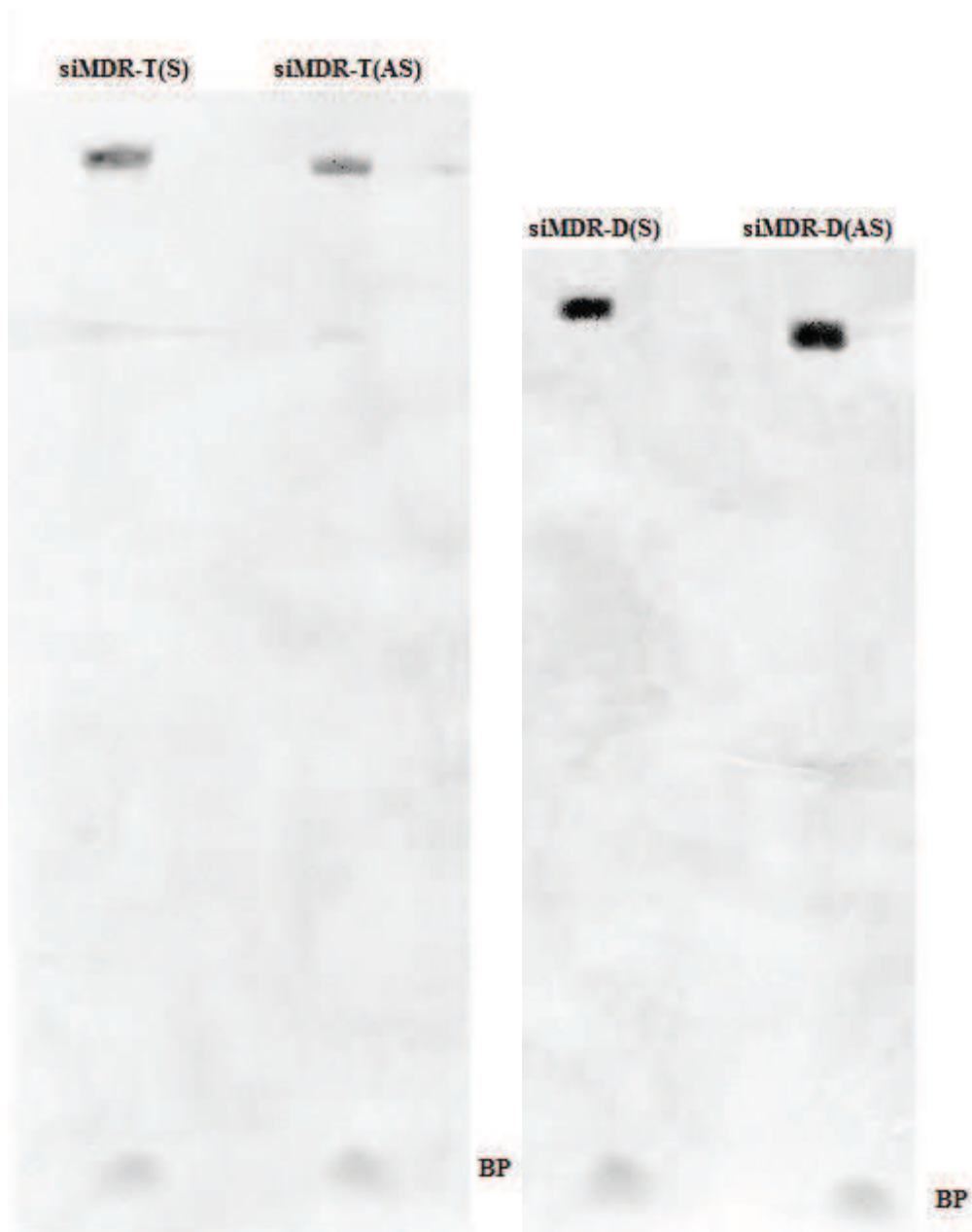
Fig. 11. Gel-electrophoretical analysis of 42- and 63 –mer oligoribpnucleotides in 12% PAAG, 8M Urea.

UNIVERSITE DE STRASBOURG

RESUME DE LA THESE DE DOCTORAT

Discipline : Sciences du Vivant

Spécialité : Aspects moléculaires et cellulaires de la biologie

Présentée par : Dovydenko Ilya

Titre : Mise au point d'aptamères aux capacités thérapeutiques basés sur les ARN importables dans les mitochondries humaines

Unité de Recherche : UMR №7156 Unistra/CNRS «Génétique Moléculaire Génomique Microbiologie»

Directeur de Thèse : ENTELIS Nina DR2 CNRS

Co-Directeur de Thèse (s'il y a lieu) : VENYAMINOVA Alia Gusejnovna PhD

Localisation : 21 rue Descartes (IPCB), Strasbourg

ECOLES DOCTORALES :
(cocher la case)

☐ ED - Sciences de l'Homme et des sociétés	☐ ED 269 - Mathématiques, sciences de l'information et de l'ingénieur
☐ ED 99 – Humanités	☐ ED 270 – Théologie et sciences religieuses
☐ ED 101 – Droit, sciences politique et histoire	☐ ED 413 – Sciences de la terre, de l'univers et de l'environnement
☐ ED 182 – Physique et chimie physique	☒ ED 414 – Sciences de la vie et de la santé
☐ ED 221 – Augustin Cournot	
☐ ED 222 - Sciences chimiques	

Résumé de la Thèse de Doctorat de M. Dovydenko Ilya

Mise au point d'aptamères aux capacités thérapeutiques basés sur les ARN importables dans les mitochondries humaines

Contexte scientifique

Les mitochondries sont des organites présents dans la majorité des cellules eucaryotes. Elles assurent la production de l'énergie nécessaire aux cellules, sous forme d'ATP, par la phosphorylation oxydative ayant lieu au niveau de la chaîne respiratoire. Le génome mitochondrial humain code pour 13 protéines de la chaîne respiratoire, 22 ARN de transfert et 2 ARN ribosomiques. Les autres protéines ou ARN nécessaires au fonctionnement des mitochondries sont quand à eux importés dans la matrice mitochondriale depuis le cytoplasme.

De multiples altérations peuvent avoir lieu dans le génome mitochondrial conduisant à l'apparition de nombreuses pathologies, pour la plupart des myopathies ou des maladies neurodégénératives. Plus de 270 mutations du génome mitochondrial ont été décrit chez l'homme. Ces mutations sont le plus souvent hétéroplasmiques, ce qui signifie que les génomes sains et mutés coexistent au sein d'une même cellule. De ce fait l'apparition, le caractère et la sévérité des symptômes dépendent du niveau d'hétéroplasmie, soit en général de 60 à 80% de génomes mutés selon la mutation ou le type de cellules.

Bien qu'à ce jour il n'existe aucun traitement efficace pour traiter de telles affections, diverses stratégies sont envisagées pour tenter d'enrayer ces maladies. L'une d'elle, appelée stratégie allotopique, consiste à exprimer dans le noyau un gène sain codant pour une protéine ou unARN, qui sont ensuite adressés dans les mitochondries et capables de remplacer fonctionnellement les produits déficients des gènes mitochondriaux mutés. D'autres stratégies ont pour but de moduler le niveau d'hétéroplasmie pour qu'il soit inférieur au seuil pathogénique. Les stratégies de type anti-génomique d'une part consistent à adresser dans les mitochondries des molécules capables de cliver spécifiquement l'ADNmt muté, comme par exemple des endonucléases de restrictions reconnaissant spécifiquement la mutation, nucléases de doigt de zinc ou de type TALEN (Transcription Activator-like Effector Nucleases). L'autre méthode pour manipuler le niveau d'hétéroplasmie consiste à inhiber

spécifiquement la réplication de l'ADNmt mutant afin de donner un avantage à la réplication de l'ADN sauvage et de permettre de réduire le niveau d'hétéroplasmie. Ceci a déjà été tenté par le passé *via* l'utilisation des PNA (Peptide Nucleic Acids), molécules artificielles présentant une forte affinité séquence-spécifique pour l'ADNmt. Il a ainsi été démontré que ces PNA pouvaient inhiber la réplication de l'ADNmt mutant *in vitro*. Bien qu'attrayante, cette approche n'a pas pu être appliquée à des cellules vivantes en raison de l'impossibilité d'importer *in vivo* ces molécules dans les mitochondries.

Notre modèle s'appuie sur l'étude des caractéristiques structurales de l'ARNt$^{Lys}_{CUU}$ de la levure *Saccharomyces cerevisiae*. De précédentes études menées au laboratoire ont pu démontrer que cet ARNt cytosolique de levure pouvait être importé dans les mitochondries humaines. Les déterminants d'import de cet ARNt ont été identifiés ouvrant la possibilité d'exploiter la flexibilité de ce système pour créer un vecteur mitochondrial pour les cellules humaines. Dans cette optique, petits ARN artificiels formés sur la base de 2 domaines induisant leur adressage dans les mitochondries et d'une séquence capable de s'hybrider spécifiquement à l'ADNmt mutant, ont été modélisés. Ces ARN transgéniques étaient capables d'induire une diminution de l'ordre de 30% du taux d'hétéroplasmie dans des cellules cybrides porteuses de la large délétion pathogénique.

Objectifs

Les objectifs poursuivis dans cette étude ont été :

1. Synthèse de nouvelles molécules antiréplicatives contenant divers nucléotides chimiquement modifiés, visant à améliorer leur protection contre les nucléases endogènes et ainsi à accroître leur stabilité intracellulaire.
2. Le développement de procédés pour la synthèse chimique des molécules contenant des groupes lipophiles fixés par l'intermédiaire d'un pont clivable au sein de la cellule.
3. Optimisation de la procédure de transfection des cellules, en vue d'améliorer son efficacité et de réduire sa toxicité, par utilisation de dérivés d'acides nucléiques synthétisés contenant des groupes lipophiles.

4. Etude de la capacité des oligonucleotides modifiés à induire la diminution du niveau de hétéroplasmie pour des mutations pathogéniques dans l'ADN mitochondrial humain.

Le but de ces travaux est donc de développer de nouveaux modèles et outils de thérapie génique s'appuyant sur la voie d'adressage des ARN dans les mitochondries pour tenter d'enrayer les maladies mitochondriales et d'améliorer l'introduction de molécules artificielles à but thérapeutique dans les cellules humaines.

Résultats

Le premier de mes objectifs a consisté à poursuivre l'étude des ARN anti-réplicatifs dirigés contre la délétion KSS (Kearns Seyre Syndrome). Pour accroître leur stabilité au sein de la cellule suivant la transfection, j'ai synthétisé et testé tout un jeu d'oligonucléotides chimériques, possédant des déterminants d'import mitochondrial d'ARN associé à l'insert anti-réplicatif ADN, ainsi que des oligonucléotides contenant les modifications 2'-OMe et 2'-F du cycle du ribose dans les sites sensibles aux nucléases et/ou une thymidine inversé à l'extrémité 3'. Les différents tests effectués sur ce panel d'ARN chimériques ont montré une très haute spécificité vis-à-vis de l'ADNmt délété, une stabilité accrue mais malheureusement aucun effet significatif sur la diminution du taux d'hétéroplasmie.

Ensuite, nous avons appliqué la stratégie anti-réplicative pour une mutation ponctuelle dans le gène ND5 (A13514>G) d'ADNmt, associées à une pathologie. Les résultats obtenus montrent que les ARNs ciblant de manière spécifique le fragment d'ADNmt porteur de la mutation, conduisent à une diminution du taux d'hétéroplasmie de cellules cybrides.

Pour diminuer la toxicité de la procédure de transfection de cellules et pour créer une approche universelle d'adressage des ARN anti-réplicatifs dans les mitochondries des cellules humaines, nous avons modélisé et synthétisé des oligoribonucléotides contenant des groupes lipophiles. Pour cela, la méthode de la synthèse chimique des molécules d'ARN contenant des groupes cholestérol, acide lithocholique, l'alcool oléique ou l'oléylamide d'acide litocholique a été développée et optimisée. L'analyse des molécules ainsi modifiées, effectué par l'équipe de Novossibirsk, a mis en évidence que parmi tous les conjugués testés, les ARN contenant un résidu de cholestérol conjugué par des ponts de 6-10 atomes de carbone démontrent la meilleur capacité de pénétrer dans les cellules sans agents de transfection additionnels .

Nous avons supposé que les conjugués de cholestérol peuvent être retenus par les membrane mitochondriales ce qui pourrait empêcher l'importation d'ARN dans la matrice mitochondriale. Pour contourner ce problème, nous avons conçu des molécules avec des ponts biodégradables, permettant l'élimination du cholestérol après la pénétration des oligonucléotides chimériques dans cellules. Un composé synthétisé contient une liaison disulfure réductible, l'autre contient une liaison hydrazone clivable dans un milieu acidique. En parallèle, pour meilleure traçabilité de molécules aux capacités thérapeutiques potentielles, nous avons développé et optimisé la synthèse de conjugués d'ARN avec un résidu de cholestérol fixé par l'intermédiaire d'un pont clivable et leurs analogues avec des groupes fluorescents.

Pour toutes les constructions, la stabilité des ponts a été estimée. Dans les conditions du pH neutre, le conjugué contenant la liaison hydrazone démontre une stabilité élevée, contrairement à une hydrolyse rapide dans des conditions acides (pH6). L'efficacité de la procédure de transfection de cellules a été estimée par cytofluorométrie. Pour le conjugué contenant la liaison hydrazone, l'efficacité assez élevé (plus que 70% des cellules transfectées) a été démontré. D'autre part, le conjugué contenant la liaison disulfure a montré une faible efficacité (jusqu'à 10% de cellules transfectées), ce fait peut être expliqué par la dégradation rapide de ces molécules dans le milieu de transfection.

L'effet de la transfection de la lignée cellulaire porteuse de la mutation ND5 avec les ARN anti-réplicatifs contenant un résidu de cholestérol sur le taux d'hétéroplasmie et les fonctions mitochondriales ont été également été étudiés.

Conclusions – perspectives

Mon projet était axé sur la création de petites molécules d'ARN stables, non toxiques, capables de pénétrer dans les cellules humaines sans ajout d'agents additionnels et de diminuer la proportion entre les génomes mitochondriales mutants et sauvage. Au cours de ma thèse j'ai synthétisé une série des nouvelles molécules antiréplicative contenant divers nucléotides chimiquement modifiés, visant à accroître leur stabilité au sein de la cellule. J'ai développé la nouvelle méthode de synthèse chimique des molécules contenant des groupes lipophiles fixé par l'intermédiaire d'un pont clivable et bio-dégradable. Cela m'a permit d'améliorer l'efficacité de transfection des cellules humaines en culture et de réduire la toxicité de cette procédure. J'ai également étudié la capacité des nouvelles molécules antireplicatives modifiées à induire la diminution du niveau de hétéroplasmie pour des mutations pathogéniques dans l'ADN mitochondrial humain.

Après avoir été testés sur des cultures de cellules humaines immortalisées et des fibroblastes primaires de patients, ces molécules pourraient être exploitées sur d'autres modèles (comme, par exemple des cellules souche ou les embryons de souris) et, à terme, pour le traitement pharmacologique des patients atteints de maladies mitochondriales provoquées par des mutations de l'ADNmt. Sur un plan fondamental, il serait intéressant d'utiliser les ARN modifiés comme un outil d'investigation pour comprendre plus en détails leur mode d'action et le mécanisme moléculaire de leur adressage dans les mitochondries.

List des publications et des communication

Publications

1. Petrova N.S., Chernikov I.V., Meschaninova M.I., Dovydenko I.S., Venyaminova A.G., Zenkova M.A., Vlassov V.V., Chernolovskaya E.L. Carrier-free cellular uptake and the gene-silencing activity of the lipophilic siRNAs is strongly affected by the length of the linker between siRNA and lipophilic group. Nucleic Acids Res. 2012. V.40. N.5. P.2330-2344.

2. Tonin Y., Heckel AM., Dovydenko I., Meschaninova M., Comte C., Venyaminova A., Pyshnyi D., Tarassov I., Entelis N. Characterization of chemically modified oligonucleotides targeting a pathogenic mutation in human mitochondrial DNA. Biochimie. 2014. V.100. P.192-199.

3. Gvozdeva O.V., Dovydenko I.S., Venyaminova A.G., Zenkova M.A., Vlassov V.V., Chernolovskaya E.L. 42- and 63-bp anti-MDR1-siRNAs bearing 2'-OMe modifications in nuclease-sensitive sites induce specific and potent gene silencing. FEBS Lett., 2014. V. 588(6)., P.1037-43.

4. Tonin Y., Heckel AM., Vysokikh M., Dovydenko I., Meschaninova M., Venyaminova A., Tarassov I., Entelis N. Modelling of antigenomic therapy of mitochondrial diseases by imported RNA targeting a pathogenic point mutation in mtDNA. J Biol Chem. 2014. V.289. N.19. P.13323-13334.

5. Dovydenko I., Heckel AM., Tonin Y., Gower A., Venyaminova A., Tarassov I., Entelis N. Mitochondrial targeting of recombinant RNA. Methods in Molecular Biology, Springer Protocols. 2015; P:209-25.

6. Ilya Dovydenko, Ivan Tarassov, Alya Venyaminova, Nina Entelis. Method of carrier-free delivery of therapeutic RNA importable into human mitochondria: lipophilic conjugates with cleavable bonds. Submited.

<u>Communication</u>

<u>Ilya S. Dovydenko</u>, Mariya I. Meschaninova, Yann Tonin, Anne-Marie Heckel, Ivan Tarasov, Aliya G. Venyaminova, Nina Entelis. SupraChem 2012 "Supramolecular Systems in Chemistry and Biology", France 2012. **Poster**

A.-M. Heckel, Y. Tonin, C. Comte, <u>I. Dovydenko</u>, A. Lombès, R. Martin, N. Entelis, I. Tarassov. 6ème Colloque Meetochondrie, France 2012. **Poster**

<u>Ilya S. Dovydenko</u>, Mariya I. Meschaninova, Yann Tonin, Anne-Marie Heckel, Ivan Tarasov, Aliya G. Venyaminova, Nina Entelis. Mitochondria in health, disease and death of the cell, France 2013. **Poster**

<u>Ilya S. Dovydenko</u>, Mariya I. Meschaninova, Yann Tonin, Anne-Marie Heckel, Ivan Tarassov, Aliya G. Venyaminova, Nina Entelis. Conférence annuelle SFBBM 2013 9ème rencontre SifrARN, France 2013. **Poster**

N. Entelis, Y. Tonin, A.-M. Heckel, <u>I. Dovydenko</u>, R. P. Martin, I. Tarassov. FEBS Congress, Russia 2013. **Oral presentation**

<u>Ilya S. Dovydenko</u>, Mariya I. Meschaninova, Yann Tonin, Anne-Marie Heckel, Ivan Tarasov, Aliya G. Venyaminova, Nina Entelis. Euromit 2014 is the 9th international conference on mitochondrial research, Finland 2014. **Poster**

<u>Ilya S. Dovydenko</u>, Yann Tonin, Anne-Marie Heckel, Aliya G. Venyaminova, Ivan Tarasov, Nina Entelis. 5th World Congress on Targeting Mitochondria, Germany 2014. **Oral presentation**

<u>Ilya Dovydenko</u>, Anne-Marie Heckel, Ivan Tarasov, Aliya G. Venyaminova, Nina Entelis. 8e colloque du réseau MeetOchondrie, France 2015. **Poster**

Résumé

Les mitochondries sont des organites présents dans la majorité des cellules eucaryotes. Elles assurent la production de l'énergie nécessaire aux cellules, sous forme d'ATP, par la phosphorylation oxydative. De multiples altérations peuvent avoir lieu dans le génome mitochondrial (ADNmt) conduisant à l'apparition des pathologies, pour la plupart des myopathies ou des maladies neurodégénératives. Ces mutations sont le plus souvent hétéroplasmiques, ce qui signifie que les génomes sains et mutés coexistent au sein d'une même cellule. De ce fait l'apparition, le caractère et la sévérité des symptômes dépendent du niveau d'hétéroplasmie. Le but du travail actuel était de développer de nouveaux modèles et outils de thérapie génique s'appuyant sur la voie d'adressage des ARN dans les mitochondries pour tenter d'enrayer les maladies mitochondriales et d'améliorer l'introduction de molécules thérapeutiques dans les cellules humaines. Bien qu'à ce jour il n'existe aucun traitement efficace pour traiter de telles affections, diverses stratégies sont envisagées pour tenter d'enrayer ces maladies. L'une d'elle a pour but de moduler le niveau d'hétéroplasmie pour qu'il soit inférieur au seuil pathogénique, en affectant la réplication de l'ADNmt mutant. Mon projet était axé sur la création de petites molécules d'ARN stables, non toxiques, capables de pénétrer dans les cellules humaines sans ajout d'agents additionnels, d'être adressées dans les mitochondries et de diminuer la proportion entre les génomes mitochondriales mutants et sauvage. Au cours de ma thèse j'ai synthétisé une série des nouvelles molécules anti-réplicatives contenant divers nucléotides chimiquement modifiés, visant à accroître leur stabilité au sein de la cellule. J'ai développé la nouvelle méthode de synthèse chimique des molécules contenant des groupes lipophiles fixé par l'intermédiaire d'un pont clivable et bio-dégradable. Cela m'a permis d'améliorer l'efficacité de transfection des cellules humaines en culture et de réduire sa toxicité. J'ai également étudié la capacité des nouvelles molécules à induire la diminution du niveau de hétéroplasmie pour des mutations pathogéniques dans l'ADNmt. Après avoir été testés sur des cultures de cellules humaines immortalisées et des fibroblastes primaires de patients, ces molécules pourraient être exploitées sur d'autres modèles (comme, par exemple des cellules souche ou les embryons de souris) et, à terme, pour le traitement pharmacologique des patients atteints de maladies mitochondriales. Sur un plan fondamental, il serait intéressant d'utiliser les ARN modifiés comme un outil d'investigation pour comprendre plus en détails leur mode d'action et le mécanisme moléculaire de leur adressage dans les mitochondries.

Abstract

Mitochondria are organelles present in most eukaryotic cells. They ensure the production of energy for cells in the form of ATP by oxidative phosphorylation. Multiple alterations may occur in the mitochondrial genome (mtDNA) leading to the appearance of pathologies, for most myopathies or neurodegenerative diseases. These mutations are usually heteroplasmic, meaning that the healthy and mutated genomes co-exist within the same cell. Hence the appearance, character and severity of symptoms depend on the level of heteroplasmy. The aim of the present work was to develop new models and gene therapy tools based on the addressing of RNA into mitochondria as a way to target pathogenic mtDNA mutations and improve the introduction of therapeutic molecules in human cells. Although to date there is no effective treatment for such diseases, various strategies has been considered. One approach of it is to modulate the level of heteroplasmy to pass below the pathogenic threshold, by affecting the replication of mutant mtDNA. My project focused on the creation of small RNA molecules stable, non-toxic, capable of penetrating human cells without adding additional agents, able to be targeted in the mitochondria and to decrease the proportion of mutant mitochondrial genomes. During my PhD study, I have synthesized a series of new anti-replication molecules containing various chemically modified nucleotides, to increase their stability in the cell. I have developed a new method for the chemical synthesis of RNA molecules containing lipophilic groups attached through a cleavable and biodegradable bridge. This allowed me to improve the efficiency of transfection of human cells in culture and reduce its toxicity. I also studied the ability of new compounds to induce a decrease in the level of heteroplasmy for pathogenic mutations in the human mtDNA. After being tested in cultures of immortalized human cells and primary fibroblasts of patients, these molecules can be exploited in more advanced models (such as, for example stem cells or mouse embryos) and, ultimately, for the treatment of the patients affected by mitochondrial diseases. On a fundamental level, it would be interesting to use the modified RNA as an investigative tool to understand more fully their mode of action and the molecular mechanism of their targeting into mitochondria.